Assessing Dredge Spoil Dispersion on the Inner Shelf off the Coast of Tauranga Harbour, Aotearoa New Zealand

A thesis

submitted in partial fulfilment

of the requirements for the degree

of

Master of Science (Research) in Earth Sciences

at

The University of Waikato

by

Charlotte Blackler

THE UNIVERSITY OF
WAIKATO
Te Whare Wānanga o Waikato

2024

Abstract

Dredging began in Te Awanui/Tauranga Harbour, the largest port in Aotearoa New Zealand, in 1919 to allow continued development of the port. The dredged material gets disposed of by depositing it into open water in a process known as spoiling. It is more important than ever to understand the impact of dredging as ships are getting ever larger, which require deeper and wider channels for safe passage into ports. This thesis investigated the composition and distribution of the dredge spoil on the Bay of Plenty inner shelf for the first time since 1992. Between August 2023 and February 2024, I used seismic and sedimentological analyses, including shallow seismic surveys, vibracoring, and surficial sediment sampling to determine the size and shape, and the grain size and organic content comprising the dredge spoil mound. Results showed that the sediments are predominantly fine to medium-grained moderately sorted sand with low organic content. The dredge spoil mound sits on average 1.5 m above the pre-deposition seafloor, and has no discernible surface texture or bedforms. This study establishes that the composition of the dredged sediment remains comparable to that of the pre-deposition seafloor. The results are compatible with past studies, suggesting that dredge spoil deposited on the inner shelf is stable, and is not subject to resuspension and transport under fair weather conditions.

Acknowledgements

I would first like to express my deepest appreciation to my supervisor, Dr Andrew La Croix. I would not have been able to complete this project without his guidance, support and invaluable knowledge. I would also like to express my gratitude to the Port of Tauranga, and specifically, Rowan Johnstone, whose support made the field work and ultimately the whole thesis possible. The operating crew at the port were also instrumental in vibracore data collection.

I also want to thank all of the University of Waikato technicians, including Ben, Holly and Bonnie, who have been invaluable with their help and time with all of the complex technical aspects involved with data collection and survey work. I would also like to acknowledge those who helped with data analysis, it's been a learning curve and I will always be grateful to those who supported me through it.

I would also like to thank my fellow postgraduate students, who have provided endless support, motivation, life lessons and laughs. Finally, I want to express my deepest appreciation to my family and partner for their boundless support and belief in me throughout this journey.

Table of Contents

List of Figures

List of Tables

Chapter 1

1.1 Introduction

Te Awanui (Tauranga Harbour) is home to the largest port in Aotearoa New Zealand (Figure 1.1). To deepen and widen the shipping channels and accommodate larger vessels to maintain navigability, dredging began in the harbour in 1919, with spoil utilization for land reclamation beginning in 1965 (Port of Tauranga, 2020). Dredging creates waste material that gets disposed of by depositing the material into open water in a process known as spoiling (Gross et al., 1979; Kester et al., 1981). A significant amount of the sediment within the harbour is deposited on the inner continental shelf at two sites; Site D/H1 receives primarily sand, and site G/H2 which is further offshore receives any silt and clay (see Figure 1.1C). Previous research into the deposition of dredge spoil onto the inner shelf disposal site has suggested that the deposited material is relatively stable and is not susceptible to erosion and shoreward transport, primarily due to the depth of the disposal ground and the predominantly fair weather conditions experienced within this area (Harms, 1989; Healy et al., 1997; Matthews, 1997; Warren et al., 1991; Warren, 1992). However, since these past studies, there has been a significant amount of additional dredge sediment deposited, and it is especially pertinent to re-assess the impacts of dredging within the harbour since the 2015-2016 capital dredging operation. Moreover, increased awareness surrounding climate and environmental change has heightened public concern over the effects of dredging and the changing dynamics of coastal environments and ecosystems.

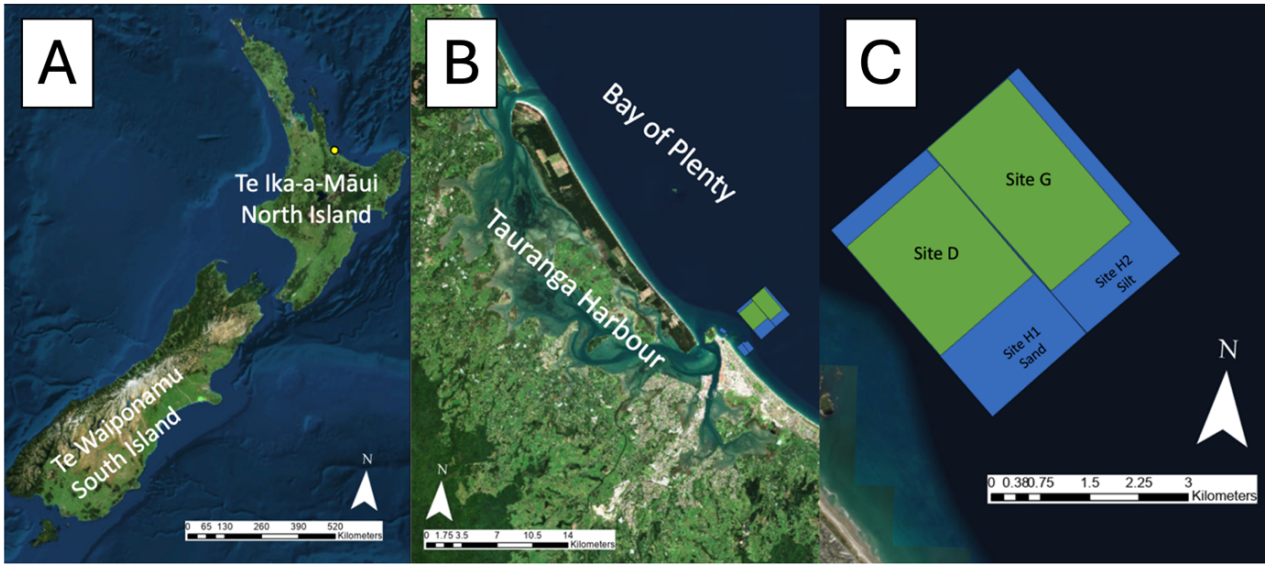

Figure1.1: A) Location of Tauranga Harbour in Aotearoa New Zealand. B) Tauranga Harbour study area showing dredge spoil deposition sites. C) Close-up of dredge spoil depositional sites.

1.1.1 Thesis Outline

This thesis is organized in "paper format" wherein Chapter One presents a review of the current knowledge and previous literature relating to the study area. Chapter Two embodies the main research for the thesis, reporting on the methods, and results, as well as providing study limitations and recommendations for future research and conclusions arranged in manuscript style. Finally, Chapter Four summarizes the key findings of the study and evaluates if the study aims were addressed.

1.2 Regional Geology and Geomorphology

New Zealand's North Island is situated on the Australian plate but adjacent to the boundary between the Pacific and Indo-Australian plates. Tauranga Harbour is located within the Tauranga Basin, a Quaternary basin in the Bay of Plenty that is primarily filled with sedimentary or volcano-sedimentary layers (MacPherson et al., 2017). The harbour is situated within a graben, associated with an extension within the Taupō Volcanic Zone that formed approximately 2-3 million years ago (Healy, 1993). A geological map of Tauranga Basin, highlighted in Figure 1.2, shows that the majority of the regional geology comprises young alluvial layers, also referred to as the Tauranga Group, and rhyolitic volcanic material ranging in age from 12-2 million years old (Ballance, 2009).

Tauranga Harbour is a large meso-tidal tombolo-bound estuarine lagoon (Davis & Healy, 1993). The estuarine lagoon system is enclosed by two tidal inlets, Katikati in the northwest, and Tauranga at the south-eastern side adjacent to the rocky headland and tombolo of Mount Maunganui.

The barrier islands, characteristic of Tauranga Harbour, were created by sediment delivered from longshore drift beginning about 7000 years before present (ka). The Holocene Highstand (HHS) in New Zealand ceased by about 4 ka (Dougherty & Dickson, 2012). Relative sea levels during the HHS were at least 2.75 m higher than present (Clement et al., 2016). The impact of the HHS has led to significant changes within the tidal inlets and margins of the harbour (De Lange et al., 2015). Rapid accretion of Holocene dunes on the barrier island between Bowentown and Mauao resulted in the closing of tidal inlets at Hunters Creek (~5 ka) and Blue Gum Bay (~3.5 ka) and the subsequent formation of the Matakana Barrier Islands (De Lange et al., 2015). The modern-day barrier system includes Matakana Island,

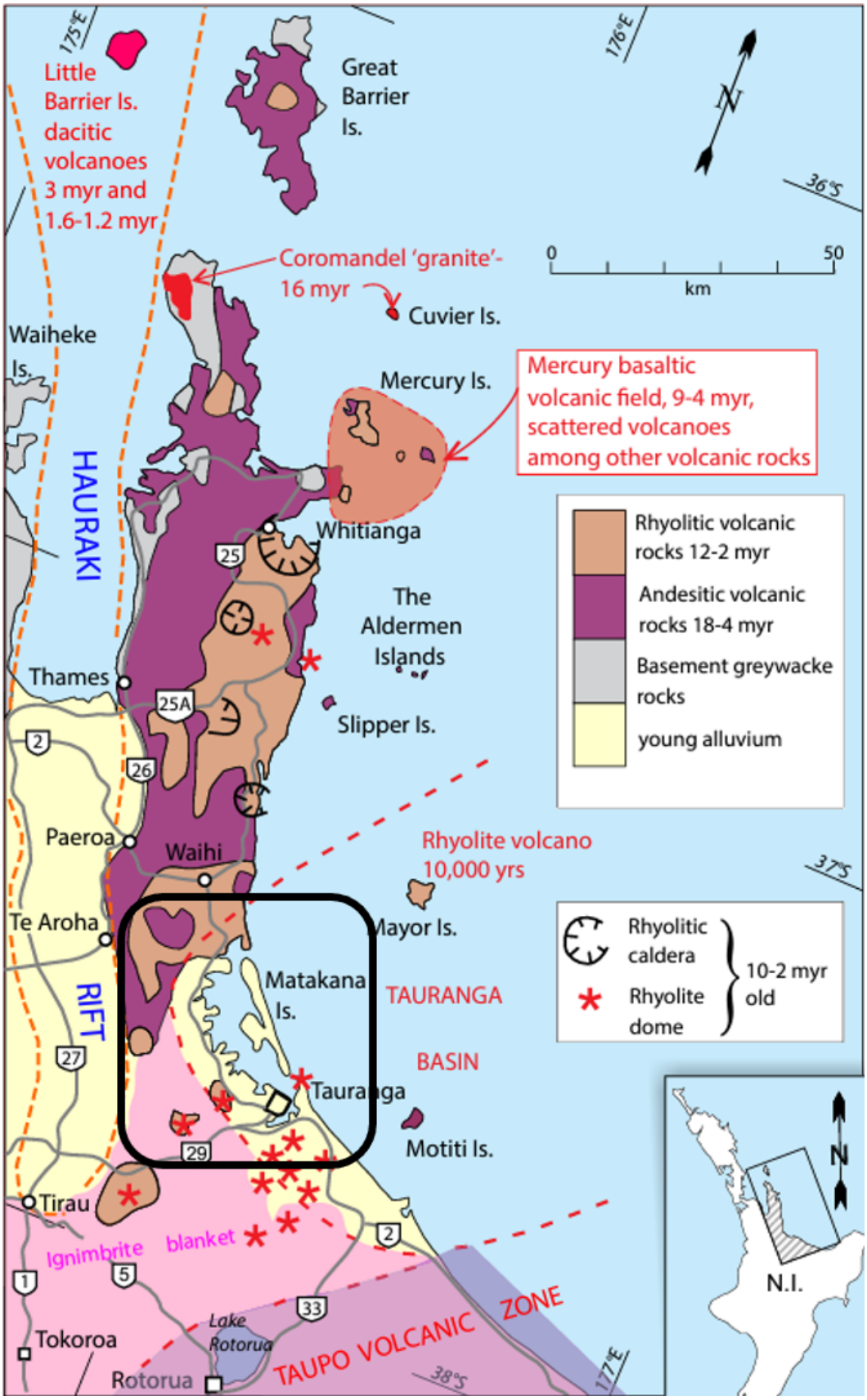

Figure 1.2 Simplified geology of the Coromandel Peninsula and the western Bay of Plenty regions of Aotearoa New Zealand's North Island. The Tauranga Harbour area is enclosed by a black rectangle (from Ballance, 2009).

The barriers eventually led to the restriction of marine sediments entering Tauranga Harbour and the development of the present-day sedimentary and hydrodynamic regime (MacPherson et al., 2017). Tauranga Harbour shows a range of other typical geomorphological features expected within a meso-tidal estuarine lagoon, including ebb and flood tidal deltas, tidal channels and tidal flats (Harms, 1989; Warren et al., 1991).

The entrance to the Tauranga inlet is approximately 500 m wide, has an average depth of 15 m, and a maximum depth of approximately 34 m (Krüger & Healy, 2006). The harbour has a water volume of approximately 455.2 x 10^6 m^3 and occupies an area of around 200 km^2. Approximately 290 billion tonnes of water flows in and out of the harbour at each end of Matakana Island (Port of Tauranga, 2011). It is estimated that 61% of the water in the harbour flows through the main entrance to the estuary at Mount Maunganui forced by tides. The tidal range within the harbour is approximately 2 m within the harbour, generating tidal currents in excess of 3.5 m/s (Davies-Colley & Healy, 1978b).

1.3 Literature Review

1.3.1 Basics of Sediment Transport

Sediment transport on the shelf can occur as bedload (grain-to-grain interaction) or as suspended load (fluid-to-grain interaction maintained above the seafloor by turbulent flows) (Komar, 1976; Warren, 1992). Whether sediments are eroded, transported, or deposited is determined by the grain size, flow velocity and water depth (Figure 1.3) (Hjulström, 1935). The critical erosion field in a Hjulström diagram shows the velocity required to entrain a sediment particle of a given diameter. In contrast, the critical deposition field shows how flow velocity and grain size control deposition. The zone between the critical erosion and critical deposition curves represents the conditions under which sediment is transported (Hjulström, 1935). The Hjulström diagram assumes that larger sediment grains require more energy to erode and transport. However, it does not account for interparticle cohesion of silt and clay-sized material. These cohesive particles require greater flow velocities than would be characteristic of noncohesive sediments (Keylock, 2004).

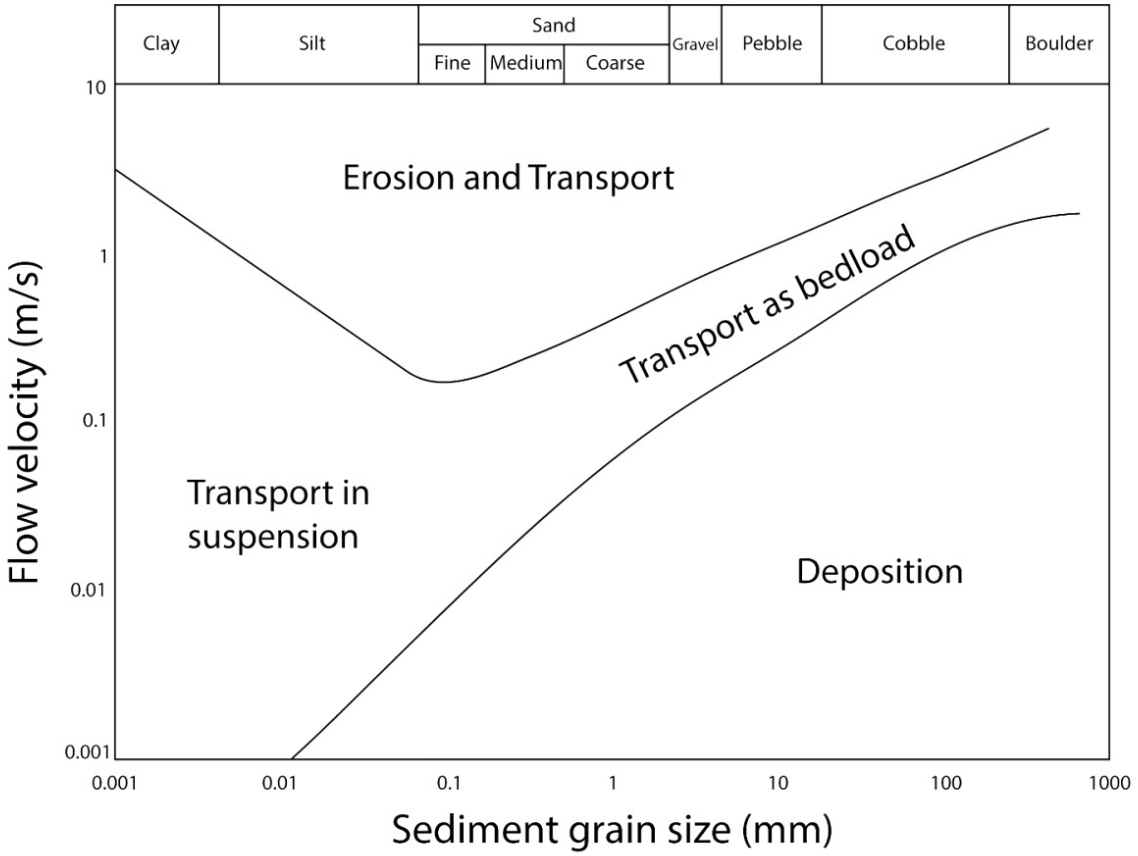

Figure 1.3 – Hjulström diagram, showing sediment erosion, transport and deposition as a function of flow velocity and sediment grain size. The assumed water depth is 1 m (Hjulström, 1935).

Currents and waves are the primary agents of sediment transport, and with the continued motion of the sediments, bedforms are eventually constructed. There are a range of different bedforms that can be built depending on the flow velocity, including ripples, megaripples, sand waves, dunes and antidunes (Figure 1.4) (Mazumder, 2003).

Ripple size generally increases in the offshore direction as wave orbital diameter increases with water depth (Miller & Komar, 1980a). The overall size of ripples is in part a function of mean sediment grain size, and therefore, with increasing grain size ripples transition into dunes (Miller & Komar, 1980b). Furthermore, as the velocities at the bed increase, the ripples become more irregular in shape, height and spacing (Bagnold, 1946; Reineck & Singh, 1980).

Bedforms generated by waves do not grow as large as current-generated bedforms (Bagnold, 1946). Waves with large wave heights and long periods following storm events can generate large ripples and megaripples. Under fair weather conditions, smaller wave velocities occur which results in a degradation of storm-generated megaripples and the subsequent formation of smaller bedforms (Harms, 1989). As flow velocity decreases, the size of the

resulting bedform also decreases due to a decrease in sediment movement, leading to the formation of massive and structureless sedimentary layers (Reineck & Singh, 1980).

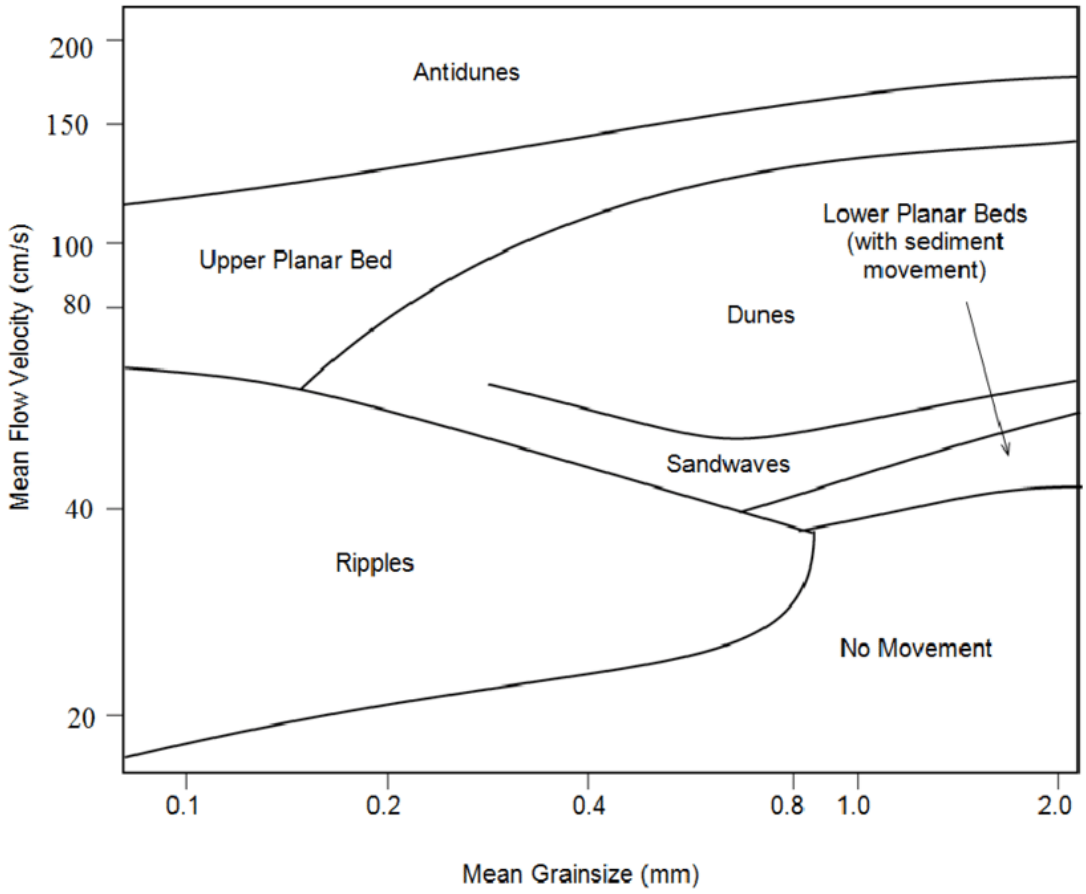

Figure 1.4- Bedform stability diagram in relation to mean flow velocity and mean grain size. Water depth is assumed to be 1 m (from Reineck & Singh, 1980).

1.3.2 Processes on the Inner Shelf

A wide range of factors influence the dynamics of the continental shelf including the influences of large-scale currents driven by the Coriolis force, regional-scale currents and tides, wind forcing, waves, storm surges, as well as indirect effects of surf zone processes (Figure 1.5) (Kombiadou & Yannis, 2013).

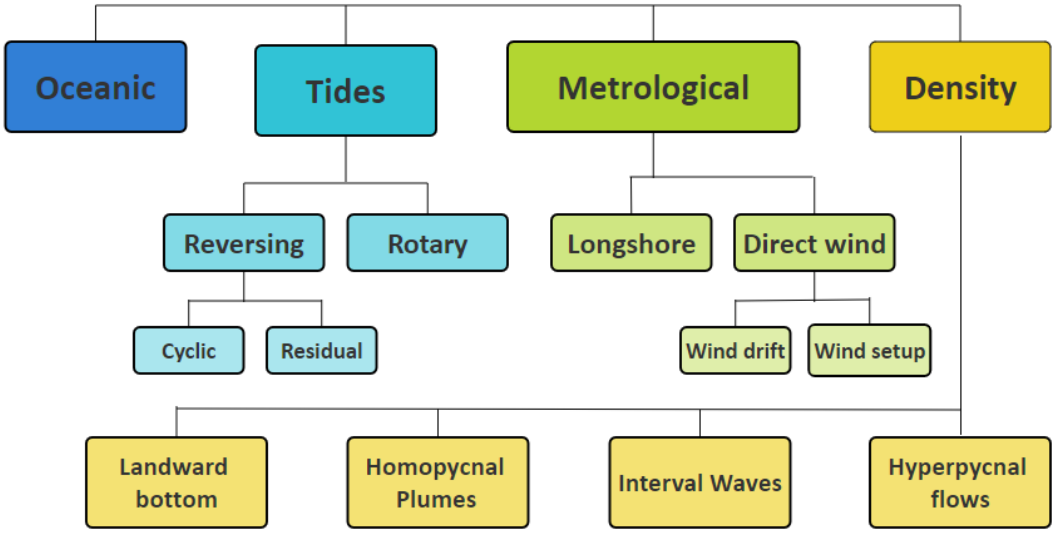

Figure 1.5 The range of processes influencing sediment dynamics on continental shelves. All currents highlighted are combined with the Coriolis force, forming geostrophic currents (from Suter, 2006).

From a sedimentological point of view (i.e., facies analysis), continental shelves fall into two main categories: 1) wave (or storm) dominated and 2) tide-dominated shelves (Davis, 1987). Shelves can also be subdivided into three major process zones (Figure 1.6). These are the shoreface, which is dominated by wave- and storm-generated waves and flows; the mid-shelf which is dominated by geostrophic flow; and, the outer shelf, which is characterised by near-bottom flows dominated by frontal processes between the shelf and open ocean water masses (Cowell & Nielsen, 1984).

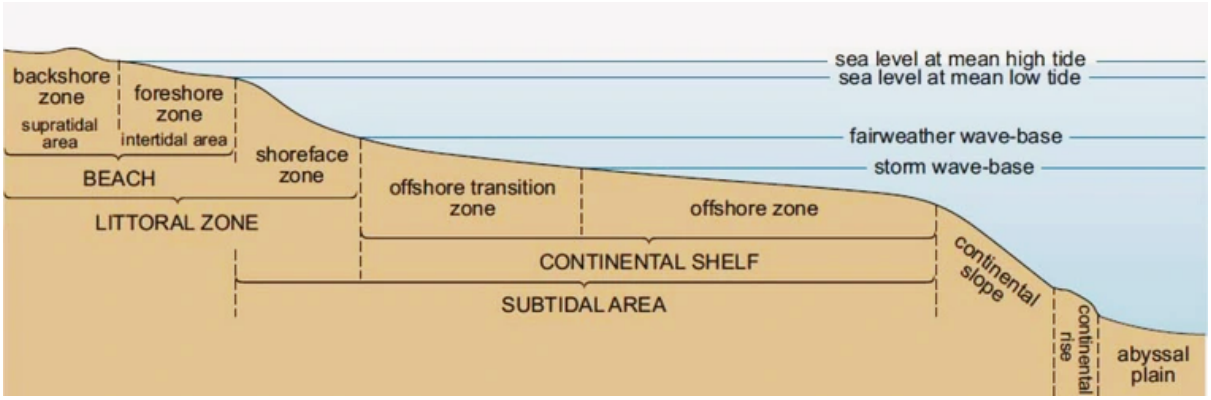

Figure 1.6 Generalised model of the shoreline to shelf transition (SEPM STRATA, 2022).

Some classic facies models for storm-dominated shelves depict a distally deepening environment where suspension settling and density-driven turbidity flows dominate the offshore below the storm wave base (Grundvåg et al., 2021).

Most sediment transport within the inner shelf occurs close to the sea bed (Harris & Wiberg, 2002). Coarser sediment is moved as bedload within a few millimetres of the sea bed (Komar, 1976; Sleath, 1986). Whereas finer sediment is predominantly transported as suspended material above the sea bed (Warren, 1992).

The New Zealand continental shelf is predominantly considered to be storm-dominated (Carter & Heath, 1975). Therefore, the leading cause of sediment movement across the shelf within the Bay of Plenty region is large waves associated with storm events (Harms, 1989; Healy et al., 1997; Michels & Healy, 1999; Warren et al., 1991). However, the impacts of tides and general circulatory currents cannot be discounted as the movement of sediment under tides and currents does occur (Stanton et al., 2001). However, it is not as common as sediment movement under storm conditions within the inner shelf environment around New Zealand.

1.3.2a Wave Processes

In water depths less than 50 m waves are the most significant process for sediment transport and deposition. At deeper water depths, over 50 m, tides induce currents that are affected by the seabed topography on a small scale or driven by wind-based forces on a larger scale (Csanady, 1988). The east coast of the North Island of New Zealand has a mixed wave climate with predominantly southerly swells, which originate in the westerlies south of New Zealand, as well as locally generated southerly and northerly storm swells (Pickrill & Mitchell, 1979). The prevailing waves are 0.5-2.0 m (Figure 1.7) and have a short period (7-11 s). These waves are generally superimposed on weak seasonal cycles resulting from an increased frequency of local northerly waves in the summer (Pickrill & Mitchell, 1979). As New Zealand's East Coast is physiographically sheltered, it generally experiences significantly smaller waves than the rest of the New Zealand coastline (Macky et al., 1995).

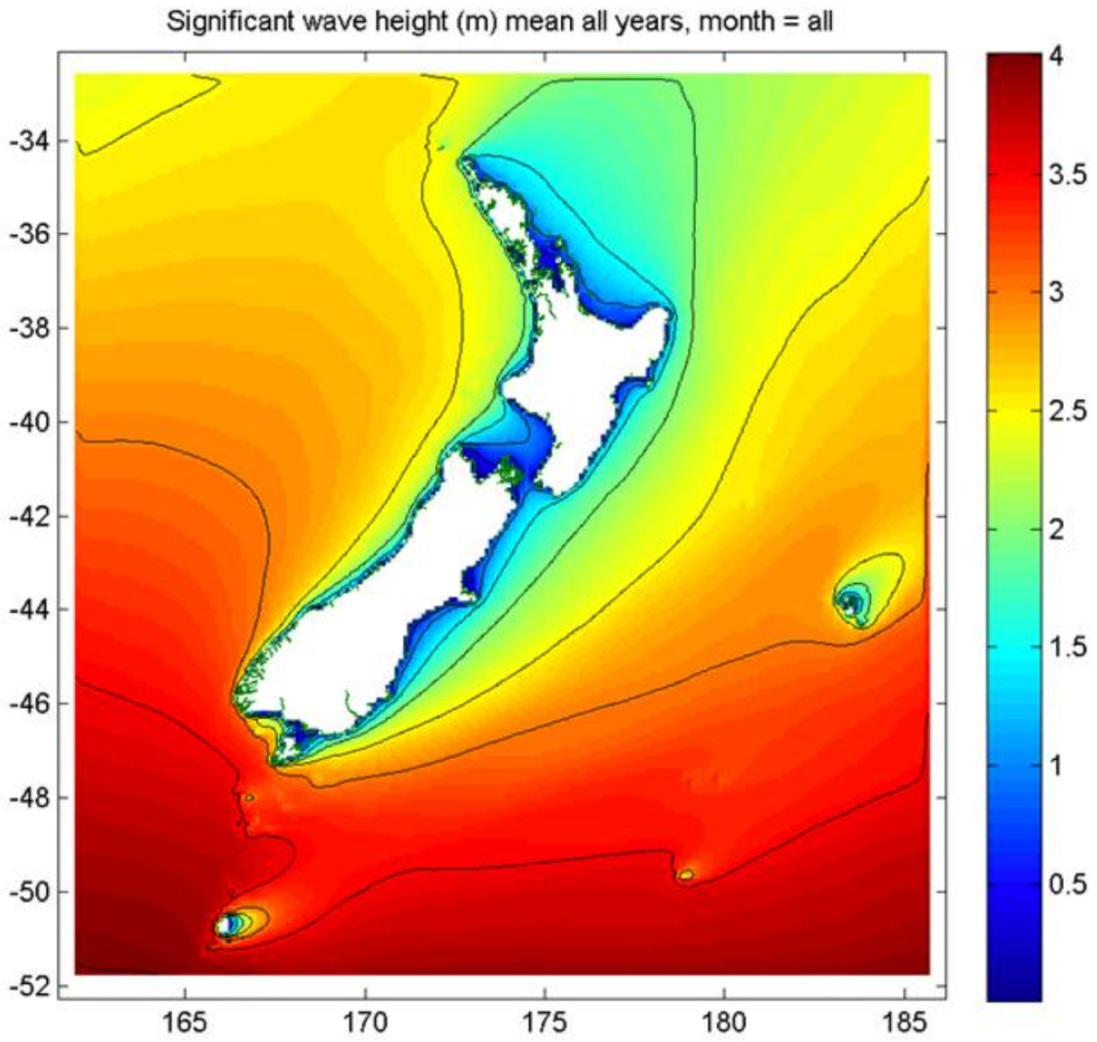

Figure 1.7- Long-term mean wave height in New Zealand using a 45-year hindcast model (from NIWA, 2024).

The Bay of Plenty is a region of low wave energy due to the sheltered nature of the coastlines from the westerly and south-westerly swell that impacts the rest of Aotearoa (Figure 1.7) (Montano Orozco, 2023). Wind-forced waves develop under westerly winds, whereas swell waves develop from the east to northeast due to the longer fetch (Harms, 1989). Variability owing to El Nino-Southern Oscillation (ENSO), as well as Tasman atmospheric depressions, increase the number of storm events evert winter-early spring, as well as ex-tropical cyclones that occur typically throughout February-April (Healy et al., 1998).

On the inner shelf where dredge spoil disposal occurs, waves have a period of between 8-11 s (Healy et al., 1998). It has been suggested by Matthews (1997) that at the dredge spoil deposition site, which is situated in water depths of 20-40 m, the primary means of sediment transport and morphological change are due to large waves and currents directly associated with storms. The potential for sediment movement from wave influence during “fair weather” conditions is low. Davies-Colley & Healy (1978) showed that tidal currents and wind-generated

waves dominate the shelf in the region of the spoil deposition site. In the case of long-term sediment transport, the largest contribution is provided by large waves that occur semi-frequently during storm conditions - defined by wave heights greater than 1.5 m, exceeding 12 s (Healy et al., 1998).

1.3.2b Tide and Current Processes

Current upwelling and downwelling in the nearshore and inner shelf environments play an important role in the transport of sediment, particularly the offshore movement of sediment associated with downwelling (Harms, 1989). The efficacy of wind-driven currents in the movement of sediment requires an understanding of the strength, direction, and duration of wind (Bradshaw, 1991). Off the east coast of New Zealand, three main currents are important for sediment transport. These currents are known as the East Cape, Southland and East Auckland currents (Heath, 1975). Seasonal variations cause the current speeds off the coast to decrease with depth down to 1000 m, whereas in the winter they are near-constant down to 300 m and decrease below this depth. The seasonal variation is thought to be related to the development of the summer thermocline (Heath, 1975).

The Bay of Plenty region has an open coastline, with a predominantly south-westerly littoral drift (Harms, 1989; Healy, 1977). The outer flows on the shelf are associated with three permanent warm water eddies (Roemmich & Sutton, 1998). Two significant currents dominate the Bay of Plenty region, the eastward flowing large-scale boundary current, the East Auckland Current (EUAC), and a relatively stationary eddy current, the East Cape Eddy (ECE) (Montaño et al., 2023). In the winter months, the EUAC and ECE currents are located further offshore, and the transport of particles is predominantly towards the central Bay of Plenty region. Whereas in the summer months, the currents tends to flow eastwards, following the EUAC (Montaño et al., 2023). Tidal currents in the spoil deposition site appear not to be the cause of currents, yet their overall importance cannot be discounted. The velocity of tidal currents varies over the tidal cycle and decreases with water depth from shore on the continental shelf (Warren, 1992).

1.3.2c Wave-Current Interactions

The interaction of wind-driven currents and waves on the inner shelf is a vital mechanism for the movement of sediment, as orbital motions are associated with the entrainment of the sediment, and currents are responsible for the transportation of the sediment (Bradshaw, 1991;

Warren, 1992). The angle between waves and the current, as well as the roughness and textural composition of the underlying bedforms, has a determining factor in the quantity and direction of sediment transport from the inner shelf (Wright, 1987). Waves determine when, and currents determine where the sediment is deposited (Bradshaw, 1991; Harms, 1989). The interaction of waves and currents contributes to sea surface and bottom shear stress (Kim, 2019). Waves only influence tidal currents through bottom friction effects in water depths less than 50 m (Kim, 2019), and this is manifested as a decrease in tidal current amplitude with increasing wave height. In order to initiate the movement of sediment in water depths of >22 m as is typical of the study area, an assumed threshold of 0.3 m/s for the initiation of medium-grained sediment transport, with wave heights greater than 1.5 m, and swell periods greater than 10 s. If these conditions are met there will be movement of medium-grained sand movement by wave action alone without the influence of tidal forces, although it is estimated that these conditions occur >5% of the time (Healy et al., 1998).

1.3.3 Deposits on the Inner Shelf

Many clastic shelves are high-energy environments, with currents capable of transporting significant amounts of sediment and having the potential to be highly erosive (Suter, 2006). The high-energy nature of clastic shelf environments means that there often is a gradation of coarser sediment at the coastline to finer sediment further out into the shelf environment (Collins & Balson, 2007; Mouton, 1952). The distribution of sand is typically limited to shallower, wave-agitated waters, whereas silt and clay are deposited further offshore in deeper undisturbed waters (Gross, 1972). The inner shelf consists of predominantly of coarse to medium grained sediment as finer-grained material is resuspended by waves and or tides and transported offshore (Nittrouer & Wright, 1994). The continental shelf is also responsible for producing a wide range of bedforms ranging from ripples to antidunes depending on flow velocity and mean grain size (Figure1.4) (Bagnold, 1946; Mazumder, 2003; Reineck & Singh, 1980).

The surficial sediments on continental shelves around New Zealand are highly influenced by a wide range of geological, oceanographic, climatic and human activities (Bostock et al., 2019). The shelf within the Bay of Plenty region is predominantly sand-dominated with small amounts of mud, suggesting that the majority of sediment is sourced from local rivers which contribute an average of 14 mt/y^{-1} of terrigenous sediments to the region (Hicks et al., 2000). There is a moderate amount of gravel and small amounts of mud off the

coast of Tauranga (Bostock et al., 2019). There is also a significant amount of sediment added to the inner shelf from volcanic sources from previous eruptive events at Moutohora (Whale Island) and Whakaari (White Island) (Bostock et al., 2019; Propp et al., 1994).

1.3.4 Deposits on the Shelf in the Study Area

Two different shelf facies (i.e., deposit types) were initially interpreted for the inner shelf environment off the coast of Tauranga; an offshore coarse sand (>50% >0.5 mm) that is located 3-4 km offshore on the natural shelf as well as inshore fine sand facies (60% <0.25 mm) (Dahm & Healy, 1980). By contrast, Harms (1989) subdivided the shelf into three facies/environments, a nearshore sand prism that displays a seaward thinning and fining wedge of nearshore-derived sand, a modern shelf blanketing muddy sediment layers, and a shelf relict sand blanket (Harms, 1989; Healy et al., 1988). This occurs due to hydrodynamic sorting of the spoil material based on grain size. The range of sediment sizes within the study area is both directly related to the disposal activities and also typical of the Eastern Coromandel Shelf (Dell et al., 1985; Healy et al., 1998). Figure 1.8 shows a generalized profile of the Tauranga shelf environment, with the study area located within the dredge spoil disposal site.

Rates of sedimentation on the inner shelf within the Bay of Plenty range from 8-45 cm 10^3 yr^{-1} and have not varied significantly over the past 30,000 years (Kohn & Glasby, 1978). Nearshore sediment is dominated by fine sand, which contains a small percentage of mafic minerals and volcanic glass (Kohn & Glasby, 1978; Kulgemeyer et al., 2016). Sediment coarsens further from shore, as well as shifts in composition to having higher mafic mineral and lithic fragment content. The sediment further offshore is linked to deposits on the inner Coromandel Shelf which are interpreted as being early to late Holocene sand reworked from Pleistocene deposits that have been overlain by allochthonous sediments (Kulgemeyer et al., 2016).

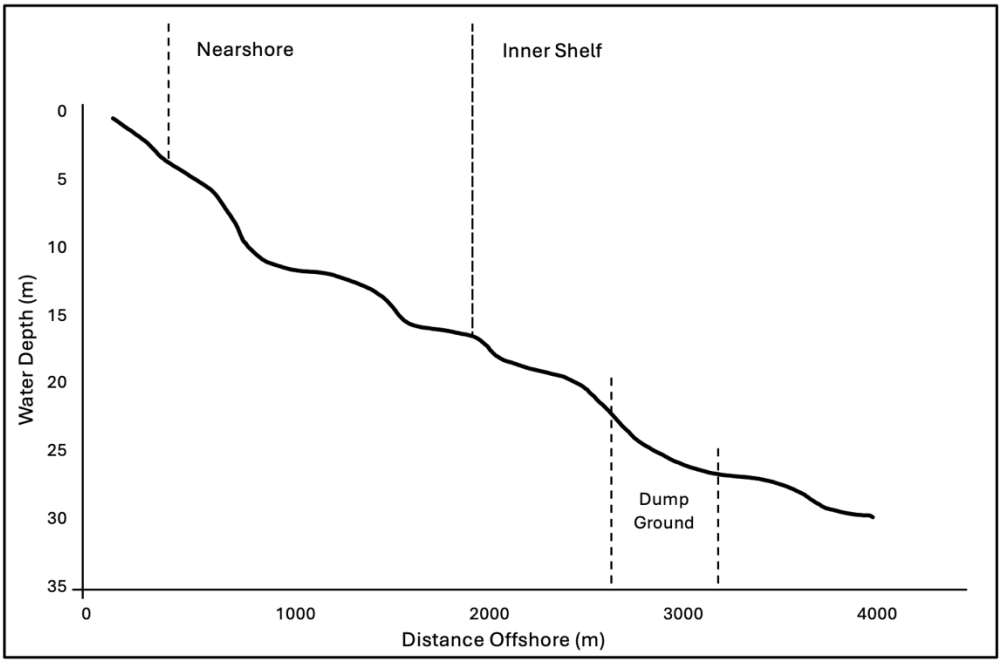

Figure 1.8 A transect across the continental shelf from the beach zone to the inner shelf, highlighting the boundary between the nearshore and inner shelf. It is modified (from Warren, 1992).

Healy et al (1997) found that the sediment composition of the inner shelf disposal ground is predominantly coarse to medium-grained moderately well-sorted sands. Further compositional analysis of the dredged sediments on the inner shelf environment found that the composition was >90% fine to medium sand, 1-10% gravel and shell fragments and <0.5% mud (Moon et al., 1994). A study performed by Michels & Healy (1999) found that the sediment composition in the dredge zone before the commencement of disposal showed that fine material ranged from 0.125 mm (fine sand) to 0.750 mm (coarse sand) with a mean of 0.320 mm (medium sand), and coarser material ranged from 0.350 mm (medium sand) – 1.0 mm (very coarse sand) with a mean size of 0.600 mm (coarse sand). It was also found that the sediments of the inner shelf site were moderately to very well sorted with a clay content of ~1% (Michels & Healy, 1999), aligning with the prior study conducted by Moon et al (1994). Further investigation into the overall silt content within the study area by Foster (1992) found that the silt content of the inner shelf sediments before sediment disposal ranged from <0.1% to 10.8%, with a mean silt content of 1.1%. The disposal site C further inshore (Figure 1.10) is predominantly featureless with few discernible bedforms, small patches of megaripples (λ = 0.8 m) were observed within newly deposited material (Harms, 1989). As sites D and G are further offshore, there is an even smaller likelihood of sediment movement leading to the formation of bedforms (Healy, 1996).

1.4 Dredging

1.4.1 Overview and Impacts

Dredging has been an essential process carried out in harbours and commercial waterways since the 1800s (Elsaeed, 2021). It is increasingly required in ports and harbours because of the ever-growing size of vessels passing through waterways, which requires deeper and wider channels (Rees, 1980). Dredging is an essential industry that has faced numerous challenges, including keeping up with the demand for dredging while limiting environmental degradation resulting from the removal and emplacement of sediment. There are three main concerns surrounding the dredging process as outlined by Riddell (2000):

1) contamination of sediments,

2) water turbidity, and

3) disposal of dredge spoil.

The process of dredging does not cause contamination of the sediments within the harbour. Rather, it is typically caused by the shipping industry, runoff from agricultural land, and other anthropogenic influences. The major impact that dredging has on the contamination of waterways is through the resuspension of sediments during uplifting (Moreira et al., 2021). Turbidity is another main concern with dredging. The motion of dredging sediment means there is a potential for sediment to become loosened, lifted and suspended in the water column (Smith & Friedrichs, 2011). Figure 1.9 highlights how dredged material is released from a hopper. As the dredged material is released it descends through the water column as a fluid-like jet (Truitt, 1988). Depending on the cohesive structure of the sediment, there may be clumps of sediment within the jet, and an increase in biological activity in the dredged material leads to an increase in sediment cohesion. Turbulent forces within the water column may also lead to water being entrained in the jet of material (Truitt, 1988).

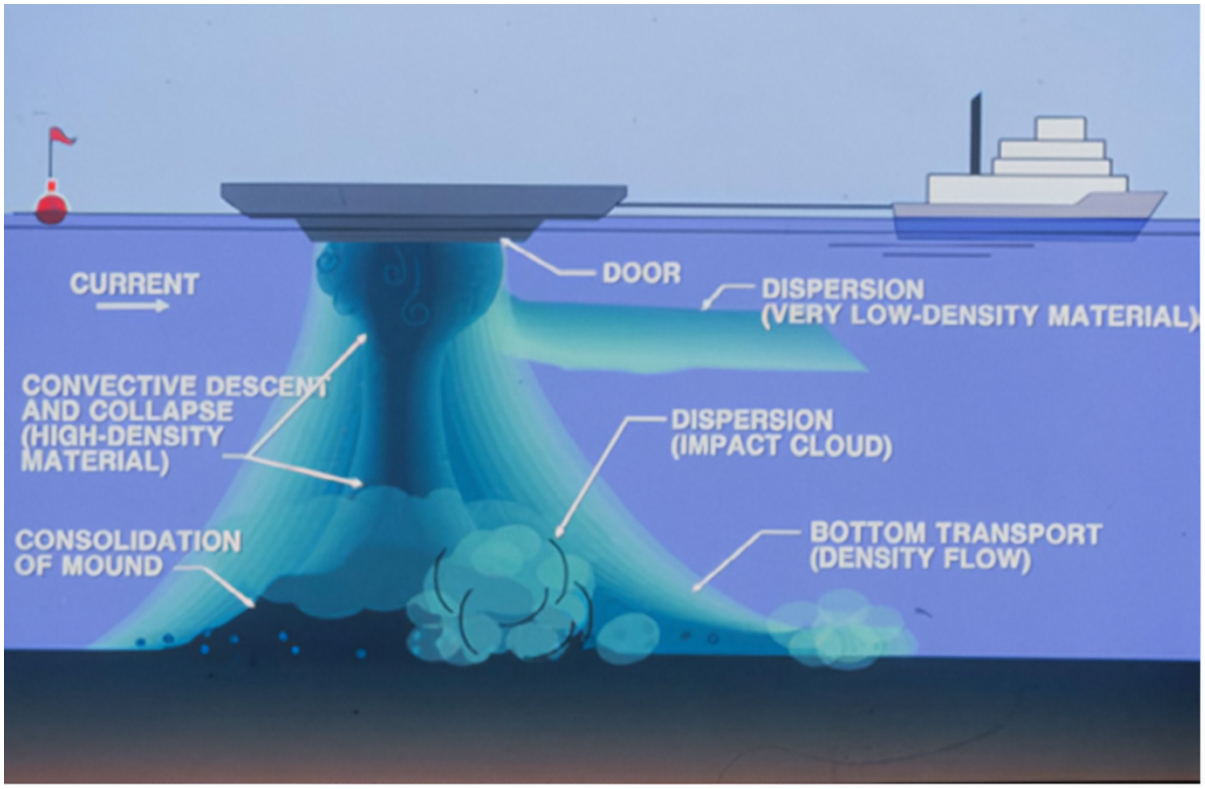

Figure 1.9- Dredge spoil descent (from US Army Corps of Engineers, 2015).

Suspended sediments caused by dredge plumes and the ability of these plumes to negatively affect marine flora and fauna is one of the key issues associated with the dredging of harbours (van Maren et al, 2015; van Rijn, 2019). Suspended sediments within the water column can reduce light availability, thereby reducing the ability of photosynthetic organisms to sustain themselves, as well as reducing visibility and feeding ability for a range of benthic organisms (Todd et al., 2015). The impacts that dredge spoil has on the environment can be divided into two main categories, short-term/acute impacts and long-term/chronic impacts. (Boyd et al., 1972; Rees, 1980; Warren, 1992). Short-term impacts include an increase in turbidity, a decrease in dissolved oxygen content, smothering of benthic organisms, and temporary inhibition of migratory routes of fish. Long-term impacts include, changes in bottom topography and composition of sediments, changes in species diversity, bioaccumulation of contaminants, and abrasion of filter-feeding organisms (Boyd et al., 1972; Gross & Palmer, 1979; Kester et al., 1981; National Research Council, 1985; Rees, 1980; Warren, 1992).

The disposal of dredged material is a concern with dredging outlined by Riddell (2000), which is increasingly of interest because of the implications for environmental management of human activities. However, dredge sediment can be seen as a resource, rather than a waste, by repurposing the large quantities of sediment removed routinely during maintenance dredging and utilising it for beach renourishment or land reclamation. This is, however, restricted to the

coarser-grained fraction; finer-grained material is often not used for beach reclamation. Dredged deposition is generally either done by building a sediment mound or spreading the spoil in a thin layer over a wider area (van Rijn, 2019).

Dredging has significant cultural implications within New Zealand which need to be considered when undertaking the dredging and spoiling processes. The Māori perspective of the world encompasses a biological-cultural perspective that positions humans within nature and emphasises ways in which cultural understandings and intergenerational connections between people and their biophysical context assist in the retention and protection of biodiversity and sustainability (Paul-Burke, 2016). The ocean is deeply rooted in the Māori worldview. It is an essential source of food and resources, as well as a place of ritual and spiritual connection (Jones, 2022). Tangata Whenua of Tauranga Moana include Ngāti Ranginui, Ngāi Te Rangi, and Ngāti Pūkenga (Bay of Plenty Regional Council, 2019), and these groups have been established in the region for generations. Preserving and sustaining the natural environment and features of Tauranga Harbour and the surrounding areas is of vital cultural and environmental importance to these groups.

1.4.2 Dredging Operations at the Port of Tauranga

The Port of Tauranga has always required regular removal of sediments through routine dredging operations to facilitate the deepening and widening of shipping channels. The majority of the sediments removed from the shipping channels are used for beach renourishment efforts at Mount Maunganui, Pilot Bay and Whareora Marae, dredge spoil is also commonly used for land reclamation at Sulphur Point, or is deposited on the inner shelf located off Mount Maunganui, see Figure 1.10 (Foster, 1992).

The dredging operations at Tauranga are undertaken with a dredger known as the “Pelican”. The Pelican is a split hopper trailing suction dredge that holds a capacity of 965 m^3 of sediments. It has been proven that the inner shelf dredge disposal zone is a suitable location to dispose of sediment with a significant silt and clay content, as these materials alongside medium and coarse-grained sediments as these materials have not been found to move during fine weather conditions (Michels and Healy, 1999; Foster, 1992).

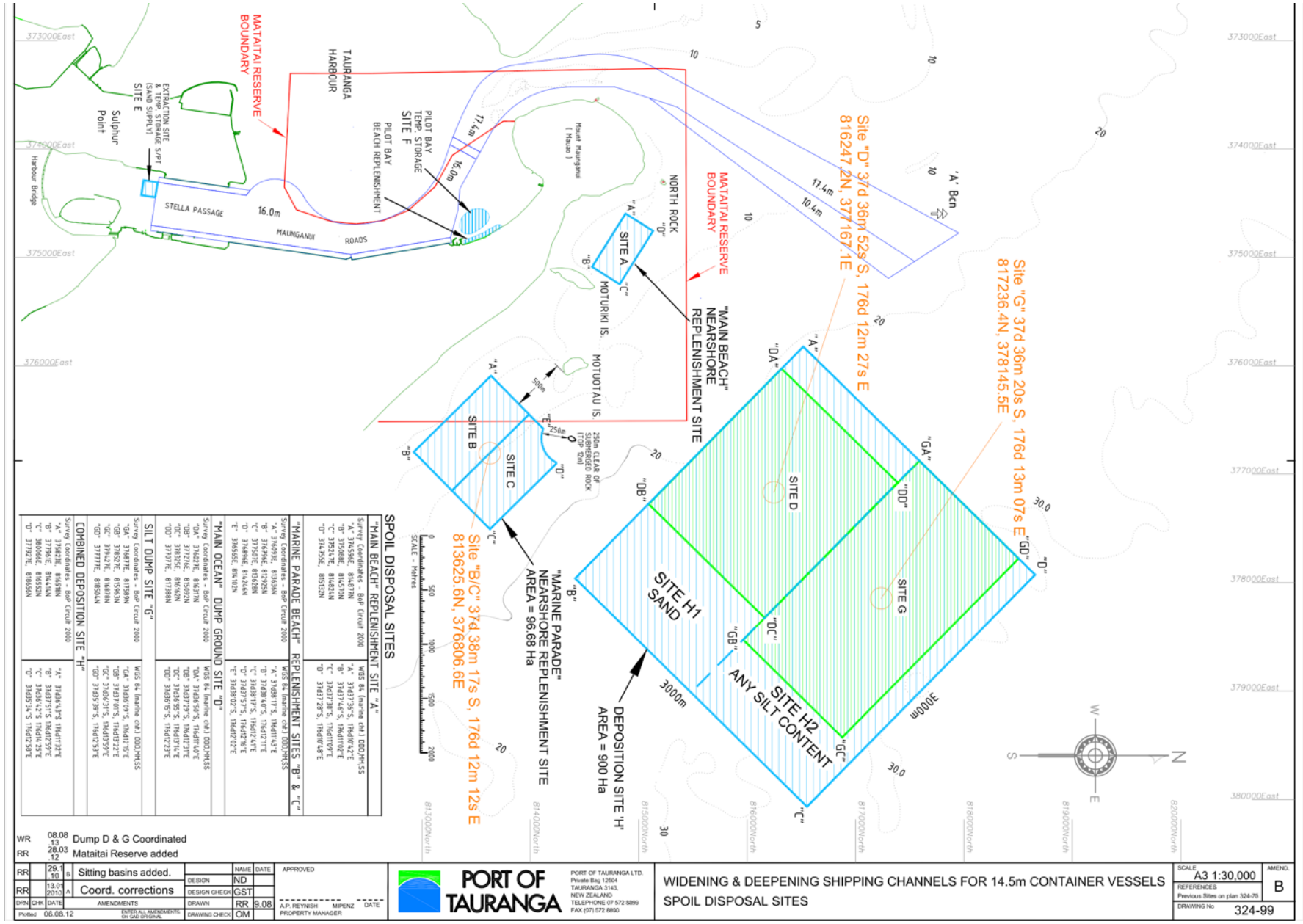

Figure 1.10: location of dredge disposal sites as proposed in 2012 by the Ports of Tauranga concerning the widening and deepening of shipping channels to accommodate larger container vessels. Highlighting the inner shelf dredge sites G, D, H1 and H2.

The most recent capital dredging programme occurred between 2015 and 2016 which allowed for the shipping channels to be widened and deepened from 12.9 m to 14.5 m inside the harbour and 15.8 m outside of the harbour (Port of Tauranga, 2016). Following the completion of the 2015-16 capital dredging programme the shoreline was monitored at Matakana Island (Panepane Point) to establish whether dredging was responsible for the erosion of the shoreline. Studies found that there have been no noticeable changes to the Matakana Island shoreline, nor are there any issues that require mitigation. It was found that the impacts that dredging had on the shoreline were no more significant than the impact natural erosive forces would have in the long term (De Lange & Moon, 2017).

1.4.4 Nature of Dredged Harbour Sediments

Seismic and core data have shown that the present-day ebb-tidal sediments is composed of a thin layer of Holocene sediments over a significantly thicker layer of Pleistocene volcaniclastic sediments (De Lange et al., 2015). Seaward of the volcanic ignimbrite deposits is a range of Quaternary alluvial valley-filling deposits with areas of estuarine and marine sediments. The basin has since been filled with up to 150 m of unconsolidated or weakly consolidated terrestrial, estuarine and marine sediments as identified through studies of boreholes and outcrop sections (MacPherson et al., 2017).

Analysis of the quantitative rates of net transportation of sediment transport near the Tauranga inlet indicates that there is a high proportion of coarse-grained sediments in this area, reflecting the high-energy nature of this environment (Davies-Colley, 1976). A study by Dahm & Healy (1980) determined both the Cutter and Maunganui channels have sediment predominantly consisting of moderate to well-sorted fine sands with a high proportion of pumice. The entrance channel, which is a more morphologically complex area, is composed of sediments grading from very coarse, poorly sorted gravelly sands on the western side, to very well-sorted fine sands on the eastern side (Dahm & Healy, 1980). Overall sediment from the harbour that are dredged consist of approximately 60% fine sand, and 25% medium sand, whereas the overall dredged material from the ebb-tidal delta channel consisted of approximately 25% fine sand, 50% medium sand, and 20% coarse sand material (Dahm & Healy, 1980).

More recent studies by Brannigan (2009) analysed surficial sedimentation patterns. Showing the majority of sediment from the dredged areas is dominated by over 50% medium-

grained sands and shelly sediments. Thus showing that the bulk composition of the sediment has remained predominantly medium-grained since the earlier studies were undertaken in 1980.

1.4.5 Dredge Sediment Composition on the Inner Shelf

Warren (1992) collected 9 samples within the current study area, and 6 samples outside of the current study area (Figure 1.11). Samples were collected before and after dredging occurred to create a baseline of sediment grain size pre and post-dredging. These provide a basis for comparison to future work on dredge sediment deposition on the inner shelf.

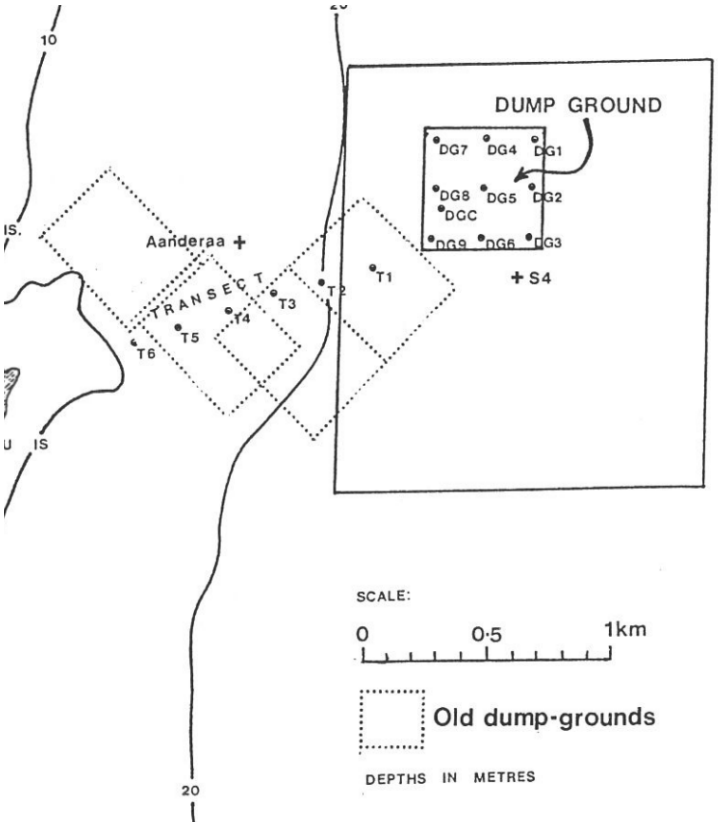

Figure 1.11- Locations of the sites sampled by Warren (1992). Transect T1-T6 are located outside of the current study area, sample locations DG1-DG9 are located within the current study area.

Table 1.1 provides a generalised summary of the findings from Warren (1992). The data represents the combination of samples taken within the current dredge spoil disposal site (DG1-9(Figure 1.11)) as well as the transect directly outside of the study area (T1-6 (Figure 1.12)). More specific data from the current study area is summarised in Table 1.2. This table highlights samples taken before and after dredging. The study area was sampled twice before dredging in October and November of 1990, samples were re-collected following dredging in February, April and June of 1991 to collect multiple comparable datasets.

Table 1.1- Summary of particle size analysis results using sieve data and the RSA statistical analysis package from each sample site in the harbour and the inner shelf dredge spoil disposal site, adapted from (Warren et al., 1992).

Sample Site	**% Gravel**	**% Sand**	**% Mud**	**Textural Description**	**Dominant Sand**	**Mean ϕ Size**
Pre-disposal Shelf *n = 6*	0.3-14	86-99	<0.5	Slightly gravelly sand	Fine sand	1.88
Harbour Sed. *n = 24*	0-40	58-99	0.5-8	Slightly gravelly sand	Medium sand	1.68
Hopper Sed. *n =4*	0.6-9	91-99	<0.5	Slightly gravelly sand	Medium sand	1.41
Post Disposal *n = 9*	0.6-7	93-99	<0.5	Slightly gravelly sand	Medium sand	1.29

Table 1.2- Summary of the results of particle size analysis using sieve data and the RSA statistical analysis package from each sample site within the dredge spoil disposal site modified from (Warren., 1991).

Sample Site	**Pre Disposal Oct 1990** **Mean ϕ Size**	**Pre Disposal Nov 1991** **Mean ϕ Size**	**Feb 1991** **Mean ϕ Size**	**April 1991** **Mean ϕ Size**	**June 1991** **Mean ϕ Size**
DG1	2.16		1.24	1.39	1.15
DG2	1.39	2.41	1.65	1.61	
DG3	1.42	1.99	1.56	1.64	0.51
DG4	1.45		0.58	0.65	
DG5	2.12	1.99	1.02	1.47	1.1
DG6	2.32	1.95	1.14	1.23	
DG7	1.53		1.32	1.93	
DG8	0.36	0.91	1.03		1.69
DG9	1.79	2.05	1.26	1.91	

This suggests that there has been a general increase in grain sizes, with the dominant sand and the mean grain size both becoming coarser following the disposal of dredge spoil (Warren, 1992). The minor differentiation in grain size between the pre-dredge and post-dredge sediments indicates that the dredged sediments are compatible with the natural inner shelf sediments (Foster, 1992; Michels & Healy, 1999; Moon et al., 1994; Warren et al., 1991; Warren, 1992).

1.4.3 Impacts of Dredging on the Tauranga Shelf

The inner shelf of Tauranga Harbour receives a large amount of dredge sediment spoil that is not utilized for land reclamation or beach renourishment. The current inner shelf dredge disposal sites have been chosen for a variety of reasons, including that there is no significant impact on the benthic ecology, no impact on tangata whenua, no risks of muddy sediment becoming transported to surrounding beaches, and no impacts on surrounding recreational areas. Furthermore, it is essential that the dredged sediment has a similar composition to the pre-existing sediment on the shelf disposal site (Michels & Healy, 1999).

Suspended sediment concentration was measured at the dredge spoil disposal site over 6 months (Moon et al., 1994). Results showed that sediment consisted of >90% fine to medium sand, 1-10% gravel and shell fragments and <0.5% mud (Moon et al., 1994). The consolidation of these sediments following the disposal of the plumes is expected to be very rapid due to the high content of coarse material. The composition of the sediments within the dredged areas is of similar textural composition to the sediments in the inner shelf dredge spoil disposal site (Cussioli et al., 2015). Background levels of Total Suspended Sediments (TSS) of 7-9 mg l^{-1} were recorded, whereas TSS during dredging was measured at 9-15 mg l^{-1} near the surface (0-2 m depth), and a TSS measurement of 24-70 mg l^{-1} at the bottom (10-12 m depth). Proving that the levels of TSS returned to the background levels within 1 hour or less of dredging, and levels of TSS of 70 mg l^{-1} and over are only harmful to flora and fauna if ongoing for over 1 hour (Cussioli et al., 2015). The speed at which the sediment settles post-dredge (<1 hour) aligns with the expectations set in the 1994 study laid out by Moon et al (1994).

Sediment is primarily transported via large waves and currents associated with storm events (Matthews, 1997). It has not been proven that sediment is transported during periods of ‘average’ conditions, and therefore, the potential for sediment to travel back onshore from the disposal site is considered to be low (Foster, 1992; Michels & Healy, 1999). In a survey of the

morphological changes of the disposal ground used during the 1991-1992 capital dredging project, bathymetric transects were analysed before, during, and after dredging. The data showed that aside from the material that was deposited during the disposal of dredge sediment, there was no notable change in the movement of the spoil mound (Matthews, 1997).

1.5 Study Aims

The primary aim of this study is to establish if any changes to the dredge spoil location on the inner shelf have occurred since the 1992 capital dredging programme carried out by the Port of Tauranga. This work will update our knowledge and set a new baseline for further sedimentary and oceanographic investigations regarding the dispersal of sediments from the inner shelf environment. This will be achieved by accomplishing the following objectives:

1) Mapping surface sediment distribution in the study area (Figure 1.1 C).
2) Examining vibracores to establish a shallow stratigraphy.
3) Mapping the thickness and structure of that shallow stratigraphy using sub-bottom profiles/shallow seismic surveys.

The seismic survey will identify the thickness and distribution of the dredge spoil mound. The sedimentological survey will determine the mineral grain size and organic matter content of the dredge spoil to determine if there has been any changes in the composition of the spoil mound. The collection of vibracores will determine the bedforms and thickness of the subsurface layers of the spoil mound. Collectively the data collected in this study will identify if there have been any changes in the spoil mound since the previous investigations were carried out in 1992, and assess the potential for sediment resuspension and transport.

1.6 References

Bagnold, A. (1946). Motion of waves in shallow water. Interaction between waves and sand bottoms. Proceedings of the Royal Society of London. Series A. Mathematical and Physical Sciences, 187(1008), 1–18. https://doi.org/10.1098/rspa.1946.0062

Ballance, P. (2009). New Zealand geology: an illustrated guide (Vol. 148). Geoscience Society of New Zealand.

Bay of Plenty Regional Council. (2019). Tauranga Moana State of the Environment Report 2019.

Bostock, H., Jenkins, C., Mackay, K., Carter, L., Nodder, S., Orpin, A., Pallentin, A., & Wysoczanski, R. (2019). Distribution of surficial sediments in the ocean around New Zealand/Aotearoa. Part B: continental shelf. New Zealand Journal of Geology and Geophysics, 62(1), 24–45. https://doi.org/10.1080/00288306.2018.1523199

Boyd, M. B., Saucier, R. T., Keely, J. W., Montgomery, R. L., & Brown, R. D. (1972). Disposal of Dredge Spoil: Problem Identification and Assessment and Research Program Development.

Bradshaw, B. E. (1991). Nearshore and inner shelf sedimentation on the East Coromandel coast, New Zealand [Unpublished DPhil Thesis]. University of Waikato .

Carter, L., & Heath, R. A. (1975). Roles of mean circulation, tides, and waves in transport of bottom sediment on the New Zealand continental shelf. New Zealand Journal of Marine and Freshwater Research, 9, 423–448.

Clement, A. J. H., Whitehouse, P. L., & Sloss, C. R. (2016). An examination of spatial variability in the timing and magnitude of Holocene relative sea-level changes in the New Zealand archipelago. Quaternary Science Reviews, 131, 73–101. https://doi.org/10.1016/j.quascirev.2015.09.025

Collins, M. B., & Balson, P. S. (2007). Coastal and shelf sediment transport: an introduction. Geological Society of London, Special Publications, 274, 1–5.

Cowell, P. J., & Nielsen, P. (1984). Predictions of sand movement on the south Sydney inner-continental shelf, South-east Australia.

Csanady, G. T. (1988). Ocean Currents Over the Continental Slope. In B. Saltzman (Ed.), Advances in Geophysics (Vol. 30, pp. 95–203). https://doi.org/10.1016/S0065-2687(08)60421-5

Cussioli, M. C., Bryan, K. R., Pilditch, C. A., & De Lange, W. P. (2015). Dispersal of dredging plumes in Tauranga Harbour, New Zealand: A field study.

Dahm, J., & Healy, T. R. (1980). A Study of Dredge Spoil Dispersion off the Entrance to the Tauranga Harbour- A Report to the Bay of Plenty Harbour Board.

Davies-Colley, R. (1976). Some Field Techniques Used in a Study of Tauranga Harbour. Proceedings (New Zealand Ecological Society), 23, 33–37.

Davies-Colley, R. J., & Healy, T. R. (1978a). Sediment and hydrodynamics of the Tauranga entrance to Tauranga harbour. New Zealand Journal of Marine and Freshwater Research, 12(3), 225–236. https://doi.org/10.1080/00288330.1978.9515747

Davies-Colley, R. J., & Healy, T. R. (1978b). Sediment transport near the Tauranga entrance to Tauranga Harbour. New Zealand Journal of Marine and Freshwater Research, 12(3), 237–243. https://doi.org/10.1080/00288330.1978.9515748

Davis, R. A. (1987). Oceanography an Introduction to the Marine Environment. Wm. C Brown Publishers.

Davis, R. A. (1991). Morphodynamics of Wave and Tide-dominated Coasts. In Coastal Engineering: Climate for Change; Proceedings of 10th Australasian Conference on Coastal and Ocean Engineering (pp. 18–21). Water Quality Centre, DSIR Marine and Freshwater.

Davis, R. A., & Healy, T. R. (1993). Holocene coastal depositional sequences on a tectonically active setting: southeastern Tauranga Harbour, New Zealand. Sedimentary Geology, 84(1–4), 57–69. https://doi.org/10.1016/0037-0738(93)90045-7

De Lange, W., Moon, V., & Johnstone, R. (2015). Evolution of the Tauranga Harbour Entrance: influences of tsunami, flooding and dredging. Australasian Coasts & Ports Conference 2015.

De Lange, W. P., & Moon, V. G. (2017). Shoreline changes for southeastern Matakana Island (Panepane Point) following capital dredging (2015-16). Environmental Research Institute Report No.95. Client report prepared for Port of Tauranga.

Dell, P. M., Healy, T. R., & Nelson, C. S. (1985). A Preliminary Investigation of the Sediments on the Eastern Coromandel Inner Shelf and the Implications for Across-Shelf Sediment Transport. 1985 Australasian Conference on Coastal and Ocean Engineering, 475–483.

Dougherty, A. J., & Dickson, M. E. (2012). Sea level and storm control on the evolution of a chenier plain, Firth of Thames, New Zealand. Marine Geology, 307–310, 58–72. https://doi.org/10.1016/j.margeo.2012.03.003

Elsaeed Gamal H. (2021). The Impact of Dredging on Coastal Environments. Australian Journal of Basic and Applied Sciences, 5(2), 74–81.

Foster, D. M. (1992). Environmental Impacts of Recent Dredging and Inner Shelf Spoil Disposal at Tauranga. University of Waikato .

Gross, M. G. (1972). Oceanography, A View of the Earth (7th ed.). Englewood Cliffs: Prentice Hill.

Gross, M. G., & Palmer, H. D. (1979). Waste Disposal and Dredging Activities: The Geological Perspective. In Ocean Dumping and Marine Pollution. Dowden, Hutchinson and Ross inc.

Grundvåg, S., Jelby, M. E., Olaussen, S., & Śliwińska, K. K. (2021). The role of shelf morphology on storm-bed variability and stratigraphic architecture, Lower Cretaceous, Svalbard. Sedimentology, 68(1), 196–237. https://doi.org/10.1111/sed.12791

Harms, C. (1989). Dredge Spoil Dispersion from an Inner Shelf Dump-Mound. University of Waikato .

Harris, C. K., & Wiberg, P. (2002). Across-shelf sediment transport: Interactions between suspended sediment and bed sediment. Journal of Geophysical Research: Oceans, 107(C1). https://doi.org/10.1029/2000JC000634

Healy, J. M., De Lange, W. P., & Mathew, J. (1997). Monitoring of a Large Inner Shelf Dump Mound Offshore Tauranga, New Zealand. Combined Australasian Coastal Engineering and Ports Conference.

Healy, T. (1996). Review of Capital Dredging Impacts for the Port of Tauranga LTD 1992 Major Channel Deepening and Widening Programme.

Healy, T., McCabe, B., Grace, R., & Harms, C. (1988). Environmental Assessment Programme for Tauranga Harbour Dredging and Inner Shelf Spoil Dumping.

Healy, T. R. (1977). Progradation at the Entrance, Tauranga Harbour, Bay of Plenty. New Zealand Geographer, 33(2), 90–91. https://doi.org/10.1111/j.1745-7939.1977.tb00858.x

Healy, T., Thompson, G., Mathew, J., Pilditch, C., & Tian, F. (1998). Assessment of Environmental Effects for Port of Tauranga LTD. Maintenance Dredging and Disposal.

Heath, R. A. (1975). Oceanic Circulation off the East Coast of New Zealand. New Zealand Oceanographic Institute.

Hicks, D. M., Gomez, B., & Trustrum, N. A. (2000). Erosion thresholds and suspended sediment yields, Waipaoa River Basin, New Zealand. Water Resources Research, 36(4), 1129–1142.

Hjulström, F. (1935). Studies of the morphological activity of rivers as illustrated by the river Fyris . Uppsala : Almqvist & Wiksell.

Jones, H. (2022). Environmentalism for the environment's sake: Towards an understanding of the influence of the Maori worldview on Western environmental management perspectives in Aotearoa New Zealand through a lens of nature connectivity [Master of Environment and Society (MEnvSoc)]. University of Waikato.

Kester, D. R., Ketchum, B. H., & Park, P. K. (1981). Future Prospects of Ocean Dumping. In Ocean Dumping of Industrial Wastes (pp. 505–517). Springer US. https://doi.org/10.1007/978-1-4684-3905-2_26

Keylock, C. (2004). Reviewing the Hjulström curve. 16–20.

Kim, S. (2019). Storm Surges. In Encyclopedia of Ocean Sciences (pp. 663–671). Elsevier. https://doi.org/10.1016/B978-0-12-409548-9.10849-8

Kohn, B. P., & Glasby, G. P. (1978). Tephra distribution and sedimentation rates m the Bay of Plenty, New Zealand. New Zealand Journal of Geology and Geophysics, 21(1), 49–70. https://doi.org/10.1080/00288306.1978.10420721

Komar, P. (1976). Beach Processes and Sedimentation. Prentice Hall.

Kombiadou, K., & Yannis, N. (2013). Modelling Cohesive Sediment Dynamics in the Marine Environment. In Sediment Transport Processes and Their Modelling Applications. InTech. https://doi.org/10.5772/51061

Krüger, J. C., & Healy, T. R. (2006). Mapping the Morphology of a Dredged Ebb Tidal Delta, Tauranga Harbour, New Zealand. Journal of Coastal Research, 223, 720–727. https://doi.org/10.2112/03-0117.1

Kulgemeyer, T., von Dobeneck, T., Müller, H., Bryan, K. R., de Lange, W. P., & Battershill, C. N. (2016). Lithofacies distribution and sediment dynamics on a storm-dominated shelf from combined photographic, acoustic and sedimentological profiling methods (Bay of Plenty, New Zealand). Marine Geology, 376, 158–174. https://doi.org/10.1016/j.margeo.2016.03.005

Macky, G. H., Latimer, G. J., & Smith, R. K. (1995). Wave climate of the western Bay of Plenty, New Zealand, 1991-93. New Zealand Journal of Marine and Freshwater Research, 29, 311–327.

MacPherson, D., Fox, B. R. S., & de Lange, W. P. (2017). Holocene evolution of the southern Tauranga Harbour. New Zealand Journal of Geology and Geophysics, 60(4), 392–409. https://doi.org/10.1080/00288306.2017.1360917

Matthews, J. (1997). Morphologic changes of the tidal deltas and an inner shelf dump ground from large scale dredging and dumping, Tauranga, New Zealand. University of Waikato .

Mazumder, R. (2003). Sediment transport, aqueous bedform stability and morphodynamics under unidirectional current: a brief overview. Journal of African Earth Sciences, 36(1–2), 1–14. https://doi.org/10.1016/S0899-5362(03)00018-6

Michels, K. H., & Healy, T. R. (1999). Evaluation of an Inner Shelf Site off Tauranga Harbour, New Zealand, for disposal of Muddy-Sandy Dredged Sediments. Journal of Coastal Research, 3, 830–838.

Miller, M. C., & Komar, P. D. (1980a). A field investigation of the relationship between oscillatory ripple spacing and near-bottom water orbital motions. Journal of Sedimentary Petrology, 50, 183–191.

Miller, M. C., & Komar, P. D. (1980b). Oscillation sand ripples generated by laboratory apparatus. Journal of Sedimentary Petrology, 50, 173–182.

Montaño, M. M., Suanda, S. H., & Souza, J. M. A. C. de. (2023). Modelled coastal circulation and Lagrangian statistics from a large coastal embayment: The case of Bay of Plenty, Aotearoa New Zealand. Estuarine, Coastal and Shelf Science, 281. https://doi.org/10.1016/j.ecss.2023.108212

Montano Orozco, M. M. (2023). Hydrodynamics and coastal dispersion from the Bay of Plenty, Aotearoa, New Zealand: A 25-year numerical modelling perspective [Doctor of Philosophy]. University of Otago.

Moon, V., de Lange, W., Warren, S., & Healy, T. (1994). Post-Disposal Behavior of Sandy Dredged Material at an Open-Water, Inner Shelf Disposal Site. Journal of Coastal Research, 10(3), 651–662.

Moreira, L. B., Braga Castro, Í., Fillmann, G., Peres, T. F., Cavalcante Belmino, I. K., Sasaki, S. T., Taniguchi, S., Bícego, M. C., Marins, R. V., Drude de Lacerda, L., Costa-Lotufo, L. V., & de Souza Abessa, D. M. (2021). Dredging impacts on the toxicity and development of sediment quality values in a semi-arid region (Ceará state, NE Brazil). Environmental Research, 193, 110525. https://doi.org/10.1016/j.envres.2020.110525

Mouton, M. W. (1952). The Continental Shelf. Springer Netherlands. https://doi.org/10.1007/978-94-017-5966-3

National Research Council. (1985). Dredging Coastal Ports An Assessment of the Issues, 212 p.

Nittrouer, C. A., & Wright, L. D. (1994). Transport of particles across continental shelves. Reviews of Geophysics, 32(1), 85–113. https://doi.org/10.1029/93RG02603

NIWA. (2024). Waves. Https://Niwa.Co.Nz/Hazards/Waves.

Paul-Burke, K. (2016). Te hekenga o te tuna: Action Plan for the enhancement and restoration of Tuna in the Rangitaiki Catchment. Report prepared for the Rangitaiki River Forum.

Pickrill, R. A., & Mitchell, J. S. (1979). Ocean wave characteristics around New Zealand. New Zealand Journal of Marine and Freshwater Research, 13(4), 501–520. https://doi.org/10.1080/00288330.1979.9515827

Port of Tauranga. (2011). Location and Transport Links, Https://www.port-tauranga.co.nz/wp-content/uploads/Location-and-Transport-Links.pdf, 2-6

Port of Tauranga. (2016). Tauranga dredging under way - Port of Tauranga Limited. Https://Www.Port-Tauranga.Co.Nz/News/Tauranga-Dredging-under-Way/#:~:Text=Danish%20dredging%20company%2C%20Rohde%20Nielsen,15.8%20metres%20outside%20the%20harbour.

Port of Tauranga. (2020). Port History to Modern Day, Https://www.port-tauranga.co.nz/wp-content/uploads/Our-Port-History-to-Modern-Day.pdf, 2-4

Propp, M. V., Odintsov, V. A., Propp, L. N., & Shulkin, V. M. (1994). Marine sediments in a region of recent volcanic activity in the Bay of Plenty, New Zealand. Journal of Marine and Freshwater Research, 28, 219–226.

Rees, C. P. (1980). Environmental Impact of Dredging Operations. Proceedings of the Third International Symposium on Dredging Technology, 373.

Reineck, H.-E., & Singh, I. B. (1980). Depositional Sedimentary Environments . Springer-Verlag, 543 p.

Roemmich, D., & Sutton, P. (1998). The mean and variability of ocean circulation past northern New Zealand: Determining the representativeness of hydrographic climatologies. Journal of Geophysical Research: Oceans, 103, 13041–13054.

Sleath, J. F. A. (1986). Sea Bed Mechanics. Journal of Fluid Mechanics, 163, 501–503. https://doi.org/10.1017/S0022112086232401

Smith, S. J., & Friedrichs, C. T. (2011). Size and settling velocities of cohesive flocs and suspended sediment aggregates in a trailing suction hopper dredge plume. Continental Shelf Research, 31(10), 50–63. https://doi.org/10.1016/j.csr.2010.04.002

Stanton, B. R., Goring, D. G., & Bell, R. G. (2001). Observed and modelled tidal currents in the New Zealand region. New Zealand Journal of Marine and Freshwater Research, 35(2), 397–415. https://doi.org/10.1080/00288330.2001.9517010

Suter, J. R. (2006). Facies Models Revisited: Clastic Shelves. In H. W. Posamentier & R. G. Walker (Eds.), Facies Models Revisited (4th ed., pp. 339–399). SEPM (Society for Sedimentary Geology).

Todd, V. L. G., Todd, I. B., Gardiner, J. C., Morrin, E. C. N., MacPherson, N. A., DiMarzio, N. A., & Thomsen, F. (2015). A review of impacts of marine dredging activities on marine mammals. ICES Journal of Marine Science, 72(2), 328–340. https://doi.org/10.1093/icesjms/fsu187

Truitt, C. L. (1988). Dredged Material Behaviour During Open-Water Disposal. Journal of Coastal Research, 4(3), 498–497.

US Army Corps of Engineers. (2015). Dredging and Dredged Material Management, 1-53.

van Maren, D. S., van Kessel, T., Cronin, K., & Sittoni, L. (2015). The impact of channel deepening and dredging on estuarine sediment concentration. Continental Shelf Research, 95, 1–14. https://doi.org/10.1016/j.csr.2014.12.010

van Rijn, L. C. (2019). Turbidity due to dredging and dumping of sediments.

Warren, S., Healy, T., Moon, V., & Foster, D. (1991). Aspects of the Geomechanics of Dredge Spoil Disposed of on the Inner Shelf, Tauranga, New Zealand. Coastal Engineering: Climate for Change; Proceedings of 20th Australasian Conference on Coastal and Ocean Engineering, 1991, 128–133.

Warren, S. K. (1992). The Geomechanics and Dispersion of Dredge Spoil Dumped in Open Water on the Inner Shelf, Tauranga, New Zealand [MSc Earth Science]. University of Waikato .

Wright, L. D. (1987). Shelf-surfzone coupling: Diabathic Shoreface Transport. American Society of Civil Engineers, 22-50.

Chapter 2

Sedimentological and Seismic Interpretation

2.1 Introduction

Dredging has been an essential process in harbours and commercial waterways since the 1800s. It is increasingly required in ports and harbours because of the ever-growing size of vessels, which requires deeper and wider channels (Rees, 1980). The process of dredging creates waste material that is usually disposed of by dumping the material into open water in a process known as spoiling, or for use in land reclamation efforts (Gross et al., 1979; Kester et al., 1981). There are three main concerns surrounding the dredging process: (1) contamination of sediments, (2) increased water turbidity, and (3) the issue of where to dispose of the dredge spoil (Riddell, 2000).

Te Awanui (Port of Tauranga) is a natural tidal harbour located within the Bay of Plenty and it is part of one of the largest barrier-enclosed estuaries in New Zealand, spanning an area of 812 km^2. Dredging commenced in the harbour in 1919, but the use of dredge spoil for land reclamation didn't begin until 1965 (Port of Tauranga, 2020). The harbour is the largest port in the country in terms of import-export tonnage, with a total cargo load of 24,698,128 tonnes in 2023 (Port of Tauranga, 2024). Dredged material that is not used for land reclamation is disposed of at a variety of sites offshore, with the majority of the spoil being disposed of on the inner continental shelf adjacent to the harbour.

Previous studies have sought to understand the processes associated with dredge sediment plumes and the potential for sediment resuspension and transport before, during and after routine disposal of dredged material at the disposal sites (Foster et al., 1996; Harms, 1989; Healy et al., 1997; Matthews, 1997; Warren, 1992). The studies found that the sediment on the inner shelf is predominantly fine to medium-grained sand that is unlikely to be subject to resuspension and transport by waves or currents due to the depth of the disposal site and its location 3-4 km offshore. However, there has been a significant amount of additional dredge sediment deposited since these past studies were undertaken. For example, a total of 1,407,300 m^3 of dredged material has been added to sites D/H1 and G/H2 during maintenance dredging operations from August 2000 to July 2023 (Table 2.1).

Table 2.1- Summary of dredge sediment volume in cubic metres deposited within sites D/H1 & G/H2 since August 2000 (R. Johnstone, pers comm., 2024). Table cells coloured black indicate no sediment was deposited during the dredging operation.

	Area D/H1 Main Ocean	Area G/H2 Silt Dump
Aug 2000	106,186	43,241
Aug 2002	35,458	45,332
Jul 2004	8,317	75,393
Jun 2006	3,066	116,543
Dec 2008	49,887	45,320
Jul 2010	6,955	
Jul 2011	13,201	38,691
Sep 2012	52,335	34,400
Sep 2013	68,105	27,678
Oct 2014	47,991	21,775
Sep 2015	12,995	3,404
Jun 2017	58,692	
Oct 2017		2,870
Jul 2018	90,874	22,117
Jun 2019	35,504	6,776
Jul 2020	59,803	8,055
Jul 2021	44,158	7,048
Jul 2022	77,975	41,012
Jul 2023	77,983	20,614

Due to the large volume (1,407,300 m^3) of sediment added to the dredge spoil disposal sites since these previous investigations, it remains unknown if the mound of dredge spoil sediment on the inner shelf has changed in shape or composition. Any potential for sediment redistribution may have negative impacts on benthic communities (van Maren et al., 2015b), such as smothering benthic habitats or attenuating light and negatively affecting the ecosystem (Todd et al, 2015). The Port of Tauranga is supporting this project to evaluate whether the inner shelf conditions are changing through time, which is especially timely given increased public awareness and concerns over anthropogenic impacts on coastal environments. This study, therefore, aims to reassess the sedimentology and stratigraphy of the dredge spoil area to determine if there is potential for sediment movement through time.

2.2 Study Area

Te Awanui Tauranga Harbour is a barrier-enclosed estuarine lagoon. The harbour has a water volume of approximately 455.2 x 10^6 m^3 and occupies an area of around 812 km^2. As the harbour is located within a tidal estuary, there is approximately 290,000,000 x 10^6 kg of water flowing in and out of each end of Matakana Island (Port of Tauranga, 2011). It is estimated that tides force 61% of the water through the main entrance to the estuary at Mount Maunganui, resulting in a tidal range of between 1.65 and 1.98 m. The tidal stream varies from 1.5 m/s during neap tides and 2.57 m/s during spring tides (Port of Tauranga, 2011).

The sediments in the harbour are predominantly sandy in the lower reaches and are sourced from eroded volcanic tephra and ignimbrite that have been reworked on the continental shelf and re-deposited within the harbour following the Holocene rise in sea level (Davies-Colley, 1976). When sediment is dredged from the harbour, that material is deposited on the inner continental shelf, at disposal sites established by the Port of Tauranga known as D/H1 and G/H2 (Figure 2.1). These locations are in water depths ranging from 20 to 40 m. A total of 1,407,300 m^3 of sediment has been added to the inner shelf spoil disposal site since 2000.

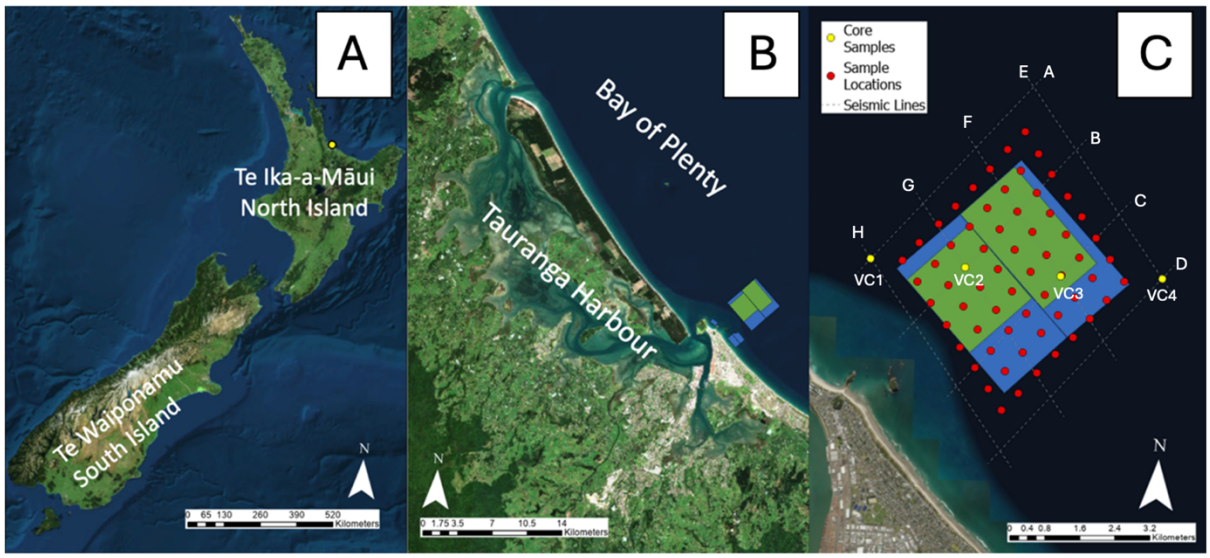

Figure 2.1: A) Location of Te Awanui Tauranga Harbour in Aotearoa New Zealand. (B) Location of the dredge spoil disposal sites offshore of the harbour. (C) Location of sediment grab samples (red dots), vibracores (yellow dots), and shallow seismic surveys (dashed lines).

Sites D/H1 and G/H2 are situated in water depths ranging from 20-40 m, a depth at which Warren (1992) found that fine weather waves do not influence the sea floor. On the inner shelf, waves move northeasterly and have mean amplitudes of 0.5 – 1.5 m (Harms, 1989). In the nearshore realm <20 m depth, landward of the disposal sites, surface sediments are predominantly featureless to rippled fine-grained sand. Further offshore >20 m depth this transitions to medium and coarse-grained sand displaying patches of ripples and mega-ripples within an otherwise primarily featureless seafloor (Warren, 1992). The combination of wave height and current speed ($0.1 m.s^{-1}$) leads to minimal movement of sediment on the shelf during periods of fair weather conditions (Warren, 1992).

2.3 Methods

Data for this study was collected between August 2023 and February 2024. These included: (1) shallow seismic/sub-bottom profile surveys, (2) vibracores, and (3) surface sediment samples (Figure 2.1 C).

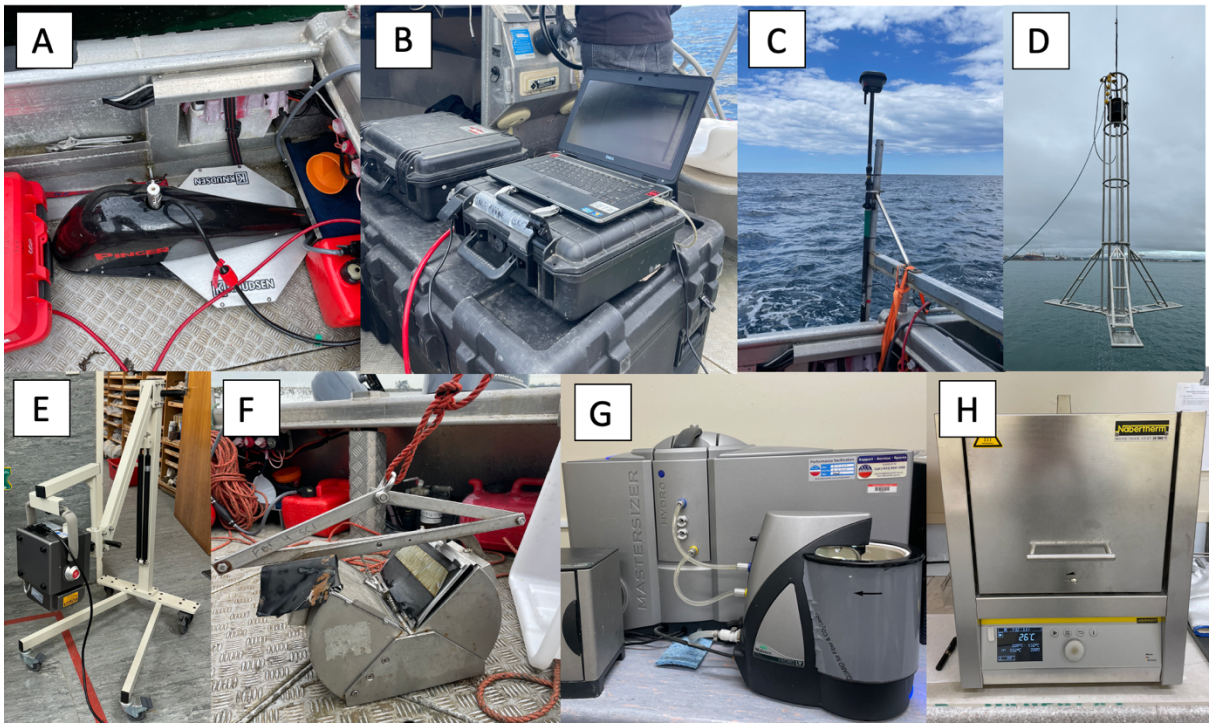

Figure 2.2- Field and laboratory equipment used in the study. (A) Wet end of Knudsen Pinger sub bottom profiler. (B) Dry end of the Knudsen Pinger. (C) Leica GPS, used alongside the Knudsen Pinger. (D) Vibracorer. (E) MX Cubex 50 x-ray for imaging sediment cores.(F) Ponar dredge grab sampler. (G) Mastersizer® particle sizer. (H) Blast furnace for determining loss on ignition.

2.3.1 Seismic Surveys

A total of 8 seismic lines were recorded (Appendix D1), spanning a combined length of 39.36 km (Figure 2.1C). Seismic surveys were collected using a Knudsen Pinger CHIRP sub-bottom profiler, operating using a 3.5 kHz transducer (Figure 2.2A). A Leica real-time GPS (Figure 2.2 C) unit provided spatial data for the seismic lines. Data processing assumed a water velocity of 1480 m s^{-1}. Seismic datasets were interpreted using the Petrel E&P Platform.

2.3.2 Vibracores

Four vibracores (VC1-VC4) were collected from the study area (Figure 2.1C). A tower-mounted corer was deployed using a barge-mounted crane provided by the Port of Tauranga

(Figure 2.2D). Coring used 5 m aluminium tubes with an inner diameter of 80 mm. Upon collection of cores, they were capped and bagged to preserve moisture and prevent sediment loss. It is estimated that sediment compaction may be up to 30%. In the lab, cores were x-rayed with an MX Cubex 50 x-ray source and Cannon Flat Panel x-ray detector (Figure 2.2E), cut in half, and subsampled at 5 cm intervals for grain size and LOI analyses. Finally, cores were logged for their sedimentological features, including grain size and physical structures.

2.3.3 Surface Sediment Samples

Sixty-four surface sediment samples were collected along eight transects inside and outside the dredge spoil disposal area. Each transect consisted of eight samples spaced approximately 570 m apart (Figure 2.1C). Samples were collected with a ponar-style grab sampler (Figure 2.2F), in water depths ranging from 17 m to 33.9 m.

Two types of analysis were undertaken on the surface sediment samples, as well as vibracore sub-samples: 1) grain size, and 2) loss on ignition. Before analysis samples were dried at 30° C for 24 hours and then were sieved through a 1 mm mesh. Dry samples were treated with 30% hydrogen peroxide to remove organic matter; hydrogen peroxide solution was added every 12 hours until reactions ceased. Following treatment with hydrogen peroxide, a 0.5% solution of sodium hexametaphosphate was added and left to sit for 24 hours to remove flocs. Samples were analysed for grain size using a Mastersizer® laser diffraction particle size analyser (Figure 2.2G). Data were processed using GRADISTAT to determine the statistical parameters of the grain size distributions (Blott & Pye, 2001). The Udden Wentworth grain size scale was used to classify the mean grain sizes using the Folk and Ward (1957) method. Following grain size analysis, sub-samples of the bulk surface sediment samples were utilised for LOI determinations.

LOI was used to estimate the total organic matter content of sediment sub-samples taken from vibracores and surface samples. Sediments were dried at 105°c for 24 hours and then weighed. Samples were heated in a blast furnace (Figure 2.2 H) for 3 hours at 550° C and then re-weighed. Total LOI was calculated using the formula:

$$LOI_{550} = ((DW_{105} – DW_{550})/DW_{105})*100$$

Where LOI_{550} represents the material lost on ignition at 550°c (as a percentage) DW_{105} represents the dry weight of the sample before combustion, and DW_{550} represents the sample

after it has been heated to 550°c. The weight loss is proportional to the amount of organic carbon contained in the sample (Heiri et al., 2001).

2.4 Results

2.4.1 Seismic Interpretation

Two prominent, semi-continuous seismic horizons were identified and correlated across the study area – Horizons A and B. A third discontinuous horizon (Horizon C) was identified in a number of the profiles (Appendix D1). Horizon A is interpreted as the top of the dredge spoil mound, as the depths correlate with the local bathymetry of the study area. Horizon B is interpreted as the base of the dredge spoil mound, inferred to represent the acoustic impedance contrast between the soft dredge spoil material and harder-packed underlying sediments. It follows that this horizon, which dips in the offshore direction, represents the original seafloor before the deposition of dredge sediment. I tentatively interpret Horizon C as representing the paleo sea floor during a lower sea level in the late Holocene as discussed by Harms (1989).

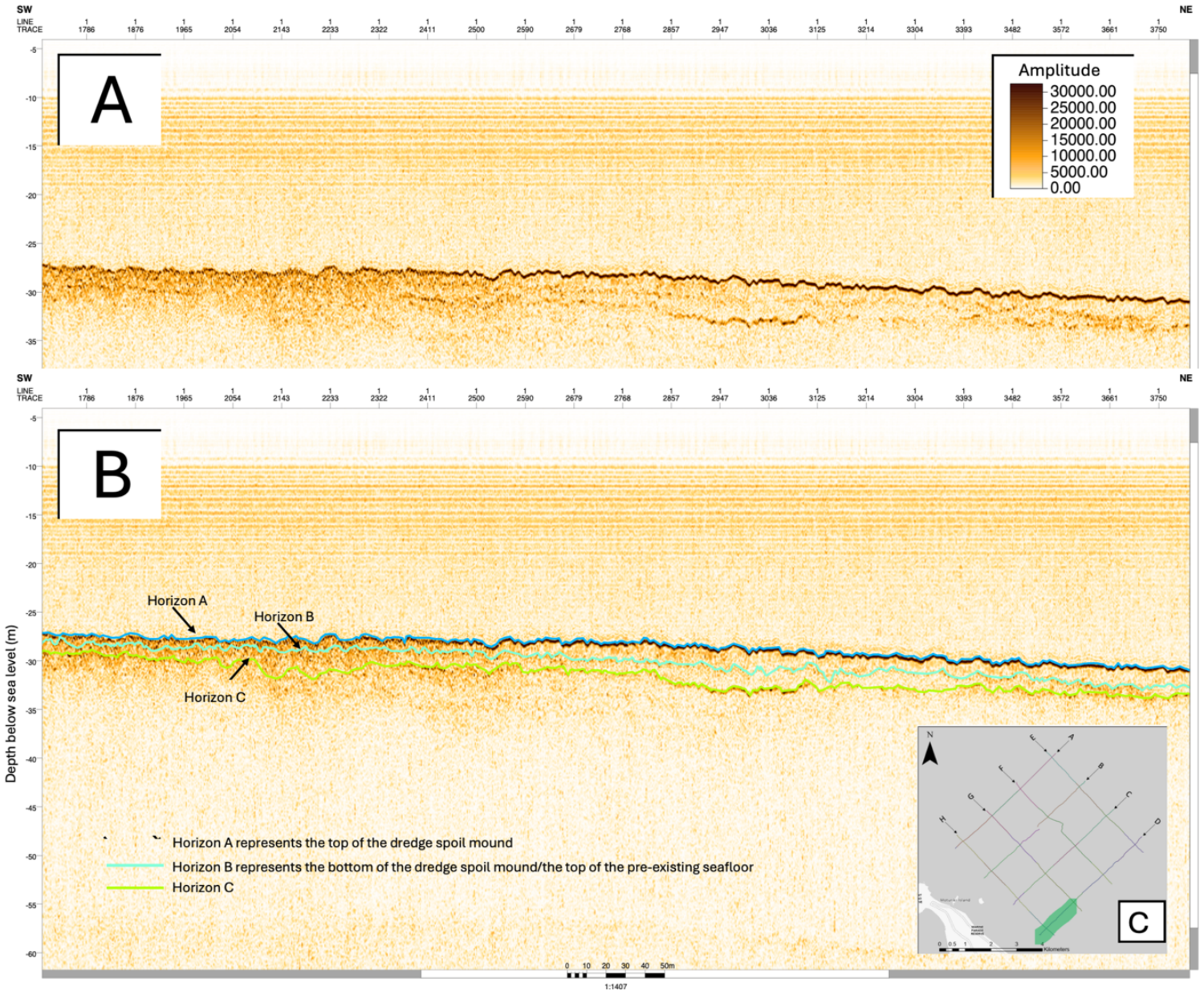

Figure 2.3- A) Uninterpreted portion of seismic line D. B) Interpreted portion of seismic horizon. C) Location of seismic profile.

Figure 2.4 displays a series of maps showcasing an interpretation of the seismic reflectors and the geometry of the sedimentary strata in the study area. These maps illustrate the depth below sea level to each horizon, as well as the thickness of the strata between horizons. All three horizon maps show an increase in depth to the northeast, as expected due to offshore deepening of the continental shelf.

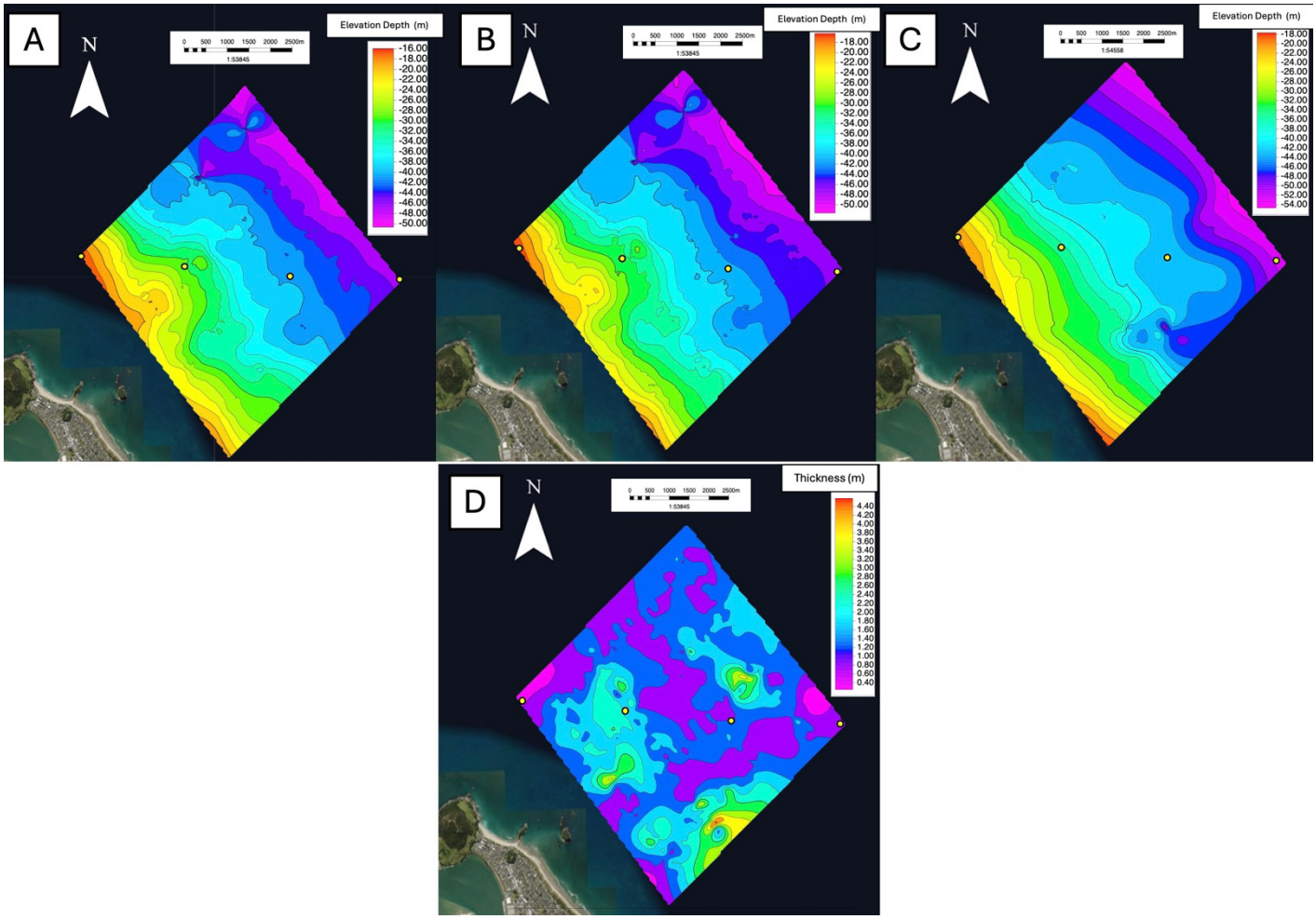

Figure 2.4 – A) Depth contour map of Seismic Horizon A, using a contour interval of 2 m. Datum is mean sea level. B) Depth contour map of Seismic Horizon B, using a contour interval of 2 m. Datum is mean sea level. C) Depth contour map of Seismic Horizon C, using a contour interval of 2 m. D) Isopach map showing thickness between horizons A and B in true vertical depth, using a contour interval of 0.5 m. Yellow dots represent the locations of virbracore samples.

The isopach map of the interval between Horizons A and B shows that the thickness of the dredge spoil mound varies from 0.5 m to 4.5 m (Figure 2.4D). The majority of the mound is between 1 and 1.5 m thick. However, there are three thicker areas, ranging between 3.5 and 4.5 m thick, all situated within the dredge spoil site. The thinnest areas of the mound, which occur on the eastern and western corners of the surveyed area towards the shoreward end of seismic lines, H, G, F, and E, are directly outside of the disposal ground.

Areas with thicker deposits in the southeastern corner of the isopach map between Horizon A and B (i.e., Figure 2.4D) indicate a possible submarine channel system that is also imaged in the seismic lines (Figure 2.5). This feature is only observed in shore-parallel profiles closer to shore such as in Seismic Profile D and its intersection with Profile G (Appendix D1). The bottom of the submarine channel extends to 4.5 m below the sea floor and ranges from 75 to 110 m wide.

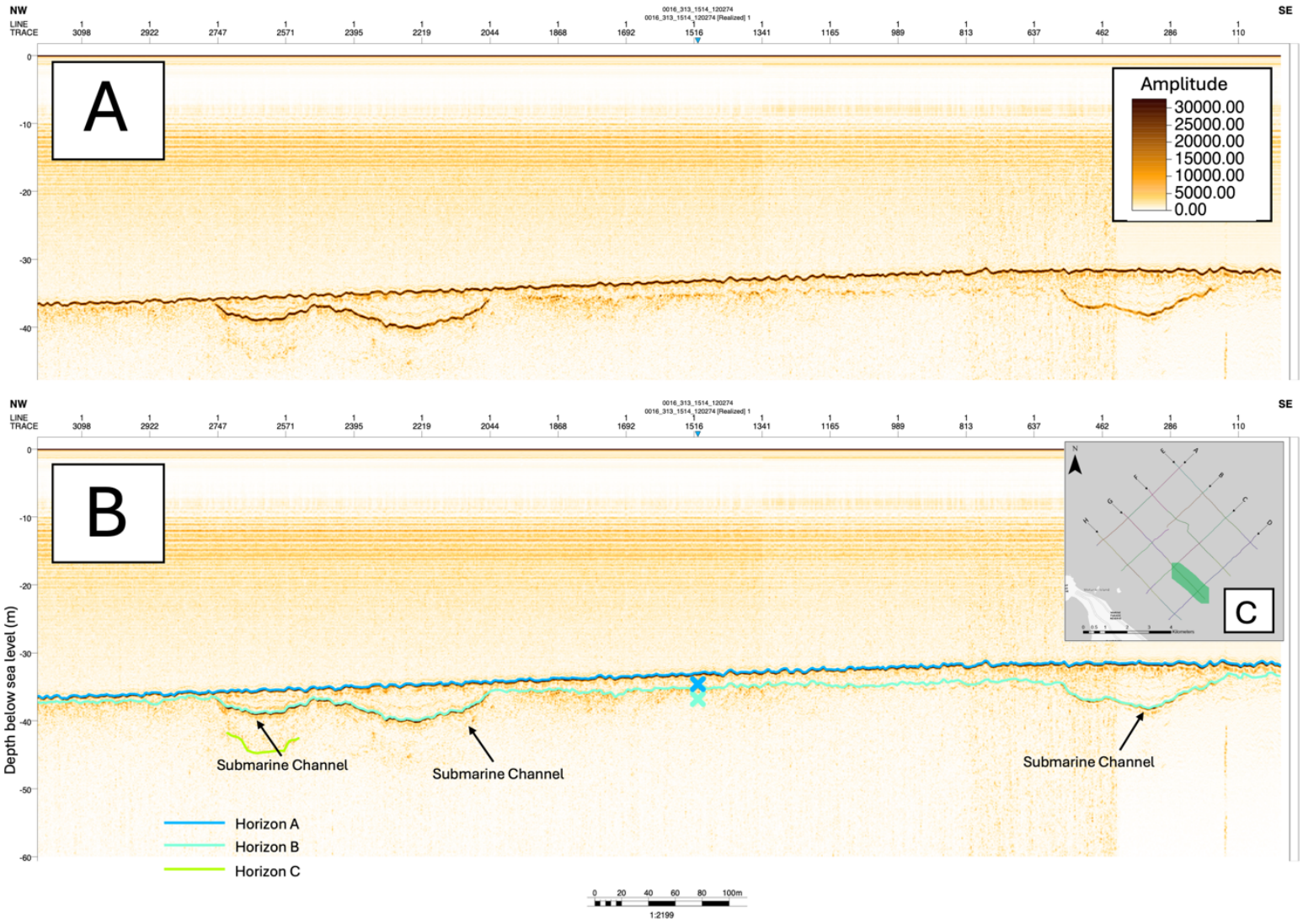

Figure 2.5- A) Uninterpreted portion of seismic horizon G. B) Interpreted portion of seismic horizon G. C) Location of seismic profiles.

2.4.2 Vibracores

Vibracore 1

Vibracore 1 (VC1) was collected from a location 2.52 km offshore (Figure 2.1C). The core measures 55 cm long (Figure 2.6). The core comprises fine-grained, moderately sorted sand. Shell debris was identified within the core between 27 cm and 35 cm depth. LOI varies from 1.43% to 2.41%, with an average of 2.07%. The core is structureless/massive, with no sedimentary structures (Figure 2.6).

Vibracore 2

Vibracore 2 (VC2) was collected from a position 4.0 km offshore (Figure 2.1C). The core is 35 cm long (Figure 2.6). The core is composed of medium-grained, moderately sorted sand. The proportion of organic matter (LOI) measured in VC2 ranges from 0.79% to 1.15% with an average of 1.10%. As VC2 is very short, there is no observable trend within the LOI or grain size data. The core is massive/structureless, with no sedimentary structures (Figure 2.6).

Vibracore 3

Vibracore 3 (VC3) was collected from a location 5.45 km offshore (Figure 2.1C). The core is 150 cm long (Figure 2.6). The top 30 cm of the core predominantly comprises medium-grained sand. Between 30 cm and 80 cm depth, there is more grain size variability, ranging from coarse-grained sand to coarse-grained silt. Most of the core is structureless, except for the basal 40 cm where planar lamination occurs. There is also a significant amount of shell hash that occurs within the core between 40 cm and 80 cm depth. This broken-up shell material is associated with higher proportions of organic matter (Figure 2.8).

The proportion of organic matter (LOI) measured in VC3 ranges from 0.45% to 3.96%, with an average of 2.36%. There is a general increase in organic content with depth, and a spike at 50 cm, which correlates to a decrease in grain size from medium-grained sand to coarse silt (Figure 2.8).

Vibracore 4

Vibracore 4 (VC4) was collected from a position 7.22 km offshore (Figure 2.1C). The core is 60 cm long (Figure 2.6). The top 20 cm of the core was damaged during collection. However, sub-samples were taken throughout the damaged core material, which provided an estimation of the grain sizes and the organic carbon content. The grain sizes throughout the undamaged core section ranges from fine to coarse-grained sand; the majority of the core comprises fine-grained sand. Sediment ranges from poorly to moderately sorted throughout the core, with all of the sub-samples being finely-skewed. Shell hash has been identified within the core at 27 cm and 35 cm depth respectively. This shelly material is associated with an increase in organic content. Overall, the core is massive/structureless (Figure 2.6). The proportion of organic matter (LOI) measured in VC4 was 1.66%. There is a substantial spike in organic matter content at 40 cm depth. Although similar to VC3, there is a general increase in organic matter with depth.

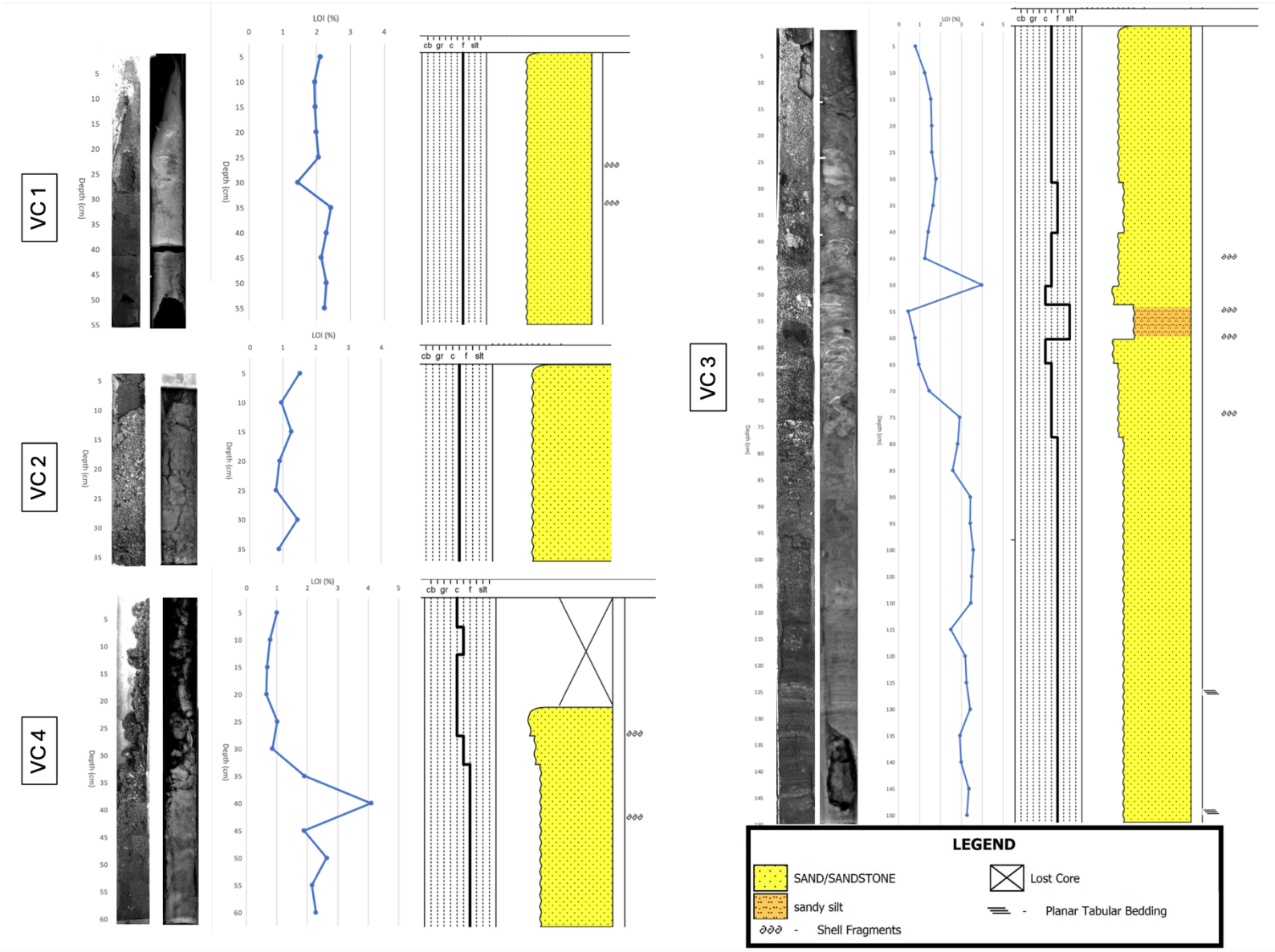

Figure 2.6 – Vibracores from the study area. From left to right displays a photograph of each core, an x-ray image, a LOI profile, a profile of mean grain size, and a sedimentological description of each core.

2.4.3 Surface Sediments

Surface samples reveal that sediment at the dredge-disposal sites predominantly consists of medium-grained, moderately sorted sand (between 250 – 500 μm; Figure 2.7A). The finest-grained sediments occur in the northern portion of the study area, as well as the south and southwestern side (Figure 2.7A). The sediment in these areas ranges from silt to very-fine sand to medium silt (31 - 125 μm). The coarsest sediment (>1000 μm) occurs in the upper north-eastern side of the study area near the edges.

Surface sediments in the study area are characterised by a range of LOI from 0.17% to 7.96%, with an average of 1.39% (Figure 2.7B). There are areas within the study area that LOI is greater, such as the northern and southern corners. The LOI in the western corner reaches 7.9%. The LOI data appear to be directly linked with grain size; finer-grained sediments tend to have a higher LOI in comparison to coarser-grained sediments.

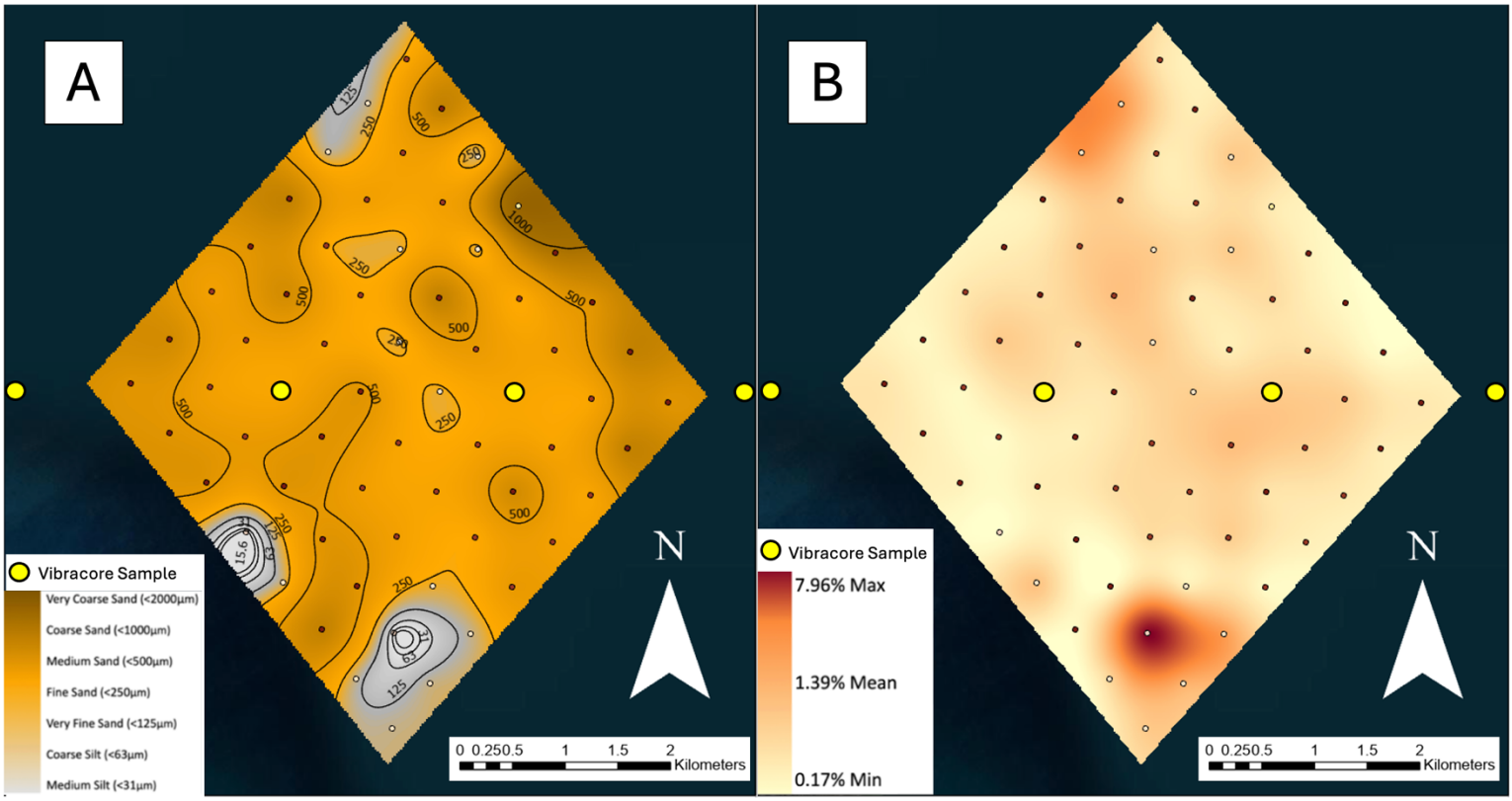

Figure 2.7 – A) Average grain size in surface sediment samples in the study area. B) LOI of surface sediment samples in the study area.

2.5 Discussion

2.5.1 Grain Size Distribution Patterns

The distribution of surface sediment samples observed in this study, with a more offshore area dominated by coarse sand and a finer-grained inshore area, matches well with the two-part facies classification of the Bay of Plenty shelf area proposed by Dahm and Healy (1980) (Figure 2.7). The present results also match the data from the same area collected by Harms (1989), Warren (1992), and Dahm and Healy (1980), showing that they predominantly consist of medium-grained, moderately to well-sorted sands. Sediment within the four vibracores was also dominated by fine to medium sand (Figure 2.8). Furthermore, grain size skewness parameters measured from sediment samples at the surface and within cores revealed a primary fine-skew or near-symmetrical skew. This also aligns with previous research that found sediment grain size distributions from both the natural shelf sediment and dredged material are primarily fine-skewed or symmetrically skewed (Dahm & Healy,1980; Harms 1989).

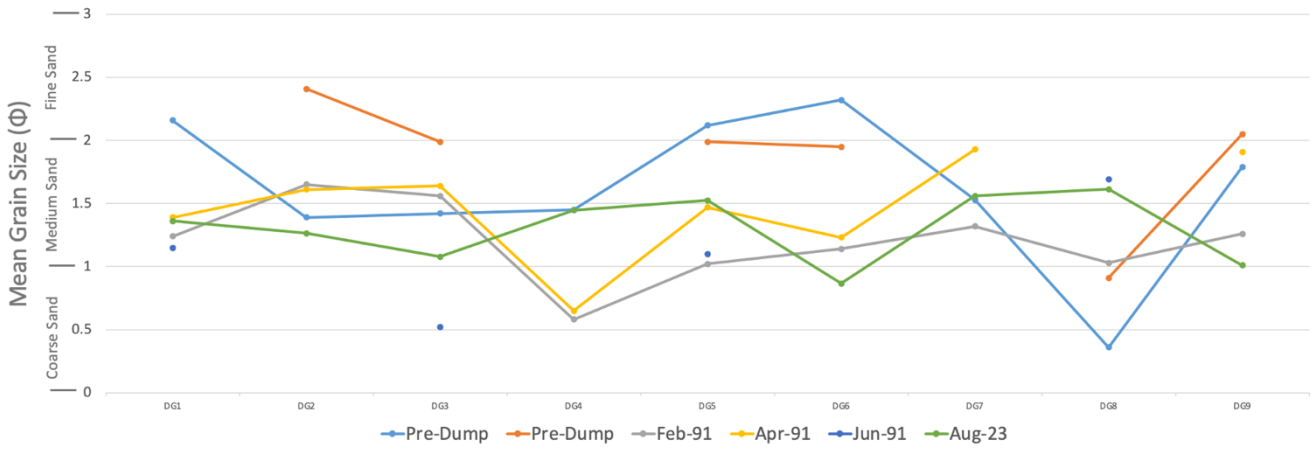

Figure 2.8 – Relationship between the pre and post-dredging grain size data collected by Warren (1992), compared to the surface grain size collected in this study.

Since this study found no significant changes in the composition of the sediment within the spoil disposal mound, it can be inferred that there has been no change in the composition of the dredged material since the Warren (1992) study. Furthermore, I concur with others in implying that the similarity in grain size between pre-dredge and post-dredge sediments indicates that the dredged sediments are compatible with the natural inner shelf sediments (Davies-Colley, 1976; Foster, 1992; Harms, 1989; Michels & Healy, 1999; Moon et al., 1994;

Warren et al., 1991; Warren, 1992). As the sediment has not changed composition it can be assumed that there is no increased risk to benthic organisms from changing the seafloor environment. Additionally, as the composition of the dredge spoil is comprised almost entirely of sandy material, it can be inferred that the consolidation of the material on the seafloor is rapid, leading to the sediment being deposited rapidly, with minimal dispersion of material occurring during disposal (Moon et al., 1994).

2.5.2 Stratigraphy

Core Stratigraphy

The study found that the core samples were predominantly structureless throughout the spoil disposal site without evidence of bedform generation. However, some thin intervals of shell debris occur within VC3 and VC4, and planar lamination was noted in the lower 40 cm of VC3 , indicating sediment movement within the spoil disposal site may have occurred in the past. I interpret the structureless nature of the stratigraphy to indicate that sediment was deposited en masse and never re-entrained or reworked to produce bedforms. The only exception is the planar lamination which suggests that at some point in the past there was sediment movement but there is no geochronological information to constrain when. Figure 2.4D shows the locations of the cores on the thickness maps, based on the thickness of VC3 (1.5 m) on the map it can be assumed that the planar laminated bedding occurred within the dredged material rather than the pre-disposal seafloor. Planar lamination in fine-grained sand indicates a flow velocity of 0.6 m s^{-1}.Thus, this interval may be the result of a past storm event.

Seismic Stratigraphy

This study mapped distinct seismic horizons which represent the top of the dredge spoil mound (Horizon A) and the seafloor before dredging (Horizon B). The results demonstrate that the thickest packages are around 4.5 m thick and occur in the northeast, southwest, and southern sides of the study area with the sediment thinning towards the edges. This thickness differs from Healy et al. (1997), who found that the maximum thickness of the mound was 7.5 m. This is not completely unexpected as when dredge sediment is initially deposited it forms a conical shape that thins away from the centre point, eventually flattening into a cohesive surface due to consolidation (Moon et al., 1994; Warren, 1992). I interpret the three thicker areas of sediment on the sea floor to be recently deposited material, as it is well known that the dredge mound takes about two years to fully consolidate and settle (Harms, 1989; Healy et al.,

1997; Healy et al., 1988). This is important to note because the long-term stability of the mound and its impacts on the surrounding environment are affected by its height, with higher mounds potentially leading to more significant changes in sedimentation and erosion patterns (Francingues & Lamb, 1991).

The seismic surveys in this study also found that the seafloor outside of the permitted spoil disposal sites D and G was covered with a thin layer of sediment (Figure 2.4D). Harms (1989) and Healy et al, (1997) inferred that there is potential for irregular disposal outside of the permitted disposal ground, and the results herein appear to support this interpretation.

Finally, this study identified a submarine channel system through the mapping of Seismic Horizon C which was most prominent directly outside of the study area (see Figure 2.8). Previous studies have also identified channels at the dredge spoil disposal site (Harms, 1989), and interpreted them to represent channels dissecting the sea floor during a lower-phase of relative sea level (Gibb, 1986; Harms, 1989).

2.5.4 Hydrodynamic Conditions and Sediment Transport

It is well known that the major controls on sediment erosion, transport and deposition are grain size, flow velocity and water depth. In the study area, sediment grain size ranges from coarse silt (63 μm) to very coarse sand (>1000 μm), with the majority of the sediment being fine to medium-grained sand (125-500 μm). Hjulström (1935) demonstrated that erosion of fine sand occurs at velocities of 0.2 m s^{-1} whereas it gets deposited when velocities decrease to 0.02 m s^{-1} (Figure 2.11). On the other hand erosion of coarse sand occurs at velocities of 0.8 m s^{-1} and it is deposited when flow velocities are below 0.08 m/s.

Previous studies demonstrated that the average current velocity at the bed in the dredge spoil disposal sites is 0.10 m s^{-1}, which is below the critical threshold to erode and transport fine-grained sand (Harms, 1989; Warren, 1992). Wave heights of at least 1 m with periods of 10-12 s are required to initiate entrainment of fine-grained sand in water deeper than 20 m (Healy, 1996; Warren, 1992). Warren (1992) clearly showed that these thresholds were only exceeded in water depths of 25 m 13.5% of the time for fine sand, 7.5% of the time for medium sand, and <1% of the time for coarse-grained sand.

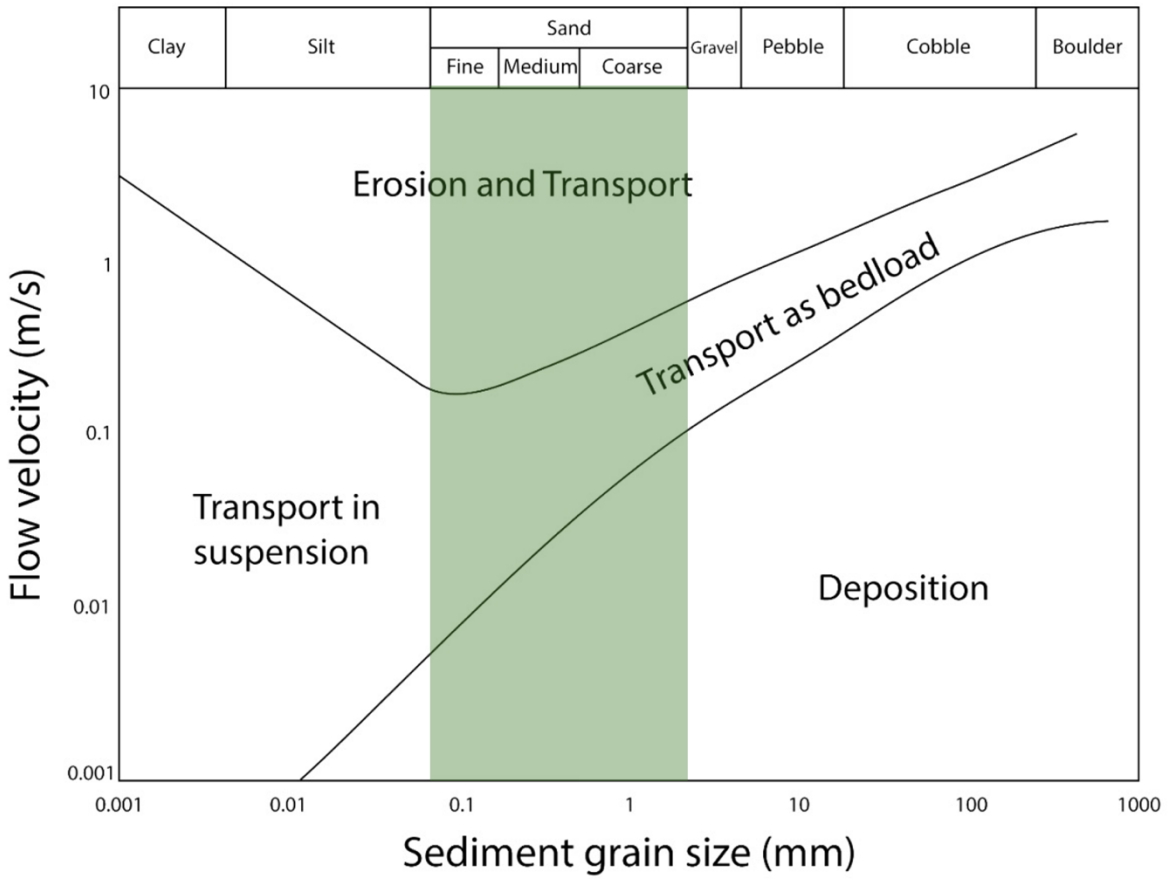

Figure 2.9 - Hjulström diagram showing sediment erosion, transport and deposition as a function of flow velocity and grain size, without an assumed water depth. The range of grain sizes within the deposition site is highlighted in green. Modified after (Hjulström, 1935).

The overwhelming dominance of structureless sediments on the sea bed and in sediment cores indicates that there is no current or wave action of sufficient energy to influence the spoil mound. This interpretation is based on the bedform stability diagram in Figure 2.10, using the range of grain sizes observed (fine to medium-grained sand) and assuming a mean flow velocity of up to 0.10 m s^{-1} (Warren, 1992).

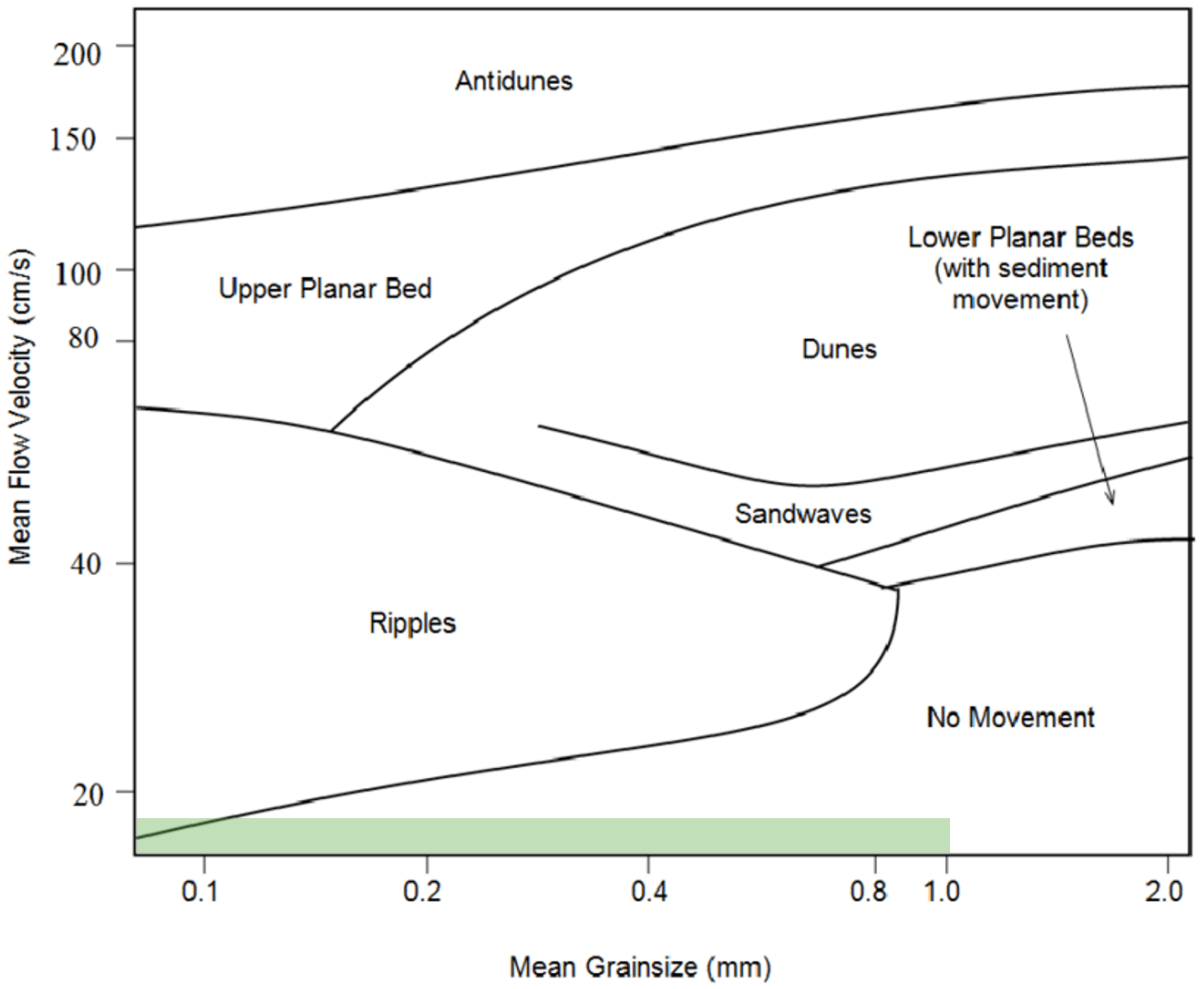

Figure 2.10- Bedform stability diagram displaying the relationship between mean flow velocity and mean grain size. Water depth was assumed to be 1. The expected mean flow velocity and range of grain sizes within the study area is highlighted in green. Modified from (Reineck & Singh, 1980).

2.6 Summary and Conclusions

Approximately 1,407,300 m^3 of sediment has been added to the inner shelf dredge disposal a Sites D and G by the Port of Tauranga since 2000. Investigations into the spoil mound were last carried out in 1992, therefore, the current composition, shape, size and sub-surface stratigraphy of the mound as well as the potential for sediment transport away from the mound was unknown. To address this knowledge gap, this study investigated sediments on the inner shelf dredge spoil disposal site using shallow seismic surveys, vibracores, and surface sediment samples, to answer the question: is there potential for sediment resuspension and transport of dredge spoil?

Mapping of the seafloor and subsurface stratigraphy show that the dredge spoil mound is predominantly about 1.5 m above the pre-disposal seafloor and thins towards the edges of the surveyed area. At its maximum thickness, the mound reaches 4.5 m, which is still at a water depth deep enough to avoid being significantly influenced by wave energy. Core samples showed that there is no well-organized layering within the stratigraphic record supporting the idea that once deposited most sediment is not re-entrained and moved any great distance. The sediment grain size distribution throughout the study area was found to primarily consist of fine to medium-grained, moderately well-sorted sand with a relatively low content organic matter content. Data from previous studies was used to estimate the potential for sediment resuspension and transport, which found that the mean current velocity of the spoil mound is 0.10 m/s^{-1} under fair-weather conditions, which is below the threshold needed to initiate the movement of fine sand.

The results of this study have shown that the dredge spoil mound is similar in composition to past studies, the spoil mound is also relatively stable and unlikely to be subject to sediment resuspension and transport under fair-weather conditions. The results of this study can be used as a baseline for further sedimentological and oceanographic investigations in the Bay of Plenty. This study also serves as evidence to support the safety of dredge-spoil disposal operations undertaken by the Port of Tauranga.

2.7 References

Blott, S. J., & Pye, K. (2001). GRADISTAT: a grain size distribution and statistics package for the analysis of unconsolidated sediments. Earth Surface Processes and Landforms, 26(11), 1237–1248. https://doi.org/10.1002/esp.261

Dahm, J., & Healy, T. R. (1980). A Study of Dredge Spoil Dispersion off the Entrance to the Tauranga Harbour- A Report to the Bay of Plenty Harbour Board.

Davies-Colley, R. (1976). Some Field Techniques Used in a Study of Tauranga Harbour. Proceedings (New Zealand Ecological Society) , 23, 33–37.

Folk, R. L., & Ward, W. C. (1957). Brazos River bar [Texas]; a study in the significance of grain size parameters. Journal of Sedimentary Research, 27(1), 3–26. https://doi.org/10.1306/74D70646-2B21-11D7-8648000102C1865D

Foster, D. M. (1992). Environmental Impacts of recent Dredging and Inner Shelf Spoil Disposal at Tauranga. University of Waikato.

Foster, G. A., Healy, T. R., & De Lange, W. P. (1996). Presaging Beach Renourishment from a Nearshore Dredge Dump Mound, Mt Maunganui Beach, New Zealand. Journal of Coastal Research , 12(2), 395–405.

Francingues, N. R., & Lamb, M. (1991). Long-term management strategy (LTMS) for dredged material: Corps of engineers assessment and summary of the national forum on implementation strategies 28-31 January, 1991, Baltimore, Maryland.

Gibb, J. G. (1986). A New Zealand regional holocene eustatic sea-level curve and its application to determination of vertical tectonic movement: A contribution to IGCP-Project 200. Royal Society of New Zealand, Bulletin , 24.

Harms, C. (1989). Dredge Spoil Dispersion from an Inner Shelf Dump-Mound. University of Waikato.

Healy, J. M., De Lange, W. P., & Mathew, J. (1997). Monitoring of a Large Inner Shelf Dump Mound Offshore Tauranga, New Zealand. Combined Australasian Coastal Engineering and Ports Conference.

Healy, T. (1996). Review of Capital Dredging Impacts for the Port of Tauranga LTD 1992 Major Channel Deepening and Widening Programme.

Healy, T., McCabe, B., Grace, R., & Harms, C. (1988). Environmental Assessment Programme for Tauranga Harbour Dredging and Inner Shelf Spoil Dumping .

Heiri, O., Lotter, A. F., & Lemcke, G. (2001). Loss on ignition as a method for estimating organic and carbonate content in sediments : reproducibility and comparability of results . Journal of Paleolimnology , 25, 101–110.

Hjulström, F. (1935). Studies of the morphological activity of rivers as illustrated by the river Fyris . Uppsala : Almqvist & Wiksell.

Matthews, J. (1997). Morphologic changes of the tidal deltas and an inner shelf dump ground from large scale dredging and dumping, Tauranga, New Zealand . University of Waikato .

Michels, K. H., & Healy, T. R. (1999). Evaluation of an Inner Shelf Site off Tauranga Harbour, New Zealand, for disposal of Muddy-Sandy Dredged Sediments. Journal of Coastal Research , 3, 830–838.

Moon, V., de Lange, W., Warren, S., & Healy, T. (1994). Post-Disposal Behavior of Sandy Dredged Material at an Open-Water, Inner Shelf Disposal Site. Journal of Coastal Research , 10(3), 651–662.

Port of Tauranga. (2011). Location and Transport Links, Https://www.port-tauranga.co.nz/wp-content/uploads/Location-and-Transport-Links.pdf, 2-6

Port of Tauranga. (2020). Port History to Modern Day, Https://www.port-tauranga.co.nz/wp-content/uploads/Our-Port-History-to-Modern-Day.pdf, 2-4

Port of Tauranga. (2024). Port Trade and Statistics Information. Https://www.port-tauranga.co.nz/wp-content/uploads/Port-Trade-and-Statistics-Information-2023.pdf. 8 p.

Rees, C. P. (1980). Envrionmental Impact of Dredging Operations. Proceedings of the Third International Symposium on Dredging Technology , 373.

Reineck, H.-E., & Singh, I. B. (1980). Depositional Sedimentary Environments . Springer-Verlag.

Riddell, J. (2000). Dredging: Opportunities and Challenges for 2000 and Beyond . Terra et Aqua , 78, 3–10.

Todd, V. L. G., Todd, I. B., Gardiner, J. C., Morrin, E. C. N., MacPherson, N. A., DiMarzio, N. A., & Thomsen, F. (2015). A review of impacts of marine dredging activities on marine mammals. ICES Journal of Marine Science, 72(2), 328–340. https://doi.org/10.1093/icesjms/fsu187

van Maren, D. S., van Kessel, T., Cronin, K., & Sittoni, L. (2015). The impact of channel deepening and dredging on estuarine sediment concentration. Continental Shelf Research, 95, 1–14. https://doi.org/10.1016/j.csr.2014.12.010

Warren, S., Healy, T., Moon, V., & Foster, D. (1991). Aspects of the Geomechanics of Dredge Spoil Disposed of on the Inner Shelf, Tauranga, New Zealand. Coastal Engineering: Climate for Change; Proceedings of 20th Australasian Conference on Coastal and Ocean Engineering, 1991 , 128–133.

Warren, S. K. (1992). The Geomechanics and Dispersion of Dredge Spoil Dumped in Open Water on the Inner Shelf, Tauranga, New Zealand [MSc Earth Science]. University of Waikato.

Chapter 3

Conclusions

The overall aim of this thesis was to investigate the inner shelf dredge disposal mound to see if any changes to the sediment have occurred since the last studies of the area undertaken in 1992. This was achieved by collecting a range of shallow seismic surveys, vibracores, and surficial sediment samples from across the dredge-disposal area. This type of study is important because a significant amount of sediment is added to the inner shelf spoil disposal sites D/G each year. Updated information regarding the composition of dredged material, thickness and distribution of the spoil mound, and the nature of the stratigraphy of the deposited material are necessary to identify potential sediment resuspension and movement inshore away from the mound. Any transported sediment has the potential to cause harm to benthic flora and fauna, as well as increase levels of suspended sediments within the Tauranga shelf. This chapter focuses on responding to the study aims posed at the beginning of the study (Chapter 1) and providing recommendations to the Port of Tauranga as to the suitability of the spoil mound for future sediment deposition.

Have there been any changes in the composition, shape or thickness of the mound?

The results of this research suggest that dredged-material deposited on the shelf has remained compositionally similar to both the pre-disposal shelf sediments and the sediments examined in past studies (Davies-Colley, 1976; Foster, 1992; Harms, 1989; Michels & Healy, 1999; Moon et al., 1994; Warren et al., 1991; Warren, 1992). Recent grain size analysis showed that sediments at Sites D and G predominantly comprise fine to medium-grained sand. This matches the two part sediment distribution model originally put forth by Dahm & Healy (1980). It follows that there has not been a compositional change in the dredged material since 1992 and that deposited material has the same textural and compositional nature as the pre-disposal sediment. This consistency between sediment grain size and texture between pre- and post-dredge disposal suggests that is little risk that sediment movement from the dredge-deposition site is impacting benthic flora and fauna outside of the deposition site.

Shallow seismic surveys found the dredge mound to typically be 1.5 m thick throughout the study area, with three small thicker areas that have been attributed to more recently

deposited material. However, past studies by Healy et al. (1997), found that the maximum thickness of the mound was 7.5 m. This is not completely unexpected as when dredge sediment is initially deposited it forms a conical shape that thins away from the centre point, eventually flattening into a cohesive surface (Moon et al., 1994; Warren, 1992). Further compression and compaction of the mound as more sediment is added on top may further lead to the mound compressing and flattening.

What is the potential for sediment resuspension and transport away from the mound?

Dredge spoil deposited on the inner shelf appears to be relatively stable and not subject to much erosion and shoreward transport. This is largely due to the location of the spoil deposition site in water depths ranging from 20-40 m. As the Bay of Plenty is sheltered and experiences relatively fair weather conditions through most of the year, large waves which would make contact with the bed are not common. Previous studies have found that the average current velocity observed at the spoil disposal site is 0.10 m s^{-1} which is below the critical threshold to initiate transport of fine-grained sand; Hjulström (1935) indicates that transport of fine sand occurs at velocities exceeding 0.2 m s^{-1}.

Structureless sediment in vibracores without primary stratification is further evidence that sediment is not being transported from the dredge-spoil location. If quasi-steady currents were able to entrain sediment on the sea floor, this would generate bedforms and this would produce cross bedding in the stratigraphic record. However, a thin interval in VC1 displayed planar bedding, which may be an indication of short-term sediment movement during a storm. Thus, we cannot completely discount that during the highest energy events (i.e., storms) that some sediment movement can occur.

3.1 Study Limitations and Future Research

The study was not without limitations. First, the vibracore sampling could not be completed as planned. The penetration of the vibracore sampler into the stratigraphic column was inadequate and therefore may have been unable to accurately capture differences between the sediments related to dredging from the older sediment layers below. Cores must be at least 2.5 m long to intersect the dredge spoil mound and original pre-disposal sediments.

It remains unsure if these challenges with coring were due to compaction of the dredge sediment, or to due to issues with the vibrating head.

Another challenge frequently encountered with sediment coring is sediment compaction. I estimated that around 30% compaction occurred in the cores from this study, which poses challenges for accurately measuring the original length of the cores. Future research might account for these uncertainties by collecting a greater number of longer vibracore samples inside and outside of the spoil disposal site, to gain a better understanding of the distribution of sub-surface facies that could be tied to the results of the shallow seismic surveys.

A third challenge of this study was the fact that neither wave height and period nor current measurements were recorded. Instead I relied on previous studies that measured the hydrodynamics. Ultimately, I was forced to assume the processes remain the same and to calculate sediment transport parameters on this basis. Future research should measure these baseline hydrodynamic parameters (waves and currents) for the inner shelf to ensure that no changes in processes are occurring through time. Long-term measurements would allow for waves and currents to be measured during periods of fine weather, as well as storm conditions, to predict the likelihood and severity of sediment transport during storm conditions.

Future studies would also benefit from using multiple seismic surveys to establish if the dredge spoil mound is subject to movement, and if so, how mobile is the sediment. This could be done by collecting annual or even sub-annual seismic profiles across the study area. Additionally, conducting more seismic surveys would also allow for the settling of the mound to be monitored post-spoil disposal. Furthermore, repeat sediment sampling of the surficial sediments may allow for a more complete understanding of the shelf sediment and if there are any changes in the composition of sediments before and after routine dredging.

3.2 Summary and Recommendations for the Port of Tauranga

I. Based on the results and interpretations of this thesis, it appears that dredge spoil deposition at Sites D and G are appropriate for the sandy and silty material coming from the Port of Tauranga. This material is similar to the original sediment on the sea floor in the area and the potential for sediment transport in the shoreward direction is low.
II. Monitoring the height and stability of the spoil mound, as well as the composition of sediment (and any associated changes in this) can be achieved through regular repeat seismic surveys following dredging operations. This would gain a more well-rounded

view of the dredge-spoil mount and if the materials are consolidating with time as we suggest in this research.

III. A repeat set of hydrodynamic measurements, perhaps over a longer period of time (i.e., months) would ensure that the process regime has not changed. It might also capture hydrodynamic process extremes, which appear to be the only time that sediment is able to be entrained and moved away from the dredge disposal site.

3.3 References

Dahm, J., & Healy, T. R. (1980). A Study of Dredge Spoil Dispersion off the Entrance to the Tauranga Harbour- A Report to the Bay of Plenty Harbour Board.

Davies-Colley, R. (1976). Some Field Techniques Used in a Study of Tauranga Harbour. Proceedings (New Zealand Ecological Society) , 23, 33–37.

Foster, D. M. (1992). Environmental Impacts of recent Dredging and Inner Shelf Spoil Disposal at Tauranga. University of Waikato .

Harms, C. (1989). Dredge Spoil Dispersion from an Inner Shelf Dump-Mound. University of Waikato .

Healy, J. M., De Lange, W. P., & Mathew, J. (1997). Monitoring of a Large Inner Shelf Dump Mound Offshore Tauranga, New Zealand. Combined Australasian Coastal Engineering and Ports Conference .

Hjulström, F. (1935). Studies of the morphological activity of rivers as illustrated by the river Fyris . Uppsala : Almqvist & Wiksell.

Michels, K. H., & Healy, T. R. (1999). Evaluation of an Inner Shelf Site off Tauranga Harbour, New Zealand, for disposal of Muddy-Sandy Dredged Sediments. Journal of Coastal Research , 3, 830–838.

Moon, V., de Lange, W., Warren, S., & Healy, T. (1994). Post-Disposal Behavior of Sandy Dredged Material at an Open-Water, Inner Shelf Disposal Site. Journal of Coastal Research , 10(3), 651–662.

Warren, S., Healy, T., Moon, V., & Foster, D. (1991). Aspects of the Geomechanics of Dredge Spoil Disposed of on the Inner Shelf, Tauranga, New Zealand. Coastal Engineering: Climate for Change; Proceedings of 20th Australasian Conference on Coastal and Ocean Engineering, 1991 , 128–133.

Warren, S. K. (1992). The Geomechanics and Dispersion of Dredge Spoil Dumped in Open Water on the Inner Shelf, Tauranga, New Zealand [MSc Earth Science]. University of Waikato .

Appendices

Appendix A. Sediment Grain Size Summary Statistics

GRADISTAT data sheets showing the proportion of samples within grain size bounds for the 64 surface sediment samples.

SAMPLE STATISTICS

		A1	A2	A3
	ANALYST AND DATE:	, 22/0/2023	, 9/20/2023	, 9/20/2023
	LOCATION	176.1945788°E 37.6108884°S	176.1972734°E 37.6142843°S	176.2005804°E 37.6176800°S
	SIEVING ERROR:	0.0%	0.0%	0.0%
	SAMPLE TYPE:	Unimodal, Poorly Sorted	Unimodal, Moderately Sorted	Unimodal, Moderately Sorted
	TEXTURAL GROUP:	Sand	Sand	Slightly Gravelly Sand
	SEDIMENT NAME:	Poorly Sorted Coarse Sand	Moderately Sorted Coarse Sand	htly Very Fine Gravelly Coarse S
FOLK AND WARD METHOD (μm)	MEAN (M_G):	327.5	517.7	506.7
	SORTING (σ_G):	2.558	1.718	1.707
	SKEWNESS (Sk_G):	-0.230	-0.069	-0.001
	KURTOSIS (K_G):	1.031	0.965	0.967
FOLK AND WARD METHOD (ϕ)	MEAN (M_G):	1.611	0.950	0.981
	SORTING (σ_G):	1.355	0.780	0.771
	SKEWNESS (Sk_G):	0.230	0.069	0.001
	KURTOSIS (K_G):	1.031	0.965	0.967
FOLK AND WARD METHOD (Description)	MEAN:	Medium Sand	Coarse Sand	Coarse Sand
	SORTING:	Poorly Sorted	Moderately Sorted	Moderately Sorted
	SKEWNESS:	Fine Skewed	Symmetrical	Symmetrical
	KURTOSIS:	Mesokurtic	Mesokurtic	Mesokurtic
	MODE 1 (μm):	545.0	545.0	545.0
	MODE 1 (ϕ):	0.881	0.881	0.881
	D_{10} (μm):	95.04	250.7	253.6
	D_{50} (μm):	355.6	526.1	506.8
	D_{90} (μm):	901.0	1008.1	1006.1
	(D_{90} / D_{10}) (μm):	9.481	4.021	3.967
	(D_{90} - D_{10}) (μm):	806.0	757.4	752.4
	(D_{75} / D_{25}) (μm):	3.621	2.115	2.092
	(D_{75} - D_{25}) (μm):	456.3	399.4	383.3
	D_{10} (ϕ):	0.150	-0.012	-0.009
	D_{50} (ϕ):	1.491	0.926	0.981
	D_{90} (ϕ):	3.395	1.996	1.979
	(D_{90} / D_{10}) (ϕ):	22.59	-172.023	-227.333
	(D_{90} - D_{10}) (ϕ):	3.245	2.008	1.988
	(D_{75} / D_{25}) (ϕ):	3.788	3.698	3.391
	(D_{75} - D_{25}) (ϕ):	1.856	1.081	1.065
	% GRAVEL:	0.0%	0.0%	0.2%
	% SAND:	93.9%	99.8%	99.4%
	% MUD:	6.1%	0.2%	0.4%
	% V COARSE GRAVEL:	0.0%	0.0%	0.0%
	% COARSE GRAVEL:	0.0%	0.0%	0.0%
	% MEDIUM GRAVEL:	0.0%	0.0%	0.0%
	% FINE GRAVEL:	0.0%	0.0%	0.0%
	% V FINE GRAVEL:	0.0%	0.0%	0.2%
	% V COARSE SAND:	6.5%	10.3%	10.0%
	% COARSE SAND:	29.3%	43.4%	40.8%
	% MEDIUM SAND:	27.0%	36.4%	39.6%
	% FINE SAND:	21.9%	9.0%	8.8%
	% V FINE SAND:	9.3%	0.7%	0.2%
	% V COARSE SILT:	1.6%	0.2%	0.4%
	% COARSE SILT:	1.5%	0.0%	0.0%
	% MEDIUM SILT:	1.0%	0.0%	0.0%
	% FINE SILT:	0.9%	0.0%	0.0%
	% V FINE SILT:	0.6%	0.0%	0.0%
	% CLAY:	0.5%	0.0%	0.0%

A4	A5	A6	A7	A8
, 9/20/2023	, 9/20/2023	, 9/20/2023	, 9/20/2023	, 9/20/2023
176.2038874ºE 37.6209785ºS	176.2071944ºE 37.6241799ºS	176.2101340ºE 37.6275751ºS	176.2134410ºE 37.6307762ºS	176.2166255ºE 37.6342681ºS
0.0%	0.0%	0.0%	0.0%	0.0%
Bimodal, Very Poorly Sorted	Unimodal, Moderately Sorted	Unimodal, Moderately Sorted	Unimodal, Poorly Sorted	Unimodal, Moderately Sorted
Sandy Mud	Sand	Slightly Gravelly Sand	Sand	Slightly Gravelly Sand
Very Fine Sandy Medium Silt	Moderately Sorted Fine Sand	htly Very Fine Gravelly Coarse S	Poorly Sorted Fine Sand	ghtly Very Fine Gravelly Fine Sa
9.756	211.2	711.4	164.4	165.4
5.678	1.734	1.723	2.001	1.888
0.090	0.020	-0.051	-0.197	-0.127
1.258	1.049	1.056	1.500	1.428
6.680	2.243	0.491	2.605	2.596
2.505	0.794	0.785	1.001	0.917
-0.090	-0.020	0.051	0.197	0.127
1.258	1.049	1.056	1.500	1.428
Medium Silt	Fine Sand	Coarse Sand	Fine Sand	Fine Sand
Very Poorly Sorted	Moderately Sorted	Moderately Sorted	Poorly Sorted	Moderately Sorted
Symmetrical	Symmetrical	Symmetrical	Fine Skewed	Fine Skewed
Leptokurtic	Mesokurtic	Mesokurtic	Leptokurtic	Leptokurtic
11.70	193.5	775.0	163.0	163.0
6.502	2.375	0.373	2.622	2.622
1.297	105.9	352.1	76.27	82.05
10.17	209.5	717.1	166.4	165.5
67.61	429.3	1391.8	330.5	327.7
52.11	4.054	3.952	4.333	3.994
66.31	323.4	1039.7	254.2	245.6
8.141	2.069	2.042	2.114	2.024
24.32	156.4	521.1	126.6	119.2
3.887	1.220	-0.477	1.597	1.610
6.619	2.255	0.480	2.588	2.595
9.590	3.239	1.506	3.713	3.607
2.467	2.655	-3.157	2.324	2.241
5.704	2.019	1.983	2.116	1.998
1.585	1.608	-33.561	1.525	1.488
3.025	1.049	1.030	1.080	1.018
0.0%	0.0%	2.2%	0.0%	0.0%
10.9%	96.9%	97.3%	92.8%	94.2%
89.1%	3.1%	0.4%	7.2%	5.7%
0.0%	0.0%	0.0%	0.0%	0.0%
0.0%	0.0%	0.0%	0.0%	0.0%
0.0%	0.0%	0.0%	0.0%	0.0%
0.0%	0.0%	0.0%	0.0%	0.0%
0.0%	0.0%	2.2%	0.0%	0.0%
1.8%	0.5%	23.9%	0.0%	1.3%
3.3%	5.6%	48.8%	1.5%	2.0%
0.1%	31.0%	20.8%	21.0%	18.0%
0.2%	46.5%	2.7%	47.3%	49.5%
5.6%	13.2%	1.1%	23.0%	23.4%
11.2%	0.5%	0.1%	1.6%	0.9%
16.8%	1.1%	0.3%	2.1%	1.8%
17.9%	0.6%	0.0%	1.3%	1.1%
15.7%	0.6%	0.0%	1.1%	1.0%
12.6%	0.3%	0.0%	0.7%	0.7%
14.9%	0.0%	0.0%	0.4%	0.2%

B1	B2	B3	B4	B5
, 9/20/2023	, 9/20/2023	, 9/20/2023	, 9/20/2023	, 9/20/2023
176.1975184°E 37.6076865°S	176.2010704°E 37.6112765°S	176.2038874°E 37.6142843°S	176.2070719°E 37.6177770°S	176.2103789°E 37.6210755°S
0.0%	0.0%	0.0%	0.0%	0.0%
Unimodal, Moderately Sorted	Unimodal, Moderately Sorted	Unimodal, Moderately Well Sorted	Unimodal, Moderately Sorted	Unimodal, Moderately Sorted
Sand	Sand	Sand	Sand	Sand
Moderately Sorted Coarse Sand	Moderately Sorted Medium Sand	derately Well Sorted Medium Sa	Moderately Sorted Coarse Sand	Moderately Sorted Coarse Sand
659.1	395.4	422.8	491.3	551.9
1.694	1.780	1.582	1.851	1.664
-0.192	-0.024	-0.055	-0.124	-0.046
1.275	0.993	0.970	0.981	0.961
0.601	1.339	1.242	1.025	0.857
0.761	0.831	0.662	0.888	0.734
0.192	0.024	0.055	0.124	0.046
1.275	0.993	0.970	0.981	0.961
Coarse Sand	Medium Sand	Medium Sand	Medium Sand	Coarse Sand
Moderately Sorted	Moderately Sorted	Moderately Well Sorted	Moderately Sorted	Moderately Sorted
Fine Skewed	Symmetrical	Symmetrical	Fine Skewed	Symmetrical
Leptokurtic	Mesokurtic	Mesokurtic	Mesokurtic	Mesokurtic
650.0	385.0	460.0	545.0	545.0
0.628	1.383	1.126	0.881	0.881
345.4	185.9	229.5	211.9	280.4
672.9	397.3	427.2	509.2	556.1
1156.4	823.4	752.0	1025.5	1046.2
3.348	4.429	3.276	4.839	3.732
811.0	637.5	522.4	813.6	765.8
1.872	2.188	1.877	2.325	2.029
424.0	317.6	271.3	431.7	399.6
-0.210	0.280	0.411	-0.036	-0.065
0.572	1.332	1.227	0.974	0.847
1.534	2.427	2.123	2.239	1.835
-7.316	8.660	5.163	-61.705	-28.146
1.743	2.147	1.712	2.275	1.900
7.671	2.460	2.158	4.039	3.969
0.904	1.130	0.908	1.217	1.021
0.0%	0.0%	0.0%	0.0%	0.0%
99.1%	99.2%	99.6%	98.8%	99.6%
0.9%	0.8%	0.4%	1.2%	0.4%
0.0%	0.0%	0.0%	0.0%	0.0%
0.0%	0.0%	0.0%	0.0%	0.0%
0.0%	0.0%	0.0%	0.0%	0.0%
0.0%	0.0%	0.0%	0.0%	0.0%
0.0%	0.0%	0.0%	0.0%	0.0%
18.0%	4.8%	1.1%	10.9%	11.7%
55.5%	29.7%	35.6%	40.3%	46.4%
20.6%	44.2%	50.3%	34.2%	35.4%
2.6%	18.4%	11.9%	11.8%	5.3%
2.4%	2.1%	0.7%	1.6%	0.9%
0.2%	0.6%	0.4%	0.6%	0.4%
0.5%	0.3%	0.0%	0.4%	0.0%
0.2%	0.0%	0.0%	0.2%	0.0%
0.0%	0.0%	0.0%	0.0%	0.0%
0.0%	0.0%	0.0%	0.0%	0.0%
0.0%	0.0%	0.0%	0.0%	0.0%

B6	B7	B8	C1	C2
, 9/20/2023	, 9/20/2023	, 9/20/2023	, 9/20/2023	, 9/20/2023
176.2138084ºE 37.6243739ºS	176.2167480ºE 37.6278661ºS	176.2198100ºE 37.6309702ºS	176.2010704ºE 37.6045814ºS	176.2042549ºE 37.6077835ºS
0.0%	0.0%	0.0%	0.0%	0.0%
Unimodal, Moderately Well Sorted	Bimodal, Very Poorly Sorted	Unimodal, Poorly Sorted	Unimodal, Moderately Sorted	Unimodal, Moderately Sorted
Sand	Sandy Mud	Slightly Gravelly Sand	Sand	Slightly Gravelly Sand
Moderately Well Sorted Coarse Sa	Fine Sandy Coarse Silt	Slightly Very Fine Gravelly Fine Sa	Moderately Sorted Medium Sand	Slightly Very Fine Gravelly Medium S
523.1	13.98	157.2	393.5	391.6
1.585	5.913	2.065	1.757	1.857
-0.038	0.004	-0.166	-0.112	-0.052
0.951	1.041	1.632	1.113	1.059
0.935	6.160	2.669	1.345	1.353
0.664	2.564	1.046	0.814	0.893
0.038	-0.004	0.166	0.112	0.052
0.951	1.041	1.632	1.113	1.059
Coarse Sand	Medium Silt	Fine Sand	Medium Sand	Medium Sand
Moderately Well Sorted	Very Poorly Sorted	Poorly Sorted	Moderately Sorted	Moderately Sorted
Symmetrical	Symmetrical	Fine Skewed	Fine Skewed	Symmetrical
Mesokurtic	Mesokurtic	Very Leptokurtic	Leptokurtic	Mesokurtic
545.0	23.30	163.0	385.0	385.0
0.881	5.507	2.622	1.383	1.383
284.2	1.389	72.56	188.1	175.3
527.5	14.32	157.8	400.3	394.5
939.6	171.0	324.7	763.5	837.9
3.307	123.0	4.476	4.058	4.781
655.4	169.6	252.2	575.4	662.7
1.906	9.892	2.096	2.055	2.256
344.3	36.95	119.2	291.0	327.8
0.090	2.548	1.623	0.389	0.255
0.923	6.126	2.664	1.321	1.342
1.815	9.491	3.785	2.410	2.512
20.19	3.725	2.332	6.191	9.849
1.725	6.943	2.162	2.021	2.257
2.999	1.718	1.501	2.269	2.536
0.931	3.306	1.068	1.039	1.173
0.0%	0.0%	0.0%	0.0%	0.1%
99.8%	18.8%	92.0%	96.8%	96.8%
0.2%	81.2%	7.9%	3.2%	3.0%
0.0%	0.0%	0.0%	0.0%	0.0%
0.0%	0.0%	0.0%	0.0%	0.0%
0.0%	0.0%	0.0%	0.0%	0.0%
0.0%	0.0%	0.0%	0.0%	0.0%
0.0%	0.0%	0.0%	0.0%	0.1%
7.0%	0.0%	1.4%	2.5%	5.4%
47.4%	0.7%	2.4%	30.9%	29.1%
39.8%	5.7%	16.0%	47.0%	42.8%
5.0%	6.3%	46.9%	14.7%	17.8%
0.5%	6.2%	25.3%	1.7%	1.9%
0.2%	11.7%	1.8%	1.3%	1.0%
0.0%	17.5%	2.4%	0.7%	0.7%
0.0%	15.8%	1.4%	0.6%	0.7%
0.0%	12.3%	1.1%	0.4%	0.5%
0.0%	10.3%	0.7%	0.1%	0.2%
0.0%	13.6%	0.5%	0.0%	0.0%

C3	C4	C5	C6	C7
, 9/20/2023	, 9/20/2023	, 9/20/2023	, 9/20/2023	, 9/20/2023
176.2074394°E 37.6113736°S	176.2106239°E 37.6147694°S	176.2140534°E 37.6179710°S	176.2168704°E 37.6211725°S	176.2202999°E 37.6241799°S
0.0%	0.0%	0.1%	0.0%	0.0%
Unimodal, Moderately Sorted	Unimodal, Moderately Well Sorted	Unimodal, Poorly Sorted	Unimodal, Moderately Well Sorted	Unimodal, Moderately Well Sorted
Sand	Sand	Slightly Gravelly Muddy Sand	Sand	Slightly Gravelly Sand
Moderately Sorted Medium Sand	oderately Well Sorted Coarse Sa	Fine Gravelly Very Coarse Silty M	derately Well Sorted Medium Sa	ightly Very Fine Gravelly Fine Sa
360.9	550.2	339.0	359.4	250.0
1.924	1.554	3.408	1.592	1.599
0.035	0.005	-0.258	-0.058	0.031
0.971	0.938	2.188	0.972	0.999
1.470	0.862	1.561	1.476	2.000
0.944	0.636	1.769	0.671	0.677
-0.035	-0.005	0.258	0.058	-0.031
0.971	0.938	2.188	0.972	0.999
Medium Sand	Coarse Sand	Medium Sand	Medium Sand	Fine Sand
Moderately Sorted	Moderately Well Sorted	Poorly Sorted	Moderately Well Sorted	Moderately Well Sorted
Symmetrical	Symmetrical	Fine Skewed	Symmetrical	Symmetrical
Mesokurtic	Mesokurtic	Very Leptokurtic	Mesokurtic	Mesokurtic
325.0	545.0	385.0	385.0	230.0
1.626	0.881	1.383	1.383	2.126
157.5	310.9	35.43	193.7	138.1
354.9	548.3	354.9	363.8	248.5
853.0	972.4	1085.8	645.7	462.9
5.416	3.128	30.64	3.334	3.352
695.5	661.5	1050.3	452.0	324.8
2.467	1.867	2.671	1.900	1.886
336.1	348.7	360.9	235.2	160.7
0.229	0.040	-0.119	0.631	1.111
1.495	0.867	1.494	1.459	2.009
2.666	1.685	4.819	2.368	2.856
11.62	41.68	-40.599	3.753	2.570
2.437	1.645	4.938	1.737	1.745
2.583	3.179	2.786	1.917	1.591
1.303	0.901	1.417	0.926	0.915
0.0%	0.0%	2.4%	0.0%	0.4%
98.0%	100.0%	85.3%	99.3%	98.7%
2.0%	0.0%	12.3%	0.7%	0.9%
0.0%	0.0%	0.0%	0.0%	0.0%
0.0%	0.0%	0.0%	0.0%	0.0%
0.0%	0.0%	0.0%	0.0%	0.0%
0.0%	0.0%	0.0%	0.0%	0.0%
0.0%	0.0%	2.4%	0.0%	0.4%
6.2%	8.6%	8.8%	0.0%	1.1%
24.7%	49.3%	19.8%	24.5%	5.7%
39.7%	39.1%	38.0%	53.6%	42.3%
24.7%	3.0%	15.9%	20.1%	44.5%
2.8%	0.0%	2.7%	1.1%	5.2%
0.4%	0.0%	2.7%	0.7%	0.2%
0.5%	0.0%	2.3%	0.0%	0.6%
0.5%	0.0%	2.5%	0.0%	0.1%
0.5%	0.0%	2.0%	0.0%	0.0%
0.0%	0.0%	1.4%	0.0%	0.0%
0.0%	0.0%	1.4%	0.0%	0.0%

C8	D1	D2	D3	D4
, 9/20/2023	, 9/22/2023	, 9/22/2023	, 9/22/2023	, 9/22/2023
176.2236069ºE 37.6277691ºS	176.2044998ºE 37.6014763ºS	176.2078068ºE 37.6046785ºS	176.2107464ºE 37.6082687ºS	176.2141759ºE 37.6113736ºS
0.0%	0.0%	0.0%	0.0%	0.0%
Unimodal, Poorly Sorted	Unimodal, Moderately Sorted	Unimodal, Poorly Sorted	Unimodal, Moderately Sorted	Unimodal, Moderately Well Sorted
Sand	Sand	Sand	Slightly Gravelly Sand	Sand
Poorly Sorted Fine Sand	Moderately Sorted Coarse Sand	Poorly Sorted Coarse Sand	htly Very Fine Gravelly Medium S	oderately Well Sorted Coarse Sa
158.4	525.7	399.5	345.4	503.2
2.124	1.694	2.915	1.969	1.562
-0.199	-0.129	-0.447	0.041	-0.037
1.671	1.035	1.637	1.008	0.944
2.658	0.928	1.324	1.534	0.991
1.087	0.760	1.543	0.977	0.643
0.199	0.129	0.447	-0.041	0.037
1.671	1.035	1.637	1.008	0.944
Fine Sand	Coarse Sand	Medium Sand	Medium Sand	Coarse Sand
Poorly Sorted	Moderately Sorted	Poorly Sorted	Moderately Sorted	Moderately Well Sorted
Fine Skewed	Fine Skewed	Very Fine Skewed	Symmetrical	Symmetrical
Very Leptokurtic	Mesokurtic	Very Leptokurtic	Mesokurtic	Mesokurtic
163.0	545.0	650.0	325.0	545.0
2.622	0.881	0.628	1.626	0.881
70.29	255.8	83.02	148.9	277.9
159.4	540.3	481.4	337.6	506.1
329.5	975.9	999.1	836.8	887.2
4.688	3.816	12.03	5.618	3.193
259.2	720.2	916.1	687.8	609.3
2.135	2.020	2.843	2.497	1.868
123.4	380.9	476.7	325.7	320.2
1.602	0.035	0.001	0.257	0.173
2.650	0.888	1.055	1.567	0.982
3.831	1.967	3.590	2.747	1.847
2.392	55.99	2762.0	10.69	10.70
2.229	1.932	3.589	2.490	1.675
1.519	3.495	4.398	2.500	2.677
1.094	1.014	1.507	1.320	0.901
0.0%	0.0%	0.0%	0.1%	0.0%
91.6%	99.2%	91.7%	97.2%	99.8%
8.4%	0.8%	8.3%	2.8%	0.2%
0.0%	0.0%	0.0%	0.0%	0.0%
0.0%	0.0%	0.0%	0.0%	0.0%
0.0%	0.0%	0.0%	0.0%	0.0%
0.0%	0.0%	0.0%	0.0%	0.0%
0.0%	0.0%	0.0%	0.1%	0.0%
0.1%	8.7%	10.0%	6.1%	4.9%
2.7%	47.2%	38.0%	22.5%	46.1%
18.0%	34.7%	28.0%	38.9%	42.8%
46.2%	7.0%	10.4%	26.3%	5.4%
24.6%	1.6%	5.4%	3.4%	0.5%
1.7%	0.3%	2.0%	0.6%	0.2%
2.4%	0.4%	1.7%	0.7%	0.0%
1.5%	0.0%	1.5%	0.6%	0.0%
1.3%	0.0%	1.3%	0.6%	0.0%
0.8%	0.0%	1.0%	0.2%	0.0%
0.8%	0.0%	1.0%	0.0%	0.0%

D5	D6	D7	D8	E1
, 9/22/2023	, 9/22/2023	, 9/22/2023	, 9/22/2023	, 9/22/2023
176.2171154ºE 37.6145753ºS	176.2205449ºE 37.6180680ºS	176.2232395ºE 37.6213666ºS	176.2267914ºE 37.6246649ºS	176.2078068ºE 37.5982739ºS
0.0%	0.0%	0.0%	0.0%	0.1%
Unimodal, Moderately Sorted	Unimodal, Moderately Sorted	Unimodal, Moderately Sorted	Unimodal, Moderately Sorted	Unimodal, Poorly Sorted
Sand	Sand	Sand	Sand	Slightly Gravelly Sand
Moderately Sorted Medium Sand	Moderately Sorted Medium Sand	Moderately Sorted Medium Sand	Moderately Sorted Medium Sand	htly Very Fine Gravelly Coarse S
304.0	324.7	274.9	429.4	555.9
1.674	1.677	1.725	1.630	2.493
-0.012	-0.081	-0.004	-0.128	-0.289
1.000	1.017	1.016	1.043	1.088
1.718	1.623	1.863	1.220	0.847
0.743	0.746	0.786	0.705	1.318
0.012	0.081	0.004	0.128	0.289
1.000	1.017	1.016	1.043	1.088
Medium Sand	Medium Sand	Medium Sand	Medium Sand	Coarse Sand
Moderately Sorted	Moderately Sorted	Moderately Sorted	Moderately Sorted	Poorly Sorted
Symmetrical	Symmetrical	Symmetrical	Fine Skewed	Fine Skewed
Mesokurtic	Mesokurtic	Mesokurtic	Mesokurtic	Mesokurtic
325.0	325.0	275.0	460.0	775.0
1.626	1.626	1.868	1.126	0.373
155.8	162.5	136.9	221.6	145.8
304.3	329.6	274.3	439.9	645.0
584.5	608.9	550.9	766.7	1481.8
3.751	3.747	4.024	3.459	10.16
428.7	446.4	414.0	545.0	1336.1
2.011	2.004	2.080	1.906	3.209
217.2	231.8	205.8	284.2	711.1
0.775	0.716	0.860	0.383	-0.567
1.716	1.601	1.866	1.185	0.633
2.682	2.621	2.869	2.174	2.778
3.462	3.663	3.335	5.671	-4.896
1.907	1.906	2.009	1.790	3.345
1.833	1.902	1.792	2.254	-34.903
1.008	1.003	1.056	0.930	1.682
0.0%	0.0%	0.0%	0.0%	3.4%
97.7%	97.1%	97.2%	98.5%	92.7%
2.3%	2.9%	2.8%	1.5%	4.0%
0.0%	0.0%	0.0%	0.0%	0.0%
0.0%	0.0%	0.0%	0.0%	0.0%
0.0%	0.0%	0.0%	0.0%	0.0%
0.0%	0.0%	0.0%	0.0%	0.0%
0.0%	0.0%	0.0%	0.0%	3.4%
0.7%	0.0%	0.7%	1.1%	23.2%
15.9%	19.8%	12.6%	38.1%	34.9%
48.2%	50.5%	43.6%	47.1%	19.3%
30.6%	24.8%	35.9%	10.5%	11.1%
2.3%	2.1%	4.4%	1.6%	4.1%
0.6%	1.1%	0.6%	0.6%	1.2%
0.6%	0.6%	0.8%	0.4%	0.9%
0.6%	0.6%	0.6%	0.4%	0.7%
0.5%	0.5%	0.6%	0.1%	0.6%
0.1%	0.1%	0.2%	0.0%	0.5%
0.0%	0.0%	0.0%	0.0%	0.0%

E2	E3	E4	E5	E6
, 9/22/2023	, 9/22/2023	, 9/22/2023	, 9/22/2023	, 9/22/2023
176.2112363ºE 37.6013792ºS	176.2142983ºE 37.6049696ºS	176.2174829ºE 37.6081716ºS	176.2206674ºE 37.6111795ºS	176.2239744ºE 37.6148664ºS
0.0%	0.0%	0.0%	0.0%	0.0%
Unimodal, Moderately Sorted	Unimodal, Poorly Sorted	Unimodal, Moderately Sorted	Unimodal, Moderately Sorted	Unimodal, Moderately Sorted
Sand	Sand	Sand	Slightly Gravelly Sand	Sand
Moderately Sorted Medium Sand	Poorly Sorted Medium Sand	Moderately Sorted Fine Sand	htly Very Fine Gravelly Medium S	Moderately Sorted Medium Sand
246.7	282.3	216.7	249.8	296.1
1.638	2.007	1.710	1.684	1.715
-0.045	-0.103	-0.041	-0.019	-0.089
0.998	1.186	1.024	1.035	1.065
2.019	1.825	2.207	2.001	1.756
0.712	1.005	0.774	0.752	0.778
0.045	0.103	0.041	0.019	0.089
0.998	1.186	1.024	1.035	1.065
Fine Sand	Medium Sand	Fine Sand	Fine Sand	Medium Sand
Moderately Sorted	Poorly Sorted	Moderately Sorted	Moderately Sorted	Moderately Sorted
Symmetrical	Fine Skewed	Symmetrical	Symmetrical	Symmetrical
Mesokurtic	Leptokurtic	Mesokurtic	Mesokurtic	Mesokurtic
275.0	275.0	230.0	230.0	325.0
1.868	1.868	2.126	2.126	1.626
128.7	117.9	107.7	127.9	145.3
248.5	284.6	217.6	250.1	301.1
458.7	633.8	422.4	484.1	567.1
3.563	5.376	3.923	3.784	3.903
329.9	515.9	314.7	356.2	421.8
1.953	2.366	2.052	2.000	2.024
168.4	251.8	159.3	176.6	215.1
1.125	0.658	1.243	1.047	0.818
2.009	1.813	2.200	2.000	1.732
2.958	3.084	3.215	2.967	2.783
2.630	4.689	2.586	2.835	3.401
1.833	2.427	1.972	1.920	1.965
1.629	2.038	1.615	1.666	1.824
0.965	1.243	1.037	1.000	1.018
0.0%	0.0%	0.0%	0.5%	0.0%
97.5%	95.1%	96.7%	96.5%	96.7%
2.5%	4.9%	3.3%	3.0%	3.3%
0.0%	0.0%	0.0%	0.0%	0.0%
0.0%	0.0%	0.0%	0.0%	0.0%
0.0%	0.0%	0.0%	0.0%	0.0%
0.0%	0.0%	0.0%	0.0%	0.0%
0.0%	0.0%	0.0%	0.5%	0.0%
0.0%	1.7%	0.0%	0.9%	0.0%
6.5%	16.7%	5.1%	7.3%	15.5%
43.0%	39.8%	34.6%	41.3%	48.2%
41.6%	30.8%	45.3%	40.9%	29.6%
6.3%	6.1%	11.7%	6.2%	3.5%
0.6%	1.3%	0.5%	0.6%	1.1%
0.8%	1.3%	1.1%	0.9%	0.8%
0.5%	1.0%	0.6%	0.6%	0.6%
0.5%	0.8%	0.7%	0.6%	0.5%
0.1%	0.5%	0.4%	0.2%	0.2%
0.0%	0.0%	0.0%	0.0%	0.0%

E7	E8	F1	F2	F3
, 9/22/2023	, 9/22/2023	, 9/22/2023	, 9/22/2023	, 9/22/2023
176.2267914ºE 37.6181651ºS	176.2300984ºE 37.6214636ºS	176.2112363ºE 37.5951685ºS	176.2144208ºE 37.5985650ºS	176.2174829ºE 37.6017674ºS
0.0%	0.0%	0.0%	0.0%	0.0%
Unimodal, Moderately Sorted	Unimodal, Moderately Sorted	Unimodal, Poorly Sorted	Unimodal, Moderately Sorted	Unimodal, Moderately Sorted
Sand	Sand	Sand	Sand	Slightly Gravelly Sand
Moderately Sorted Coarse Sand	Moderately Sorted Medium Sand	Poorly Sorted Fine Sand	Moderately Sorted Medium Sand	ightly Very Fine Gravelly Fine Sa
500.9	360.6	174.4	376.9	231.1
1.977	1.743	2.104	1.647	1.755
-0.232	-0.088	-0.166	-0.068	0.035
1.184	1.031	1.510	1.000	1.040
0.997	1.472	2.520	1.408	2.113
0.983	0.802	1.073	0.720	0.811
0.232	0.088	0.166	0.068	-0.035
1.184	1.031	1.510	1.000	1.040
Coarse Sand	Medium Sand	Fine Sand	Medium Sand	Fine Sand
Moderately Sorted	Moderately Sorted	Poorly Sorted	Moderately Sorted	Moderately Sorted
Fine Skewed	Symmetrical	Fine Skewed	Symmetrical	Symmetrical
Leptokurtic	Mesokurtic	Very Leptokurtic	Mesokurtic	Mesokurtic
650.0	385.0	163.0	385.0	230.0
0.628	1.383	2.622	1.383	2.126
192.4	171.0	76.90	194.6	114.5
531.2	366.7	175.2	381.6	228.7
1042.6	705.0	378.2	696.3	481.2
5.419	4.123	4.918	3.578	4.203
850.2	534.0	301.3	501.7	366.7
2.306	2.099	2.220	1.971	2.106
440.9	275.3	143.4	261.7	175.3
-0.060	0.504	1.403	0.522	1.055
0.913	1.447	2.513	1.390	2.128
2.378	2.548	3.701	2.361	3.127
-39.531	5.052	2.638	4.522	2.963
2.438	2.044	2.298	1.839	2.071
4.338	2.154	1.594	2.073	1.679
1.205	1.070	1.151	0.979	1.074
0.0%	0.0%	0.0%	0.0%	0.3%
96.5%	97.3%	92.7%	97.4%	97.1%
3.5%	2.7%	7.3%	2.6%	2.5%
0.0%	0.0%	0.0%	0.0%	0.0%
0.0%	0.0%	0.0%	0.0%	0.0%
0.0%	0.0%	0.0%	0.0%	0.0%
0.0%	0.0%	0.0%	0.0%	0.0%
0.0%	0.0%	0.0%	0.0%	0.3%
11.5%	1.3%	0.1%	0.7%	1.2%
42.5%	26.7%	4.0%	28.4%	7.3%
31.0%	47.1%	23.0%	50.7%	34.7%
9.3%	20.2%	44.8%	17.1%	43.7%
2.2%	2.0%	20.8%	0.7%	10.2%
1.0%	1.0%	1.7%	0.9%	0.3%
0.8%	0.6%	2.0%	0.5%	0.9%
0.7%	0.5%	1.3%	0.6%	0.5%
0.6%	0.4%	1.1%	0.5%	0.6%
0.4%	0.1%	0.8%	0.1%	0.2%
0.0%	0.0%	0.5%	0.0%	0.0%

F4	F5	F6	F7	F8
, 9/22/2023	, 9/22/2023	, 9/22/2023	, 9/22/2023	, 9/22/2023
176.2205449ºE 37.6051636ºS	176.2238519ºE 37.6083657ºS	176.2271589ºE 37.6116646ºS	176.2303434ºE 37.6153515ºS	176.2335279ºE 37.6183591ºS
0.1%	0.0%	0.0%	0.0%	0.0%
Unimodal, Moderately Sorted	Unimodal, Moderately Sorted	Unimodal, Moderately Sorted	Unimodal, Moderately Sorted	Unimodal, Moderately Sorted
Slightly Gravelly Sand	Sand	Sand	Sand	Sand
htly Very Fine Gravelly Coarse S	Moderately Sorted Medium Sand	Moderately Sorted Medium Sand	Moderately Sorted Medium Sand	Moderately Sorted Medium Sand
793.2	447.2	309.0	318.9	327.4
1.737	1.715	1.902	1.627	1.666
-0.078	-0.131	-0.133	-0.071	-0.018
1.111	1.052	1.069	0.998	0.993
0.334	1.161	1.694	1.649	1.611
0.797	0.778	0.927	0.702	0.736
0.078	0.131	0.133	0.071	0.018
1.111	1.052	1.069	0.998	0.993
Coarse Sand	Medium Sand	Medium Sand	Medium Sand	Medium Sand
Moderately Sorted	Moderately Sorted	Moderately Sorted	Moderately Sorted	Moderately Sorted
Symmetrical	Fine Skewed	Fine Skewed	Symmetrical	Symmetrical
Leptokurtic	Mesokurtic	Mesokurtic	Mesokurtic	Mesokurtic
775.0	460.0	325.0	325.0	325.0
0.373	1.126	1.626	1.626	1.626
384.7	216.7	130.1	166.8	169.4
803.8	458.9	319.4	323.3	327.5
1545.6	836.5	658.2	577.4	626.6
4.018	3.860	5.061	3.461	3.699
1161.0	619.8	528.1	410.6	457.2
2.020	2.037	2.313	1.941	2.006
573.2	328.5	270.6	216.7	232.9
-0.628	0.258	0.603	0.792	0.674
0.315	1.124	1.647	1.629	1.611
1.378	2.206	2.943	2.584	2.562
-2.194	8.566	4.876	3.261	3.798
2.007	1.949	2.339	1.791	1.887
-4.537	2.624	2.132	1.824	1.908
1.014	1.026	1.210	0.957	1.004
3.5%	0.0%	0.0%	0.0%	0.0%
96.5%	97.6%	96.3%	97.4%	97.4%
0.0%	2.4%	3.7%	2.6%	2.6%
0.0%	0.0%	0.0%	0.0%	0.0%
0.0%	0.0%	0.0%	0.0%	0.0%
0.0%	0.0%	0.0%	0.0%	0.0%
0.0%	0.0%	0.0%	0.0%	0.0%
3.5%	0.0%	0.0%	0.0%	0.0%
29.9%	3.7%	0.8%	0.0%	0.5%
47.9%	39.8%	21.4%	17.4%	19.8%
14.6%	42.4%	42.8%	52.4%	49.9%
3.1%	10.4%	25.9%	26.1%	26.2%
1.0%	1.4%	5.4%	1.4%	1.0%
0.0%	0.8%	1.1%	0.9%	0.8%
0.0%	0.6%	1.0%	0.5%	0.6%
0.0%	0.5%	0.7%	0.5%	0.6%
0.0%	0.4%	0.6%	0.5%	0.5%
0.0%	0.1%	0.3%	0.1%	0.1%
0.0%	0.0%	0.0%	0.0%	0.0%

G1	G2	G3	G4	G5
, 9/22/2023	, 9/22/2023	, 9/22/2023	, 9/22/2023	, 9/22/2023
176.2147883ºE 37.5918688ºS	176.2177278ºE 37.5952655ºS	176.2210348ºE 37.5984680ºS	176.2242193ºE 37.6018644ºS	176.2270364ºE 37.6053577ºS
0.0%	0.0%	0.0%	0.0%	0.0%
Unimodal, Poorly Sorted	Unimodal, Moderately Sorted	Unimodal, Moderately Sorted	Unimodal, Moderately Sorted	Unimodal, Poorly Sorted
Sand	Sand	Sand	Sand	Sand
Poorly Sorted Fine Sand	Moderately Sorted Medium Sand	Moderately Sorted Medium Sand	Moderately Sorted Fine Sand	Poorly Sorted Medium Sand
152.1	379.1	392.6	227.0	257.5
2.129	1.684	1.748	1.723	2.007
-0.204	-0.053	-0.069	-0.014	-0.136
1.640	0.974	1.013	1.004	1.231
2.717	1.399	1.349	2.139	1.958
1.090	0.752	0.806	0.785	1.005
0.204	0.053	0.069	0.014	0.136
1.640	0.974	1.013	1.004	1.231
Fine Sand	Medium Sand	Medium Sand	Fine Sand	Medium Sand
Poorly Sorted	Moderately Sorted	Moderately Sorted	Moderately Sorted	Poorly Sorted
Fine Skewed	Symmetrical	Symmetrical	Symmetrical	Fine Skewed
Very Leptokurtic	Mesokurtic	Mesokurtic	Mesokurtic	Leptokurtic
163.0	385.0	385.0	230.0	275.0
2.622	1.383	1.383	2.126	1.868
65.91	189.6	187.0	112.3	108.6
153.8	382.9	398.2	227.0	261.6
318.2	726.1	781.0	454.4	563.4
4.827	3.829	4.177	4.047	5.188
252.3	536.5	594.0	342.1	454.8
2.155	2.050	2.121	2.086	2.322
120.5	278.7	303.2	170.6	225.1
1.652	0.462	0.357	1.138	0.828
2.701	1.385	1.329	2.140	1.934
3.923	2.399	2.419	3.155	3.203
2.375	5.196	6.783	2.772	3.869
2.271	1.937	2.062	2.017	2.375
1.514	2.180	2.353	1.659	1.908
1.108	1.036	1.085	1.061	1.216
0.0%	0.0%	0.0%	0.0%	0.0%
90.8%	98.4%	98.0%	97.2%	94.7%
9.2%	1.6%	2.0%	2.8%	5.3%
0.0%	0.0%	0.0%	0.0%	0.0%
0.0%	0.0%	0.0%	0.0%	0.0%
0.0%	0.0%	0.0%	0.0%	0.0%
0.0%	0.0%	0.0%	0.0%	0.0%
0.0%	0.0%	0.0%	0.0%	0.0%
0.2%	1.5%	3.0%	0.0%	0.7%
2.2%	28.9%	30.9%	6.8%	13.3%
16.8%	48.2%	45.5%	36.1%	38.9%
45.1%	18.6%	17.0%	43.7%	34.0%
26.5%	1.2%	1.7%	10.6%	7.8%
2.4%	0.7%	0.8%	0.4%	1.4%
2.3%	0.3%	0.5%	1.0%	1.5%
1.5%	0.4%	0.4%	0.6%	1.0%
1.2%	0.1%	0.3%	0.6%	0.8%
0.9%	0.0%	0.0%	0.2%	0.5%
0.8%	0.0%	0.0%	0.0%	0.0%

G6	G7	G8	H1	H2
, 9/22/2023	, 9/22/2023	, 9/22/2023	, 9/22/2023	, 9/22/2023
176.2305884ºE 37.6085598ºS	176.2336504ºE 37.6120527ºS	176.2369574ºE 37.6152545ºS	176.2176053ºE 37.5886660ºS	176.2210348ºE 37.5920629ºS
0.0%	0.0%	0.0%	0.0%	0.0%
Unimodal, Moderately Sorted	Unimodal, Moderately Sorted	Unimodal, Moderately Well Sorted	Unimodal, Moderately Sorted	Unimodal, Moderately Sorted
Sand	Sand	Slightly Gravelly Sand	Sand	Sand
Moderately Sorted Medium Sand	Moderately Sorted Medium Sand	htly Very Fine Gravelly Coarse S	Moderately Sorted Medium Sand	Moderately Sorted Coarse Sand
353.6	324.3	773.4	239.0	641.2
1.742	1.803	1.622	1.730	1.948
-0.067	-0.132	-0.026	-0.083	-0.312
1.049	1.168	0.990	0.968	1.314
1.500	1.625	0.371	2.065	0.641
0.801	0.851	0.698	0.790	0.962
0.067	0.132	0.026	0.083	0.312
1.049	1.168	0.990	0.968	1.314
Medium Sand	Medium Sand	Coarse Sand	Fine Sand	Coarse Sand
Moderately Sorted	Moderately Sorted	Moderately Well Sorted	Moderately Sorted	Moderately Sorted
Symmetrical	Fine Skewed	Symmetrical	Symmetrical	Very Fine Skewed
Mesokurtic	Leptokurtic	Mesokurtic	Mesokurtic	Leptokurtic
385.0	325.0	775.0	275.0	775.0
1.383	1.626	0.373	1.868	0.373
170.3	152.6	412.3	114.1	211.0
357.0	330.2	776.9	244.5	696.9
698.3	638.1	1419.6	470.1	1258.2
4.101	4.181	3.443	4.119	5.963
528.0	485.5	1007.4	356.0	1047.2
2.084	2.085	1.934	2.132	2.128
266.5	245.6	520.8	186.2	514.8
0.518	0.648	-0.506	1.089	-0.331
1.486	1.598	0.364	2.032	0.521
2.554	2.712	1.278	3.131	2.245
4.930	4.185	-2.529	2.876	-6.775
2.036	2.064	1.784	2.042	2.576
2.098	1.979	-7.714	1.723	26.92
1.059	1.060	0.951	1.092	1.089
0.0%	0.0%	1.9%	0.0%	0.0%
96.7%	95.8%	97.0%	98.1%	98.0%
3.3%	4.2%	1.1%	1.9%	2.0%
0.0%	0.0%	0.0%	0.0%	0.0%
0.0%	0.0%	0.0%	0.0%	0.0%
0.0%	0.0%	0.0%	0.0%	0.0%
0.0%	0.0%	0.0%	0.0%	0.0%
0.0%	0.0%	1.9%	0.0%	0.0%
1.6%	0.6%	28.0%	0.0%	22.9%
24.8%	20.7%	51.8%	7.4%	48.4%
47.8%	48.1%	16.0%	41.1%	17.0%
21.0%	23.9%	0.5%	39.0%	6.8%
1.6%	2.5%	0.7%	10.6%	2.9%
1.1%	1.4%	0.1%	0.3%	0.6%
0.7%	0.9%	0.4%	0.7%	0.5%
0.7%	0.8%	0.4%	0.4%	0.4%
0.5%	0.7%	0.2%	0.4%	0.4%
0.2%	0.4%	0.0%	0.1%	0.1%
0.0%	0.0%	0.0%	0.0%	0.0%

H3	H4	H5	H6	H7	H8
, 9/22/2023	, 9/22/2023	, 9/22/2023	, 9/22/2023	, 9/22/2023	, 9/22/2023
176.2240968ºE 37.5953626ºS	176.2274038ºE 37.5987591ºS	176.2304659ºE 37.6020585ºS	176.2336504ºE 37.6054547ºS	176.2370799ºE 37.6086568ºS	176.2400194ºE 37.6118587ºS
0.0%	0.5%	0.0%	0.0%	0.0%	0.0%
Unimodal, Poorly Sorted	Unimodal, Moderately Sorted	Unimodal, Moderately Well Sorted	Unimodal, Moderately Sorted	Unimodal, Moderately Sorted	Unimodal, Moderately Well Sorted
Slightly Gravelly Sand	Gravelly Sand	Slightly Gravelly Sand	Sand	Sand	Sand
ightly Very Fine Gravelly Fine Sa	ry Fine Gravelly Very Coarse Sa	htly Very Fine Gravelly Coarse S	Moderately Sorted Coarse Sand	Moderately Sorted Coarse Sand	derately Well Sorted Coarse Sar
203.9	1169.6	882.7	491.6	660.2	559.9
2.200	1.746	1.530	1.630	1.635	1.538
-0.141	-0.075	0.024	-0.124	-0.105	-0.055
1.523	0.944	1.004	1.034	1.007	0.964
2.294	-0.226	0.180	1.025	0.599	0.837
1.137	0.804	0.613	0.705	0.709	0.621
0.141	0.075	-0.024	0.124	0.105	0.055
1.523	0.944	1.004	1.034	1.007	0.964
Fine Sand	Very Coarse Sand	Coarse Sand	Medium Sand	Coarse Sand	Coarse Sand
Poorly Sorted	Moderately Sorted	Moderately Well Sorted	Moderately Sorted	Moderately Sorted	Moderately Well Sorted
Fine Skewed	Symmetrical	Symmetrical	Fine Skewed	Fine Skewed	Symmetrical
Very Leptokurtic	Mesokurtic	Mesokurtic	Mesokurtic	Mesokurtic	Mesokurtic
193.5	1300.0	920.0	545.0	775.0	545.0
2.375	-0.373	0.126	0.881	0.373	0.881
86.07	554.9	515.0	252.8	341.1	315.9
203.8	1190.4	876.7	502.4	674.2	565.8
468.8	2319.6	1537.5	876.2	1187.2	958.1
5.447	4.180	2.986	3.466	3.480	3.032
382.7	1764.7	1022.5	623.4	846.1	642.1
2.314	2.188	1.782	1.917	1.942	1.818
176.2	946.2	514.1	328.0	449.7	341.6
1.093	-1.214	-0.621	0.191	-0.248	0.062
2.295	-0.251	0.190	0.993	0.569	0.822
3.538	0.850	0.957	1.984	1.552	1.662
3.237	-0.700	-1.543	10.40	-6.267	26.91
2.445	2.064	1.578	1.793	1.799	1.600
1.717	-0.410	-2.642	2.726	9.760	3.168
1.210	1.130	0.833	0.939	0.958	0.862
0.0%	17.1%	2.9%	0.0%	0.0%	0.0%
93.2%	82.9%	97.1%	99.1%	100.0%	99.9%
6.8%	0.0%	0.0%	0.9%	0.0%	0.1%
0.0%	0.0%	0.0%	0.0%	0.0%	0.0%
0.0%	0.0%	0.0%	0.0%	0.0%	0.0%
0.0%	0.0%	0.0%	0.0%	0.0%	0.0%
0.0%	0.0%	0.0%	0.0%	0.0%	0.0%
0.0%	17.1%	2.9%	0.0%	0.0%	0.0%
1.6%	44.6%	34.9%	4.4%	19.5%	7.6%
6.7%	31.2%	53.7%	46.0%	52.9%	53.3%
28.6%	5.7%	7.1%	40.0%	23.4%	35.5%
41.6%	1.0%	0.8%	7.1%	3.3%	2.6%
14.6%	0.4%	0.6%	1.7%	0.9%	0.8%
1.5%	0.0%	0.0%	0.3%	0.0%	0.1%
1.9%	0.0%	0.0%	0.3%	0.0%	0.0%
1.2%	0.0%	0.0%	0.3%	0.0%	0.0%
1.0%	0.0%	0.0%	0.0%	0.0%	0.0%
0.7%	0.0%	0.0%	0.0%	0.0%	0.0%
0.6%	0.0%	0.0%	0.0%	0.0%	0.0%

GRADISTAT data sheets showing the proportion of sample within grain size bounds for the 60 sub-samples taken from the 4 core samples.

SAMPLE STATISTICS

		VC1 1	VC1 2
	ANALYST AND DATE:	C. Blackler , 5/21/2024 9:45:18 AM	C. Blackler , 5/21/2024 9:53:18 AM
	LOCATION	176.112678°E 37.366425°S	
	DEPTH (cm)	55	50
	SIEVING ERROR:	0.0%	0.0%
	SAMPLE TYPE:	Unimodal, Moderately Well Sorted	Unimodal, Moderately Sorted
	TEXTURAL GROUP:	Sand	Sand
	SEDIMENT NAME:	Moderately Well Sorted Fine Sand	Moderately Sorted Fine Sand
FOLK AND WARD METHOD (μm)	MEAN (M_G):	187.5	180.8
	SORTING (σ_G):	1.592	1.665
	SKEWNESS (Sk_G):	0.005	0.002
	KURTOSIS (K_G):	0.986	1.069
FOLK AND WARD METHOD (ϕ)	MEAN (M_Z):	2.415	2.467
	SORTING (σ_I):	0.671	0.736
	SKEWNESS (Sk_I):	-0.005	-0.002
	KURTOSIS (K_G):	0.986	1.069
FOLK AND WARD METHOD (Description)	MEAN:	Fine Sand	Fine Sand
	SORTING:	Moderately Well Sorted	Moderately Sorted
	SKEWNESS:	Symmetrical	Symmetrical
	KURTOSIS:	Mesokurtic	Mesokurtic
	MODE 1 (μm):	193.5	193.5
	MODE 1 (ϕ):	2.375	2.375
	D_{10} (μm):	103.7	94.96
	D_{50} (μm):	187.3	180.4
	D_{90} (μm):	341.4	344.6
	(D_{90} / D_{10}) (μm):	3.291	3.629
	(D_{90} - D_{10}) (μm):	237.7	249.6
	(D_{75} / D_{25}) (μm):	1.892	1.944
	(D_{75} - D_{25}) (μm):	121.7	122.5
	D_{10} (ϕ):	1.550	1.537
	D_{50} (ϕ):	2.417	2.471
	D_{90} (ϕ):	3.269	3.397
	(D_{90} / D_{10}) (ϕ):	2.108	2.210
	(D_{90} - D_{10}) (ϕ):	1.719	1.859
	(D_{75} / D_{25}) (ϕ):	1.471	1.483
	(D_{75} - D_{25}) (ϕ):	0.920	0.959
	% GRAVEL:	0.0%	0.0%
	% SAND:	97.7%	96.2%
	% MUD:	2.3%	3.8%
	% V COARSE GRAVEL:	0.0%	0.0%
	% COARSE GRAVEL:	0.0%	0.0%
	% MEDIUM GRAVEL:	0.0%	0.0%
	% FINE GRAVEL:	0.0%	0.0%
	% V FINE GRAVEL:	0.0%	0.0%
	% V COARSE SAND:	0.0%	0.5%
	% COARSE SAND:	1.5%	2.6%
	% MEDIUM SAND:	25.5%	22.4%
	% FINE SAND:	54.1%	52.1%
	% V FINE SAND:	16.6%	18.6%
	% V COARSE SILT:	0.2%	0.4%
	% COARSE SILT:	1.0%	1.2%
	% MEDIUM SILT:	0.6%	0.8%
	% FINE SILT:	0.5%	0.8%
	% V FINE SILT:	0.1%	0.6%
	% CLAY:	0.0%	0.0%

VC1 3	VC1 4	VC1 5	VC1 6	VC1 7
C. Blackler , 5/21/2024 10:00:54 AM	C. Blackler , 5/21/2024 10:09:43 AM	C. Blackler , 5/21/2024 10:17:59 AM	C. Blackler , 5/21/2024 10:26:03 AM	C. Blackler , 5/21/2024 10:34:22 AM
45	40	35	30	25
0.0%	0.0%	0.0%	0.0%	0.0%
Unimodal, Moderately Sorted	Unimodal, Moderately Sorted	Unimodal, Moderately Sorted	Unimodal, Moderately Sorted	Unimodal, Moderately Sorted
Sand	Sand	Sand	Sand	Sand
Moderately Sorted Fine Sand	Moderately Sorted Fine Sand	Moderately Sorted Fine Sand	Moderately Sorted Fine Sand	Moderately Sorted Fine Sand
183.5	179.4	193.1	214.5	192.0
1.727	1.708	1.739	1.848	1.736
0.039	-0.005	0.037	0.114	0.055
1.097	1.080	1.062	1.083	1.063
2.446	2.479	2.373	2.221	2.380
0.788	0.772	0.798	0.886	0.796
-0.039	0.005	-0.037	-0.114	-0.055
1.097	1.080	1.062	1.083	1.063
Fine Sand	Fine Sand	Fine Sand	Fine Sand	Fine Sand
Moderately Sorted	Moderately Sorted	Moderately Sorted	Moderately Sorted	Moderately Sorted
Symmetrical	Symmetrical	Symmetrical	Coarse Skewed	Symmetrical
Mesokurtic	Mesokurtic	Mesokurtic	Mesokurtic	Mesokurtic
193.5	193.5	193.5	193.5	193.5
2.375	2.375	2.375	2.375	2.375
93.54	91.47	97.27	103.9	97.57
181.8	179.0	190.5	206.5	189.2
371.7	351.3	399.0	496.9	398.1
3.974	3.840	4.102	4.784	4.080
278.1	259.8	301.7	393.1	300.5
2.017	2.004	2.064	2.205	2.059
131.2	127.4	142.6	171.6	141.3
1.428	1.509	1.325	1.009	1.329
2.460	2.482	2.392	2.276	2.402
3.418	3.450	3.362	3.267	3.357
2.394	2.286	2.536	3.238	2.526
1.990	1.941	2.036	2.258	2.029
1.521	1.508	1.564	1.683	1.559
1.013	1.003	1.045	1.140	1.042
0.0%	0.0%	0.0%	0.0%	0.0%
96.3%	95.9%	96.5%	97.1%	97.0%
3.7%	4.1%	3.5%	2.9%	3.0%
0.0%	0.0%	0.0%	0.0%	0.0%
0.0%	0.0%	0.0%	0.0%	0.0%
0.0%	0.0%	0.0%	0.0%	0.0%
0.0%	0.0%	0.0%	0.0%	0.0%
0.0%	0.0%	0.0%	0.0%	0.0%
0.8%	0.1%	0.1%	1.2%	0.4%
3.9%	3.1%	5.0%	8.7%	4.9%
22.5%	22.8%	25.6%	27.5%	24.9%
50.0%	50.1%	48.8%	45.2%	49.0%
19.1%	19.8%	17.0%	14.6%	17.7%
0.6%	0.7%	0.4%	0.3%	0.4%
1.4%	1.5%	1.2%	1.0%	1.1%
0.7%	0.7%	0.8%	0.7%	0.7%
0.7%	0.8%	0.7%	0.7%	0.7%
0.4%	0.4%	0.4%	0.3%	0.3%
0.0%	0.0%	0.0%	0.0%	0.0%

VC1 8	VC1 9	VC1 10	VC1 11	VC2 1
C. Blackler , 5/21/2024 10:42:09 AM	C. Blackler , 5/21/2024 10:49:56 AM	C. Blackler , 5/21/2024 10:57:54 AM	C. Blackler , 5/21/2024 11:05:20 AM	C. Blackler , 5/21/2024 11:13:15 AM
				176.124454°E 37.36683°S
20	15	10	5	35
0.0%	0.0%	0.0%	0.0%	0.0%
Unimodal, Moderately Sorted	Unimodal, Moderately Sorted	Unimodal, Moderately Well Sorted	Unimodal, Moderately Well Sorted	Unimodal, Moderately Sorted
Sand	Sand	Sand	Sand	Sand
Moderately Sorted Fine Sand	Moderately Sorted Fine Sand	Moderately Well Sorted Fine Sand	Moderately Well Sorted Fine Sand	Moderately Sorted Coarse Sand
185.9	187.1	187.5	183.7	495.4
1.684	1.626	1.609	1.572	1.777
0.063	0.037	0.051	0.027	-0.075
1.074	1.032	1.017	0.994	0.971
2.428	2.418	2.415	2.444	1.013
0.752	0.701	0.686	0.652	0.829
-0.063	-0.037	-0.051	-0.027	0.075
1.074	1.032	1.017	0.994	0.971
Fine Sand	Fine Sand	Fine Sand	Fine Sand	Medium Sand
Moderately Sorted	Moderately Sorted	Moderately Well Sorted	Moderately Well Sorted	Moderately Sorted
Symmetrical	Symmetrical	Symmetrical	Symmetrical	Symmetrical
Mesokurtic	Mesokurtic	Mesokurtic	Mesokurtic	Mesokurtic
193.5	193.5	193.5	193.5	545.0
2.375	2.375	2.375	2.375	0.881
98.48	102.3	104.4	104.1	228.8
183.6	185.7	185.7	182.7	505.1
367.9	350.1	349.1	331.0	1003.8
3.736	3.422	3.343	3.178	4.386
269.4	247.8	244.6	226.8	775.0
1.971	1.913	1.897	1.848	2.207
128.2	123.4	121.8	114.2	405.7
1.443	1.514	1.518	1.595	-0.005
2.446	2.429	2.429	2.452	0.985
3.344	3.289	3.259	3.263	2.128
2.318	2.172	2.147	2.046	-389.978
1.901	1.775	1.741	1.668	2.133
1.504	1.479	1.472	1.442	3.651
0.979	0.936	0.924	0.886	1.142
0.0%	0.0%	0.0%	0.0%	0.0%
97.4%	97.5%	98.1%	98.3%	99.4%
2.6%	2.5%	1.9%	1.7%	0.6%
0.0%	0.0%	0.0%	0.0%	0.0%
0.0%	0.0%	0.0%	0.0%	0.0%
0.0%	0.0%	0.0%	0.0%	0.0%
0.0%	0.0%	0.0%	0.0%	0.0%
0.0%	0.0%	0.0%	0.0%	0.0%
1.1%	0.4%	0.2%	0.0%	10.1%
3.5%	2.8%	2.9%	1.5%	40.6%
22.7%	23.7%	23.7%	23.1%	36.9%
51.6%	53.6%	54.2%	55.9%	10.7%
18.6%	17.0%	17.2%	17.7%	1.2%
0.2%	0.1%	0.1%	0.1%	0.5%
0.9%	0.9%	0.7%	0.6%	0.1%
0.6%	0.7%	0.6%	0.6%	0.0%
0.6%	0.6%	0.4%	0.4%	0.0%
0.2%	0.2%	0.1%	0.1%	0.0%
0.0%	0.0%	0.0%	0.0%	0.0%

VC2 2	VC2 3	VC2 4	VC2 5	VC2 6
C. Blackler , 5/21/2024 11:20:46 AM	C. Blackler , 5/21/2024 11:28:26 AM	C. Blackler , 5/21/2024 11:35:50 AM	C. Blackler , 5/21/2024 11:43:19 AM	C. Blackler , 5/21/2024 11:53:45 AM
30	25	20	15	10
0.0%	0.0%	0.0%	0.0%	0.0%
Unimodal, Moderately Sorted	Unimodal, Moderately Well Sorted	Unimodal, Moderately Sorted	Unimodal, Moderately Sorted	Unimodal, Moderately Sorted
Sand	Sand	Sand	Sand	Sand
Moderately Sorted Medium Sand	Moderately Well Sorted Medium San	Moderately Sorted Medium Sand	Moderately Sorted Coarse Sand	Moderately Sorted Medium Sand
381.7	480.3	478.6	498.2	398.2
1.766	1.606	1.674	1.700	1.627
-0.063	-0.041	-0.030	-0.035	-0.004
1.016	0.951	0.964	0.948	0.949
1.389	1.058	1.063	1.005	1.328
0.820	0.684	0.744	0.765	0.702
0.063	0.041	0.030	0.035	0.004
1.016	0.951	0.964	0.948	0.949
Medium Sand	Medium Sand	Medium Sand	Medium Sand	Medium Sand
Moderately Sorted	Moderately Well Sorted	Moderately Sorted	Moderately Sorted	Moderately Sorted
Symmetrical	Symmetrical	Symmetrical	Symmetrical	Symmetrical
Mesokurtic	Mesokurtic	Mesokurtic	Mesokurtic	Mesokurtic
385.0	545.0	460.0	545.0	385.0
1.383	0.881	1.126	0.881	1.383
180.3	255.7	243.9	248.2	212.9
386.1	483.7	481.7	502.9	397.9
769.6	873.9	922.4	976.2	746.1
4.268	3.418	3.783	3.933	3.505
589.3	618.3	678.5	728.0	533.2
2.149	1.936	2.039	2.099	1.974
300.1	324.5	349.7	379.9	275.5
0.378	0.194	0.117	0.035	0.423
1.373	1.048	1.054	0.992	1.329
2.471	1.968	2.036	2.010	2.232
6.541	10.12	17.46	57.91	5.281
2.094	1.773	1.919	1.976	1.809
2.325	2.657	2.892	3.311	2.167
1.104	0.953	1.028	1.070	0.981
0.0%	0.0%	0.0%	0.0%	0.0%
97.8%	99.7%	99.7%	99.6%	99.5%
2.2%	0.3%	0.3%	0.4%	0.5%
0.0%	0.0%	0.0%	0.0%	0.0%
0.0%	0.0%	0.0%	0.0%	0.0%
0.0%	0.0%	0.0%	0.0%	0.0%
0.0%	0.0%	0.0%	0.0%	0.0%
0.0%	0.0%	0.0%	0.0%	0.0%
2.8%	4.8%	6.8%	8.9%	1.9%
29.3%	42.6%	40.4%	41.5%	30.5%
45.4%	43.6%	42.1%	39.4%	50.2%
18.5%	8.3%	9.8%	9.6%	16.6%
1.8%	0.5%	0.6%	0.3%	0.3%
0.9%	0.3%	0.3%	0.4%	0.5%
0.5%	0.0%	0.0%	0.0%	0.0%
0.5%	0.0%	0.0%	0.0%	0.0%
0.4%	0.0%	0.0%	0.0%	0.0%
0.0%	0.0%	0.0%	0.0%	0.0%
0.0%	0.0%	0.0%	0.0%	0.0%

VC2 7	VC3 1	VC3 2	VC3 3	VC3 4
C. Blackler , 5/21/2024 12:01:24 PM	C. Blackler , 5/21/2024 12:08:50 PM	C. Blackler , 5/21/2024 12:16:46 PM	C. Blackler , 5/21/2024 12:46:31 PM	C. Blackler , 5/21/2024 12:54:02 PM
	176.136123°E 37.36695°S			
5	150	145	140	135
0.0%	0.0%	0.1%	0.1%	0.0%
Unimodal, Moderately Sorted	Unimodal, Moderately Sorted	Unimodal, Poorly Sorted	Unimodal, Poorly Sorted	Unimodal, Moderately Sorted
Sand	Sand	Muddy Sand	Sand	Sand
Moderately Sorted Medium Sand	Moderately Sorted Fine Sand	Very Coarse Silty Fine Sand	Poorly Sorted Fine Sand	Moderately Sorted Fine Sand
439.7	153.8	143.3	150.7	141.5
1.725	1.947	2.046	2.107	1.825
-0.025	-0.204	-0.274	-0.189	-0.231
0.951	1.533	1.645	1.666	1.503
1.185	2.701	2.803	2.730	2.822
0.786	0.962	1.033	1.075	0.868
0.025	0.204	0.274	0.189	0.231
0.951	1.533	1.645	1.666	1.503
Medium Sand	Fine Sand	Fine Sand	Fine Sand	Fine Sand
Moderately Sorted	Moderately Sorted	Poorly Sorted	Poorly Sorted	Moderately Sorted
Symmetrical	Fine Skewed	Fine Skewed	Fine Skewed	Fine Skewed
Mesokurtic	Very Leptokurtic	Very Leptokurtic	Very Leptokurtic	Very Leptokurtic
460.0	163.0	163.0	163.0	163.0
1.126	2.622	2.622	2.622	2.622
215.1	73.04	59.03	65.36	71.31
441.5	155.8	148.4	152.4	144.0
879.7	298.1	280.9	314.1	254.3
4.089	4.081	4.759	4.805	3.567
664.6	225.1	221.9	248.7	183.0
2.140	2.032	2.063	2.112	1.914
343.7	111.9	107.6	116.1	94.13
0.185	1.746	1.832	1.671	1.975
1.179	2.682	2.753	2.714	2.796
2.217	3.775	4.082	3.935	3.810
11.99	2.162	2.229	2.355	1.929
2.032	2.029	2.251	2.265	1.835
2.736	1.469	1.462	1.495	1.400
1.098	1.023	1.045	1.079	0.937
0.0%	0.0%	0.0%	0.0%	0.0%
99.4%	92.2%	89.5%	90.7%	92.3%
0.6%	7.8%	10.5%	9.3%	7.7%
0.0%	0.0%	0.0%	0.0%	0.0%
0.0%	0.0%	0.0%	0.0%	0.0%
0.0%	0.0%	0.0%	0.0%	0.0%
0.0%	0.0%	0.0%	0.0%	0.0%
0.0%	0.0%	0.0%	0.0%	0.0%
5.7%	0.2%	0.0%	0.5%	0.0%
35.6%	1.3%	0.2%	2.8%	0.0%
43.1%	16.1%	14.6%	14.9%	10.6%
14.3%	48.8%	47.8%	45.9%	51.0%
0.8%	25.9%	27.0%	26.5%	30.7%
0.5%	2.1%	3.1%	2.6%	2.2%
0.0%	2.4%	2.9%	2.6%	2.4%
0.0%	1.4%	1.8%	1.6%	1.3%
0.0%	1.2%	1.4%	1.3%	1.1%
0.0%	0.7%	0.8%	0.8%	0.6%
0.0%	0.1%	0.4%	0.4%	0.0%

VC3 5	VC3 6	VC3 7	VC3 8	VC3 9
C. Blackler , 5/21/2024 1:01:31 PM	C. Blackler , 5/21/2024 1:09:18 PM	C. Blackler , 5/21/2024 1:17:00 PM	C. Blackler , 5/21/2024 1:24:27 PM	C. Blackler , 5/21/2024 1:32:00 PM
130	125	120	115	110
0.0%	0.1%	0.0%	0.2%	0.2%
Unimodal, Poorly Sorted	Unimodal, Poorly Sorted	Unimodal, Moderately Sorted	Unimodal, Poorly Sorted	Unimodal, Poorly Sorted
Sand	Muddy Sand	Sand	Muddy Sand	Muddy Sand
Poorly Sorted Fine Sand	Very Coarse Silty Fine Sand	Moderately Sorted Fine Sand	Very Coarse Silty Fine Sand	Very Coarse Silty Fine Sand
161.1	146.2	146.3	141.8	126.6
2.008	2.080	1.950	2.140	2.128
-0.165	-0.241	-0.202	-0.199	-0.315
1.554	1.619	1.532	1.723	1.680
2.634	2.774	2.773	2.818	2.981
1.006	1.056	0.963	1.098	1.090
0.165	0.241	0.202	0.199	0.315
1.554	1.619	1.532	1.723	1.680
Fine Sand	Fine Sand	Fine Sand	Fine Sand	Fine Sand
Poorly Sorted	Poorly Sorted	Moderately Sorted	Poorly Sorted	Poorly Sorted
Fine Skewed	Fine Skewed	Fine Skewed	Fine Skewed	Very Fine Skewed
Very Leptokurtic	Very Leptokurtic	Very Leptokurtic	Very Leptokurtic	Very Leptokurtic
163.0	163.0	163.0	137.0	137.0
2.622	2.622	2.622	2.873	2.873
75.77	62.07	68.07	58.48	37.58
161.9	149.9	148.6	144.5	133.8
328.5	295.4	288.1	296.4	250.1
4.336	4.760	4.232	5.069	6.655
252.7	233.4	220.0	238.0	212.5
2.083	2.115	2.030	2.109	2.111
121.2	113.4	106.4	109.1	99.70
1.606	1.759	1.795	1.754	1.999
2.627	2.738	2.750	2.791	2.902
3.722	4.010	3.877	4.096	4.734
2.318	2.280	2.159	2.335	2.368
2.116	2.251	2.081	2.342	2.734
1.504	1.487	1.453	1.475	1.449
1.058	1.081	1.022	1.077	1.078
0.0%	0.0%	0.0%	0.0%	0.0%
92.7%	89.9%	91.5%	89.4%	86.1%
7.3%	10.1%	8.5%	10.6%	13.9%
0.0%	0.0%	0.0%	0.0%	0.0%
0.0%	0.0%	0.0%	0.0%	0.0%
0.0%	0.0%	0.0%	0.0%	0.0%
0.0%	0.0%	0.0%	0.0%	0.0%
0.0%	0.0%	0.0%	0.0%	0.0%
0.7%	0.0%	0.3%	0.4%	0.0%
2.6%	1.2%	1.4%	3.1%	0.0%
17.6%	15.5%	13.7%	12.2%	10.0%
47.8%	46.1%	47.5%	44.9%	45.0%
24.1%	27.0%	28.5%	28.8%	31.0%
1.7%	3.0%	2.7%	3.1%	4.7%
2.3%	2.7%	2.4%	3.0%	3.7%
1.4%	1.8%	1.4%	1.8%	2.4%
1.1%	1.4%	1.2%	1.4%	1.6%
0.7%	0.8%	0.7%	0.9%	1.0%
0.1%	0.4%	0.1%	0.4%	0.5%

VC3 10	VC3 11	VC3 12	VC3 13	VC3 14
C. Blackler , 5/21/2024 1:40:57 PM	C. Blackler , 5/21/2024 1:48:17 PM	C. Blackler , 5/21/2024 1:55:31 PM	C. Blackler , 5/21/2024 2:02:54 PM	C. Blackler , 5/21/2024 2:10:33 PM
105	100	95	90	85
0.1%	0.3%	0.3%	0.3%	0.3%
Unimodal, Poorly Sorted	Unimodal, Poorly Sorted	Unimodal, Poorly Sorted	Unimodal, Poorly Sorted	Unimodal, Poorly Sorted
Muddy Sand	Muddy Sand	Muddy Sand	Muddy Sand	Muddy Sand
Very Coarse Silty Fine Sand	Coarse Silty Fine Sand	Very Coarse Silty Fine Sand	Very Coarse Silty Fine Sand	Very Coarse Silty Fine Sand
135.8	148.7	139.0	140.3	155.9
2.088	2.583	2.631	2.574	2.470
-0.265	-0.313	-0.256	-0.227	-0.186
1.660	1.699	1.718	1.763	1.681
2.880	2.749	2.847	2.834	2.681
1.062	1.369	1.396	1.364	1.304
0.265	0.313	0.256	0.227	0.186
1.660	1.699	1.718	1.763	1.681
Fine Sand	Fine Sand	Fine Sand	Fine Sand	Fine Sand
Poorly Sorted	Poorly Sorted	Poorly Sorted	Poorly Sorted	Poorly Sorted
Fine Skewed	Very Fine Skewed	Fine Skewed	Fine Skewed	Fine Skewed
Very Leptokurtic	Very Leptokurtic	Very Leptokurtic	Very Leptokurtic	Very Leptokurtic
137.0	163.0	163.0	163.0	163.0
2.873	2.622	2.622	2.622	2.622
53.81	26.47	26.28	28.77	45.40
140.3	161.3	147.5	147.3	158.9
271.3	357.9	351.2	348.7	391.2
5.042	13.52	13.36	12.12	8.616
217.5	331.4	324.9	320.0	345.8
2.098	2.509	2.535	2.451	2.445
104.4	148.5	139.1	134.0	145.8
1.882	1.482	1.510	1.520	1.354
2.834	2.632	2.761	2.763	2.654
4.216	5.239	5.250	5.119	4.461
2.240	3.534	3.477	3.368	3.295
2.334	3.757	3.740	3.599	3.107
1.460	1.658	1.633	1.604	1.639
1.069	1.327	1.342	1.294	1.290
0.0%	0.0%	0.0%	0.0%	0.0%
88.4%	85.1%	84.3%	85.1%	87.7%
11.6%	14.9%	15.7%	14.9%	12.3%
0.0%	0.0%	0.0%	0.0%	0.0%
0.0%	0.0%	0.0%	0.0%	0.0%
0.0%	0.0%	0.0%	0.0%	0.0%
0.0%	0.0%	0.0%	0.0%	0.0%
0.0%	0.0%	0.0%	0.0%	0.0%
0.7%	0.0%	0.4%	0.9%	0.6%
0.7%	3.3%	4.2%	4.4%	5.3%
11.5%	21.0%	16.5%	15.1%	18.4%
45.7%	40.4%	38.8%	39.9%	40.2%
29.8%	20.4%	24.4%	24.9%	23.2%
3.7%	3.9%	4.8%	4.5%	3.7%
3.1%	4.0%	4.0%	4.0%	3.2%
2.1%	3.0%	3.0%	2.8%	2.2%
1.5%	2.1%	2.1%	1.9%	1.6%
0.9%	1.2%	1.3%	1.1%	1.0%
0.4%	0.6%	0.6%	0.6%	0.5%

VC3 15	VC3 16	VC3 17	VC3 18	VC3 19
C. Blackler , 5/21/2024 2:20:56 PM	C. Blackler , 5/21/2024 2:28:17 PM	C. Blackler , 5/21/2024 2:35:40 PM	C. Blackler , 5/21/2024 2:43:35 PM	C. Blackler , 5/21/2024 2:51:14 PM
80	75	70	65	60
0.6%	0.6%	0.4%	0.1%	0.0%
Trimodal, Poorly Sorted	Unimodal, Poorly Sorted	Unimodal, Poorly Sorted	Unimodal, Moderately Sorted	Unimodal, Moderately Sorted
Muddy Sand	Muddy Sand	Sand	Sand	Sand
Very Coarse Silty Fine Sand	Very Coarse Silty Fine Sand	Poorly Sorted Coarse Sand	Moderately Sorted Medium Sand	Moderately Sorted Coarse Sand
193.6	181.1	406.4	420.2	461.4
3.570	3.484	2.338	1.941	1.764
-0.276	-0.250	-0.334	-0.260	-0.192
1.284	1.363	1.558	1.282	1.159
2.369	2.465	1.299	1.251	1.116
1.836	1.801	1.225	0.957	0.819
0.276	0.250	0.334	0.260	0.192
1.284	1.363	1.558	1.282	1.159
Fine Sand	Fine Sand	Medium Sand	Medium Sand	Medium Sand
Poorly Sorted	Poorly Sorted	Poorly Sorted	Moderately Sorted	Moderately Sorted
Fine Skewed	Fine Skewed	Very Fine Skewed	Fine Skewed	Fine Skewed
Leptokurtic	Leptokurtic	Very Leptokurtic	Leptokurtic	Leptokurtic
193.5	163.0	545.0	545.0	545.0
2.375	2.622	0.881	0.881	0.881
21.90	21.47	125.0	166.5	215.2
215.0	196.3	440.2	444.9	478.0
692.2	645.7	885.4	827.7	861.3
31.61	30.07	7.083	4.971	4.002
670.3	624.2	760.4	661.2	646.1
4.401	4.000	2.416	2.177	2.029
343.7	295.0	383.3	343.5	338.4
0.531	0.631	0.176	0.273	0.215
2.218	2.349	1.184	1.168	1.065
5.513	5.541	3.000	2.586	2.216
10.39	8.780	17.08	9.478	10.29
4.982	4.910	2.824	2.314	2.001
2.829	2.486	3.077	2.715	2.749
2.138	2.000	1.273	1.122	1.021
0.0%	0.0%	0.0%	0.0%	0.0%
83.5%	83.3%	93.7%	96.0%	97.7%
16.5%	16.7%	6.3%	4.0%	2.3%
0.0%	0.0%	0.0%	0.0%	0.0%
0.0%	0.0%	0.0%	0.0%	0.0%
0.0%	0.0%	0.0%	0.0%	0.0%
0.0%	0.0%	0.0%	0.0%	0.0%
0.0%	0.0%	0.0%	0.0%	0.0%
1.9%	1.6%	5.7%	3.3%	4.2%
18.9%	15.7%	36.2%	38.4%	42.4%
23.9%	23.4%	36.2%	39.5%	39.8%
24.2%	26.9%	12.0%	11.7%	8.9%
14.5%	15.7%	3.7%	3.2%	2.3%
4.5%	4.5%	1.6%	1.2%	0.8%
4.0%	4.0%	1.3%	0.8%	0.6%
3.2%	3.2%	1.2%	0.7%	0.5%
2.4%	2.4%	1.0%	0.6%	0.4%
1.6%	1.6%	0.8%	0.5%	0.1%
0.9%	1.0%	0.5%	0.1%	0.0%

VC3 20	VC3 21	VC3 22	VC3 23	VC3 24
C. Blackler , 5/21/2024 2:59:19 PM	C. Blackler , 5/21/2024 3:07:00 PM	C. Blackler , 5/21/2024 3:14:56 PM	C. Blackler , 5/21/2024 3:22:39 PM	C. Blackler , 5/21/2024 3:31:01 PM
55	50	45	40	35
0.0%	2.5%	0.0%	0.0%	1.3%
Unimodal, Moderately Well Sorted	Unimodal, Very Poorly Sorted	Unimodal, Moderately Sorted	Unimodal, Moderately Sorted	Unimodal, Poorly Sorted
Sand	Sandy Mud	Sand	Sand	Muddy Sand
Moderately Well Sorted Coarse San	Very Fine Sandy Very Coarse Silt	Moderately Sorted Coarse Sand	Moderately Sorted Coarse Sand	Coarse Silty Medium Sand
559.2	29.05	548.7	454.7	265.3
1.515	4.422	1.869	1.867	2.950
-0.057	-0.170	-0.216	-0.148	-0.376
0.970	0.941	1.206	1.053	1.538
0.839	5.105	0.866	1.137	1.914
0.599	2.145	0.903	0.901	1.561
0.057	0.170	0.216	0.148	0.376
0.970	0.941	1.206	1.053	1.538
Coarse Sand	Coarse Silt	Coarse Sand	Medium Sand	Medium Sand
Moderately Well Sorted	Very Poorly Sorted	Moderately Sorted	Moderately Sorted	Poorly Sorted
Symmetrical	Fine Skewed	Fine Skewed	Fine Skewed	Very Fine Skewed
Mesokurtic	Mesokurtic	Leptokurtic	Mesokurtic	Very Leptokurtic
545.0	48.50	650.0	545.0	385.0
0.881	4.372	0.628	0.881	1.383
322.7	3.548	230.7	192.3	37.41
565.1	34.63	573.4	472.6	304.3
942.5	170.8	1078.5	941.3	704.4
2.921	48.14	4.674	4.895	18.83
619.8	167.3	847.8	749.0	666.9
1.777	7.919	2.145	2.274	3.072
328.3	74.02	435.3	389.8	333.9
0.085	2.550	-0.109	0.087	0.506
0.823	4.852	0.802	1.081	1.716
1.632	8.139	2.116	2.378	4.740
19.10	3.192	-19.398	27.26	9.375
1.546	5.589	2.225	2.291	4.235
3.004	1.838	4.745	3.264	2.596
0.830	2.985	1.101	1.185	1.619
0.0%	0.0%	0.0%	0.0%	0.0%
99.9%	33.3%	97.4%	97.7%	87.7%
0.1%	66.7%	2.6%	2.3%	12.3%
0.0%	0.0%	0.0%	0.0%	0.0%
0.0%	0.0%	0.0%	0.0%	0.0%
0.0%	0.0%	0.0%	0.0%	0.0%
0.0%	0.0%	0.0%	0.0%	0.0%
0.0%	0.0%	0.0%	0.0%	0.0%
6.8%	0.0%	13.1%	7.5%	1.7%
54.5%	0.5%	46.5%	38.8%	22.8%
35.5%	4.6%	29.2%	36.8%	34.8%
1.9%	10.7%	6.5%	12.4%	21.8%
1.2%	17.6%	2.1%	2.1%	6.7%
0.1%	19.5%	0.9%	0.8%	3.1%
0.0%	16.2%	0.7%	0.6%	3.3%
0.0%	11.0%	0.5%	0.5%	2.6%
0.0%	9.0%	0.4%	0.4%	2.0%
0.0%	6.9%	0.1%	0.1%	0.4%
0.0%	4.1%	0.0%	0.0%	0.8%

VC3 25	VC3 26	VC3 27	VC3 28	VC3 29
C. Blackler , 5/21/2024 3:38:26 PM	C. Blackler , 5/21/2024 3:46:13 PM	C. Blackler , 5/21/2024 3:53:49 PM	C. Blackler , 5/21/2024 4:01:55 PM	C. Blackler , 5/21/2024 4:09:44 PM
30	25	20	15	10
0.9%	1.8%	0.2%	0.2%	0.1%
Bimodal, Very Poorly Sorted	Bimodal, Poorly Sorted	Unimodal, Moderately Sorted	Unimodal, Moderately Sorted	Unimodal, Moderately Sorted
Muddy Sand	Muddy Sand	Slightly Gravelly Sand	Sand	Sand
Very Coarse Silty Medium Sand	Very Coarse Silty Medium Sand	Slightly Very Fine Gravelly Fine Sand	Moderately Sorted Medium Sand	Moderately Sorted Medium Sand
147.5	141.8	256.4	402.9	380.0
4.369	3.390	1.959	1.962	1.767
-0.413	-0.406	-0.004	-0.084	-0.107
0.919	1.108	1.139	1.079	1.047
2.761	2.818	1.963	1.312	1.396
2.127	1.761	0.970	0.972	0.821
0.413	0.406	0.004	0.084	0.107
0.919	1.108	1.139	1.079	1.047
Fine Sand	Fine Sand	Medium Sand	Medium Sand	Medium Sand
Very Poorly Sorted	Poorly Sorted	Moderately Sorted	Moderately Sorted	Moderately Sorted
Very Fine Skewed	Very Fine Skewed	Symmetrical	Symmetrical	Fine Skewed
Mesokurtic	Mesokurtic	Leptokurtic	Mesokurtic	Mesokurtic
385.0	230.0	230.0	460.0	385.0
1.383	2.126	2.126	1.126	1.383
15.23	20.79	112.7	165.2	177.2
216.4	190.7	253.2	408.5	388.0
665.1	487.1	593.0	905.7	749.3
43.66	23.43	5.264	5.483	4.228
649.8	466.3	480.3	740.5	572.1
8.346	4.567	2.333	2.405	2.123
378.9	253.7	223.2	366.7	294.6
0.588	1.038	0.754	0.143	0.416
2.208	2.391	1.982	1.292	1.366
6.037	5.588	3.150	2.598	2.496
10.26	5.385	4.178	18.19	5.996
5.448	4.550	2.396	2.455	2.080
3.517	2.351	1.901	2.885	2.287
3.061	2.191	1.222	1.266	1.086
0.0%	0.0%	0.0%	0.0%	0.0%
72.1%	76.7%	95.4%	96.8%	97.6%
27.9%	23.3%	4.6%	3.2%	2.4%
0.0%	0.0%	0.0%	0.0%	0.0%
0.0%	0.0%	0.0%	0.0%	0.0%
0.0%	0.0%	0.0%	0.0%	0.0%
0.0%	0.0%	0.0%	0.0%	0.0%
0.0%	0.0%	0.0%	0.0%	0.0%
1.5%	0.1%	2.4%	7.1%	2.0%
17.8%	9.1%	12.4%	30.5%	30.0%
26.1%	28.1%	35.9%	39.5%	45.8%
17.1%	27.9%	36.7%	17.0%	17.5%
9.6%	11.5%	7.9%	2.7%	2.4%
10.3%	9.5%	1.3%	1.1%	1.0%
7.4%	6.4%	1.5%	0.8%	0.6%
4.7%	3.6%	0.9%	0.7%	0.5%
3.1%	2.7%	0.8%	0.5%	0.4%
1.6%	0.4%	0.2%	0.1%	0.0%
0.8%	0.7%	0.0%	0.0%	0.0%

VC3 30	VC4 1	VC4 2	VC4 3	VC4 4
C. Blackler , 5/21/2024 4:17:32 PM	C. Blackler , 5/21/2024 4:29:47 PM	C. Blackler , 5/21/2024 4:37:07 PM	C. Blackler , 5/21/2024 4:44:43 PM	C. Blackler , 5/21/2024 4:51:57 PM
	176.148632°E 37.366691°S			
5	60	55	50	45
-1.2%	0.5%	-0.1%	0.2%	0.5%
Unimodal, Moderately Sorted	Unimodal, Poorly Sorted	Unimodal, Poorly Sorted	Unimodal, Poorly Sorted	Unimodal, Poorly Sorted
Sand	Muddy Sand	Muddy Sand	Muddy Sand	Muddy Sand
Moderately Sorted Medium Sand	Coarse Silty Fine Sand	Coarse Silty Fine Sand	Coarse Silty Fine Sand	Very Coarse Silty Fine Sand
419.3	170.7	187.6	154.8	182.4
1.753	2.763	2.717	2.525	2.985
-0.129	-0.266	-0.171	-0.257	-0.164
1.046	1.666	1.609	1.771	1.576
1.254	2.551	2.414	2.691	2.455
0.810	1.466	1.442	1.336	1.578
0.129	0.266	0.171	0.257	0.164
1.046	1.666	1.609	1.771	1.576
Medium Sand	Fine Sand	Fine Sand	Fine Sand	Fine Sand
Moderately Sorted	Poorly Sorted	Poorly Sorted	Poorly Sorted	Poorly Sorted
Fine Skewed	Fine Skewed	Fine Skewed	Fine Skewed	Fine Skewed
Mesokurtic	Very Leptokurtic	Very Leptokurtic	Very Leptokurtic	Very Leptokurtic
460.0	193.5	193.5	163.0	163.0
1.126	2.375	2.375	2.622	2.622
195.9	28.40	48.56	32.59	31.80
431.5	182.3	188.1	161.2	182.4
812.7	458.7	529.8	369.2	577.3
4.148	16.15	10.91	11.33	18.15
616.7	430.3	481.2	336.6	545.5
2.104	2.713	2.769	2.427	3.060
322.6	184.7	201.0	145.1	218.2
0.299	1.124	0.917	1.437	0.793
1.213	2.456	2.410	2.633	2.455
2.352	5.138	4.364	4.939	4.975
7.857	4.570	4.762	3.436	6.276
2.052	4.014	3.448	3.502	4.182
2.530	1.812	1.881	1.634	1.993
1.073	1.440	1.470	1.279	1.614
0.0%	0.0%	0.0%	0.0%	0.0%
97.5%	85.8%	88.6%	87.0%	86.5%
2.5%	14.2%	11.4%	13.0%	13.5%
0.0%	0.0%	0.0%	0.0%	0.0%
0.0%	0.0%	0.0%	0.0%	0.0%
0.0%	0.0%	0.0%	0.0%	0.0%
0.0%	0.0%	0.0%	0.0%	0.0%
0.0%	0.0%	0.0%	0.0%	0.0%
3.1%	0.8%	1.4%	0.3%	1.9%
36.1%	7.2%	9.8%	4.2%	11.2%
43.2%	24.5%	23.9%	19.8%	22.0%
13.5%	36.9%	36.2%	41.0%	33.5%
1.6%	16.4%	17.4%	21.7%	18.1%
0.6%	3.7%	2.8%	3.1%	3.6%
0.4%	3.8%	2.9%	3.3%	3.4%
0.3%	3.0%	2.3%	2.7%	2.6%
0.0%	2.2%	1.7%	2.0%	2.0%
1.2%	1.0%	1.2%	1.3%	1.2%
0.0%	0.6%	0.4%	0.6%	0.7%

VC45	VC46	VC47	VC48	VC49
C. Blackler , 5/21/2024 4:59:54 PM	C. Blackler , 5/21/2024 5:07:41 PM	C. Blackler , 5/21/2024 5:15:15 PM	C. Blackler , 5/21/2024 5:22:56 PM	C. Blackler , 5/21/2024 5:30:31 PM
40	35	30	25	20
0.5%	1.1%	0.2%	0.2%	0.0%
Unimodal, Poorly Sorted	Unimodal, Poorly Sorted	Unimodal, Poorly Sorted	Unimodal, Moderately Sorted	Unimodal, Moderately Sorted
Muddy Sand	Muddy Sand	Sand	Sand	Sand
Very Coarse Silty Fine Sand	Very Coarse Silty Fine Sand	Poorly Sorted Coarse Sand	Moderately Sorted Coarse Sand	Moderately Sorted Coarse Sand
168.9	219.5	489.9	510.4	562.0
2.913	2.915	2.180	1.919	1.834
-0.158	-0.141	-0.274	-0.237	-0.222
1.617	1.332	1.164	1.183	1.168
2.566	2.188	1.029	0.970	0.831
1.542	1.543	1.125	0.940	0.875
0.158	0.141	0.274	0.237	0.222
1.617	1.332	1.164	1.183	1.168
Fine Sand	Fine Sand	Medium Sand	Coarse Sand	Coarse Sand
Poorly Sorted	Poorly Sorted	Poorly Sorted	Moderately Sorted	Moderately Sorted
Fine Skewed	Fine Skewed	Fine Skewed	Fine Skewed	Fine Skewed
Very Leptokurtic	Leptokurtic	Leptokurtic	Leptokurtic	Leptokurtic
163.0	193.5	650.0	650.0	650.0
2.622	2.375	0.628	0.628	0.628
30.32	56.01	151.8	199.1	236.1
169.4	215.4	542.3	542.7	592.1
530.6	687.9	1127.4	1028.9	1090.0
17.50	12.28	7.428	5.168	4.616
500.3	631.9	975.6	829.8	853.8
2.920	3.468	2.592	2.212	2.116
192.0	295.3	504.3	427.6	438.9
0.914	0.540	-0.173	-0.041	-0.124
2.562	2.215	0.883	0.882	0.756
5.044	4.158	2.720	2.329	2.082
5.517	7.704	-15.723	-56.654	-16.749
4.130	3.618	2.893	2.370	2.207
1.871	2.414	5.831	4.203	5.076
1.546	1.794	1.374	1.145	1.082
0.0%	0.0%	0.0%	0.0%	0.0%
86.0%	89.3%	96.4%	97.6%	98.4%
14.0%	10.7%	3.6%	2.4%	1.6%
0.0%	0.0%	0.0%	0.0%	0.0%
0.0%	0.0%	0.0%	0.0%	0.0%
0.0%	0.0%	0.0%	0.0%	0.0%
0.0%	0.0%	0.0%	0.0%	0.0%
0.0%	0.0%	0.0%	0.0%	0.0%
1.5%	2.6%	14.7%	11.0%	13.8%
9.6%	16.4%	40.0%	44.6%	48.0%
19.9%	24.6%	26.8%	30.3%	27.4%
34.8%	29.8%	10.6%	8.7%	6.9%
20.3%	15.8%	4.2%	2.9%	2.3%
3.9%	2.9%	1.1%	0.7%	0.5%
3.6%	2.8%	0.9%	0.7%	0.5%
2.7%	2.2%	0.8%	0.6%	0.4%
2.0%	1.8%	0.6%	0.5%	0.2%
1.2%	0.5%	0.2%	0.0%	0.0%
0.7%	0.6%	0.0%	0.0%	0.0%

VC4 10	VC4 11	VC4 12
C. Blackler , 5/21/2024 5:38:00 PM	C. Blackler , 5/21/2024 5:45:42 PM	C. Blackler , 5/21/2024 5:53:02 PM
15	10	5
-0.2%	0.1%	0.1%
Unimodal, Moderately Sorted	Unimodal, Poorly Sorted	Unimodal, Moderately Sorted
Sand	Sand	Sand
Moderately Sorted Coarse Sand	Poorly Sorted Coarse Sand	Moderately Sorted Coarse Sand
538.4	493.7	600.1
1.908	2.076	1.725
-0.225	-0.287	-0.163
1.156	1.184	1.125
0.893	1.018	0.737
0.932	1.054	0.786
0.225	0.287	0.163
1.156	1.184	1.125
Coarse Sand	Medium Sand	Coarse Sand
Moderately Sorted	Poorly Sorted	Moderately Sorted
Fine Skewed	Fine Skewed	Fine Skewed
Leptokurtic	Leptokurtic	Leptokurtic
650.0	650.0	650.0
0.628	0.628	0.628
213.8	159.0	286.6
571.1	545.5	617.8
1091.6	1069.4	1117.4
5.105	6.728	3.899
877.7	910.5	830.8
2.228	2.407	2.002
452.9	467.7	429.5
-0.126	-0.097	-0.160
0.808	0.874	0.695
2.225	2.653	1.803
-17.610	-27.406	-11.257
2.352	2.750	1.963
5.080	4.937	5.532
1.156	1.267	1.002
0.0%	0.0%	0.0%
97.8%	97.2%	98.2%
2.2%	2.8%	1.8%
0.0%	0.0%	0.0%
0.0%	0.0%	0.0%
0.0%	0.0%	0.0%
0.0%	0.0%	0.0%
0.0%	0.0%	0.0%
13.7%	12.6%	15.2%
45.2%	42.9%	50.4%
28.4%	27.3%	26.9%
8.1%	10.0%	4.1%
2.5%	4.4%	1.6%
0.6%	0.9%	0.5%
0.6%	0.8%	0.5%
0.4%	0.6%	0.4%
0.3%	0.5%	0.4%
0.2%	0.1%	0.0%
0.0%	0.0%	0.0%

Appendix B. Raw Mastersizer Data

Mastersizer® data sheets showing the proportion of samples under grain size boundaries for the 64 surfice sediment samples.

	Sample Name	A1	A2	A3
	Measurement Date Time	20/09/2023 13:15	20/09/2023 13:23	20/09/2023 13:31
	Sample Location	176.1945788°E 37.6108884°S	176.1972734°E 37.6142843°S	176.2005804°E 37.6176800°S
Grain Size (um)	0.05	0	0	0
	0.06	0	0	0
	0.12	0	0	0
	0.24	0	0	0
	0.49	0.21	0	0
	0.98	0.25	0	0
	2	0.61	0	0
	3.9	0.86	0	0
	7.8	1.04	0	0
	15.6	1.44	0	0
	31	0.36	0	0.02
	37	0.32	0	0.1
	44	0.39	0.08	0.14
	53	0.61	0.09	0.13
	63	0.95	0.09	0.11
	74	1.74	0.11	0.01
	88	2.8	0.19	0
	105	3.75	0.35	0.07
	125	4.81	0.79	0.46
	149	5.38	1.48	1.24
	177	5.7	2.47	2.48
	210	6.02	4.25	4.67
	250	6.44	6.46	7.26
	300	5.68	7.25	8.12
	350	7.29	10.87	11.81
	420	7.59	11.86	12.41
	500	7.69	11.89	11.91
	590	8.59	12.8	12.18
	710	7.11	10.28	9.37
	840	5.89	8.42	7.34
	1000	3.97	5.84	4.9
	1190	2.13	3.41	2.95
	1410	0.38	1.02	1.5
	1680	0	0	0.61
	2000	0	0	0.21
	2380	0	0	0
	2830	0	0	0
	3360	0	0	0
Statistics	Dx (10)	95.9	251	254
	Dx (50)	356	526	507
	Dx (90)	897	1010	1010
	D [4,3]	431	582	579
	D [3,2]	74.2	435	429
	Kurtosis [3]	0.132	0.268	2.437
	Skew [3]	0.87	0.819	1.35
	Mode	596	555	507
	Span	2.25	1.437	1.482
	Laser Obscuration	17.48	11.1	4.82
	Weighted Residual	0.37	0.48	0.47
	Residual	0.36	0.54	0.52

A4	A5	A6	A7	A8
20/09/2023 13:39	20/09/2023 13:47	20/09/2023 13:55	20/09/2023 14:03	20/09/2023 14:11
176.2038874°E 37.6209785°S	176.2071944°E 37.6241799°S	176.2101340°E 37.6275751°S	176.2134410°E 37.6307762°S	176.2166255°E 37.6342681°S
0	0	0	0	0
0	0	0	0	0
0	0	0	0	0
0.08	0	0	0	0
6.53	0	0	0.23	0.2
8.62	0	0	0.19	0.05
12.26	0.26	0	0.7	0.72
15.65	0.65	0	1.07	1.03
17.92	0.61	0	1.28	1.08
16.65	1.1	0.33	2.1	1.75
3.41	0.24	0.01	0.29	0.22
2.97	0.12	0	0.15	0.05
2.81	0.01	0.01	0.27	0.05
2.28	0.1	0.1	0.93	0.62
1.87	0.56	0.15	2.05	1.77
1.65	1.87	0.24	4.25	4.13
1.21	4.16	0.33	7.13	7.38
0.72	6.64	0.4	9.54	10.12
0.23	9.68	0.44	11.83	12.69
0	11.61	0.48	12.49	13.33
0	12.58	0.62	12.15	12.7
0	12.62	1.15	10.79	10.81
0	11.72	2.25	9.03	8.52
0	8.1	3.27	5.62	4.86
0	6.82	6.47	4.13	3.14
0.07	4.38	8.76	2.26	1.5
0.35	2.59	10.56	1.05	0.65
0.86	1.59	13.67	0.4	0.43
1.02	0.89	12.64	0.07	0.4
1.06	0.56	11.95	0	0.47
0.86	0.34	9.66	0	0.47
0.58	0.18	7.02	0	0.39
0.29	0.02	4.6	0	0.28
0.05	0	2.64	0	0.16
0	0	1.41	0	0.03
0	0	0.58	0	0
0	0	0.23	0	0
0	0	0	0	0
1.31	106	353	77	82.9
10.2	209	717	166	166
67.3	428	1390	329	326
64.6	246	809	186	202
3.97	123	534	59.2	66.5
21.795	8.08	2.928	1.967	29.837
4.631	2.196	1.368	1.102	4.615
14	205	730	169	165
6.443	1.536	1.448	1.516	1.468
3.43	19.46	10.76	18.18	19.15
1.18	0.28	0.92	0.26	0.3
1.08	0.27	0.98	0.26	0.3

B1	B2	B3	B4	B5
20/09/2023 14:19	20/09/2023 14:27	20/09/2023 14:35	20/09/2023 14:43	20/09/2023 14:51
176.1975184°E 37.6076865°S	176.2010704°E 37.6112765°S	176.2038874°E 37.6142843°S	176.2070719°E 37.6177770°S	176.2103789°E 37.6210755°S
0	0	0	0	0
0	0	0	0	0
0	0	0	0	0
0	0	0	0	0
0	0	0	0	0
0	0	0	0	0
0	0	0	0	0
0	0	0	0	0
0.18	0	0	0.24	0
0.52	0.28	0	0.44	0
0.08	0.13	0	0.15	0
0	0.14	0.06	0.14	0.05
0.01	0.16	0.16	0.14	0.14
0.14	0.14	0.21	0.14	0.2
0.27	0.15	0.21	0.14	0.22
0.49	0.27	0.19	0.23	0.26
0.76	0.56	0.15	0.43	0.22
0.89	1.07	0.19	0.78	0.18
0.87	2.13	0.66	1.42	0.25
0.65	3.49	1.66	2.25	0.6
0.46	5.16	3.3	3.25	1.36
0.6	7.63	6.29	4.84	3.08
1.51	10.09	9.77	6.66	5.47
2.81	9.89	10.75	6.98	6.77
6.6	12.54	14.97	9.95	10.86
9.7	11.7	14.76	10.64	12.27
12.17	10	12.91	10.69	12.56
15.9	8.97	11.3	11.75	13.66
14.41	6.24	7.2	9.69	11.05
12.97	4.46	4.16	8.2	9.13
9.59	2.76	1.1	5.88	6.43
6.04	1.56	0	3.63	3.9
2.37	0.48	0	1.34	1.34
0.01	0	0	0	0
0	0	0	0	0
0	0	0	0	0
0	0	0	0	0
0	0	0	0	0
346	188	232	212	283
674	397	427	509	556
1150	822	744	1020	1040
707	458	460	568	613
434	316	367	340	459
-0.097	1.611	0.081	0.164	0.26
0.358	1.222	0.681	0.775	0.793
707	401	440	573	568
1.193	1.597	1.2	1.591	1.363
15.02	13.96	13.82	11.9	13.95
0.93	0.51	0.5	0.44	0.74
0.94	0.53	0.53	0.46	0.78

B6	B7	B8	C1	C2
20/09/2023 15:00	20/09/2023 15:08	20/09/2023 15:16	20/09/2023 15:24	20/09/2023 15:31
176.2138084°E 37.6243739°S	176.2167480°E 37.6278661°S	176.2198100°E 37.6309702°S	176.2010704°E 37.6045814°S	176.2042549°E 37.6077835°S
0	0	0	0	0
0	0	0	0	0
0	0	0	0	0
0	0.09	0	0	0
0	6.2	0.24	0	0
0	7.58	0.26	0	0
0	10.01	0.73	0.12	0.19
0	12.25	1.12	0.44	0.52
0	15.82	1.36	0.62	0.65
0	17.39	2.42	0.74	0.67
0	3.73	0.35	0.25	0.23
0	3.18	0.16	0.29	0.25
0.08	2.86	0.3	0.39	0.28
0.16	2.17	1.05	0.4	0.25
0.18	1.7	2.29	0.37	0.21
0.2	1.58	4.75	0.36	0.26
0.09	1.45	7.89	0.37	0.47
0	1.38	10.36	0.55	0.92
0.04	1.42	12.49	1.22	1.95
0.41	1.49	12.75	2.41	3.34
1.28	1.6	11.85	4.12	5.02
3.29	1.74	9.83	6.94	7.46
6.08	1.84	7.6	9.99	9.83
7.66	1.45	4.28	10.35	9.57
12.3	1.41	2.76	13.66	12.08
13.78	0.96	1.37	12.99	11.27
13.78	0.53	0.71	11.09	9.7
14.38	0.17	0.57	9.63	8.81
10.97	0	0.53	6.25	6.16
8.28	0	0.57	3.92	4.41
4.97	0	0.53	1.95	2.71
1.96	0	0.42	0.56	1.55
0.11	0	0.28	0.02	0.78
0	0	0.15	0	0.33
0	0	0.03	0	0.13
0	0	0	0	0
0	0	0	0	0
0	0	0	0	0
286	1.4	72.8	190	176
528	14.5	158	401	395
933	171	323	754	838
572	52.3	197	439	461
457	4.43	55.5	196	182
0.136	8.891	26.201	0.771	3.686
0.728	2.92	4.358	0.818	1.533
539	19.1	158	417	400
1.226	11.737	1.584	1.409	1.678
10.17	11.73	18.68	15.33	18.54
0.46	0.9	0.29	0.42	0.28
0.52	0.42	0.29	0.42	0.27

C3	C4	C5	C6	C7
20/09/2023 15:39	20/09/2023 15:47	20/09/2023 15:54	20/09/2023 16:02	20/09/2023 16:09
176.2074394°E 37.6113736°S	176.2106239°E 37.6147694°S	176.2140534°E 37.6179710°S	176.2168704°E 37.6211725°S	176.2202999°E 37.6241799°S
0	0	0	0	0
0	0	0	0	0
0	0	0	0	0
0	0	0	0	0
0	0	0.47	0	0
0	0	0.94	0	0
0	0	1.38	0	0
0.52	0	2.02	0	0
0.51	0	2.46	0	0.11
0.52	0	2.27	0	0.6
0.18	0	0.6	0.12	0.12
0.14	0	0.65	0.18	0.04
0.1	0	0.78	0.23	0
0	0	0.75	0.22	0
0	0	0.67	0.16	0
0.22	0	0.63	0.12	0.26
0.83	0	0.6	0.2	1.43
1.8	0	0.79	0.59	3.5
3.49	0	1.54	1.71	6.95
5.24	0.07	2.8	3.45	10.15
6.98	0.56	4.5	5.74	12.72
8.95	2.38	7.02	9.19	14.64
10.48	5.3	9.34	12.54	14.98
9.23	7.3	8.94	12.33	11.14
10.62	12.35	10.62	15.23	9.84
9.37	14.11	9.09	13.5	6.31
7.86	14.23	7.04	10.58	3.42
7.24	14.9	5.71	8.03	1.59
5.35	11.44	3.89	4.36	0.53
4.2	8.77	3.16	1.52	0.19
2.97	5.56	2.7	0	0.19
1.97	2.81	2.38	0	0.28
1.02	0.22	2.09	0	0.33
0.21	0	1.66	0	0.27
0	0	1.24	0	0.22
0	0	0.78	0	0.14
0	0	0.42	0	0.05
0	0	0	0	0
159	313	35.6	195	139
355	548	355	364	248
851	966	1090	640	456
439	599	492	392	293
203	502	35.9	310	213
2.311	0.213	6.729	0.14	44.196
1.463	0.831	2.339	0.699	5.52
329	543	356	375	244
1.95	1.191	2.962	1.223	1.274
22.49	9.48	9.06	15.67	13.56
0.28	0.52	0.49	0.51	0.43
0.27	0.6	0.47	0.55	0.44

C8	D1	D2	D3	D4
20/09/2023 16:17	22/09/2023 12:46	22/09/2023 12:54	22/09/2023 13:01	22/09/2023 13:09
176.2236069°E 37.6277691°S	176.2044998°E 37.6014763°S	176.2078068°E 37.6046785°S	176.2107464°E 37.6082687°S	176.2141759°E 37.6113736°S
0	0	0	0	0
0	0	0	0	0
0	0	0	0	0
0	0	0	0	0
0.35	0	0.4	0	0
0.44	0	0.57	0	0
0.83	0	0.93	0.24	0
1.25	0	1.26	0.6	0
1.49	0.04	1.49	0.63	0
2.35	0.37	1.67	0.73	0
0.3	0	0.41	0.24	0
0.14	0.05	0.43	0.21	0
0.29	0.12	0.54	0.13	0.09
1.03	0.18	0.68	0	0.16
2.25	0.24	0.83	0.01	0.18
4.62	0.34	1.19	0.28	0.2
7.64	0.47	1.54	0.99	0.09
10.03	0.55	1.78	2.07	0
12.13	0.77	2.04	3.88	0.04
12.45	1.14	2.26	5.7	0.41
11.7	1.79	2.6	7.41	1.36
9.91	3.27	3.48	9.27	3.59
7.92	5.37	4.83	10.6	6.69
4.73	6.53	5.37	9.15	8.38
3.4	10.57	8.3	10.27	13.24
1.98	12.22	9.45	8.91	14.53
1.15	12.77	9.9	7.34	14.15
0.79	14.12	11.13	6.64	14.19
0.48	11.33	9.22	4.81	10.39
0.27	9.02	7.74	3.74	7.37
0.08	5.77	5.47	2.64	3.98
0	2.78	3.33	1.81	0.95
0	0.19	1.16	1.14	0.01
0	0	0	0.49	0
0	0	0	0.07	0
0	0	0	0	0
0	0	0	0	0
0	0	0	0	0
70.9	257	83.3	149	281
159	541	482	338	506
328	970	999	837	880
185	580	519	427	546
46.3	398	49.9	163	442
7.277	-0.086	-0.138	3.542	0.064
2.038	0.565	0.569	1.707	0.695
160	585	600	311	516
1.615	1.319	1.898	2.037	1.184
21.32	8.13	19.38	15.85	8.07
0.26	0.54	0.4	0.3	0.48
0.26	0.58	0.39	0.29	0.53

D5	D6	D7	D8	E1
22/09/2023 13:17	22/09/2023 13:24	22/09/2023 13:32	22/09/2023 13:40	22/09/2023 13:48
176.2171154°E 37.6145753°S	176.2205449°E 37.6180680°S	176.2232395°E 37.6213666°S	176.2267914°E 37.6246649°S	176.2078068°E 37.5982739°S
0	0	0	0	0
0	0	0	0	0
0	0	0	0	0
0	0	0	0	0
0	0	0	0	0
0	0	0	0	0.03
0.06	0.12	0.15	0	0.47
0.49	0.45	0.6	0.07	0.61
0.55	0.57	0.62	0.41	0.73
0.57	0.59	0.81	0.43	0.91
0.21	0.25	0.26	0.09	0.26
0.19	0.29	0.22	0.11	0.27
0.16	0.34	0.13	0.19	0.32
0.06	0.28	0	0.25	0.39
0	0.2	0	0.3	0.5
0.04	0.22	0.3	0.38	0.8
0.58	0.48	1.27	0.43	1.21
1.66	1.15	2.83	0.49	1.61
3.8	2.68	5.42	0.83	2.15
6.27	4.72	7.95	1.55	2.57
8.81	7.09	10.21	2.82	2.96
11.71	10.27	12.36	5.33	3.44
13.74	12.99	13.48	8.51	4.01
11.82	11.98	10.89	9.72	3.81
12.65	13.86	10.96	14.2	5.34
9.97	11.66	8.24	14.65	6.12
7.06	8.73	5.63	13.37	6.99
4.93	6.33	3.84	12.22	9.27
2.62	3.33	2.05	7.99	9.14
1.32	1.39	1.08	4.54	9.46
0.53	0.03	0.48	1.12	8.45
0.19	0	0.2	0	6.73
0.01	0	0.02	0	4.89
0	0	0	0	3.13
0	0	0	0	1.91
0	0	0	0	0.98
0	0	0	0	0.47
0	0	0	0	0
157	165	138	223	146
304	330	274	440	647
583	607	548	757	1480
343	359	314	466	747
183	182	154	293	152
2.66	0.444	3.547	-0.082	1.923
1.295	0.72	1.486	0.463	1.216
304	342	271	470	838
1.4	1.34	1.494	1.213	2.055
15.34	14.75	18.87	7.97	16.48
0.3	0.28	0.25	0.46	0.65
0.29	0.27	0.25	0.47	0.62

E2	E3	E4	E5	E6
22/09/2023 13:56	22/09/2023 14:04	22/09/2023 14:12	22/09/2023 14:20	22/09/2023 14:27
176.2112363°E 37.6013792°S	176.2142983°E 37.6049696°S	176.2174829°E 37.6081716°S	176.2206674°E 37.6111795°S	176.2239744°E 37.6148664°S
0	0	0	0	0
0	0	0	0	0
0	0	0	0	0
0	0	0	0	0
0	0	0	0	0
0	0.04	0	0	0
0.14	0.53	0.35	0.23	0.2
0.55	0.83	0.68	0.62	0.52
0.5	0.97	0.64	0.63	0.64
0.77	1.25	1.11	0.9	0.77
0.26	0.38	0.27	0.28	0.29
0.21	0.35	0.17	0.2	0.3
0.1	0.31	0.02	0.09	0.32
0	0.27	0.1	0	0.25
0.08	0.39	0.53	0.07	0.22
0.58	0.84	1.64	0.54	0.38
1.9	1.8	3.63	1.84	0.93
3.78	3.07	5.91	3.72	1.91
6.74	5.05	8.89	6.67	3.82
9.46	6.9	11.03	9.35	6.05
11.74	8.58	12.38	11.53	8.41
13.67	10.3	12.99	13.31	11.28
14.4	11.44	12.59	13.89	13.44
11.12	9.58	9.03	10.65	11.76
10.42	10.31	7.87	9.93	12.81
7.09	8.43	5.1	6.81	10.21
4.11	6.41	2.89	4.07	7.22
1.99	5.09	1.49	2.18	4.89
0.39	3.17	0.55	0.83	2.42
0	1.98	0.14	0.25	0.96
0	1.05	0	0.12	0
0	0.5	0	0.18	0
0	0.18	0	0.3	0
0	0	0	0.3	0
0	0	0	0.26	0
0	0	0	0.18	0
0	0	0	0.07	0
0	0	0	0	0
129	119	108	129	146
248	285	218	250	301
453	630	422	482	565
271	336	244	297	330
150	110	118	139	158
0.592	3.184	1.966	40.165	0.697
0.78	1.478	1.143	5.21	0.808
254	288	220	251	313
1.301	1.796	1.441	1.412	1.391
16.43	20.91	14.16	18.76	14.32
0.24	0.26	0.23	0.28	0.3
0.23	0.23	0.22	0.28	0.29

E7	E8	F1	F2	F3
22/09/2023 14:35	22/09/2023 14:43	22/09/2023 14:51	22/09/2023 14:59	22/09/2023 15:06
176.2267914°E 37.6181651°S	176.2300984°E 37.6214636°S	176.2112363°E 37.5951685°S	176.2144208°E 37.5985650°S	176.2174829°E 37.6017674°S
0	0	0	0	0
0	0	0	0	0
0	0	0	0	0
0	0	0	0	0
0	0	0.23	0	0
0	0	0.27	0	0
0.4	0.05	0.75	0.14	0.24
0.59	0.42	1.09	0.48	0.58
0.69	0.54	1.25	0.57	0.53
0.81	0.64	2.01	0.46	0.87
0.23	0.23	0.34	0.17	0.19
0.23	0.26	0.21	0.22	0.07
0.27	0.3	0.32	0.28	0
0.28	0.25	0.87	0.25	0.04
0.31	0.21	1.82	0.18	0.32
0.44	0.26	3.79	0.09	1.28
0.63	0.52	6.42	0.06	3.18
0.85	1.04	8.68	0.34	5.44
1.28	2.24	10.92	1.25	8.43
1.78	3.8	11.72	2.8	10.62
2.48	5.7	11.58	4.89	12.01
3.73	8.43	10.57	8.12	12.66
5.39	11.04	9.14	11.36	12.33
6	10.68	5.97	11.44	8.95
9.19	13.27	4.83	14.54	8.01
10.42	12.09	3.07	13.34	5.45
10.93	9.98	1.86	10.96	3.39
12.38	8.37	1.2	9.01	2.13
10.37	5.24	0.64	5.45	1.11
8.81	3.09	0.34	2.95	0.63
6.3	1.21	0.11	0.65	0.39
3.85	0.14	0	0	0.29
1.36	0	0	0	0.27
0	0	0	0	0.24
0	0	0	0	0.19
0	0	0	0	0.12
0	0	0	0	0.04
0	0	0	0	0
194	172	77.7	196	116
532	367	175	382	229
1040	704	376	693	478
577	405	206	414	281
167	202	57.9	198	135
-0.015	0.614	5.129	0.329	33.97
0.594	0.826	1.778	0.669	4.634
609	385	174	393	221
1.587	1.451	1.701	1.303	1.587
13.1	12.31	17.09	12.6	18.92
0.39	0.33	0.25	0.28	0.23
0.37	0.32	0.25	0.28	0.23

F4	F5	F6	F7	F8
22/09/2023 15:14	22/09/2023 15:21	22/09/2023 15:30	22/09/2023 15:37	22/09/2023 15:45
176.2205449°E 37.6051636°S	176.2238519°E 37.6083657°S	176.2271589°E 37.6116646°S	176.2303434°E 37.6153515°S	176.2335279°E 37.6183591°S
0	0	0	0	0
0	0	0	0	0
0	0	0	0	0
0	0	0	0	0
0	0	0	0	0
0	0	0	0	0
0	0.05	0.3	0.14	0.06
0	0.4	0.6	0.49	0.49
0	0.54	0.73	0.55	0.58
0	0.61	0.98	0.5	0.64
0	0.15	0.28	0.22	0.23
0	0.18	0.26	0.26	0.24
0	0.22	0.28	0.27	0.23
0	0.26	0.32	0.18	0.13
0.06	0.27	0.45	0.04	0.03
0.18	0.3	0.84	0.03	0
0.31	0.34	1.57	0.32	0.15
0.47	0.45	2.49	1.04	0.86
0.63	0.86	3.99	2.72	2.64
0.73	1.63	5.54	4.94	5
0.79	2.83	7.14	7.54	7.64
0.99	5.06	9.19	10.91	10.88
1.5	7.78	11	13.75	13.39
2.06	8.69	9.94	12.57	11.98
4.39	12.65	11.65	14.32	13.44
6.6	13.24	10.24	11.79	11.09
8.86	12.53	8.23	8.53	8.29
12.85	12.32	6.74	5.76	6.19
12.94	8.86	4.13	2.68	3.48
13.24	6.11	2.32	0.45	1.81
11.45	3.07	0.75	0	0.53
8.74	0.6	0.04	0	0
6.02	0	0	0	0
3.63	0	0	0	0
2.08	0	0	0	0
0.98	0	0	0	0
0.44	0	0	0	0
0	0	0	0	0
390	218	131	169	171
805	460	320	323	328
1540	836	652	576	623
899	494	359	349	365
635	233	144	180	188
2.506	0.019	0.619	0.275	1.066
1.288	0.553	0.871	0.627	0.961
825	493	348	335	326
1.425	1.346	1.632	1.259	1.38
8.94	9.29	9.32	11.32	8.34
1.11	0.32	0.25	0.31	0.33
1.19	0.33	0.24	0.31	0.33

G1	G2	G3	G4	G5
22/09/2023 15:53	22/09/2023 16:00	22/09/2023 16:08	22/09/2023 16:15	22/09/2023 16:22
176.2147883°E 37.5918688°S	176.2177278°E 37.5952655°S	176.2210348°E 37.5984680°S	176.2242193°E 37.6018644°S	176.2270364°E 37.6053577°S
0	0	0	0	0
0	0	0	0	0
0	0	0	0	0
0	0	0	0	0
0.36	0	0	0	0
0.45	0	0	0	0
0.86	0	0	0.24	0.48
1.24	0.14	0.34	0.6	0.84
1.53	0.38	0.42	0.56	1.03
2.27	0.3	0.45	0.97	1.47
0.31	0.15	0.16	0.24	0.42
0.22	0.19	0.18	0.13	0.36
0.54	0.23	0.23	0.02	0.33
1.45	0.18	0.21	0.06	0.34
2.74	0.13	0.2	0.39	0.52
5.2	0.12	0.24	1.4	1.15
8.14	0.25	0.41	3.29	2.33
10.33	0.69	0.8	5.47	3.77
12.13	1.77	1.74	8.4	5.93
12.21	3.33	3.08	10.55	7.79
11.32	5.31	4.8	11.99	9.39
9.48	8.2	7.41	12.78	10.91
7.53	11.03	10.06	12.6	11.77
4.43	10.85	10.07	9.27	9.57
3.13	13.69	13.01	8.43	9.87
1.74	12.65	12.34	5.78	7.72
0.95	10.58	10.66	3.56	5.56
0.63	9.06	9.54	2.08	4.09
0.39	5.76	6.44	0.9	2.35
0.26	3.47	4.23	0.29	1.3
0.13	1.37	2.22	0	0.54
0.03	0.17	0.73	0	0.16
0	0	0.03	0	0.01
0	0	0	0	0
0	0	0	0	0
0	0	0	0	0
0	0	0	0	0
0	0	0	0	0
67.1	191	189	114	110
154	383	398	227	262
316	723	774	449	561
179	423	444	258	304
45.1	265	237	132	109
10.079	0.581	0.784	1.992	2.472
2.328	0.852	0.911	1.208	1.312
156	394	414	226	270
1.619	1.39	1.47	1.48	1.727
17.34	11.32	10.75	12.55	20.13
0.26	0.39	0.42	0.25	0.23
0.25	0.39	0.42	0.25	0.2

G6	G7	G8	H1	H2
22/09/2023 16:30	22/09/2023 16:37	22/09/2023 16:45	22/09/2023 16:53	22/09/2023 17:00
176.2305884°E 37.6085598°S	176.2336504°E 37.6120527°S	176.2369574°E 37.6152545°S	176.2176053°E 37.5886660°S	176.2210348°E 37.5920629°S
0	0	0	0	0
0	0	0	0	0
0	0	0	0	0
0	0	0	0	0
0	0	0	0	0
0	0	0	0	0
0.2	0.39	0	0.06	0.12
0.53	0.65	0.2	0.45	0.38
0.69	0.83	0.38	0.41	0.41
0.71	0.86	0.43	0.7	0.54
0.26	0.31	0.06	0.08	0.14
0.29	0.35	0	0	0.12
0.34	0.41	0	0.02	0.13
0.27	0.37	0	0.24	0.18
0.2	0.3	0.06	0.69	0.28
0.19	0.35	0.15	1.69	0.54
0.35	0.62	0.21	3.29	0.89
0.86	1.24	0.23	4.96	1.22
2.12	2.68	0.19	7.23	1.56
3.86	4.59	0.06	9.04	1.7
6	6.82	0.01	10.59	1.74
8.97	9.79	0.27	12.09	1.83
11.65	12.35	1.06	12.95	2.24
11.06	11.38	2.1	10.4	2.59
13.31	13.2	5.11	10.3	4.97
11.74	11.21	7.76	7.44	7.15
9.4	8.55	10.16	4.56	9.36
7.69	6.49	14.17	2.34	13.24
4.79	3.7	13.8	0.47	13
2.88	1.94	13.64	0	12.81
1.35	0.6	11.38	0	10.45
0.29	0.02	8.36	0	7.34
0	0	5.4	0	4.06
0	0	2.9	0	1.01
0	0	1.37	0	0
0	0	0.44	0	0
0	0	0.1	0	0
0	0	0	0	0
171	153	414	115	211
357	330	777	245	698
696	633	1420	466	1250
398	364	856	270	725
172	138	427	158	263
1.045	0.823	1.862	0.332	-0.285
0.948	0.834	1.091	0.781	0.339
364	343	787	265	790
1.47	1.453	1.289	1.435	1.483
15.25	19.8	8.99	16.84	11.89
0.28	0.31	1	0.26	0.82
0.27	0.3	1.03	0.26	0.81

H3	H4	H5	H6	H7	H8
22/09/2023 17:07	22/09/2023 17:15	22/09/2023 17:22	22/09/2023 17:30	22/09/2023 17:38	22/09/2023 17:46
176.2240968°E 37.5953626°S	176.2274038°E 37.5987591°S	176.2304659°E 37.6020585°S	176.2336504°E 37.6054547°S	176.2370799°E 37.6086568°S	176.2400194°E 37.6118587°S
0	0	0	0	0	0
0	0	0	0	0	0
0	0	0	0	0	0
0	0	0	0	0	0
0.3	0	0	0	0	0
0.26	0	0	0	0	0
0.7	0	0	0	0	0
1.03	0	0	0	0	0
1.15	0	0	0.25	0	0
1.88	0	0	0.34	0	0
0.43	0	0	0	0	0
0.31	0	0	0	0	0
0.27	0	0	0.09	0	0.01
0.49	0	0	0.19	0	0.13
1.07	0	0	0.27	0.07	0.19
2.42	0.08	0.09	0.39	0.17	0.25
4.5	0.15	0.19	0.48	0.28	0.23
6.58	0.21	0.29	0.52	0.35	0.13
9.02	0.26	0.35	0.66	0.44	0.01
10.43	0.26	0.29	1.02	0.56	0.09
11.1	0.24	0.18	1.79	0.8	0.53
11.06	0.24	0	3.62	1.47	1.97
10.39	0.38	0	6.22	2.71	4.37
7.35	0.65	0.31	7.67	3.78	6.22
6.48	1.72	2.04	12.29	7.25	11.24
4.41	2.96	4.79	13.8	9.7	13.68
2.81	4.45	8.24	13.82	11.63	14.66
1.92	7.42	14.02	14.24	14.97	16.22
1.15	8.58	15.24	10.55	13.69	12.76
0.83	10.57	16.19	7.4	12.61	9.69
0.62	11.56	14.02	3.69	9.65	5.62
0.47	11.5	10.42	0.7	6.39	1.91
0.34	11.3	6.76	0	3.04	0.09
0.19	9.99	3.72	0	0.44	0
0.04	8.25	1.9	0	0	0
0	5.63	0.75	0	0	0
0	3.1	0.21	0	0	0
0	0	0	0	0	0
86.8	558	520	253	342	318
204	1190	876	502	675	566
464	2340	1520	869	1190	951
255	1330	960	533	722	602
58.4	944	768	360	557	491
14.282	0.009	2.177	-0.114	-0.006	-0.034
3.049	0.746	1.202	0.488	0.606	0.591
202	1250	862	537	716	587
1.852	1.491	1.146	1.225	1.252	1.119
22.99	13.75	8.1	11.73	7.89	6.43
0.22	0.88	1.35	0.57	0.9	0.69
0.21	1.06	1.42	0.59	0.97	0.75

Mastersizer® data sheets showing proportion of samples under grain size boundaries for the 60 sub-samples taken from the 4 core samples.

	Sample Name	VC1 1	VC1 2	VC1 3
	Measurement Date Time	21/05/2024 9:45	21/05/2024 9:53	21/05/2024 10:00
	Location	176.112678°E 37.366425°S		
Depth (cm)		55	50	45
Grain Size (um)	0.05	0	0	0
	0.06	0	0	0
	0.12	0	0	0
	0.24	0	0	0
	0.49	0	0	0
	0.98	0	0	0
	2	0	0.04	0
	3.9	0.13	0.61	0.37
	7.8	0.6	1.38	1.09
	15.6	1.15	2.19	1.77
	31	2.12	3.43	3.13
	37	2.22	3.62	3.36
	44	2.23	3.68	3.42
	53	2.23	3.68	3.44
	63	2.3	3.82	3.75
	74	2.88	4.68	4.86
	88	5.1	7.45	7.91
	105	10.36	13.37	13.96
	125	18.88	22.39	22.87
	149	31.11	34.72	34.78
	177	45.22	48.48	47.95
	210	59.71	62.23	61.08
	250	73.02	74.51	72.85
	300	84.23	84.59	82.62
	350	91.11	90.61	88.58
	420	95.98	94.77	92.89
	500	98.51	96.94	95.33
	590	99.59	98.01	96.71
	710	99.95	98.65	97.74
	840	100	99.1	98.51
	1000	100	99.5	99.18
	1190	100	99.8	99.64
	1410	100	99.98	99.91
	1680	100	100	100
	2000	100	100	100
	2380	100	100	100
	2830	100	100	100
	3360	100	100	100
Statistics	Dx (10)	104	96.4	94.5
	Dx (50)	187	180	182
	Dx (90)	341	344	369
	D [4,3]	207	209	219
	D [3,2]	128	93.8	105
	Kurtosis [3]	1.991	15.732	14.296
	Skew [3]	1.121	3.025	3.088
	Mode	184	178	177
	Span	1.265	1.374	1.512
	Laser Obscuration	14.32	12.44	12.03
	Weighted Residual	0.37	0.37	0.34
	Residual	0.37	0.36	0.33

VC1 4	VC1 5	VC1 6	VC1 7	VC1 8
21/05/2024 10:09	21/05/2024 10:17	21/05/2024 10:26	21/05/2024 10:34	21/05/2024 10:42
40	35	30	25	20
0	0	0	0	0
0	0	0	0	0
0	0	0	0	0
0	0	0	0	0
0	0	0	0	0
0	0	0	0	0
0	0	0	0	0
0.4	0.4	0.26	0.26	0.24
1.17	1.14	0.91	0.91	0.8
1.88	1.89	1.57	1.56	1.41
3.37	3.11	2.59	2.64	2.34
3.63	3.32	2.76	2.8	2.42
3.71	3.39	2.81	2.84	2.42
3.73	3.39	2.81	2.84	2.42
4.12	3.54	2.91	3.03	2.57
5.38	4.38	3.55	3.97	3.43
8.63	6.95	5.66	6.71	6.21
14.88	12.33	10.28	12.34	12.16
23.94	20.51	17.48	20.77	21.2
35.94	31.74	27.56	32.2	33.47
49.15	44.43	39.16	44.98	47.11
62.28	57.34	51.19	57.89	60.69
74.07	69.27	62.66	69.74	72.81
83.89	79.56	72.92	79.91	82.8
89.91	86.19	79.88	86.4	88.83
94.33	91.49	85.9	91.5	93.11
96.85	94.88	90.15	94.67	95.47
98.24	97.02	93.18	96.63	96.76
99.11	98.53	95.72	98.05	97.67
99.62	99.4	97.51	98.97	98.35
99.91	99.87	98.83	99.6	98.95
100	100	99.63	99.93	99.43
100	100	99.98	100	99.76
100	100	100	100	99.95
100	100	100	100	100
100	100	100	100	100
100	100	100	100	100
100	100	100	100	100
92.1	98.8	104	99	99.8
179	191	206	189	183
351	395	497	394	366
206	225	263	227	223
101	107	123	116	119
6.837	5.313	5.909	7.823	19.687
1.988	1.889	2.156	2.292	3.649
176	183	189	181	177
1.446	1.555	1.901	1.56	1.45
13.44	16.51	15.51	15.72	14.44
0.35	0.39	0.3	0.31	0.34
0.34	0.37	0.29	0.31	0.34

VC1 9	VC1 10	VC1 11	VC2 1	VC2 2
21/05/2024 10:49	21/05/2024 10:57	21/05/2024 11:05	21/05/2024 11:13	21/05/2024 11:20
			176.124454°E 37.36683°S	
15	10	5	35	30
0	0	0	0	0
0	0	0	0	0
0	0	0	0	0
0	0	0	0	0
0	0	0	0	0
0	0	0	0	0
0	0	0	0	0
0.24	0.11	0.05	0	0
0.81	0.52	0.44	0	0.36
1.46	1.09	1.03	0	0.82
2.33	1.8	1.66	0.06	1.33
2.4	1.8	1.66	0.16	1.52
2.4	1.8	1.66	0.27	1.73
2.4	1.8	1.66	0.41	1.98
2.48	1.87	1.73	0.56	2.2
3.07	2.43	2.3	0.71	2.39
5.37	4.69	4.62	0.91	2.62
10.79	10.17	10.26	1.22	3.07
19.51	19.03	19.42	1.75	3.99
31.89	31.63	32.44	2.82	5.98
45.98	45.95	47.24	4.68	9.43
60.23	60.37	62.1	7.63	14.68
73.06	73.25	75.3	12.44	22.52
83.64	83.8	86.01	19.43	32.91
89.99	90.11	92.27	26.97	43.08
94.43	94.52	96.42	37.82	55.93
96.79	96.9	98.44	49.31	67.89
97.98	98.15	99.29	60.58	78.08
98.7	98.94	99.65	72.51	87.1
99.17	99.44	99.83	82.04	93.15
99.56	99.78	99.95	89.88	97.15
99.83	99.96	100	95.4	99.26
99.99	100	100	98.79	99.97
100	100	100	100	100
100	100	100	100	100
100	100	100	100	100
100	100	100	100	100
100	100	100	100	100
103	105	104	230	181
186	186	183	505	386
350	349	330	1000	762
215	214	204	566	433
119	133	135	397	227
14.997	10.658	7.651	0.36	0.893
2.953	2.486	1.882	0.863	0.955
180	179	179	534	399
1.332	1.317	1.233	1.53	1.503
14.07	14.87	14.05	11.26	18.25
0.33	0.34	0.34	0.56	0.28
0.33	0.34	0.34	0.6	0.27

VC2 3	VC2 4	VC2 5	VC2 6	VC2 7
21/05/2024 11:28	21/05/2024 11:35	21/05/2024 11:43	21/05/2024 11:53	21/05/2024 12:01
25	20	15	10	5
0	0	0	0	0
0	0	0	0	0
0	0	0	0	0
0	0	0	0	0
0	0	0	0	0
0	0	0	0	0
0	0	0	0	0
0	0	0	0	0
0	0	0	0	0
0	0	0	0	0
0	0	0	0	0
0	0	0.02	0.11	0.11
0	0.05	0.12	0.24	0.25
0.11	0.18	0.26	0.41	0.42
0.28	0.33	0.39	0.55	0.56
0.46	0.48	0.5	0.59	0.67
0.63	0.61	0.51	0.59	0.69
0.7	0.73	0.51	0.6	0.86
0.77	0.93	0.64	0.81	1.32
1.13	1.54	1.23	1.93	2.58
2.16	2.96	2.67	4.59	5.05
4.42	5.68	5.35	9.38	9.1
9.06	10.72	10.2	17.39	15.62
16.69	18.53	17.56	28.6	24.72
25.53	27.23	25.66	39.87	34.05
38.71	39.77	37.32	54.26	46.49
52.64	52.78	49.58	67.57	58.73
65.89	65.06	61.45	78.69	69.83
78.96	77.25	73.76	88.2	80.55
88.46	86.33	83.38	94.31	88.44
95.24	93.17	91.06	98.09	94.33
98.97	97.51	96.25	99.74	98.02
99.97	99.74	99.22	100	99.87
100	100	100	100	100
100	100	100	100	100
100	100	100	100	100
100	100	100	100	100
100	100	100	100	100
257	245	249	213	216
484	482	503	398	441
867	916	971	740	874
527	536	562	442	498
416	408	422	345	366
0.169	0.483	0.449	0.711	0.573
0.749	0.895	0.899	0.958	0.953
497	490	517	397	447
1.261	1.393	1.436	1.323	1.491
12.4	15.22	12.4	8.42	16.4
0.46	0.47	0.49	0.46	0.55
0.5	0.51	0.54	0.5	0.59

VC3 1	VC3 2	VC3 3	VC3 4	VC3 5
21/05/2024 12:08	21/05/2024 12:16	21/05/2024 12:46	21/05/2024 12:54	21/05/2024 13:01
176.136123°E 37.366425°S				
155	150	145	140	135
0	0	0	0	0
0	0	0	0	0
0	0	0	0	0
0	0	0	0	0
0	0	0	0	0
0	0.14	0.13	0	0
0.11	0.56	0.51	0.04	0.1
0.8	1.38	1.29	0.68	0.78
1.95	2.78	2.61	1.76	1.91
3.31	4.54	4.24	3.05	3.28
5.7	7.44	6.86	5.49	5.61
6.1	8.03	7.3	5.82	5.96
6.33	8.5	7.62	5.98	6.14
6.72	9.21	8.17	6.38	6.4
7.84	10.68	9.52	7.76	7.33
10.19	13.37	12.13	10.67	9.4
15.01	18.54	17.21	16.54	13.81
23.03	26.82	25.38	26.07	21.32
33.65	37.54	35.91	38.36	31.39
46.55	50.38	48.4	52.79	43.79
59.8	63.4	60.94	67.04	56.67
72.17	75.43	72.43	79.71	68.85
82.42	85.27	81.77	89.38	79.14
90.27	92.69	88.85	95.97	87.25
94.61	96.68	92.76	98.95	91.92
97.28	98.96	95.31	100	95.06
98.48	99.81	96.67	100	96.71
99	100	97.51	100	97.59
99.33	100	98.29	100	98.27
99.6	100	98.96	100	98.83
99.83	100	99.51	100	99.33
99.97	100	99.85	100	99.7
100	100	99.99	100	99.92
100	100	100	100	100
100	100	100	100	100
100	100	100	100	100
100	100	100	100	100
100	100	100	100	100
73.2	59.4	65.8	71.8	76.6
156	148	152	144	162
298	278	311	254	327
176	160	182	153	193
71.7	50.7	53.9	72.9	73.9
13.96	0.908	14.412	0.248	17.889
2.592	0.73	3.071	0.472	3.369
160	157	155	151	163
1.442	1.472	1.61	1.261	1.546
19.07	16.26	16.91	13.92	19.36
0.33	0.28	0.31	0.35	0.3
0.32	0.28	0.3	0.34	0.29

VC3 6	VC3 7	VC3 8	VC3 9	VC3 10
21/05/2024 13:09	21/05/2024 13:17	21/05/2024 13:24	21/05/2024 13:32	21/05/2024 13:40
130	125	120	115	110
0	0	0	0	0
0	0	0	0	0
0	0	0	0	0
0	0	0	0	0
0	0	0	0	0
0.13	0	0.22	0.24	0.14
0.52	0.1	0.67	0.74	0.57
1.33	0.79	1.51	1.69	1.43
2.71	1.97	2.9	3.32	2.94
4.47	3.41	4.73	5.67	5
7.16	5.82	7.69	9.38	8.04
7.63	6.21	8.19	10.15	8.58
8.02	6.5	8.58	10.88	9.07
8.7	7.09	9.27	12.05	9.96
10.25	8.61	10.9	14.24	11.85
13.05	11.5	13.9	17.82	15.15
18.33	17.05	19.58	24.13	21.13
26.62	25.83	28.42	33.54	30.23
37.18	37.05	39.54	45.09	41.56
49.64	50.19	52.33	58.14	54.53
62.18	63.27	64.8	70.69	67.18
73.74	75.11	75.82	81.68	78.44
83.27	84.57	84.33	90.01	87.2
90.63	91.55	90.42	95.76	93.47
94.78	95.24	93.57	98.48	96.61
97.47	97.38	95.48	99.7	98.19
98.79	98.3	96.53	99.98	98.66
99.39	98.7	97.31	100	98.7
99.71	99.05	98.2	100	98.77
99.89	99.39	98.99	100	99.01
100	99.72	99.61	100	99.35
100	99.94	99.93	100	99.68
100	100	100	100	99.9
100	100	100	100	100
100	100	100	100	100
100	100	100	100	100
100	100	100	100	100
100	100	100	100	100
61.8	69	58.8	35.7	53.3
150	149	144	134	140
295	286	296	250	268
168	170	174	142	161
52.2	69.7	47.1	41.8	48.2
5.881	17.996	13.139	0.548	33.514
1.638	3.165	3.028	0.609	4.595
155	153	148	145	148
1.556	1.461	1.64	1.604	1.53
19.14	17.3	20	18.48	17.81
0.28	0.34	0.32	0.33	0.28
0.28	0.33	0.32	0.32	0.27

VC3 11	VC3 12	VC3 13	VC3 14	VC3 15
21/05/2024 13:48	21/05/2024 13:55	21/05/2024 14:02	21/05/2024 14:10	21/05/2024 14:20
100	*95*	90	85	80
0	0	0	0	0
0	0	0	0	0
0	0	0	0	0
0	0	0	0	0
0	0	0	0	0
0.29	0.31	0.29	0.25	0.58
0.9	0.98	0.88	0.77	1.52
2.09	2.23	1.99	1.75	3.03
4.22	4.35	3.92	3.39	5.39
7.25	7.31	6.74	5.62	8.59
11.16	11.22	10.69	8.77	12.5
12.02	12.09	11.53	9.44	13.45
12.79	12.94	12.32	10.07	14.39
13.76	14.16	13.43	10.99	15.57
15.19	16.1	15.28	12.59	17.09
17.41	19.05	18.17	15.17	19.08
21.33	24.02	23.18	19.76	22.13
27.46	31.33	30.69	26.76	26.35
35.45	40.35	40.02	35.63	31.44
45.3	50.76	50.84	46.12	37.34
55.82	61.17	61.62	56.83	43.43
66.21	70.84	71.54	66.95	49.48
75.74	79.06	79.77	75.73	55.48
84.04	85.78	86.27	83.04	61.62
89.49	89.97	90.12	87.7	66.81
93.91	93.29	92.98	91.51	73.12
96.7	95.5	94.79	94.11	79.29
98.35	97.01	96.07	95.95	85.06
99.34	98.24	97.29	97.5	90.85
99.82	99.08	98.3	98.59	95.12
100	99.65	99.15	99.37	98.13
100	99.94	99.71	99.8	99.69
100	100	99.98	99.99	100
100	100	100	100	100
100	100	100	100	100
100	100	100	100	100
100	100	100	100	100
100	100	100	100	100
25.2	24.9	27.3	43.1	20.1
161	147	147	159	213
356	350	348	388	689
186	182	187	201	297
37.8	36	38.4	43.6	29.8
3.222	7.855	10.578	8.139	0.662
1.414	2.3	2.784	2.392	1.114
175	155	154	160	177
2.056	2.212	2.182	2.173	3.14
22.19	20.36	19.71	23.17	18.91
0.21	0.24	0.25	0.22	0.28
0.19	0.22	0.24	0.21	0.25

VC3 16	VC3 17	VC3 18	VC3 19	VC3 20
21/05/2024 14:28	21/05/2024 14:35	21/05/2024 14:43	21/05/2024 14:51	21/05/2024 14:59
75	70	65	60	55
0	0	0	0	0
0	0	0	0	0
0	0	0	0	0
0	0	0	0	0
0	0	0	0	0
0.63	0.39	0.13	0	0
1.63	0.94	0.23	0	0
3.16	1.71	0.71	0.12	0
5.5	2.68	1.33	0.52	0
8.71	3.83	2.06	1.03	0
12.7	5.1	2.89	1.59	0
13.66	5.42	3.11	1.72	0
14.58	5.76	3.36	1.85	0
15.74	6.19	3.71	2.06	0.01
17.26	6.69	4.14	2.36	0.15
19.33	7.29	4.65	2.75	0.37
22.57	8.09	5.33	3.29	0.7
27.18	9.11	6.21	3.94	1.06
32.8	10.35	7.27	4.68	1.31
39.39	12.03	8.75	5.65	1.39
46.21	14.31	10.87	7.1	1.39
52.98	17.48	13.97	9.41	1.67
59.56	22.3	18.91	13.59	3.22
66.07	29.18	26.21	20.3	7.15
71.33	36.58	34.24	28.17	13.17
77.3	47.19	45.96	40.23	24.56
82.81	58.33	58.38	53.39	38.72
87.74	69.04	70.29	66.29	53.97
92.51	79.94	82.17	79.38	70.72
95.98	88.17	90.77	89.02	83.68
98.44	94.36	96.7	95.83	93.25
99.73	98.14	99.51	99.31	98.54
100	99.88	100	100	99.96
100	100	100	100	100
100	100	100	100	100
100	100	100	100	100
100	100	100	100	100
100	100	100	100	100
19.6	119	167	216	325
195	439	445	479	565
642	879	826	856	936
274	476	473	508	599
28.7	54.9	113	225	488
1.315	0.047	-0.144	-0.116	-0.061
1.299	0.591	0.451	0.454	0.529
175	509	506	522	582
3.194	1.728	1.482	1.336	1.081
21.62	13.82	17.89	15.61	15.63
0.27	0.25	0.33	0.4	0.6
0.24	0.23	0.31	0.39	0.66

VC3 21	VC3 22	VC3 23	VC3 24	VC3 25
21/05/2024 15:07	21/05/2024 15:14	21/05/2024 15:22	21/05/2024 15:31	21/05/2024 15:38
50	45	40	35	30
0	0	0	0	0
0	0	0	0	0
0	0	0	0	0
0	0	0	0	0
0	0	0	0.03	0
2.45	0	0	0.79	0.68
6.54	0	0	1.15	1.52
13.14	0.12	0.05	2.51	3.32
21.96	0.52	0.46	4.52	6.34
32.66	1	0.96	7.08	10.96
48.25	1.67	1.55	10.29	18.22
53	1.87	1.72	11.12	20.69
57.77	2.08	1.91	11.9	23.26
62.96	2.33	2.12	12.7	26.08
67.74	2.63	2.34	13.46	28.62
72.1	2.98	2.59	14.29	30.86
76.6	3.45	2.96	15.52	33.16
80.86	4.05	3.55	17.4	35.51
84.69	4.76	4.46	20.03	38.06
88.04	5.67	6	23.79	41.18
90.82	6.86	8.35	28.59	44.96
93.17	8.52	11.75	34.4	49.49
95.11	11.26	16.88	41.53	55.01
96.79	15.63	24.04	49.94	61.46
97.94	20.96	31.6	57.63	67.28
98.92	29.82	42.34	67.05	74.3
99.55	40.43	53.65	75.83	80.84
99.89	51.99	64.7	83.47	86.59
100	65.51	76.27	90.43	92
100	77.01	85.33	95.17	95.84
100	86.91	92.48	98.29	98.47
100	94.02	97.15	99.75	99.76
100	98.41	99.63	100	100
100	99.99	100	100	100
100	100	100	100	100
100	100	100	100	100
100	100	100	100	100
100	100	100	100	100
2.95	233	194	29.2	13.8
33.1	574	473	300	214
168	1070	936	701	659
64.9	615	522	344	277
7.99	239	231	33.1	25.1
8.296	-0.059	0.192	0.303	0.567
2.59	0.524	0.725	0.812	1.058
49.5	635	528	393	381
4.973	1.459	1.569	2.236	3.02
13.07	14.32	15.74	17.41	18.65
0.55	0.44	0.31	0.22	0.27
0.28	0.43	0.3	0.2	0.22

VC3 26	VC3 27	VC3 28	VC3 29	VC3 30
21/05/2024 15:46	21/05/2024 15:53	21/05/2024 16:01	21/05/2024 16:09	21/05/2024 16:17
15	20	15	10	5
0	0	0	0	0
0	0	0	0	0
0	0	0	0	0
0	0	0	0	0
0	0	0	0	0
0.62	0	0	0	0
1.3	0	0	0	0
2.89	0.41	0.21	0.05	0
5.5	1.16	0.75	0.43	0
9.03	2.03	1.43	0.91	0.31
15.22	3.52	2.23	1.46	0.71
17.54	3.99	2.49	1.64	0.83
19.94	4.38	2.76	1.86	0.97
22.52	4.64	3.06	2.14	1.15
24.8	4.81	3.37	2.44	1.34
26.86	5.14	3.68	2.75	1.54
29.22	6.13	4.11	3.16	1.81
32.17	8.51	4.84	3.8	2.22
35.98	12.65	6.02	4.83	2.91
41.22	19.28	8.16	6.78	4.28
47.67	27.92	11.47	10.01	6.66
55.09	38.06	16.21	14.9	10.45
63.35	49.3	23.02	22.35	16.56
71.95	60.84	31.91	32.47	25.33
78.75	69.76	40.61	42.61	34.59
85.63	78.52	51.78	55.71	47.4
90.98	85.16	62.48	68.08	60.31
94.84	89.92	72	78.7	72.16
97.66	93.59	81.08	88.04	83.47
99.22	95.94	87.79	94.17	91.45
99.93	97.57	92.94	98.03	96.86
100	98.64	96.42	99.73	99.5
100	99.34	98.59	100	100
100	99.76	99.73	100	100
100	99.97	100	100	100
100	100	100	100	100
100	100	100	100	100
100	100	100	100	100
18	113	166	177	206
187	253	408	388	435
483	592	900	743	812
222	316	478	427	474
28.3	116	176	214	306
1.186	7.963	1.66	0.438	0.128
1.118	2.312	1.211	0.774	0.69
250	242	423	412	466
2.481	1.896	1.799	1.458	1.393
17.14	18.3	16.7	14.22	15.86
0.23	0.25	0.3	0.25	0.37
0.19	0.23	0.29	0.25	0.39

VC4 1	VC4 2	VC4 3	VC4 4	VC4 5
21/05/2024 16:29	21/05/2024 16:37	21/05/2024 16:44	21/05/2024 16:51	21/05/2024 16:59
176.148632°E 37.366691°S				
60	55	50	45	40
0	0	0	0	0
0	0	0	0	0
0	0	0	0	0
0	0	0	0	0
0	0	0	0	0
0.25	0.14	0.27	0.41	0.4
0.85	0.59	0.87	1.11	1.08
2.06	1.52	2.04	2.35	2.28
4.24	3.19	4.06	4.31	4.23
7.24	5.52	6.72	6.93	6.96
10.95	8.45	10.01	10.3	10.53
11.81	9.04	10.61	11.03	11.28
12.6	9.55	11.13	11.7	11.97
13.5	10.23	11.86	12.58	12.93
14.7	11.35	13.22	13.94	14.48
16.45	13.18	15.52	16.02	16.88
19.53	16.52	19.74	19.59	20.96
24.41	21.8	26.34	25	27.03
30.94	28.72	34.86	31.85	34.59
39.31	37.32	45.18	40.08	43.47
48.62	46.61	55.95	48.73	52.56
58.24	55.98	66.4	57.24	61.31
67.63	64.92	75.74	65.19	69.19
76.34	73.16	83.7	72.48	76.15
82.5	79.05	88.82	77.73	80.97
88.05	84.58	92.91	82.87	85.45
92.01	88.84	95.54	87.05	89
94.77	92.13	97.22	90.5	91.91
96.89	95.03	98.45	93.78	94.71
98.26	97.09	99.23	96.25	96.87
99.2	98.61	99.73	98.15	98.53
99.75	99.54	99.95	99.36	99.55
99.98	99.97	100	99.96	99.97
100	100	100	100	100
100	100	100	100	100
100	100	100	100	100
100	100	100	100	100
100	100	100	100	100
26	50.2	31	29	27.8
181	188	161	182	169
453	528	367	575	528
226	249	193	254	235
39.4	50	39.5	36.2	36.2
5.351	4.391	6.7	3.668	4.4
1.924	1.895	2.051	1.82	1.964
193	182	168	173	163
2.354	2.537	2.088	3.01	2.967
17.84	15.89	16.2	21.56	19.44
0.22	0.21	0.22	0.21	0.22
0.2	0.2	0.2	0.19	0.19

VC4 6	VC4 7	VC4 8	VC4 9	VC4 10
21/05/2024 17:07	21/05/2024 17:15	21/05/2024 17:22	21/05/2024 17:30	21/05/2024 17:38
35	20	25	20	15
0	0	0	0	0
0	0	0	0	0
0	0	0	0	0
0	0	0	0	0
0	0	0	0	0
0.4	0	0	0	0
1.05	0	0	0	0
2.19	0.42	0.2	0	0
3.94	1.06	0.69	0.2	0.35
6.16	1.81	1.24	0.6	0.79
8.87	2.73	1.91	1.11	1.36
9.43	2.95	2.06	1.22	1.49
9.94	3.16	2.21	1.32	1.62
10.64	3.44	2.39	1.44	1.77
11.79	3.82	2.64	1.62	1.99
13.59	4.34	2.99	1.89	2.28
16.7	5.19	3.56	2.35	2.78
21.39	6.41	4.4	3.04	3.52
27.32	7.97	5.48	3.95	4.49
34.44	9.95	6.89	5.1	5.78
41.97	12.27	8.64	6.49	7.41
49.5	15.02	10.88	8.25	9.51
56.83	18.58	14.19	10.85	12.59
63.97	23.35	19.08	14.86	17.14
69.56	28.49	24.74	19.72	22.41
75.68	36.33	33.83	28.01	30.93
81.19	45.36	44.46	38.23	41.04
86.09	55.05	55.84	49.73	52.08
90.94	66.47	68.9	63.61	65.14
94.63	76.4	79.82	75.69	76.43
97.43	85.3	88.98	86.24	86.32
99.16	92.15	95.33	93.83	93.59
99.95	96.86	98.99	98.43	98.18
100	99.41	100	100	99.99
100	100	100	100	100
100	100	100	100	100
100	100	100	100	100
100	100	100	100	100
45	150	197	238	217
212	542	543	592	572
683	1120	1030	1080	1080
299	595	581	629	615
39.6	156	208	313	272
1.824	0.053	-0.07	-0.145	-0.131
1.425	0.676	0.535	0.485	0.544
180	651	618	664	649
3.004	1.784	1.526	1.421	1.513
20.47	14.71	19.93	14.87	13.89
0.23	0.45	0.42	0.49	0.44
0.21	0.42	0.41	0.5	0.45

VC4 11	VC4 12
21/05/2024 17:45	21/05/2024 17:53
10	5
0	0
0	0
0	0
0	0
0	0
0	0
0	0
0.19	0.05
0.66	0.44
1.25	0.87
2.03	1.34
2.2	1.44
2.36	1.54
2.59	1.66
2.95	1.83
3.48	2.07
4.38	2.42
5.69	2.88
7.32	3.4
9.3	3.98
11.5	4.66
14.02	5.63
17.27	7.49
21.75	10.9
26.8	15.49
34.9	23.83
44.53	34.4
55.05	46.4
67.46	60.96
78.13	73.66
87.41	84.81
94.16	92.95
98.38	98.05
99.99	99.99
100	100
100	100
100	100
100	100
158	288
546	618
1060	1100
584	658
199	284
-0.187	-0.071
0.531	0.48
645	665
1.656	1.322
18.85	16.12
0.45	0.52
0.44	0.52

Appendix C. Loss on Ignition Data

Surface Sediment Samples

Table Including the location of each sample, weights before and after samples have been processed using the blast furnace, the average grain size of each sample, the percentage of organic matter lost on ignition, and the total amount of weight lost from each sample.

Sample Name	Location	Weight (g) at 105	Minus container	weight (g) at 550	Minus Container	% LOI	Avg. Grain size	weight loss (g)
A1	176.1945788°E 37.6108884°S	6.95	6.4	6.88	6.33	1.09375	medium sand	0.07
A2	176.1972734°E 37.6142843°S	5.63	5.08	5.59	5.04	0.787401575	coarse sand	0.04
A3	176.2005804°E 37.6176800°S	6.84	6.29	6.8	6.25	0.635930048	coarse sand	0.04
A4	176.2038874°E 37.6209785°S	6.32	5.77	6.31	5.76	0.173310225	medium silt	0.01
A5	176.2071944°E 37.6241799°S	4.16	3.61	4.08	3.53	2.216066482	fine sand	0.08
A6	176.2101340°E 37.6275751°S	8.89	8.34	8.86	8.31	0.35971223	coarse sand	0.03
A7	176.2134410°E 37.6307762°S	3.92	3.37	3.87	3.32	1.483679525	fine sand	0.05
A8	176.2166255°E 37.6342681°S	4.59	4.04	4.51	3.96	1.98019802	fine sand	0.08
B1	176.1975184°E 37.6076865°S	8.89	8.34	8.85	8.3	0.479616307	coarse sand	0.04
B2	176.2010704°E 37.6112765°S	7.21	6.66	7.18	6.63	0.45045045	medium sand	0.03
B3	176.2038874°E 37.6142843°S	6.81	6.26	6.79	6.24	0.319488818	medium sand	0.02
B4	176.2070719°E 37.6177770°S	7.87	7.32	7.81	7.26	0.819672131	medium sand	0.06
B5	176.2103789°E 37.6210755°S	6.23	5.68	6.21	5.66	0.352112676	coarse sand	0.02
B6	176.2138084°E 37.6243739°S	8.05	7.5	8.03	7.48	0.266666667	coarse sand	0.02
B7	176.2167480°E 37.6278661°S	2.57	2.02	2.41	1.86	7.920792079	medium silt	0.16
B8	176.2198100°E 37.6309702°S	4.49	3.94	4.38	3.83	2.791878173	fine sand	0.11
C1	176.2010704°E 37.6045814°S	8.26	7.71	8.18	7.63	1.037613489	medium sand	0.08
C2	176.2042549°E 37.6077835°S	4.73	4.18	4.65	4.1	1.913875598	medium sand	0.08
C3	176.2074394°E 37.6113736°S	6.35	5.8	6.27	5.72	1.379310345	medium sand	0.08
C4	176.2106239°E 37.6147694°S	5.85	5.3	5.81	5.26	0.754716981	coarse sand	0.04
C5	176.2140534°E 37.6179710°S	5.08	4.53	5.02	4.47	1.324503311	medium sand	0.06
C6	176.2168704°E 37.6211725°S	5.29	4.74	5.25	4.7	0.843881857	medium sand	0.04
C7	176.2202999°E 37.6241799°S	4.9	4.35	4.84	4.29	1.379310345	fine sand	0.06
C8	176.2236069°E 37.6277691°S	3.62	3.07	3.51	2.96	3.583061889	fine sand	0.11
D1	176.2044998°E 37.6014763°S	5.69	5.14	5.65	5.1	0.778210117	coarse sand	0.04
D2	176.2078068°E 37.6046785°S	5.95	5.4	5.88	5.33	1.296296296	medium sand	0.07
D3	176.2107464°E 37.6082687°S	6.1	5.55	6.03	5.48	1.261261261	medium sand	0.07
D4	176.2141759°E 37.6113736°S	6.03	5.48	5.97	5.42	1.094890511	coarse sand	0.06
D5	176.2171154°E 37.6145753°S	5.11	4.56	5.04	4.49	1.535087719	medium sand	0.07
D6	176.2205449°E 37.6180680°S	4.61	4.06	4.55	4	1.477832512	medium sand	0.06
D7	176.2232395°E 37.6213666°S	3.73	3.18	3.67	3.12	1.886792453	medium sand	0.06
D8	176.2267914°E 37.6246649°S	5.87	5.32	5.85	5.3	0.37593985	medium sand	0.02

Sample Name	Location	Weight (g) at 105	Minus container	weight (g) at 550	Minus Container	% LOI	Avg. Grain size	weight loss (g)
E1	176.2078068°E 37.5982739°S	6.75	6.2	6.69	6.14	0.967741935	coarse sand	0.06
E2	176.2112363°E 37.6013792°S	4.34	3.79	4.27	3.72	1.846965699	fine sand	0.07
E3	176.2142983°E 37.6049696°S	4.06	3.51	3.98	3.43	2.279202279	medium sand	0.08
E4	176.2174829°E 37.6081716°S	4.66	4.11	4.57	4.02	2	fine sand	0.09
E5	176.2206674°E 37.6111795°S	5.54	4.99	5.45	4.9	1.803607214	fine sand	0.09
E6	176.2239744°E 37.6148664°S	4.8	4.25	4.7	4.15	2.352941176	medium sand	0.1
E7	176.2267914°E 37.6181651°S	4.89	4.34	4.84	4.29	1.152073733	coarse sand	0.05
E8	176.2300984°E 37.6214636°S	4.5	3.95	4.47	3.92	0.759493671	medium sand	0.03
F1	176.2112363°E 37.5951685°S	2.97	2.42	2.87	2.32	4.132231405	fine sand	0.1
F2	176.2144208°E 37.5985650°S	4.53	3.98	4.46	3.91	1.75879397	medium sand	0.07
F3	176.2174829°E 37.6017674°S	4.7	4.15	4.62	4.07	1.927710843	fine sand	0.08
F4	176.2205449°E 37.6051636°S	5.78	5.23	5.73	5.18	0.956022945	coarse sand	0.05
F5	176.2238519°E 37.6083657°S	2.98	2.43	2.96	2.41	0.823045267	medium sand	0.02
F6	176.2271589°E 37.6116646°S	4.93	4.38	4.79	4.24	2.04778157	medium sand	0.14
F7	176.2303434°E 37.6153515°S	4.39	3.84	4.32	3.77	1.822916667	medium sand	0.07
F8	176.2335279°E 37.6183591°S	5.88	5.33	5.83	5.28	0.938086304	medium sand	0.05
G1	176.2147883°E 37.5918688°S	3.84	3.29	3.72	3.17	3.647416413	fine sand	0.12
G2	176.2177278°E 37.5952655°S	6.53	5.98	6.47	5.92	1.003344482	medium sand	0.06
G3	176.2210348°E 37.5984680°S	5.49	4.94	5.44	4.89	1.012145749	medium sand	0.05
G4	176.2242193°E 37.6018644°S	4.19	3.64	4.12	3.57	1.923076923	fine sand	0.07
G5	176.2270364°E 37.6053577°S	3.51	2.96	3.47	2.92	1.351351351	medium sand	0.04
G6	176.2305884°E 37.6085598°S	4.89	4.34	4.84	4.29	1.152073733	medium sand	0.05
G7	176.2336504°E 37.6120527°S	4.43	3.88	4.36	3.81	1.804123711	medium sand	0.07
G8	176.2369574°E 37.6152545°S	5.52	4.97	5.19	4.64	0.84033613	coarse sand	0.33
H1	176.2176053°E 37.5886660°S	7.2	6.65	7.13	6.58	1.052631579	fine sand	0.07
H2	176.2210348°E 37.5920629°S	6.67	6.12	6.62	6.07	0.816993464	coarse sand	0.05
H3	176.2240968°E 37.5953626°S	3.6	3.05	3.54	2.99	1.967213115	fine sand	0.06
H4	176.2274038°E 37.5987591°S	8.32	7.77	8.25	7.7	0.900900901	Very coarse sand	0.07
H5	176.2304659°E 37.6020585°S	6.59	6.04	6.55	6	0.662251656	coarse sand	0.04
H6	176.2336504°E 37.6054547°S	5.2	4.65	5.18	4.63	0.430107527	medium sand	0.02
H7	176.2370799°E 37.6086568°S	7.58	7.03	7.56	7.01	0.284495021	coarse sand	0.02
H8	176.2400194°E 37.6118587°S	5.68	5.13	5.63	5.08	0.974658869	coarse sand	0.05

Vibracore Samples

Loss on Ignition data for the 60 sub samples taken from the 4 core samples. Including location, weights before and after samples have been processed using the blast furnace, the average grain size of each sample, the percentage of organic matter lost on ignition, and the total amount of weight lost from each sample.

Sample Name	Location	Depth (cm)	Weight (g) at 105	Minus container	weight (g) at 550	Minus Container	% LOI	Avg. grain size	weight loss (g)
VC1 1	176.112678°E 37.366425°S	55	5.03	4.48	4.93	4.38	2.232142857	fine sand	0.1
VC1 2		50	4.48	3.93	4.39	3.84	2.290076336	fine sand	0.09
VC1 3		45	5.69	5.14	5.58	5.03	2.140077821	fine sand	0.11
VC1 4		40	6.24	5.69	6.11	5.56	2.284710018	fine sand	0.13
VC1 5		35	5.51	4.96	5.39	4.84	2.419354839	fine sand	0.12
VC1 6		30	5.42	4.87	5.35	4.8	1.437371663	fine sand	0.07
VC1 7		25	6.38	5.83	6.26	5.71	2.058319039	fine sand	0.12
VC1 8		20	6.59	6.04	6.47	5.92	1.986754967	fine sand	0.12
VC1 9		15	7.21	6.66	7.08	6.53	1.951951952	fine sand	0.13
VC1 10		10	6.21	5.66	6.1	5.55	1.943462898	fine sand	0.11
VC1 11		5	6.26	5.71	6.14	5.59	2.101576182	fine sand	0.12
VC2 1	176.124454°E 37.36683°S	35	5.12	4.57	5.08	4.53	0.875273523	medium sand	0.04
VC2 2		30	5.39	4.84	5.32	4.77	1.446280992	medium sand	0.07
VC2 3		25	6.83	6.28	6.78	6.23	0.796178344	medium sand	0.05
VC2 4		20	6.1	5.55	6.05	5.5	0.900900901	medium sand	0.05
VC2 5		15	6.12	5.57	6.05	5.5	1.256732496	medium sand	0.07
VC2 6		10	6.8	6.25	6.74	6.19	0.96	medium sand	0.06
VC2 7		5	7.79	7.24	7.68	7.13	1.519337017	medium sand	0.11
VC3 1	176.136123°E 37.36695°S	150	4.84	4.29	4.7	4.15	3.263403263	fine sand	0.14
VC3 2		145	4.43	3.88	4.3	3.75	3.350515464	fine sand	0.13
VC3 3		140	5.58	5.03	5.43	4.88	2.982107356	fine sand	0.15
VC3 4		135	5.34	4.79	5.2	4.65	2.922755741	fine sand	0.14
VC3 5		130	4.94	4.39	4.79	4.24	3.416856492	fine sand	0.15
VC3 6		125	4.26	3.71	4.14	3.59	3.234501348	fine sand	0.12
VC3 7		120	4.96	4.41	4.82	4.27	3.174603175	fine sand	0.14
VC3 8		115	5.78	5.23	5.65	5.1	2.485659656	fine sand	0.13
VC3 9		110	4.61	4.06	4.47	3.92	3.448275862	fine sand	0.14
VC3 10		105	4.57	4.02	4.43	3.88	3.482587065	fine sand	0.14
VC3 11		100	4.76	4.21	4.61	4.06	3.562945368	fine sand	0.15
VC3 12		95	4.94	4.39	4.79	4.24	3.416856492	fine sand	0.15

Sample Name	Location	Depth	Weight (g) at 105	Minus container	weight (g) at 550	Minus Container	% LOI	Avg. grain size	weight loss (g)
VC3 13		90	4.35	3.8	4.22	3.67	3.421052632	fine sand	0.13
VC3 14		85	5.98	5.43	5.84	5.29	2.578268877	fine sand	0.14
VC3 15		80	5.51	4.96	5.37	4.82	2.822580645	fine sand	0.14
VC3 16		75	5.7	5.15	5.55	5	2.912621359	fine sand	0.15
VC3 17		70	6.75	6.2	6.66	6.11	1.451612903	medium sand	0.09
VC3 18		65	6.86	6.31	6.8	6.25	0.950871632	medium sand	0.06
VC3 19		60	7.07	6.52	7.02	6.47	0.766871166	medium sand	0.05
VC3 20		55	7.19	6.64	7.16	6.61	0.451807229	coarse sand	0.03
VC3 21		50	5.34	4.79	5.15	4.6	3.966597077	coarse silt	0.19
VC3 22		45	6.97	6.42	6.89	6.34	1.246105919	coarse sand	0.08
VC3 23		40	6.26	5.71	6.18	5.63	1.401050788	medium sand	0.08
VC3 24		35	6.06	5.51	5.97	5.42	1.633393829	medium sand	0.09
VC3 25		30	5.63	5.08	5.54	4.99	1.771653543	fine sand	0.09
VC3 26		25	5.62	5.07	5.54	4.99	1.57790927	fine sand	0.08
VC3 27		20	5.63	5.08	5.55	5	1.57480315	medium sand	0.08
VC3 28		15	6.43	5.88	6.34	5.79	1.530612245	medium sand	0.09
VC3 29		10	6.19	5.64	6.12	5.57	1.241134752	medium sand	0.07
VC3 30		5	5.65	5.1	5.61	5.06	0.784313725	medium sand	0.04
VC4 1	176.148632°E 37.366691°S	60	5.38	4.83	5.27	4.72	2.277432712	fine sand	0.11
VC4 2		55	6.13	5.58	6.01	5.46	2.150537634	fine sand	0.12
VC4 3		50	4.72	4.17	4.61	4.06	2.637889688	fine sand	0.11
VC4 4		45	5.85	5.3	5.75	5.2	1.886792453	fine sand	0.1
VC4 5		40	5.878	5.328	5.66	5.11	4.091591592	fine sand	0.218
VC4 6		35	6.34	5.79	6.23	5.68	1.899827288	fine sand	0.11
VC4 7		30	7.62	7.07	7.56	7.01	0.848656294	medium sand	0.06
VC4 8		25	6.47	5.92	6.41	5.86	1.013513514	coarse sand	0.06
VC4 9		20	6.62	6.07	6.58	6.03	0.658978583	coarse sand	0.04
VC4 10		15	6.38	5.83	6.34	5.79	0.686106346	coarse sand	0.04
VC4 11		10	6.97	6.42	6.92	6.37	0.778816199	medium sand	0.05
VC4 12		5	7.53	6.98	7.46	6.91	1.00286533	coarse sand	0.07

Appendix D1. Seismic Profiles

Seismic line survey A, shore-to-sea.

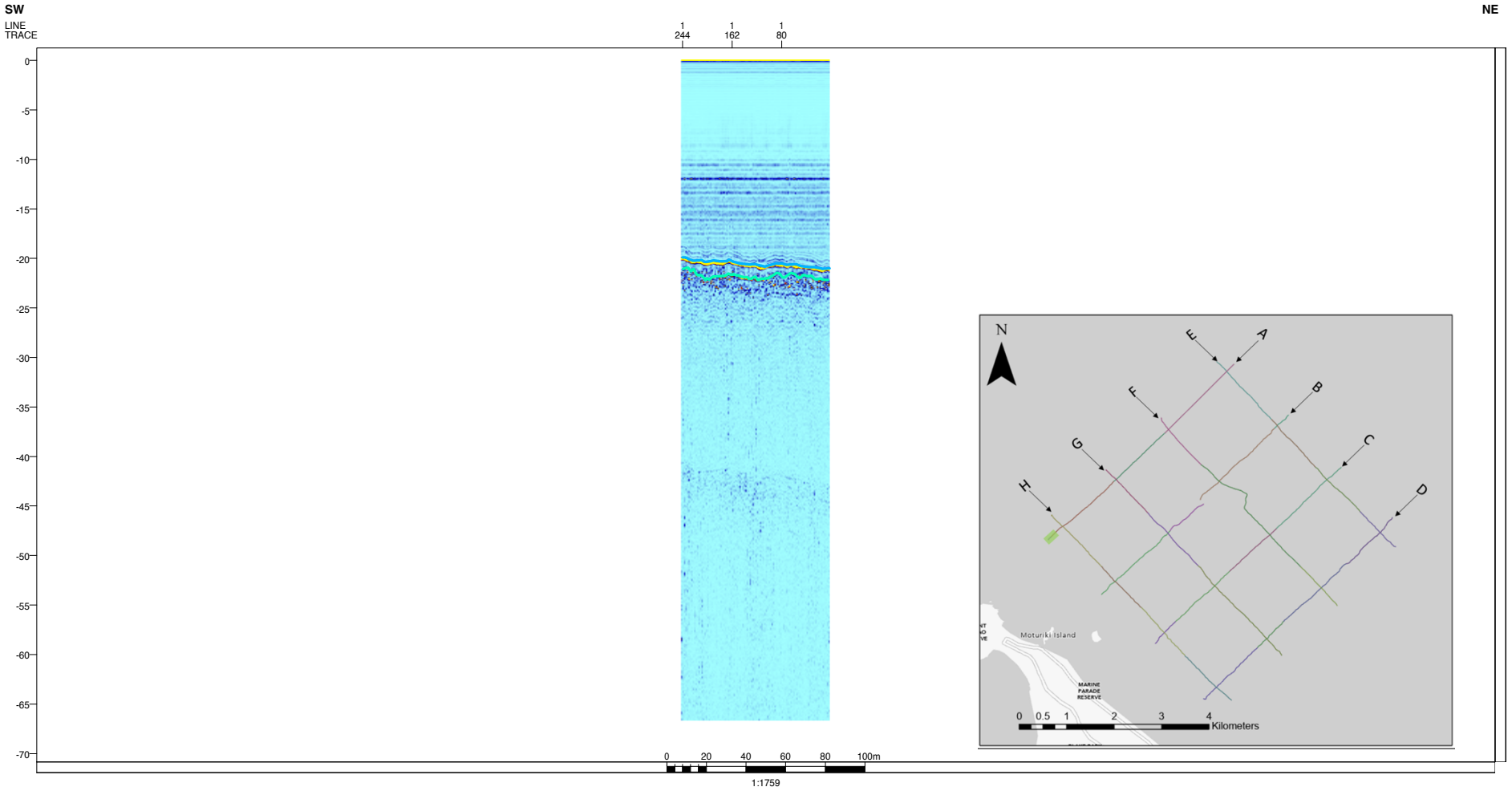

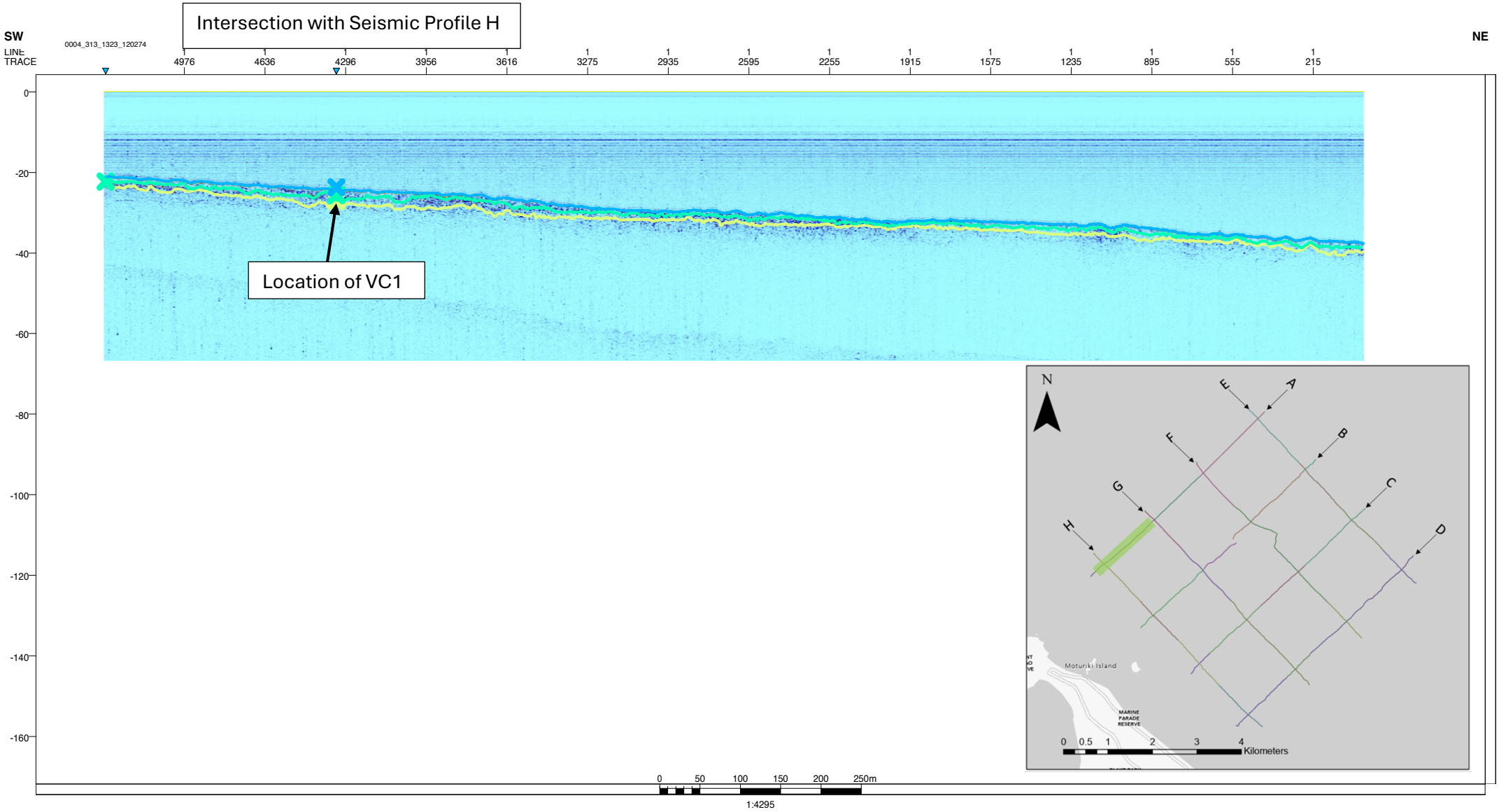
Intersection with Seismic Profile H
SW
NE
0004_313_1323_120274
LINE
TRACE
4976
4636
4296
3956
3616
3275
2935
2595
2255
1915
1575
1235
895
555
215
0
-20
-40
-60
-80
-100
-120
-140
-160
Location of VC1
N
A
B
C
D
E
F
G
H
Moturiki Island
MARINE PARADE RESERVE
0 0.5 1 2 3 4
Kilometers
0 50 100 150 200 250m
1:4295

Intersection with Seismic Profile G

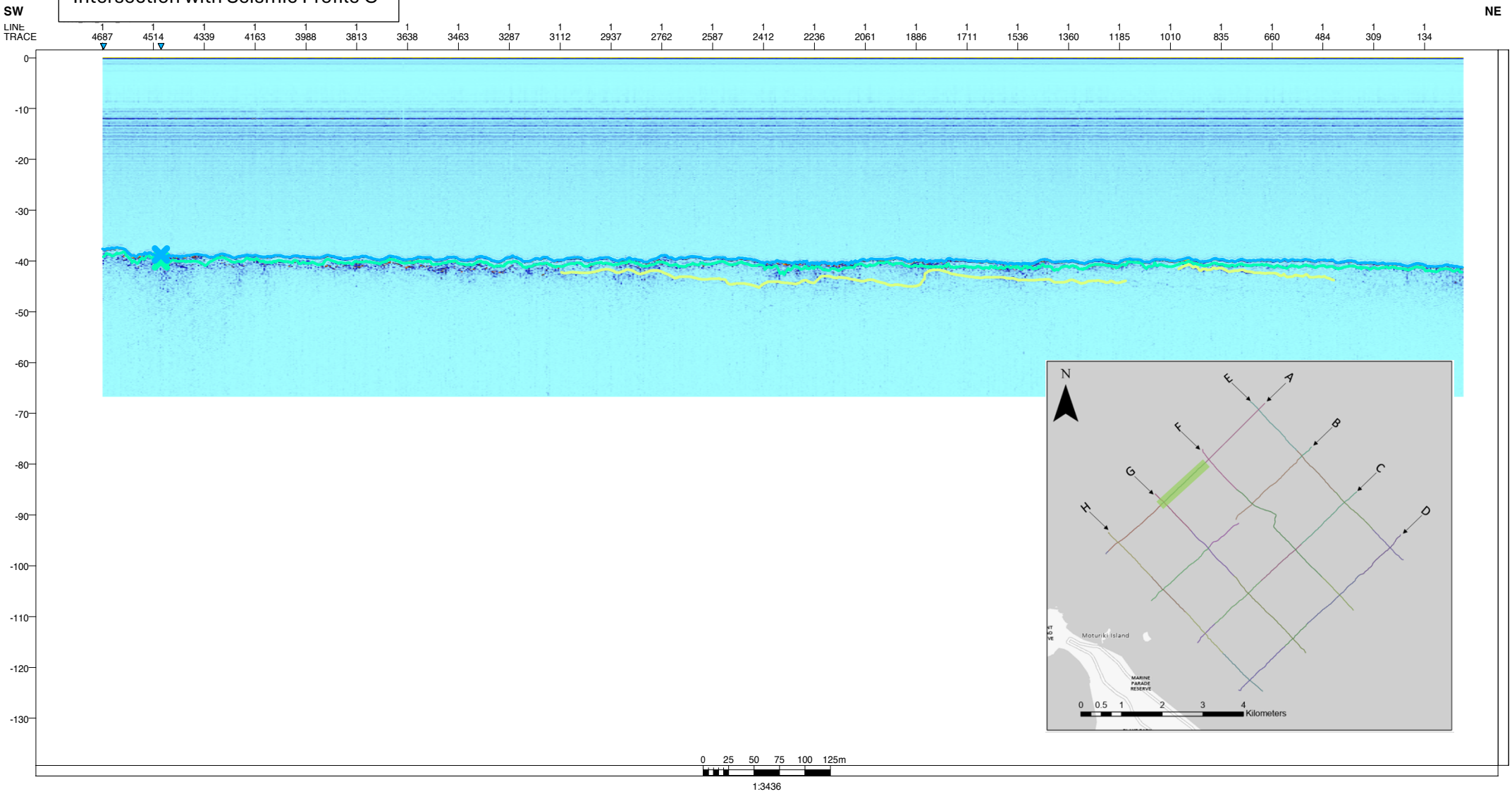

Intersection with Seismic Profile F

Intersection with Seismic Profile E

SW

NE

LINE
TRACE

1 361 1 720 1 1080 1 1440 1 1800 1 2159 1 2519 1 2879 1 3238 1 3598 1 3958 1 4318 1 4677 1 5037 1 5397 1 5756 1 6116 1 6476

0
-20
-40
-60
-80
-100
-120
-140
-160
-180
-200

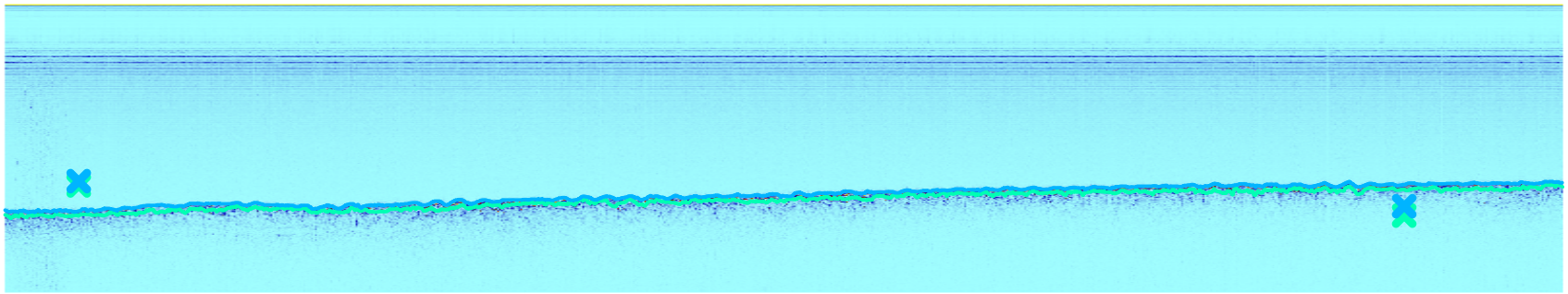

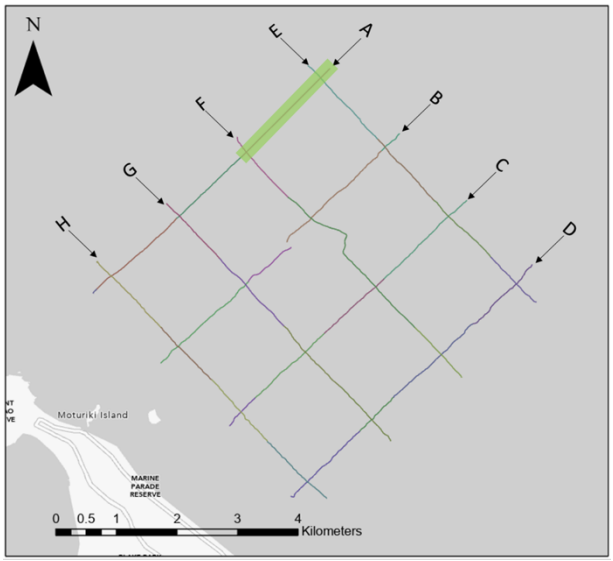

0 50 100 150 200 250m

1:5369

Seismic line survey B, shore-to-sea.

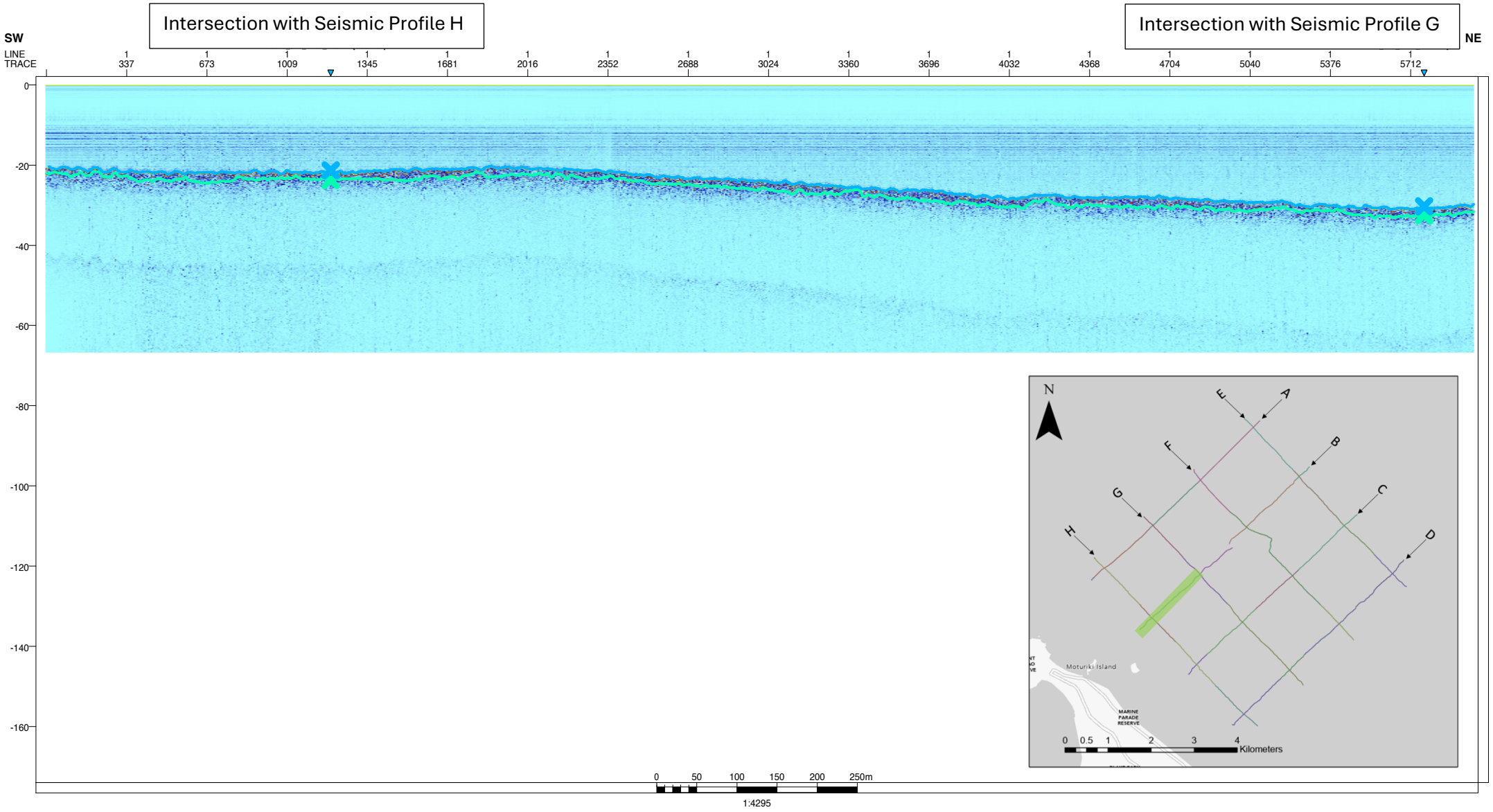

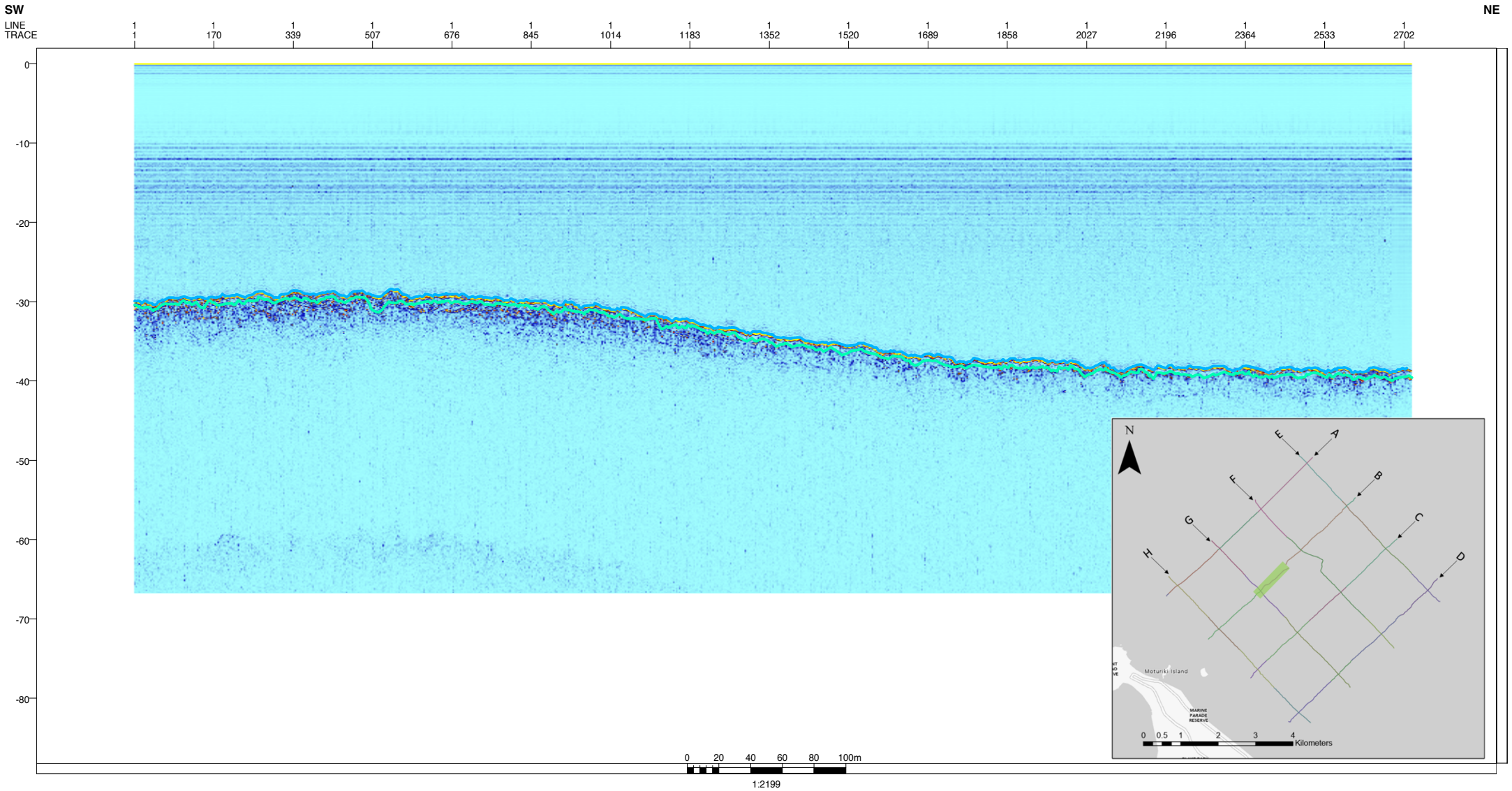
SW
NE
LINE
TRACE
1 1
1 170
1 339
1 507
1 676
1 845
1 1014
1 1183
1 1352
1 1520
1 1689
1 1858
1 2027
1 2196
1 2364
1 2533
1 2702
0
-10
-20
-30
-40
-50
-60
-70
-80
N
A
B
C
D
E
F
G
H
Moturiki Island
MARINE PARADE RESERVE
0 0.5 1 2 3 4 Kilometers
0 20 40 60 80 100m
1:2199

Intersection with Seismic Profile F

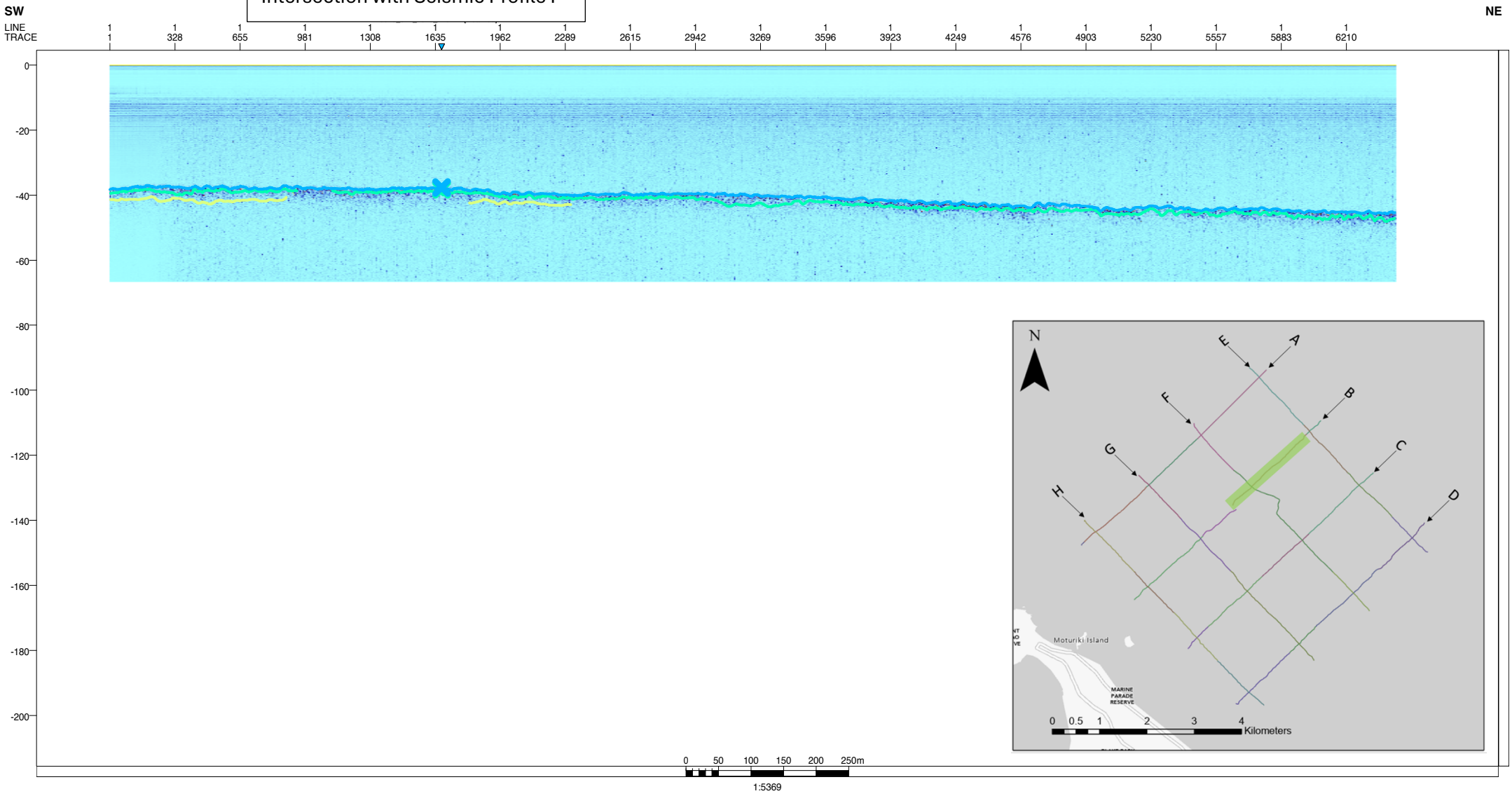

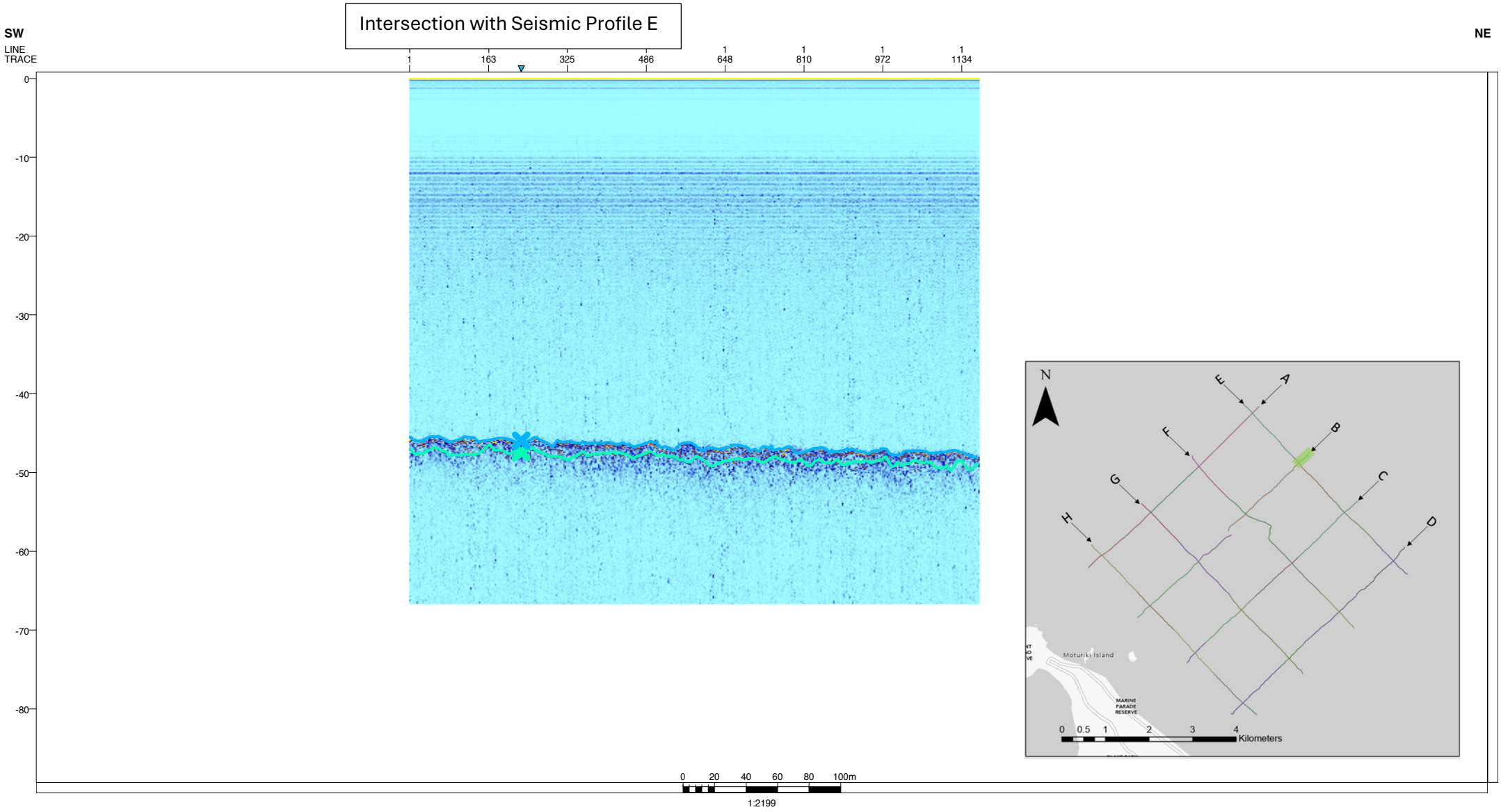
Intersection with Seismic Profile E
SW
NE
LINE
TRACE
1
163
325
486
1 648
1 810
1 972
1 1134
0
-10
-20
-30
-40
-50
-60
-70
-80
0 20 40 60 80 100m
1:2199
N
A
B
C
D
E
F
G
H
Moturiki Island
MARINE PARADE RESERVE
0 0.5 1 2 3 4
Kilometers

Seismic line survey C, shore-to-sea.

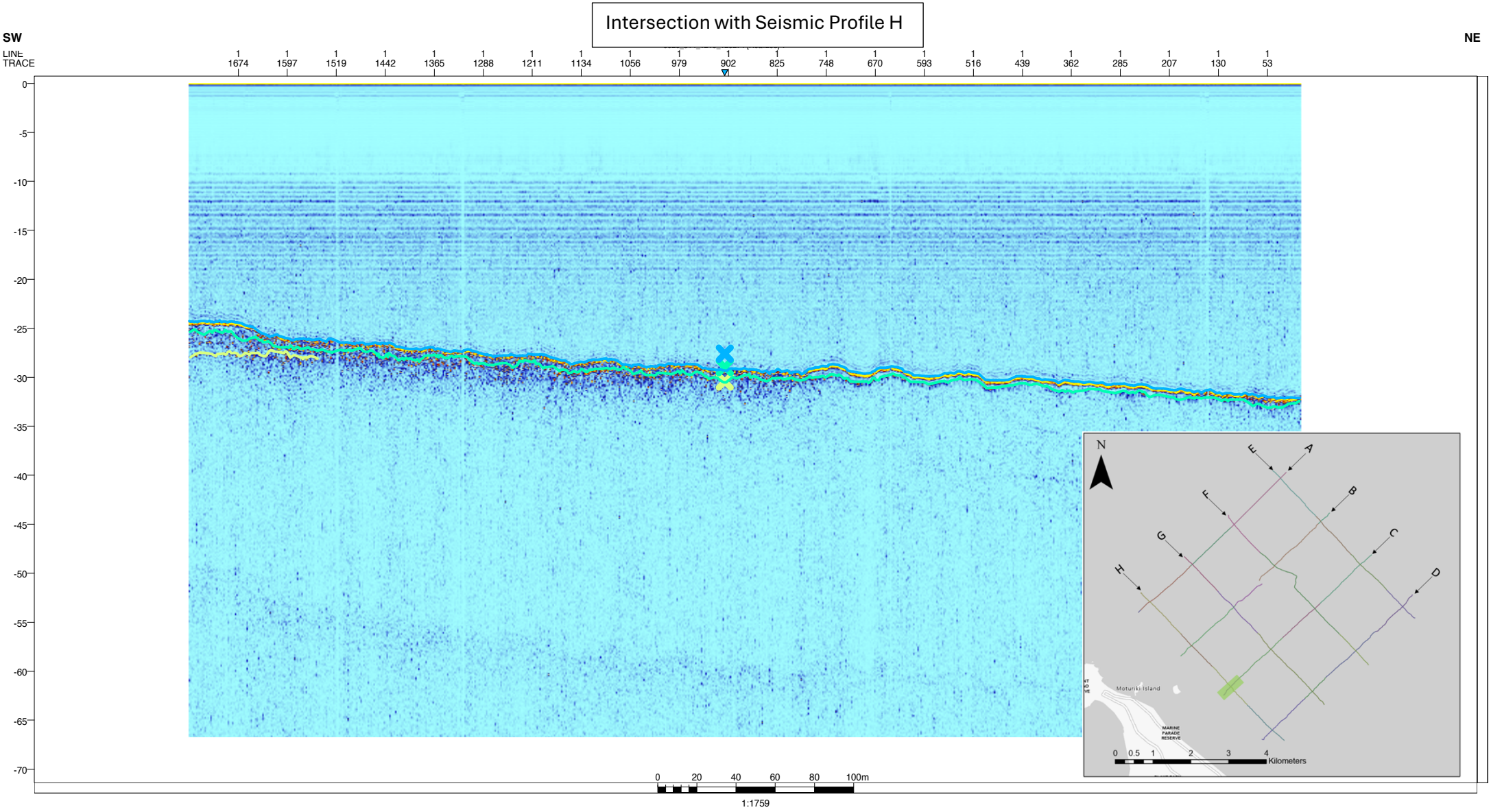

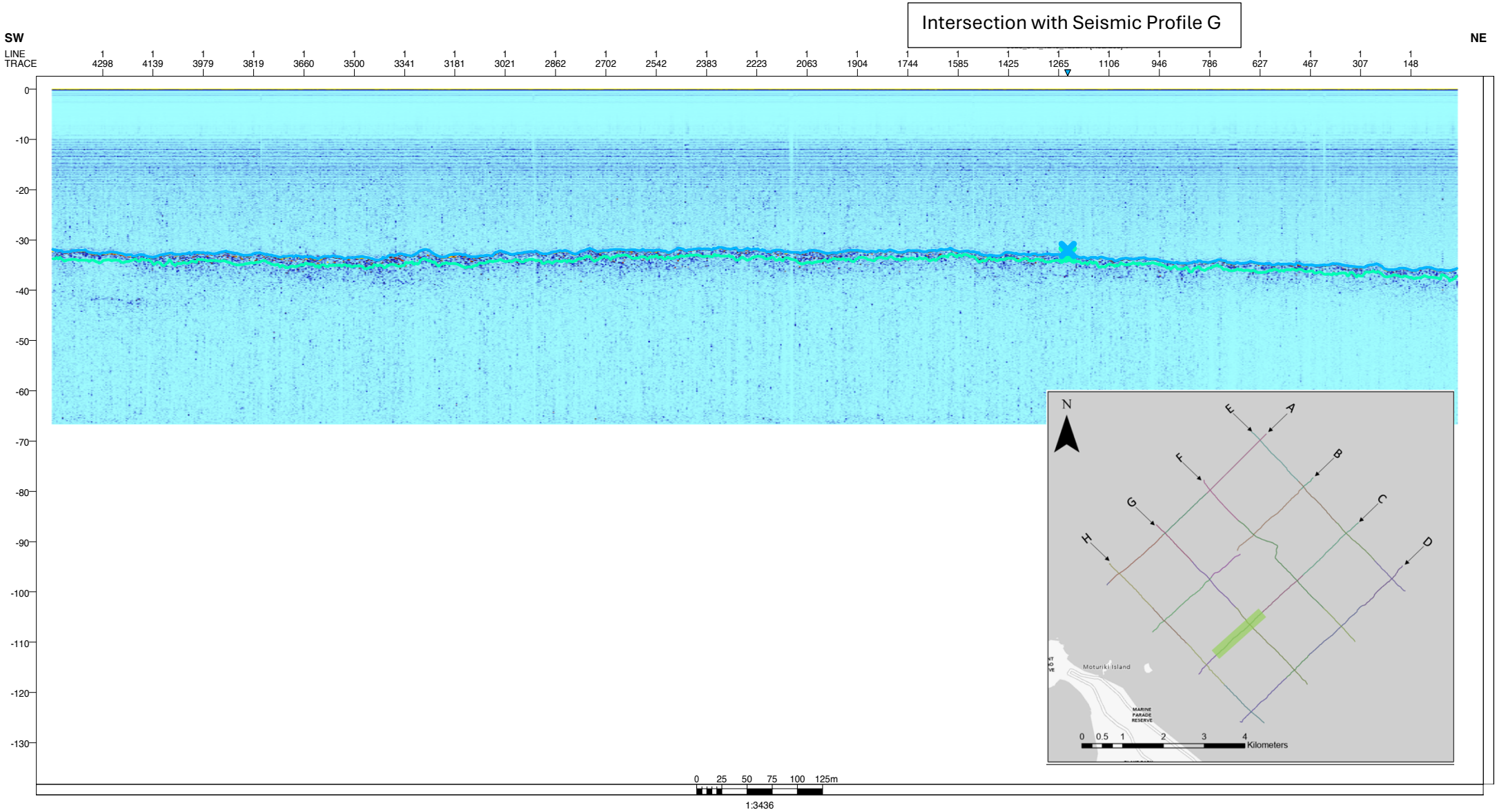
Intersection with Seismic Profile G
SW
NE
LINE
TRACE
1 4298
1 4139
1 3979
1 3819
1 3660
1 3500
1 3341
1 3181
1 3021
1 2862
1 2702
1 2542
1 2383
1 2223
1 2063
1 1904
1 1744
1 1585
1 1425
1 1265
1 1106
1 946
1 786
1 627
1 467
1 307
1 148
0
-10
-20
-30
-40
-50
-60
-70
-80
-90
-100
-110
-120
-130
N
A
B
C
D
E
F
G
H
Moturiki Island
MARINE PARADE RESERVE
0 0.5 1 2 3 4
Kilometers
0 25 50 75 100 125m
1:3436

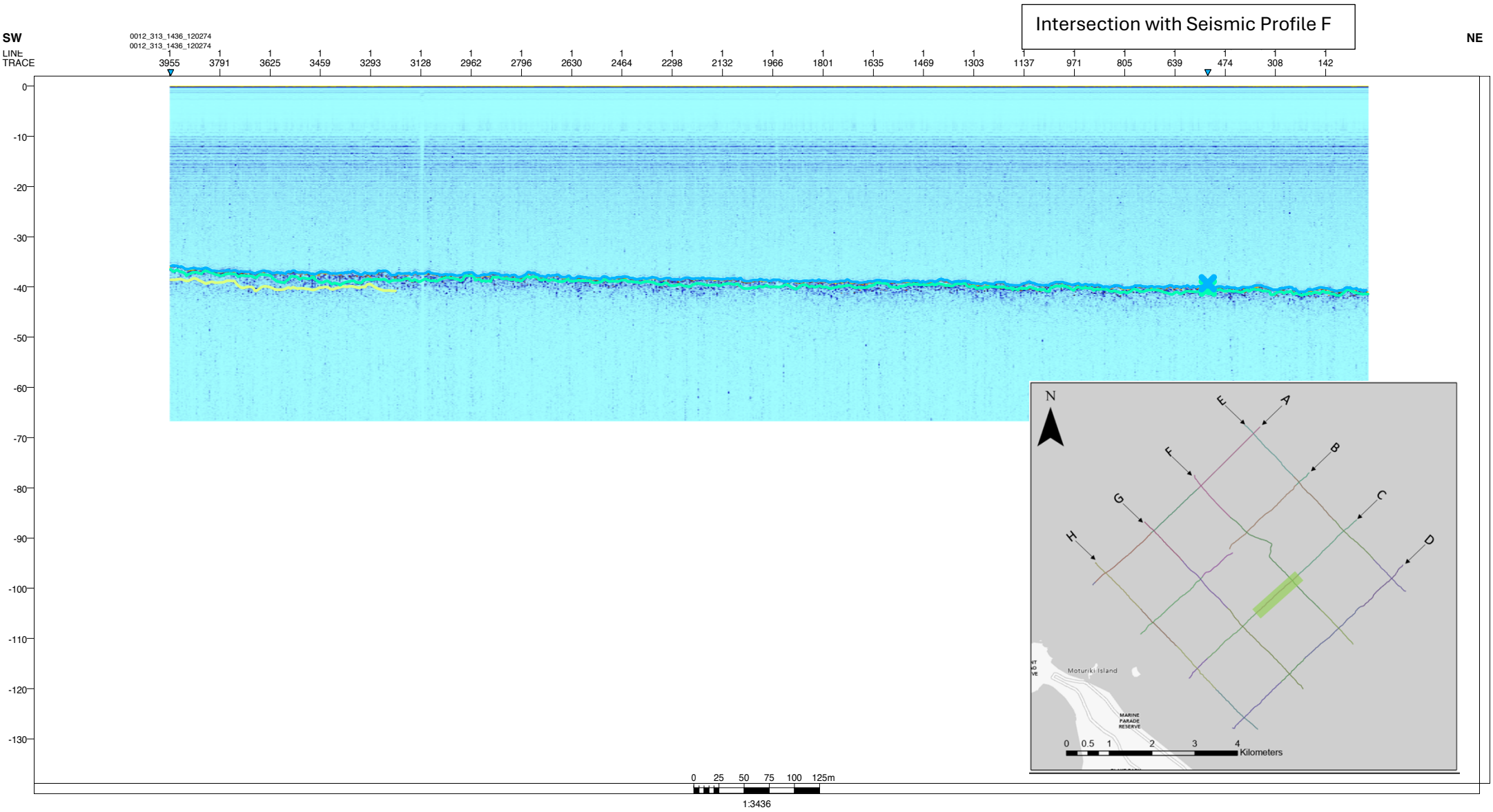
Intersection with Seismic Profile F
SW
NE
0012_313_1436_120274
0012_313_1436_120274
LINE
TRACE
3955
3791
3625
3459
3293
3128
2962
2796
2630
2464
2298
2132
1966
1801
1635
1469
1303
1137
971
805
639
474
308
142
0
-10
-20
-30
-40
-50
-60
-70
-80
-90
-100
-110
-120
-130
N
A
B
C
D
E
F
G
H
Moturiki Island
MARINE PARADE RESERVE
0 0.5 1 2 3 4
Kilometers
0 25 50 75 100 125m
1:3436

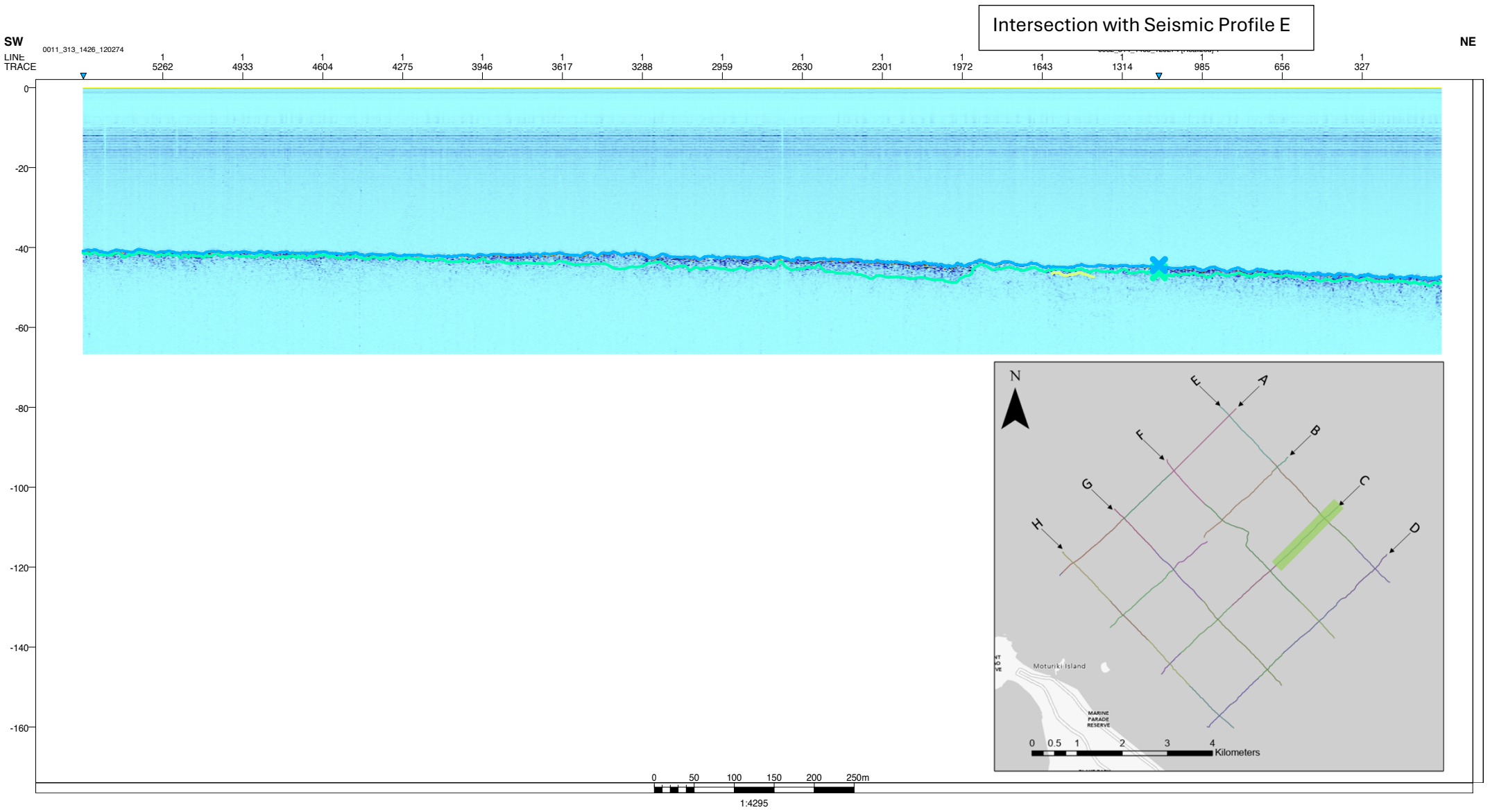
Intersection with Seismic Profile E
SW
NE
0011_313_1426_120274
LINE
TRACE
1 5262
1 4933
1 4604
1 4275
1 3946
1 3617
1 3288
1 2959
1 2630
1 2301
1 1972
1 1643
1 1314
1 985
1 656
1 327
0
-20
-40
-60
-80
-100
-120
-140
-160
N
E
A
F
B
G
C
H
D
Moturiki Island
MARINE PARADE RESERVE
0 0.5 1 2 3 4
Kilometers
0 50 100 150 200 250m
1:4295

Seismic line survey D, shore-to-sea.

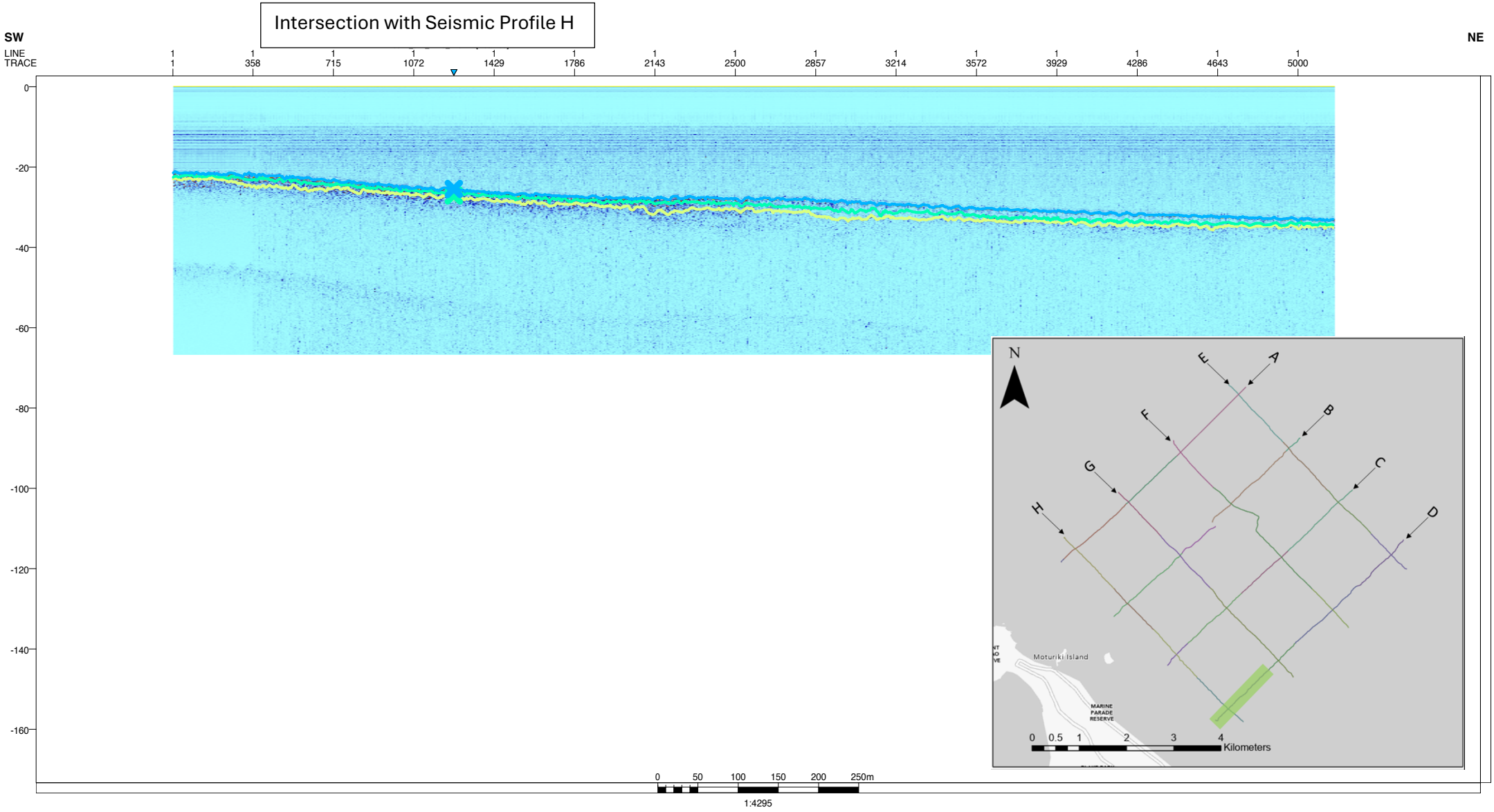

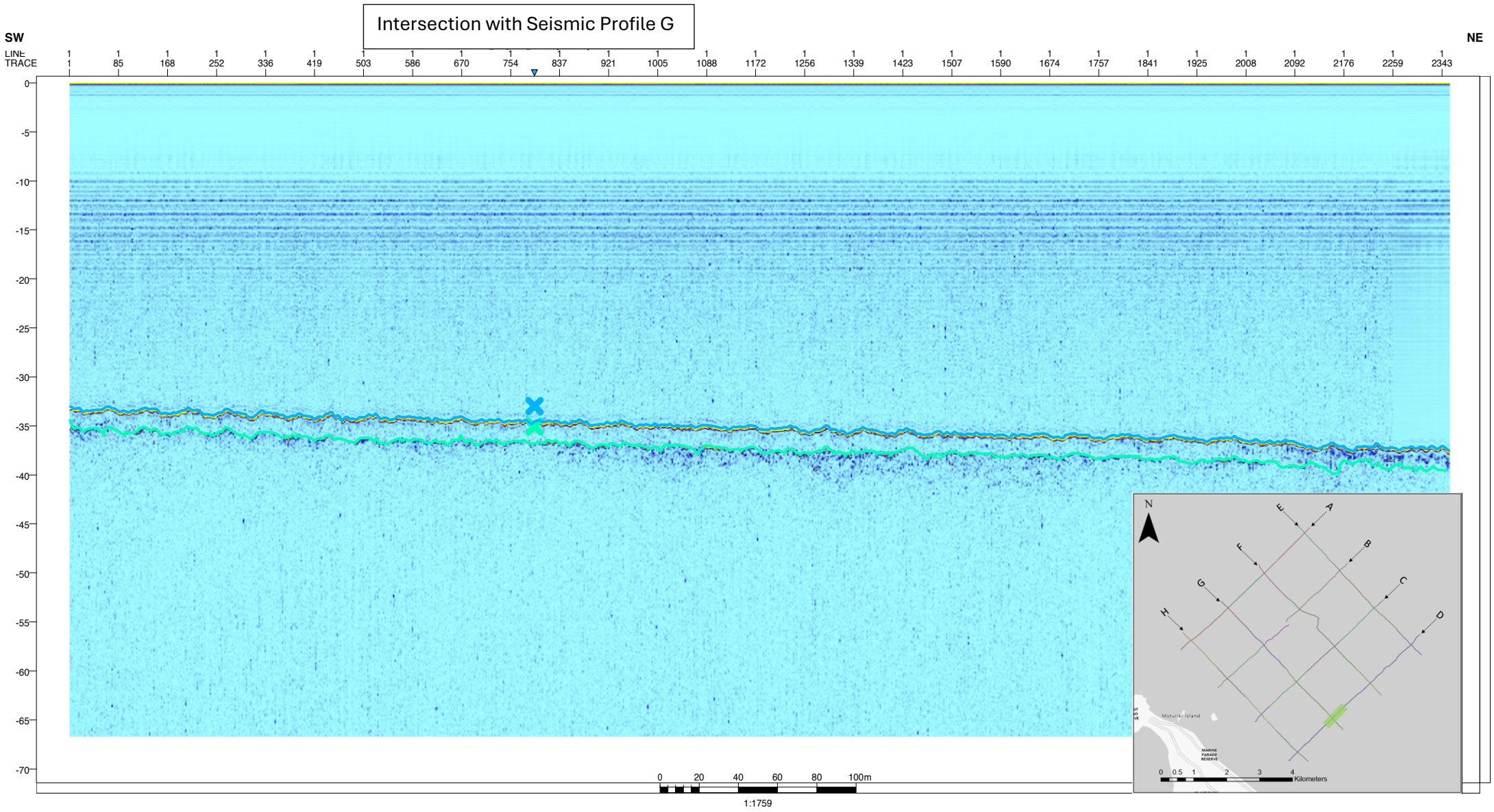
Intersection with Seismic Profile G
SW
NE
LINE
TRACE
1 1
1 85
1 168
1 252
1 336
1 419
1 503
1 586
1 670
1 754
1 837
1 921
1 1005
1 1088
1 1172
1 1256
1 1339
1 1423
1 1507
1 1590
1 1674
1 1757
1 1841
1 1925
1 2008
1 2092
1 2176
1 2259
1 2343
0
-5
-10
-15
-20
-25
-30
-35
-40
-45
-50
-55
-60
-65
-70
0 20 40 60 80 100m
1:1759
N
E
A
F
B
G
C
H
D
Moturiki Island
MARINE PARADE RESERVE
0 0.5 1 2 3 4 Kilometers

Intersection with Seismic Profile F

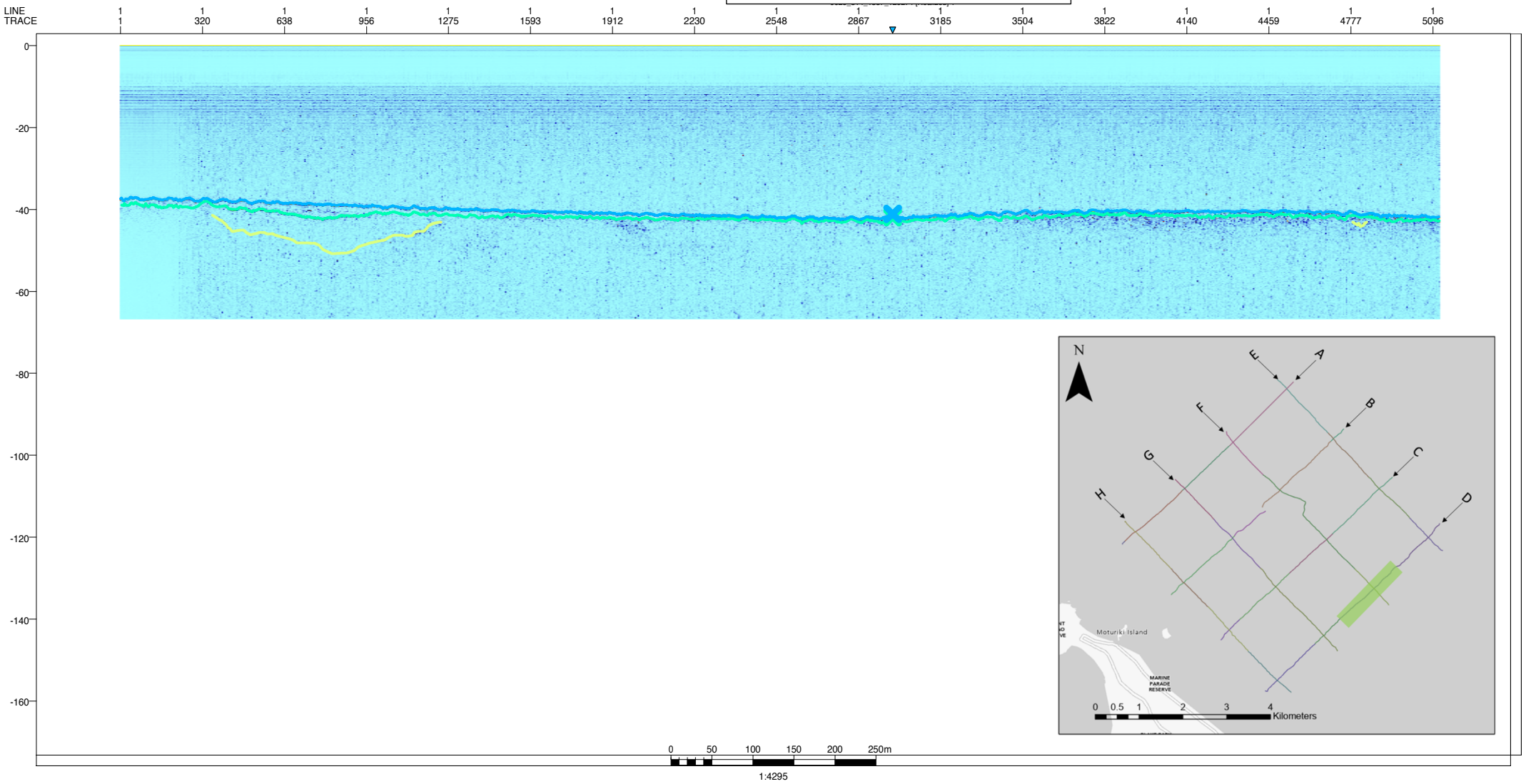

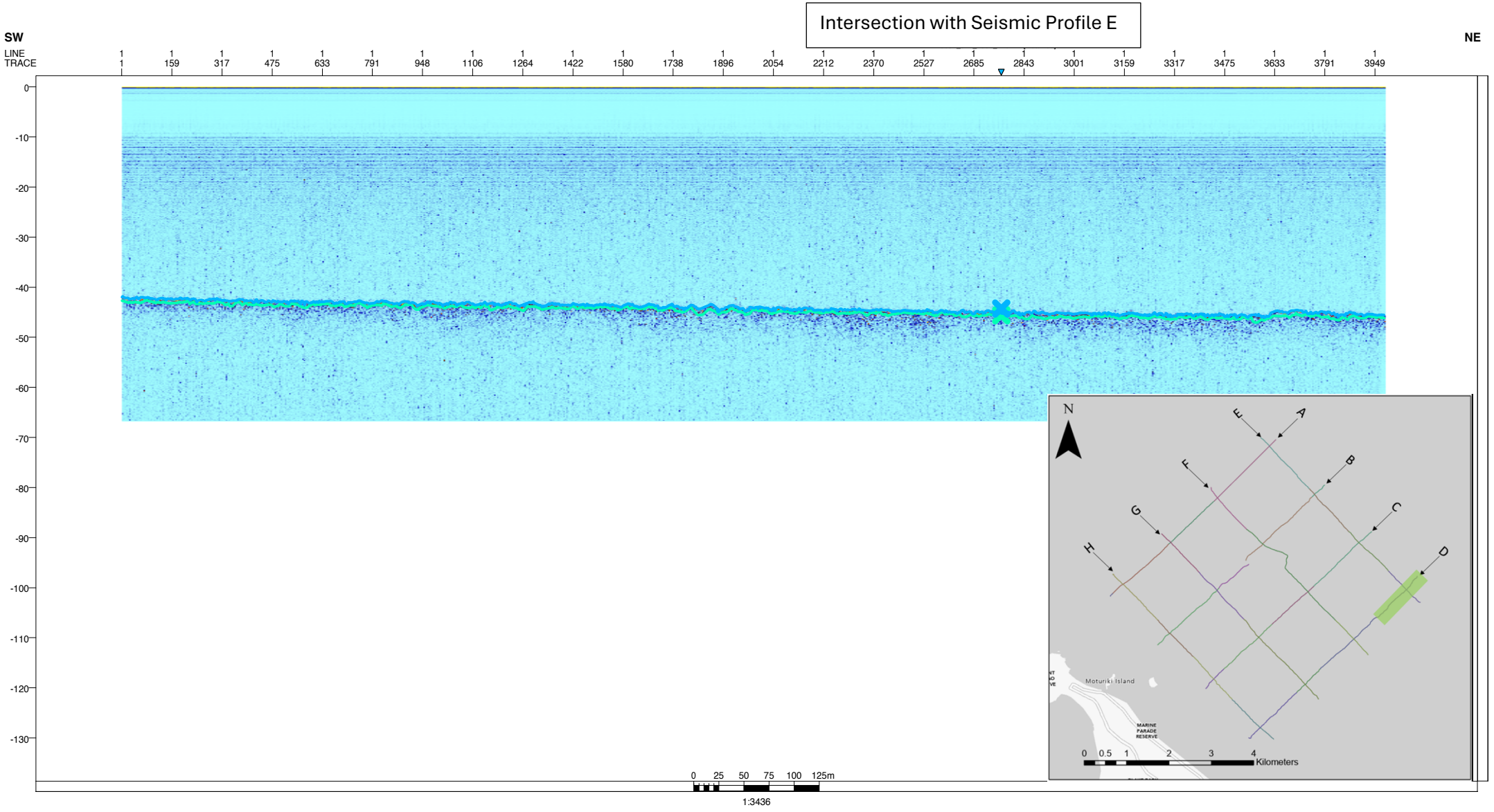
Intersection with Seismic Profile E
SW
NE
LINE
TRACE
1 1
1 159
1 317
1 475
1 633
1 791
1 948
1 1106
1 1264
1 1422
1 1580
1 1738
1 1896
1 2054
1 2212
1 2370
1 2527
1 2685
1 2843
1 3001
1 3159
1 3317
1 3475
1 3633
1 3791
1 3949
0
-10
-20
-30
-40
-50
-60
-70
-80
-90
-100
-110
-120
-130
N
A
B
C
D
E
F
G
H
Moturiki Island
MARINE PARADE RESERVE
0 0.5 1 2 3 4
Kilometers
0 25 50 75 100 125m
1:3436

Seismic line survey E, from northwest to southwest

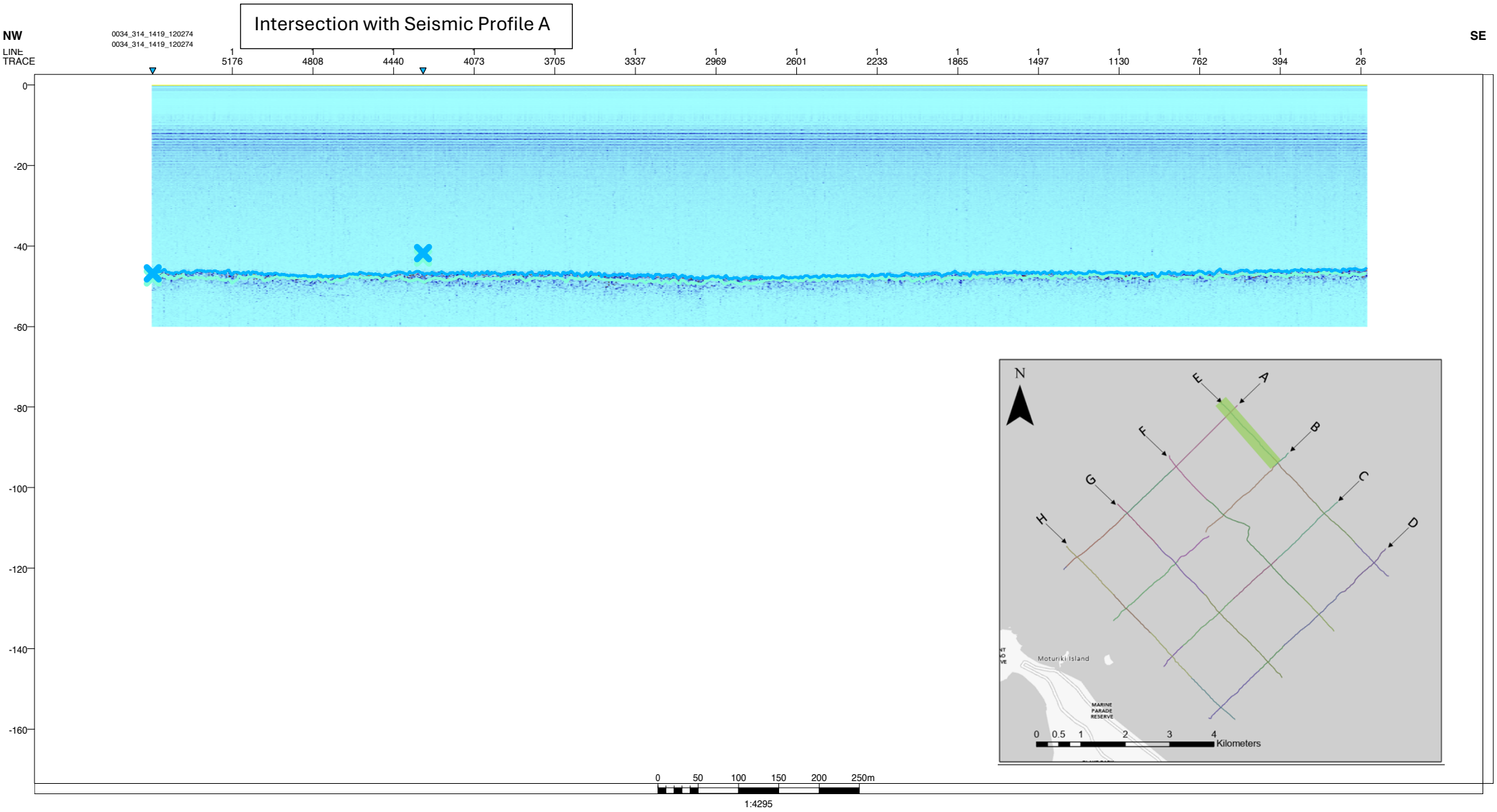

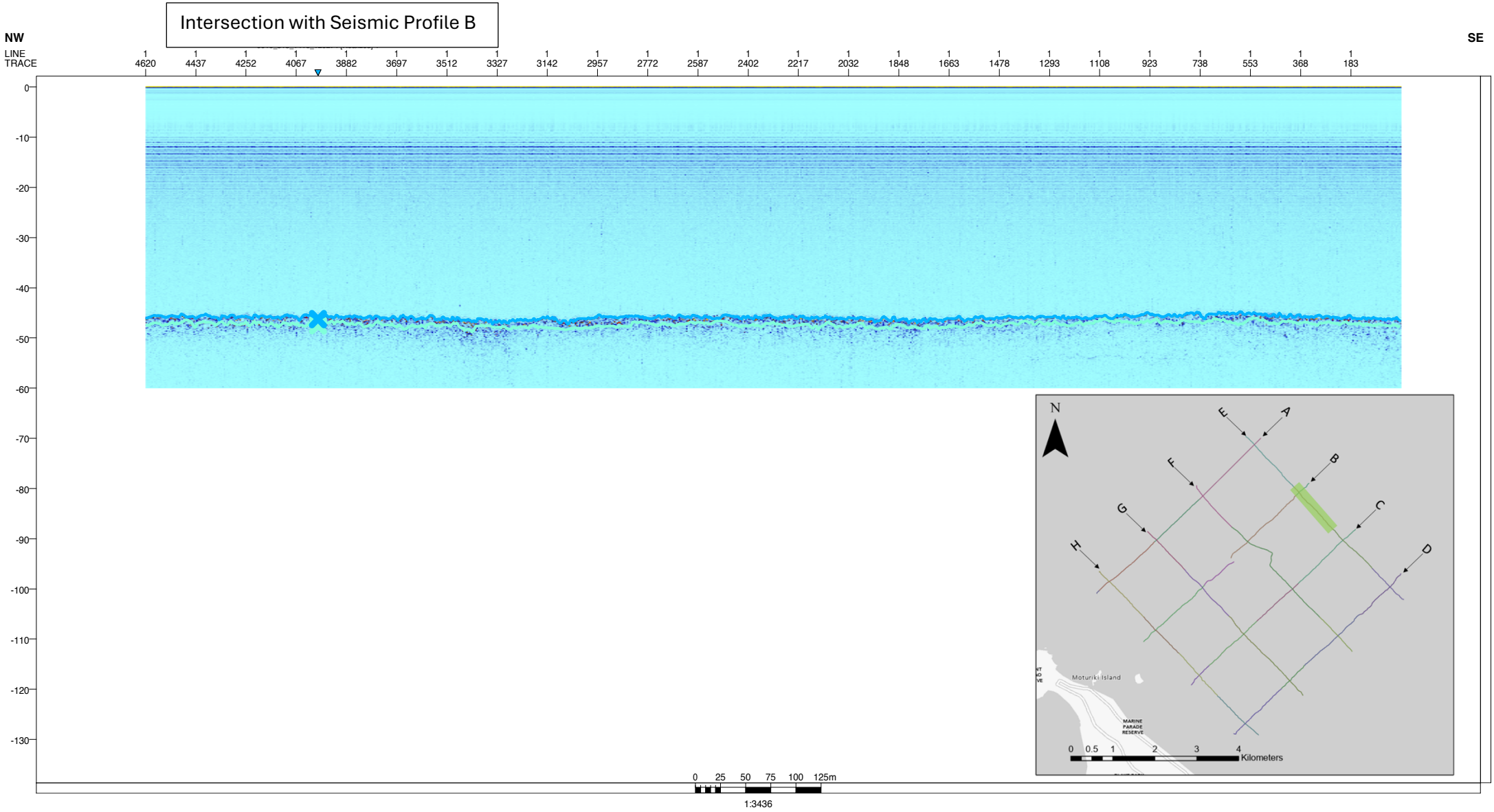
Intersection with Seismic Profile B
NW
SE
LINE
TRACE
1 4620
1 4437
1 4252
1 4067
1 3882
1 3697
1 3512
1 3327
1 3142
1 2957
1 2772
1 2587
1 2402
1 2217
1 2032
1 1848
1 1663
1 1478
1 1293
1 1108
1 923
1 738
1 553
1 368
1 183
0
-10
-20
-30
-40
-50
-60
-70
-80
-90
-100
-110
-120
-130
N
A
B
C
D
E
F
G
H
Moturiki Island
MARINE PARADE RESERVE
0 0.5 1 2 3 4
Kilometers
0 25 50 75 100 125m
1:3436

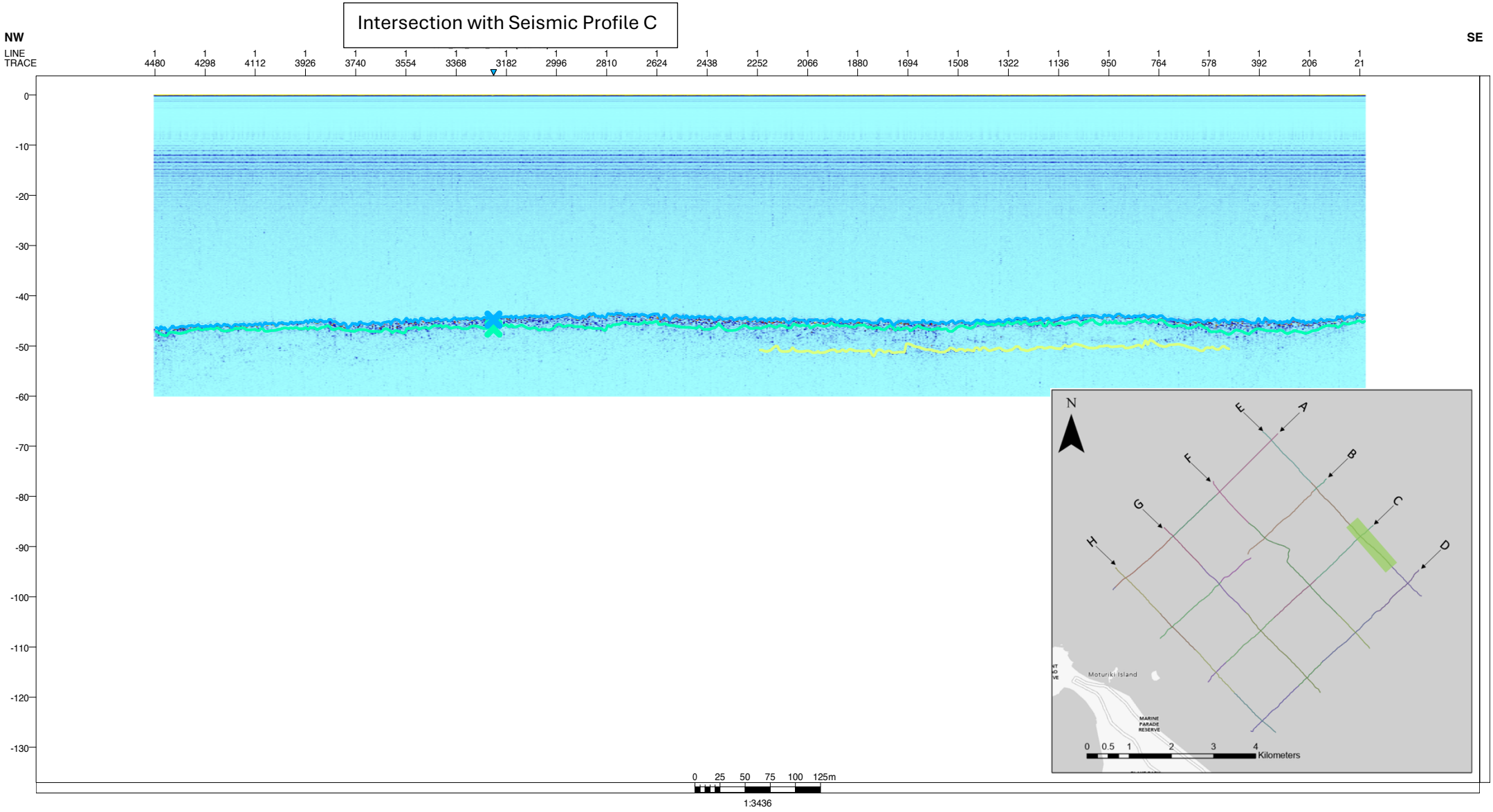
Intersection with Seismic Profile C
NW
SE
LINE
TRACE
1 4480
1 4298
1 4112
1 3926
1 3740
1 3554
1 3368
1 3182
1 2996
1 2810
1 2624
1 2438
1 2252
1 2066
1 1880
1 1694
1 1508
1 1322
1 1136
1 950
1 764
1 578
1 392
1 206
1 21
0
-10
-20
-30
-40
-50
-60
-70
-80
-90
-100
-110
-120
-130
N
A
B
C
D
E
F
G
H
Moturiki Island
MARINE PARADE RESERVE
0 0.5 1 2 3 4
Kilometers
0 25 50 75 100 125m
1:3436

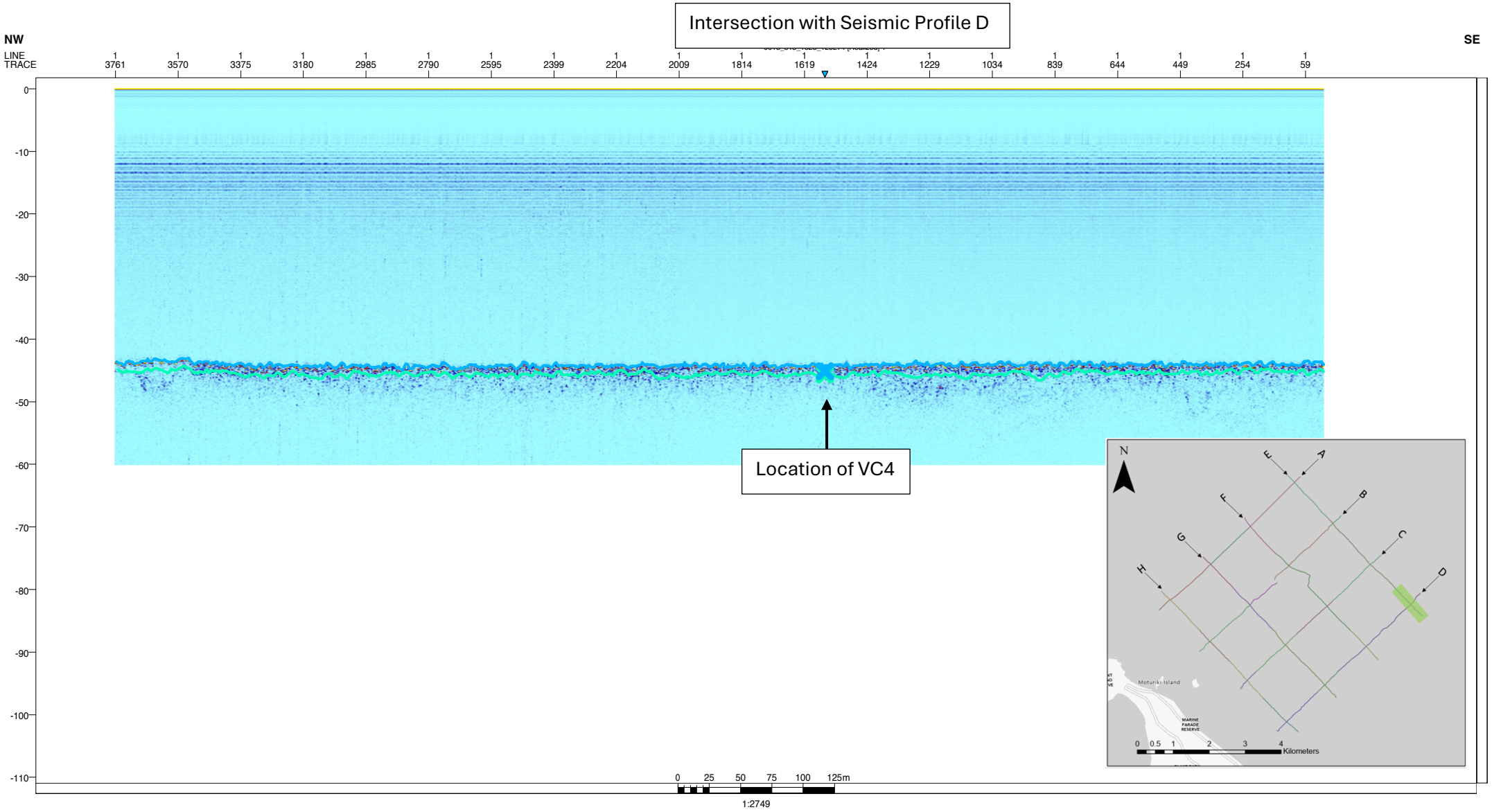
Intersection with Seismic Profile D
NW
SE
LINE
TRACE
1 3761
1 3570
1 3375
1 3180
1 2985
1 2790
1 2595
1 2399
1 2204
1 2009
1 1814
1 1619
1 1424
1 1229
1 1034
1 839
1 644
1 449
1 254
1 59
0
-10
-20
-30
-40
-50
-60
-70
-80
-90
-100
-110
Location of VC4
N
A
B
C
D
E
F
G
H
Moturiki Island
MARINE PARADE RESERVE
0 0.5 1 2 3 4 Kilometers
0 25 50 75 100 125m
1:2749

Seismic line survey F, from northwest to southwest

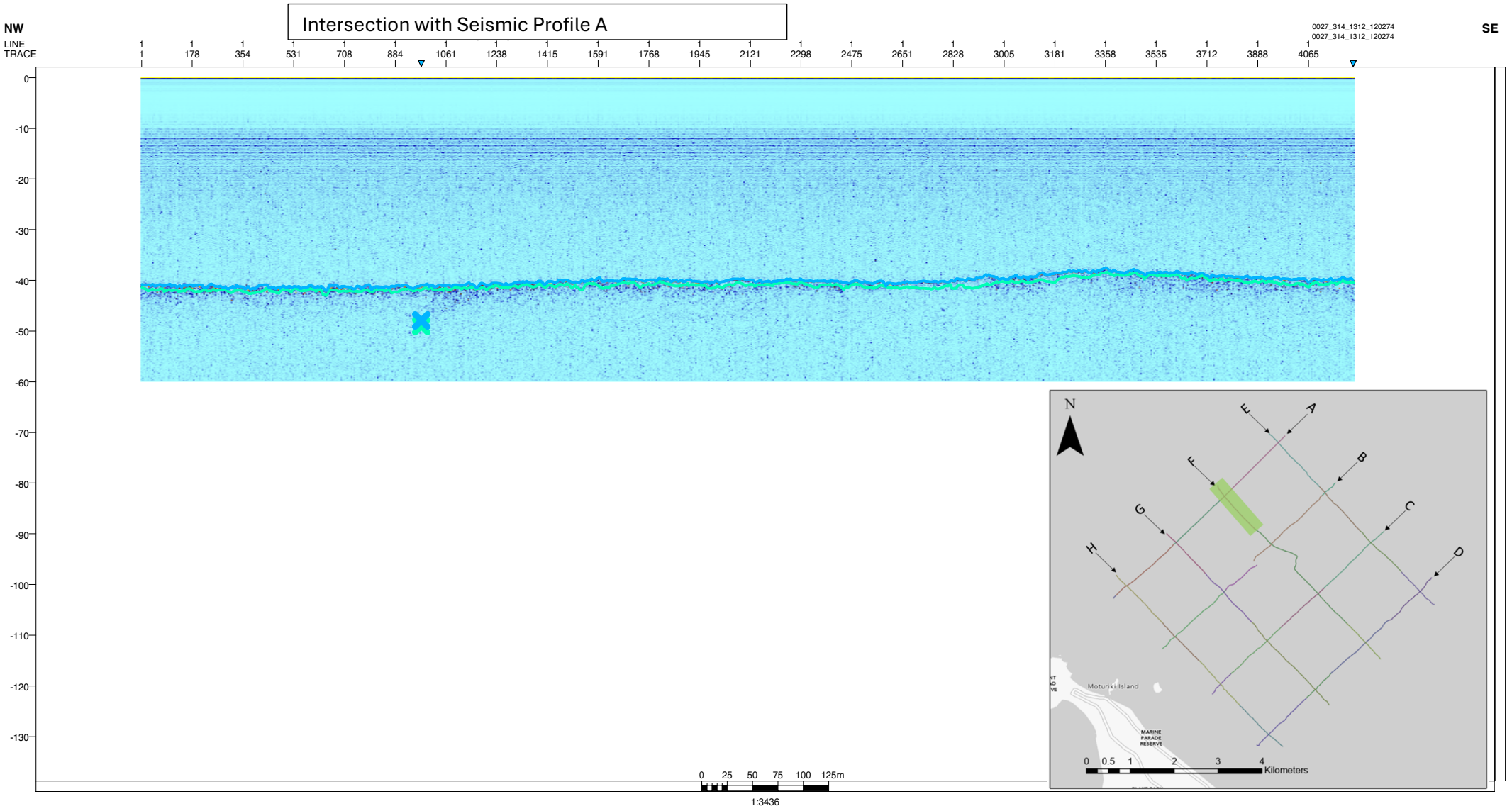

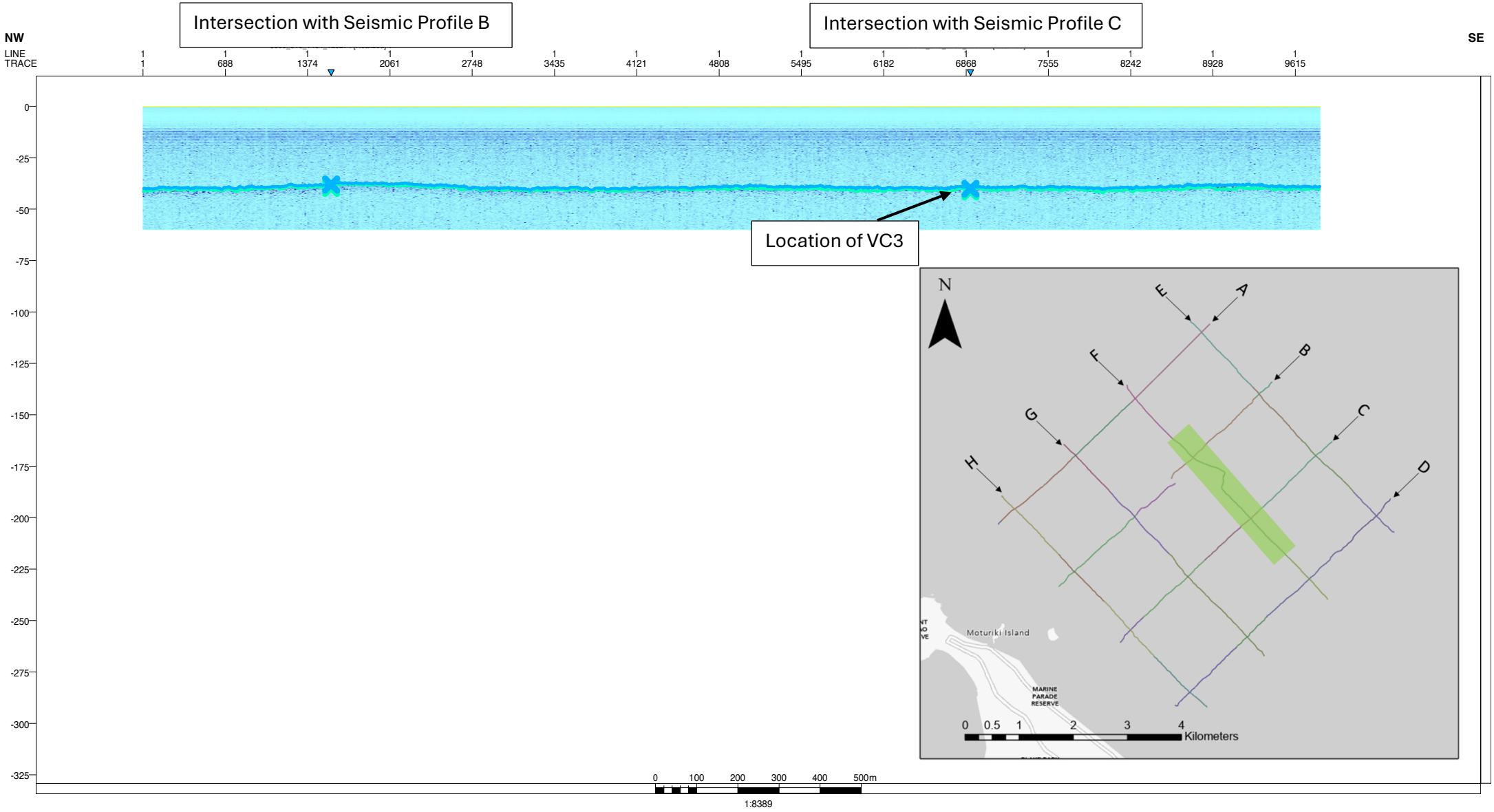
Intersection with Seismic Profile B
Intersection with Seismic Profile C
NW
SE
LINE
TRACE
1 1
1 688
1 1374
1 2061
1 2748
1 3435
1 4121
1 4808
1 5495
1 6182
1 6868
1 7555
1 8242
1 8928
1 9615
0
-25
-50
-75
-100
-125
-150
-175
-200
-225
-250
-275
-300
-325
Location of VC3
N
A
B
C
D
E
F
G
H
Moturiki Island
MARINE PARADE RESERVE
0 0.5 1 2 3 4
Kilometers
0 100 200 300 400 500m
1:8389

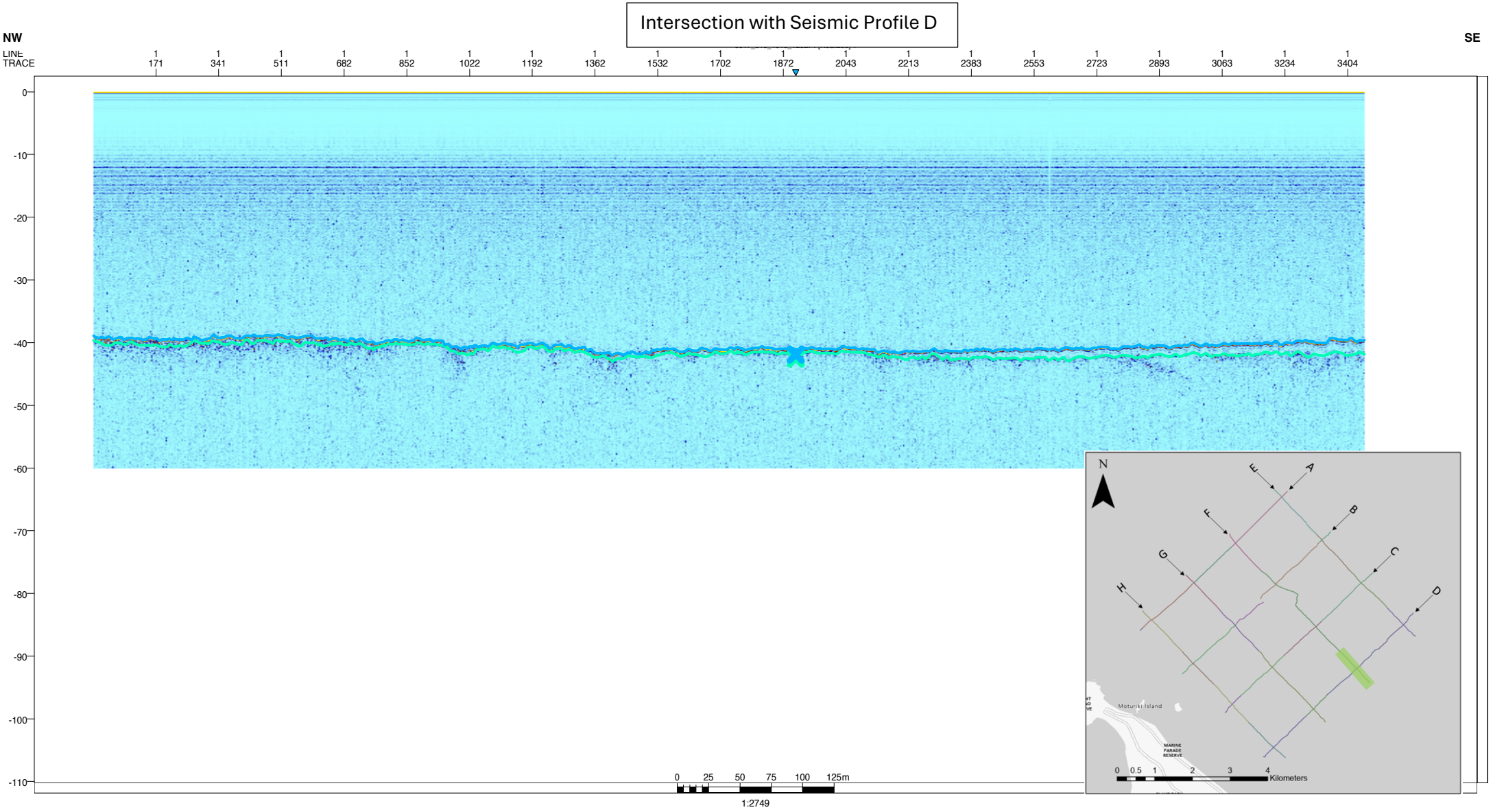
Intersection with Seismic Profile D
NW
SE
LINE
TRACE
1 171
1 341
1 511
1 682
1 852
1 1022
1 1192
1 1362
1 1532
1 1702
1 1872
1 2043
1 2213
1 2383
1 2553
1 2723
1 2893
1 3063
1 3234
1 3404
0
-10
-20
-30
-40
-50
-60
-70
-80
-90
-100
-110
0 25 50 75 100 125m
1:2749
N
A
B
C
D
E
F
G
H
Moturiki Island
MARINE PARADE RESERVE
0 0.5 1 2 3 4 Kilometers

Seismic line survey G, from northwest to southwest

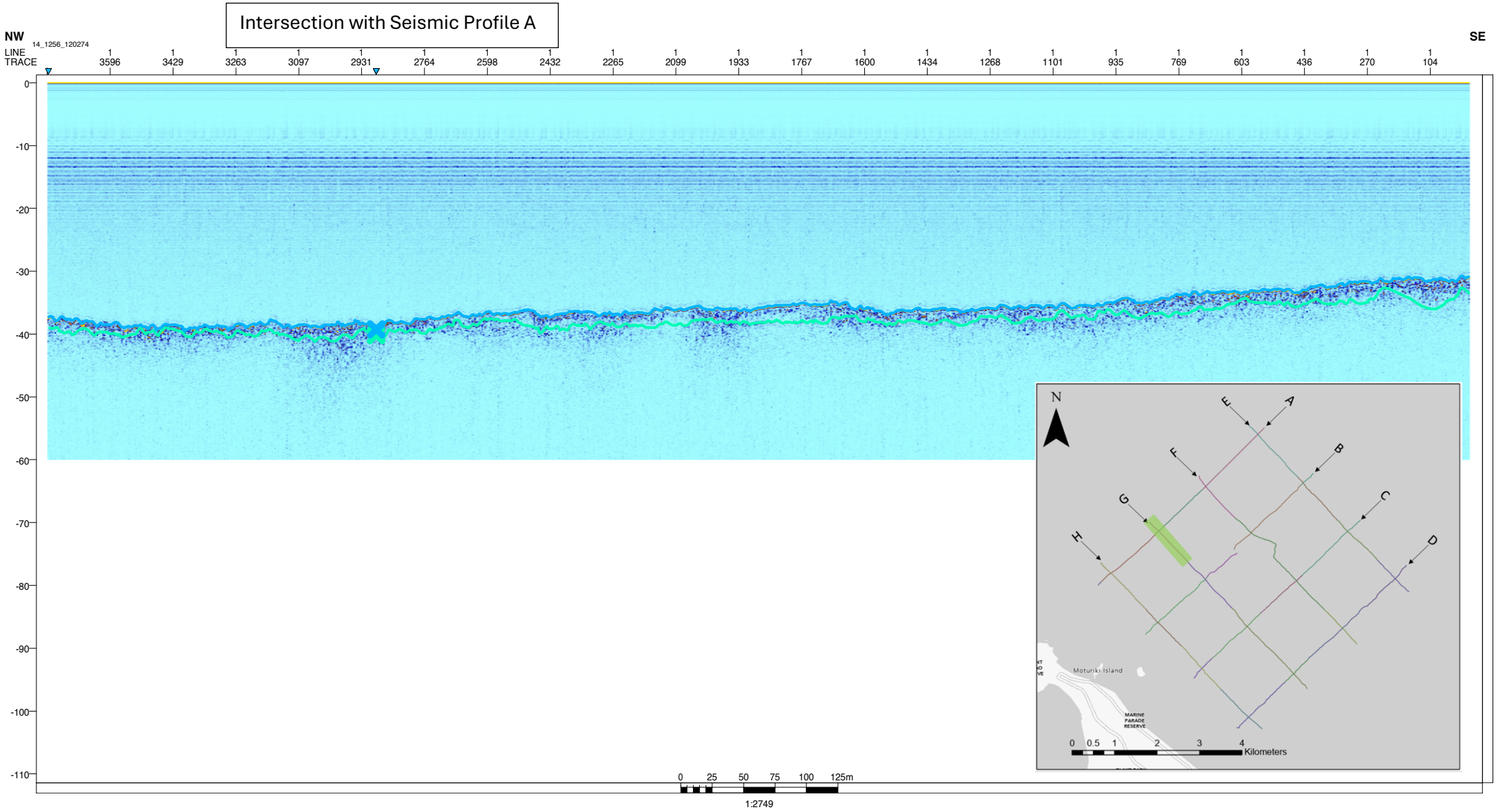

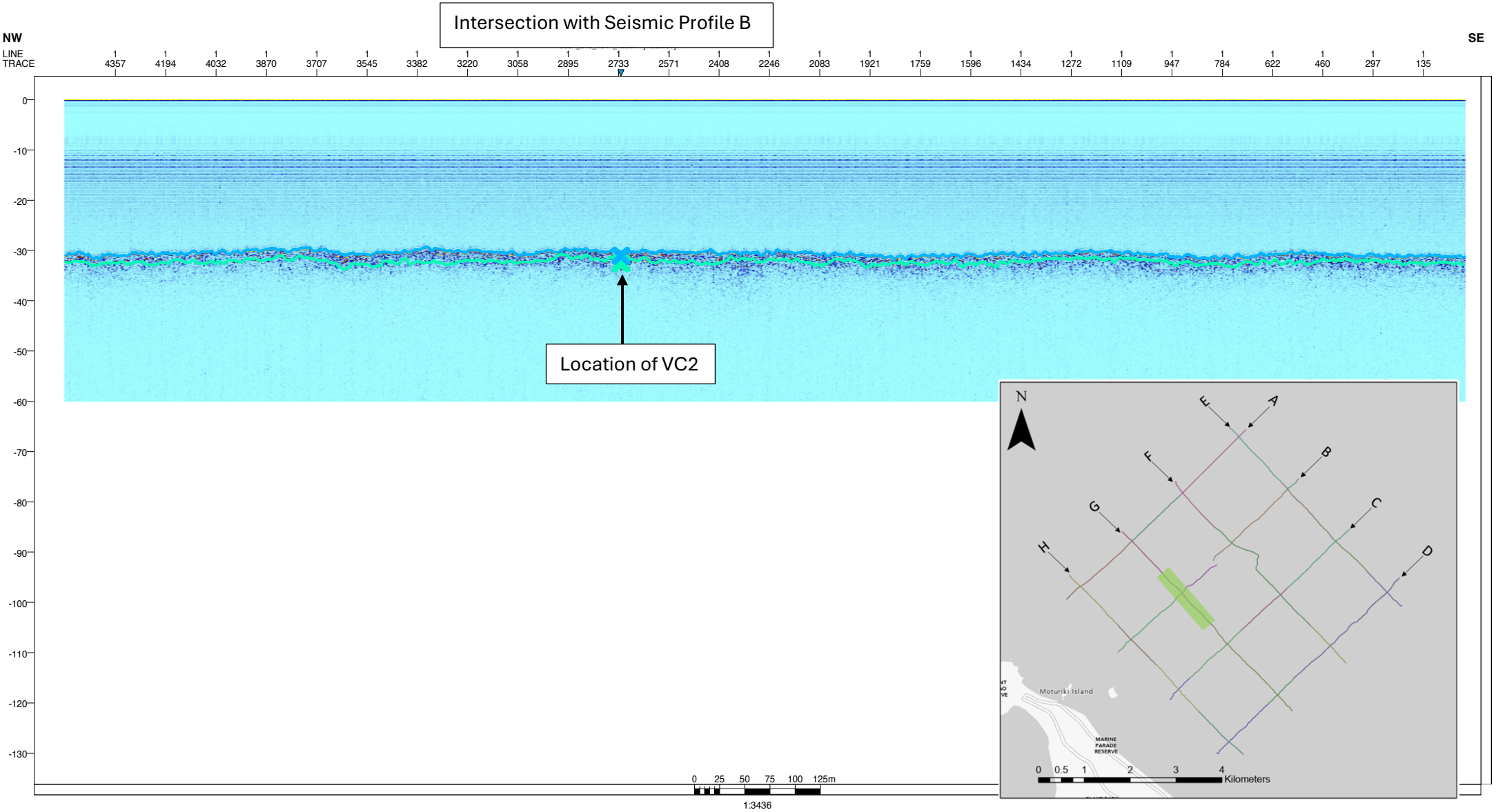
Intersection with Seismic Profile B
NW
SE
LINE
TRACE
1 4357
1 4194
1 4032
1 3870
1 3707
1 3545
1 3382
1 3220
1 3058
1 2895
1 2733
1 2571
1 2408
1 2246
1 2083
1 1921
1 1759
1 1596
1 1434
1 1272
1 1109
1 947
1 784
1 622
1 460
1 297
1 135
0
-10
-20
-30
-40
-50
-60
-70
-80
-90
-100
-110
-120
-130
Location of VC2
0 25 50 75 100 125m
1:3436
N
A
B
C
D
E
F
G
H
Moturiki Island
MARINE PARADE RESERVE
0 0.5 1 2 3 4
Kilometers

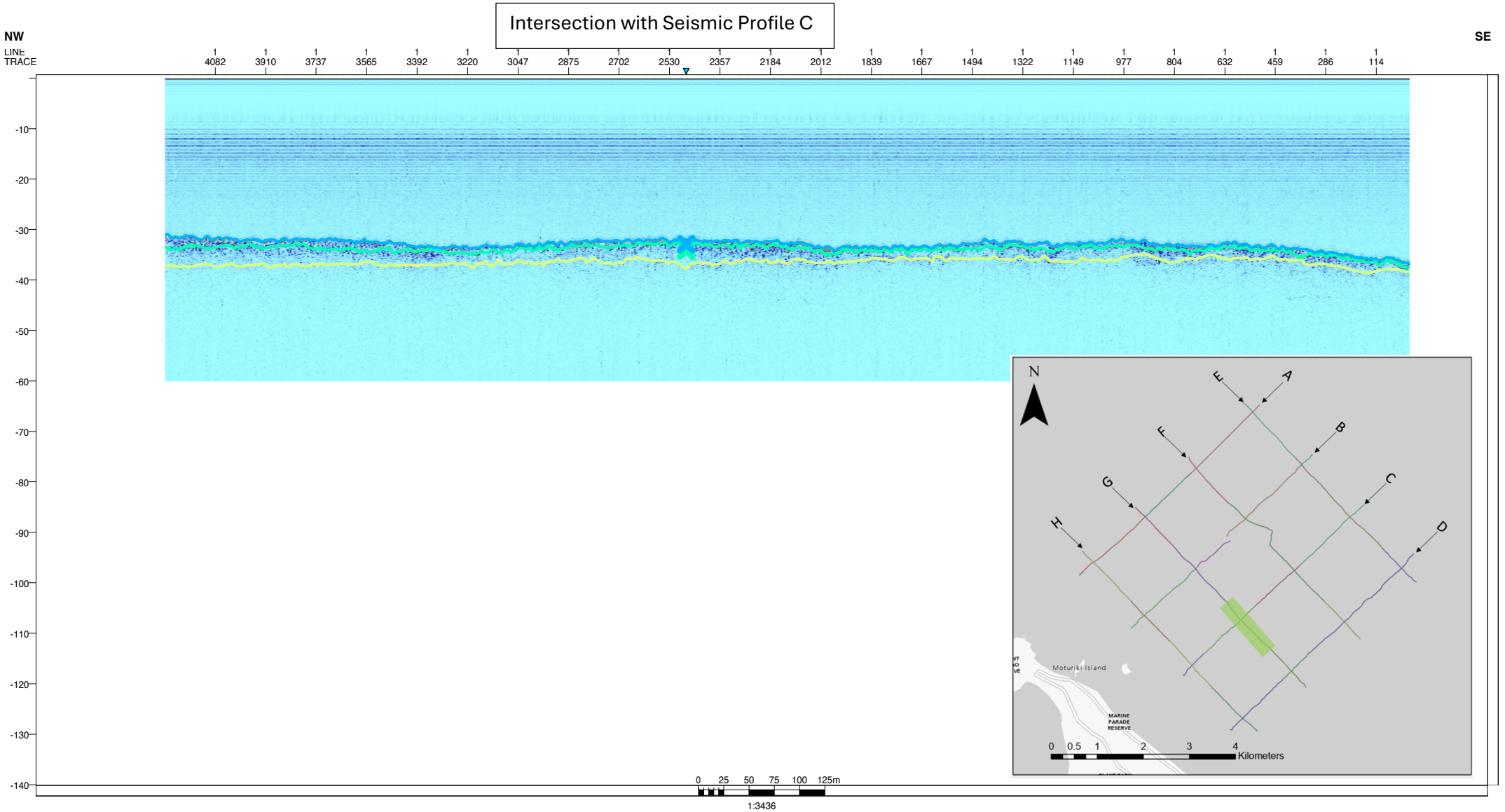
Intersection with Seismic Profile C
NW
SE
LINE
TRACE
1 4082
1 3910
1 3737
1 3565
1 3392
1 3220
1 3047
1 2875
1 2702
1 2530
1 2357
1 2184
1 2012
1 1839
1 1667
1 1494
1 1322
1 1149
1 977
1 804
1 632
1 459
1 286
1 114
-10
-20
-30
-40
-50
-60
-70
-80
-90
-100
-110
-120
-130
-140
0 25 50 75 100 125m
1:3436
N
A
B
C
D
E
F
G
H
Moturiki Island
MARINE PARADE RESERVE
0 0.5 1 2 3 4 Kilometers

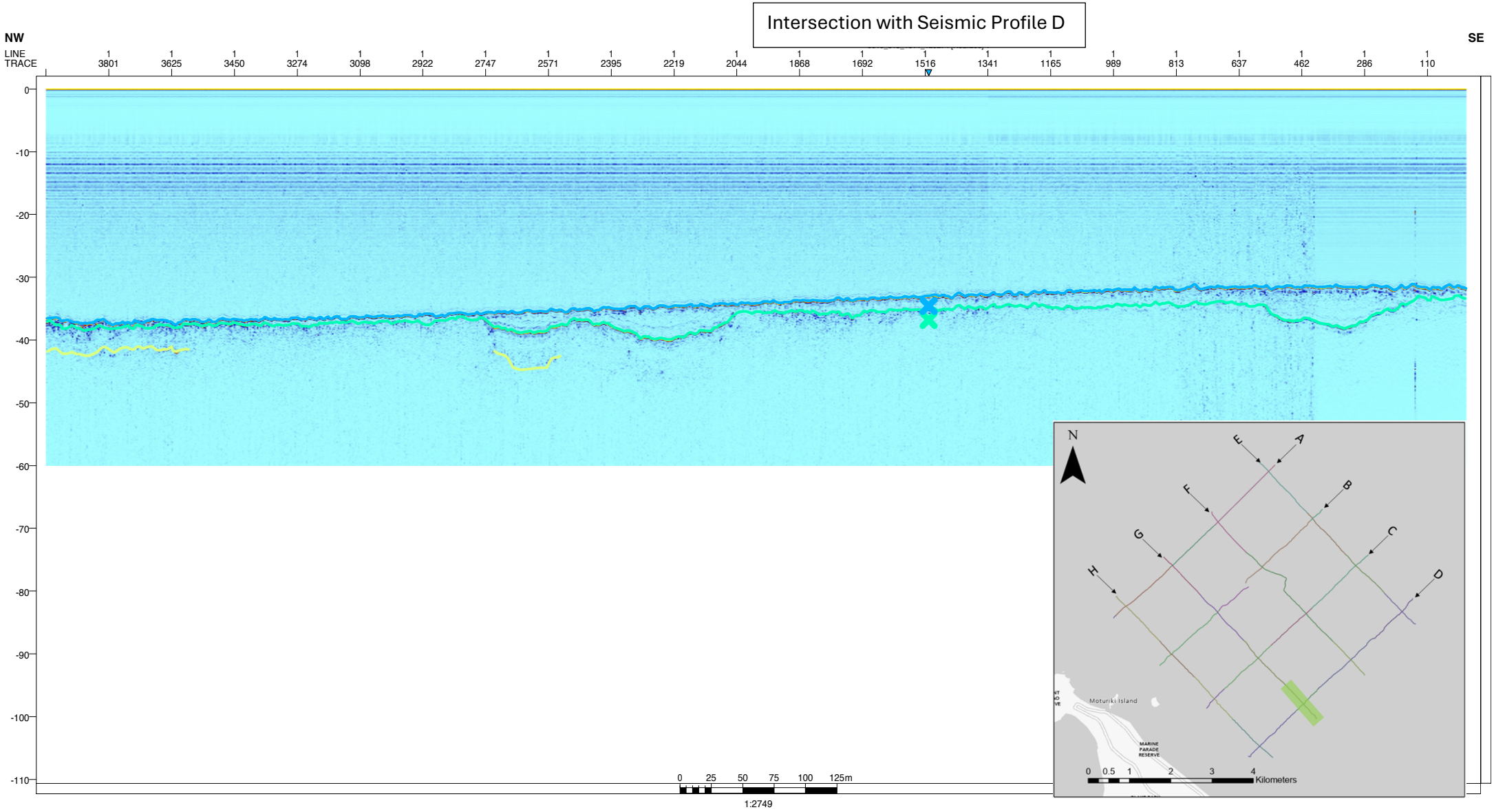
Intersection with Seismic Profile D
NW
SE
LINE
TRACE
1 3801
1 3625
1 3450
1 3274
1 3098
1 2922
1 2747
1 2571
1 2395
1 2219
1 2044
1 1868
1 1692
1 1516
1 1341
1 1165
1 989
1 813
1 637
1 462
1 286
1 110
0
-10
-20
-30
-40
-50
-60
-70
-80
-90
-100
-110
0 25 50 75 100 125m
1:2749
N
A
B
C
D
E
F
G
H
Moturiki Island
MARINE PARADE RESERVE
0 0.5 1 2 3 4
Kilometers

Seismic line survey H, from northwest to southwest

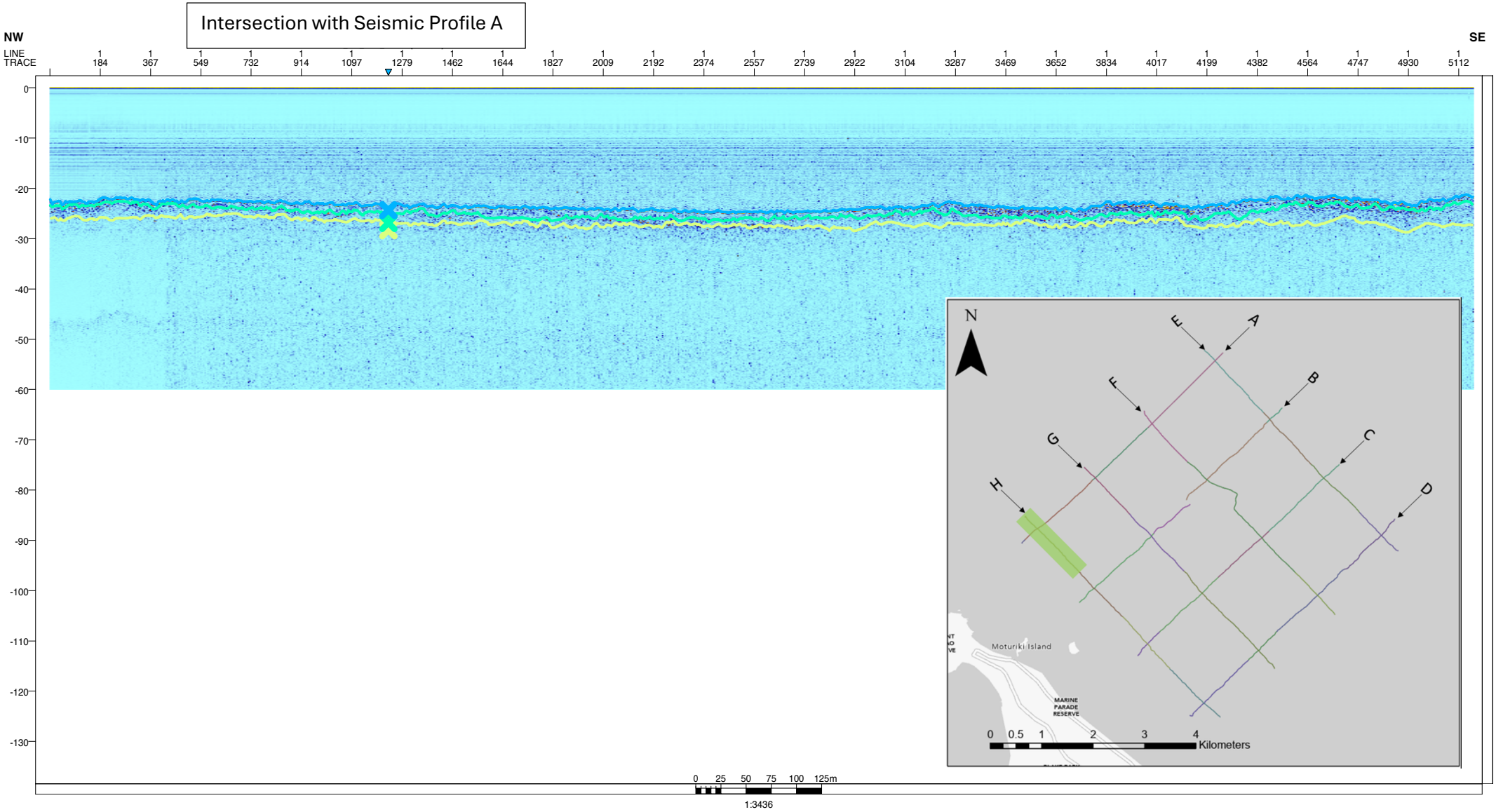

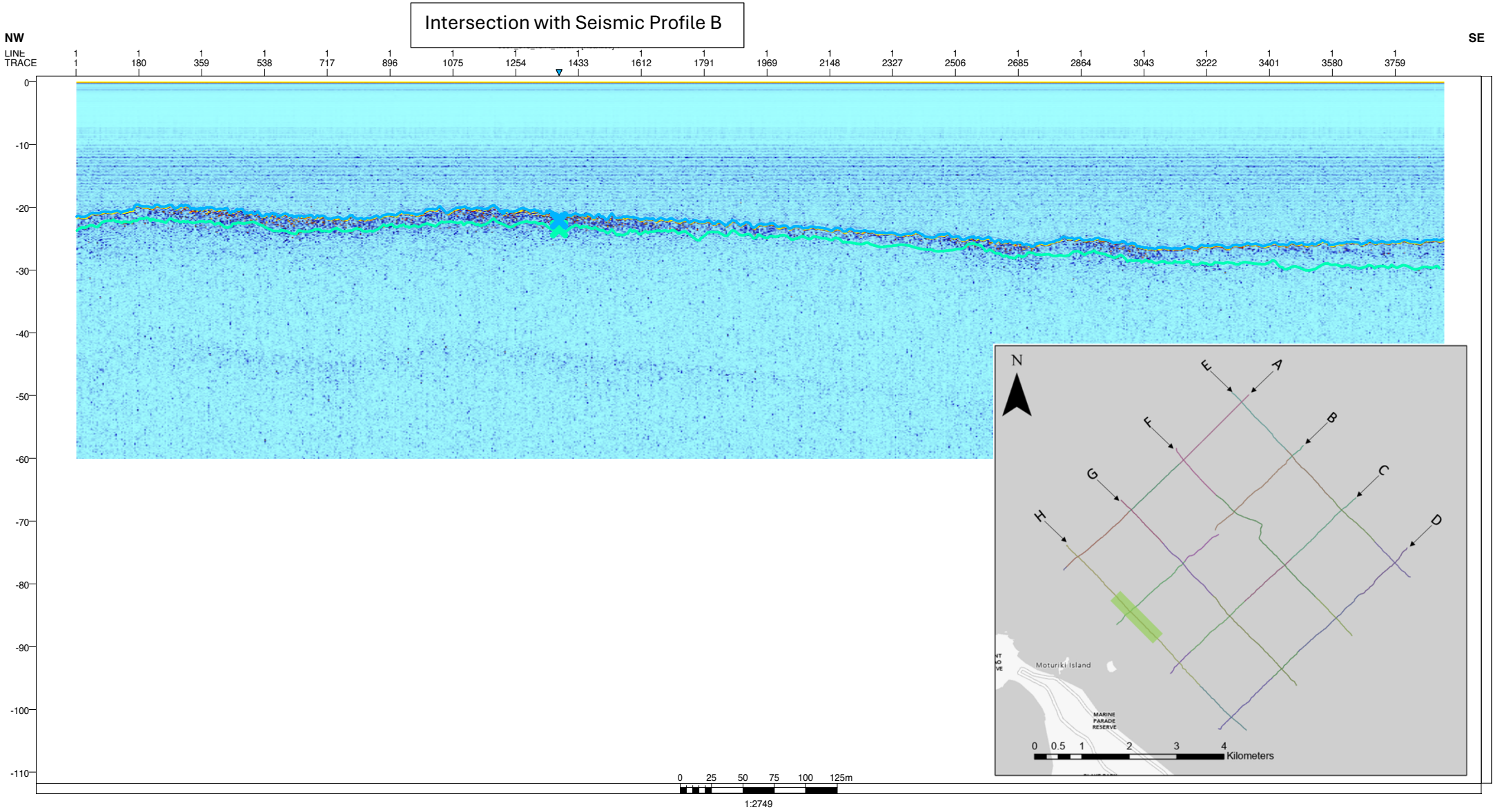
Intersection with Seismic Profile B
NW
SE
LINE
TRACE
1 1
1 180
1 359
1 538
1 717
1 896
1 1075
1 1254
1 1433
1 1612
1 1791
1 1969
1 2148
1 2327
1 2506
1 2685
1 2864
1 3043
1 3222
1 3401
1 3580
1 3759
0
-10
-20
-30
-40
-50
-60
-70
-80
-90
-100
-110
N
A
B
C
D
E
F
G
H
Moturiki Island
MARINE PARADE RESERVE
0 0.5 1 2 3 4
Kilometers
0 25 50 75 100 125m
1:2749

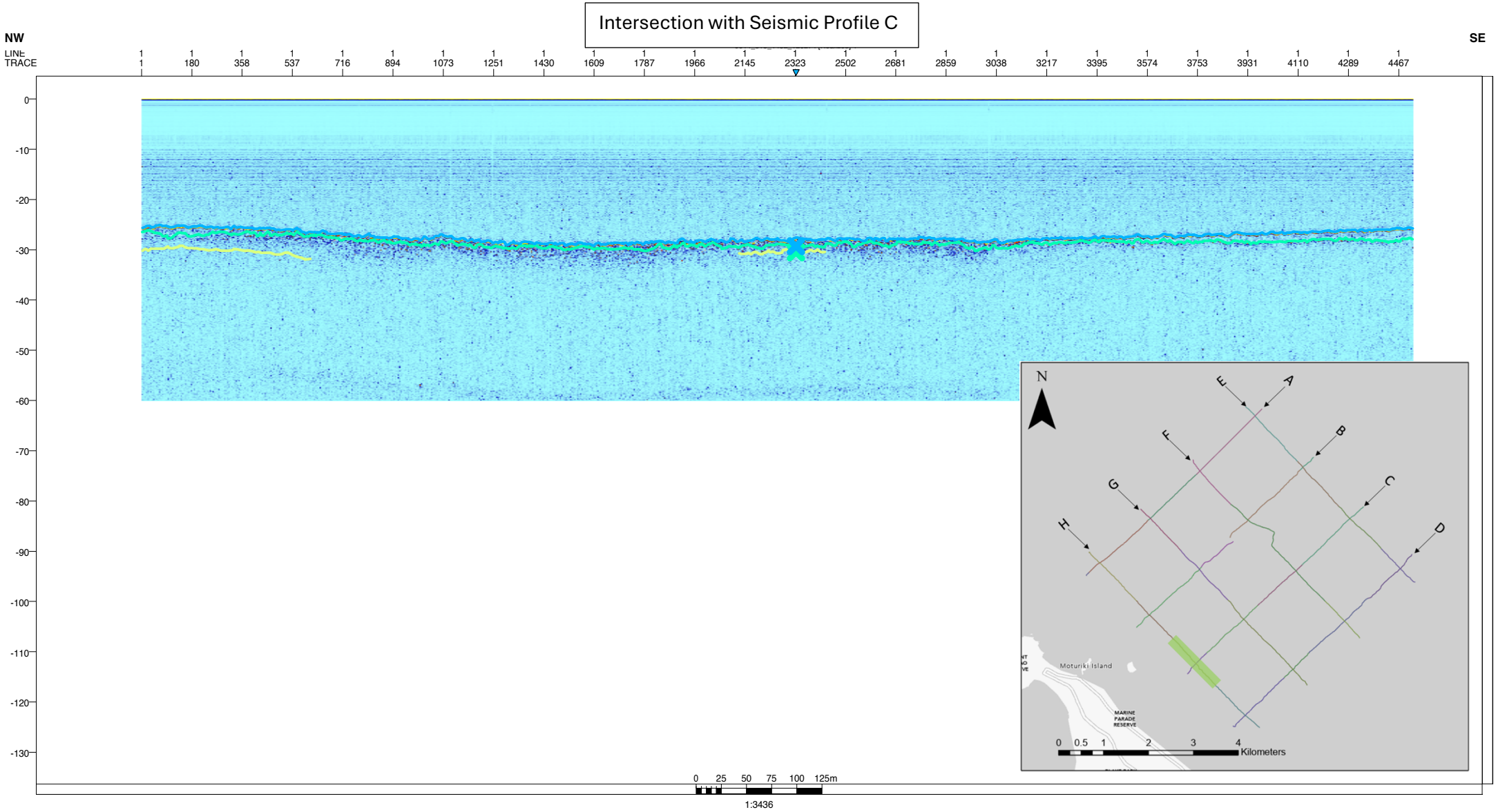
Intersection with Seismic Profile C
NW
SE
LINE
TRACE
1 1
1 180
1 358
1 537
1 716
1 894
1 1073
1 1251
1 1430
1 1609
1 1787
1 1966
1 2145
1 2323
1 2502
1 2681
1 2859
1 3038
1 3217
1 3395
1 3574
1 3753
1 3931
1 4110
1 4289
1 4467
0
-10
-20
-30
-40
-50
-60
-70
-80
-90
-100
-110
-120
-130
N
A
B
C
D
E
F
G
H
Moturiki Island
MARINE PARADE RESERVE
0 0.5 1 2 3 4
Kilometers
0 25 50 75 100 125m
1:3436

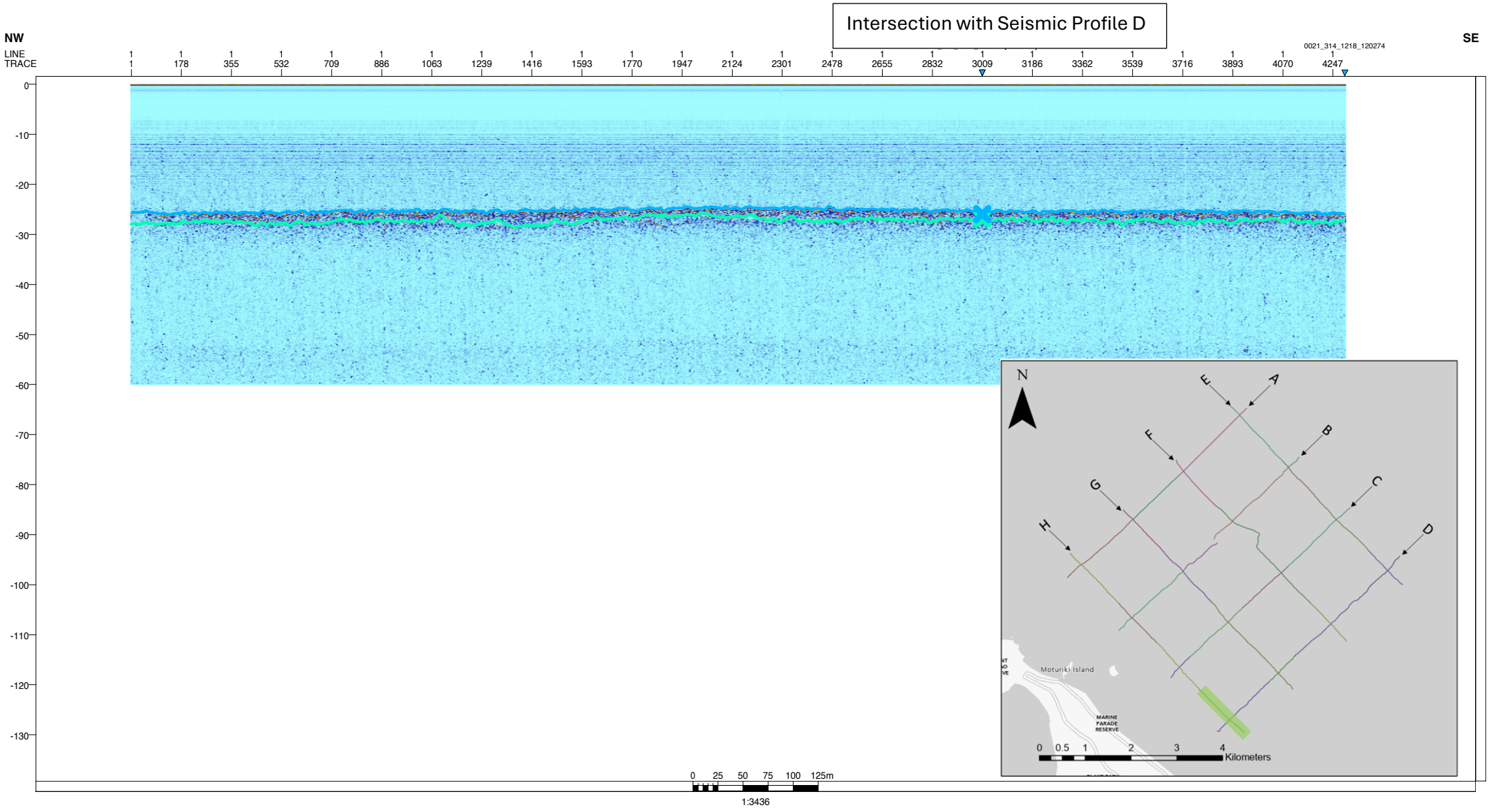
Intersection with Seismic Profile D
NW
SE
LINE
TRACE
0021_314_1218_120274
1 1
1 178
1 355
1 532
1 709
1 886
1 1063
1 1239
1 1416
1 1593
1 1770
1 1947
1 2124
1 2301
1 2478
1 2655
1 2832
1 3009
1 3186
1 3362
1 3539
1 3716
1 3893
1 4070
1 4247
0
-10
-20
-30
-40
-50
-60
-70
-80
-90
-100
-110
-120
-130
N
A
B
C
D
E
F
G
H
Moturiki Island
MARINE PARADE RESERVE
0 0.5 1 2 3 4
Kilometers
0 25 50 75 100 125m
1:3436

Distribution of Horizon C throughout the study area, red areas represent areas where Horizon C is present.

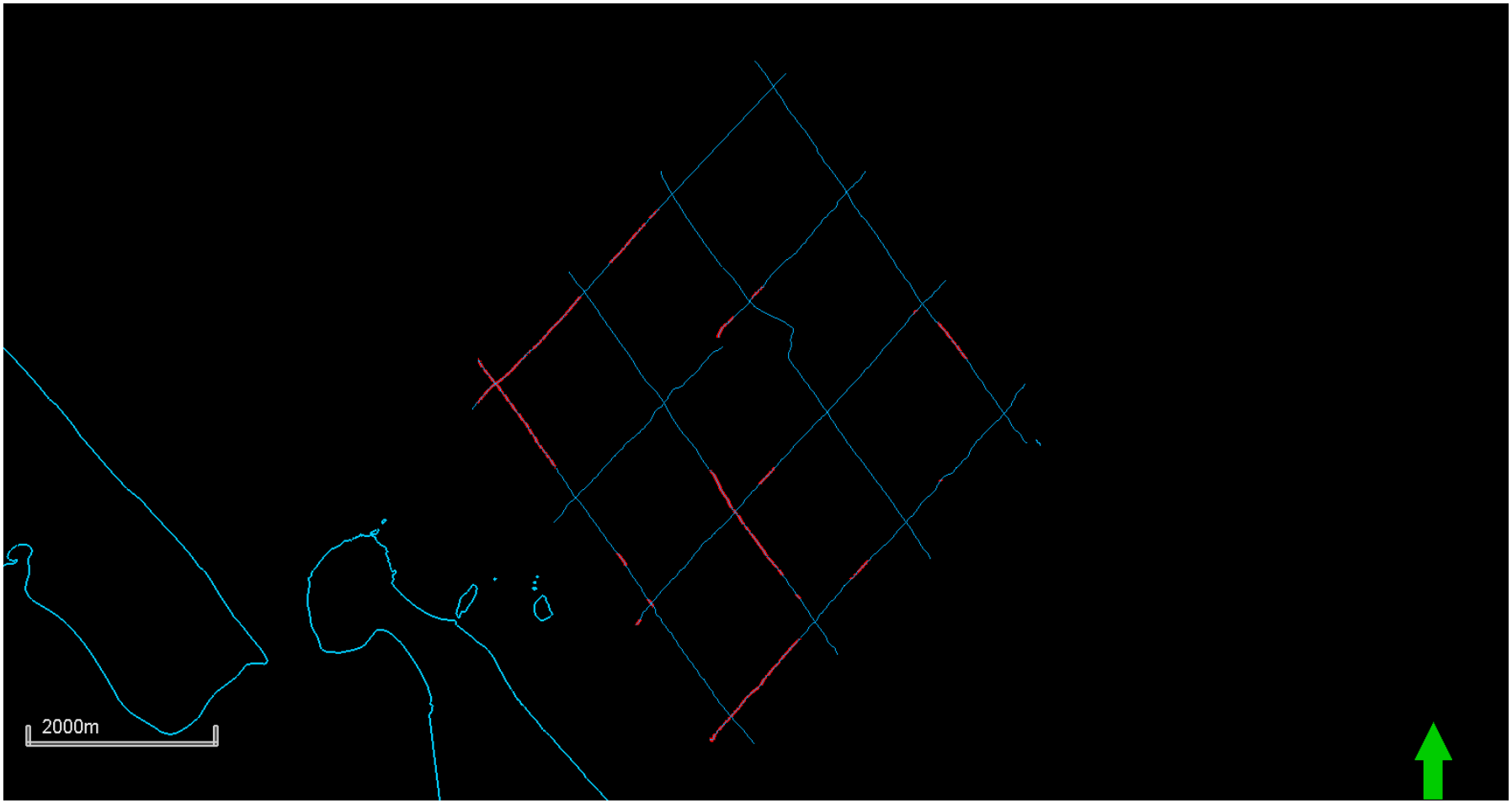

Appendix D2. Uninterpreted Seismic Profiles

Seismic line survey A, from shore-to-sea.

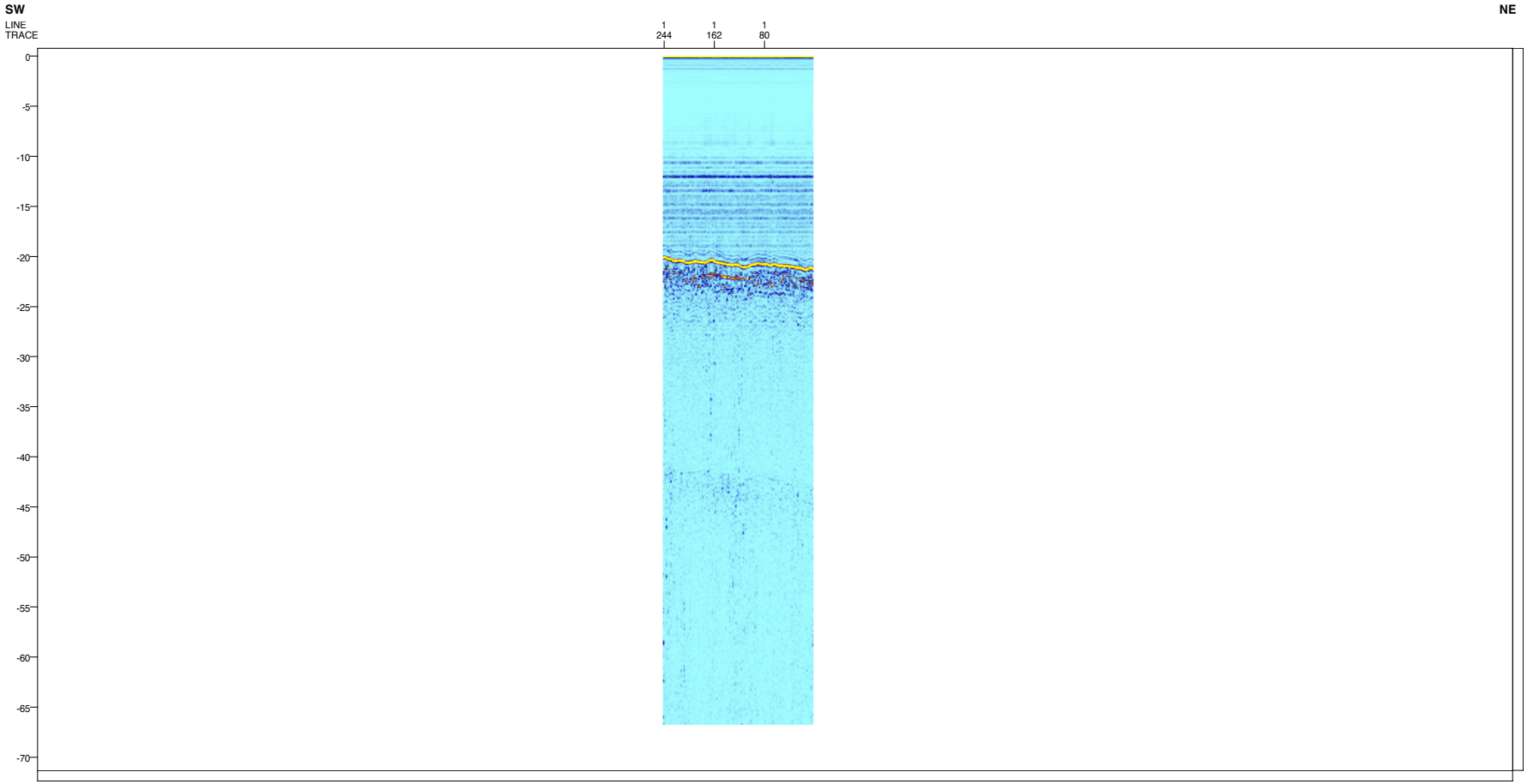

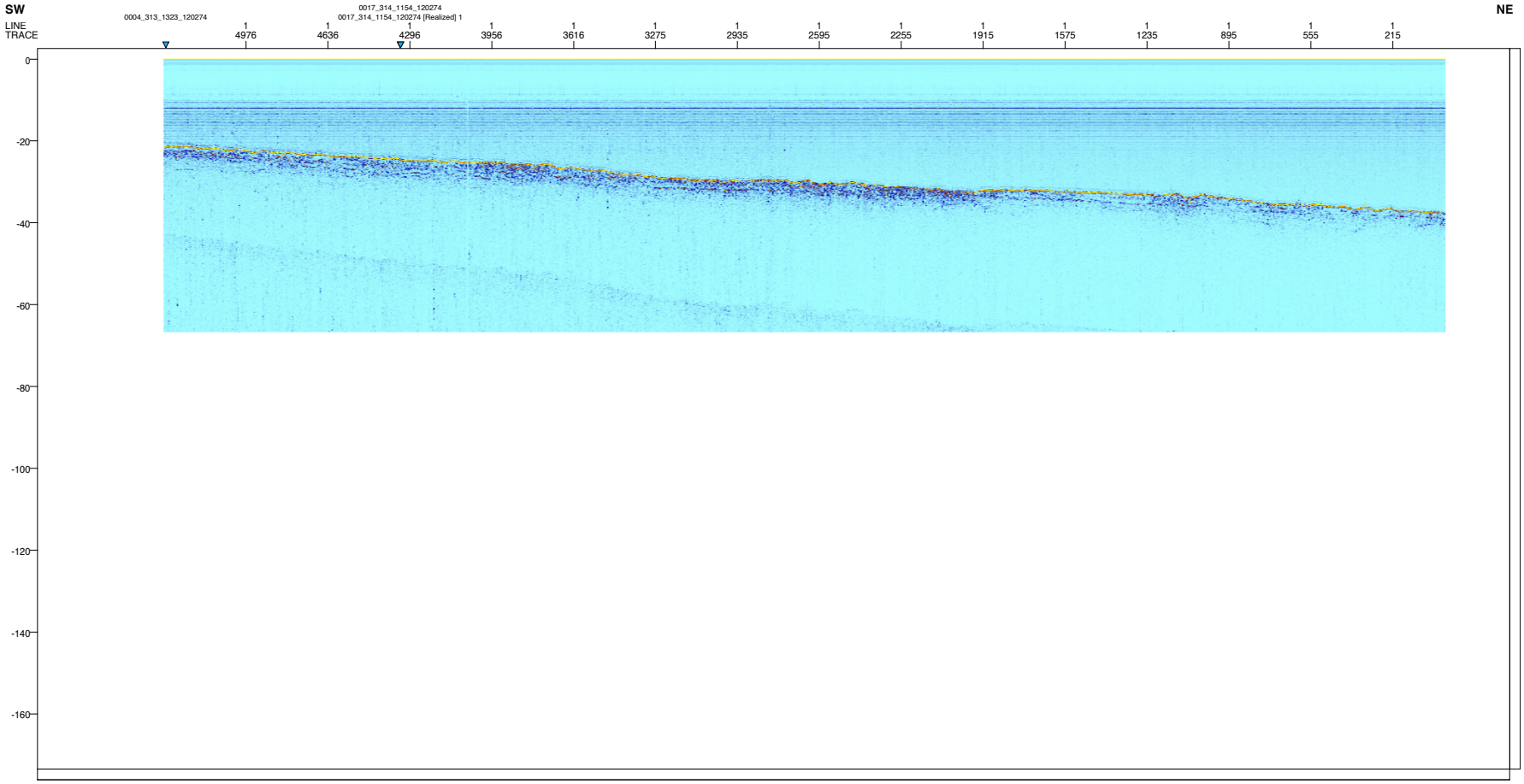
SW
NE
LINE
TRACE
0004_313_1323_120274
0017_314_1154_120274
0017_314_1154_120274 [Realized] 1
1 4976
1 4636
1 4296
1 3956
1 3616
1 3275
1 2935
1 2595
1 2255
1 1915
1 1575
1 1235
1 895
1 555
1 215
0
-20
-40
-60
-80
-100
-120
-140
-160

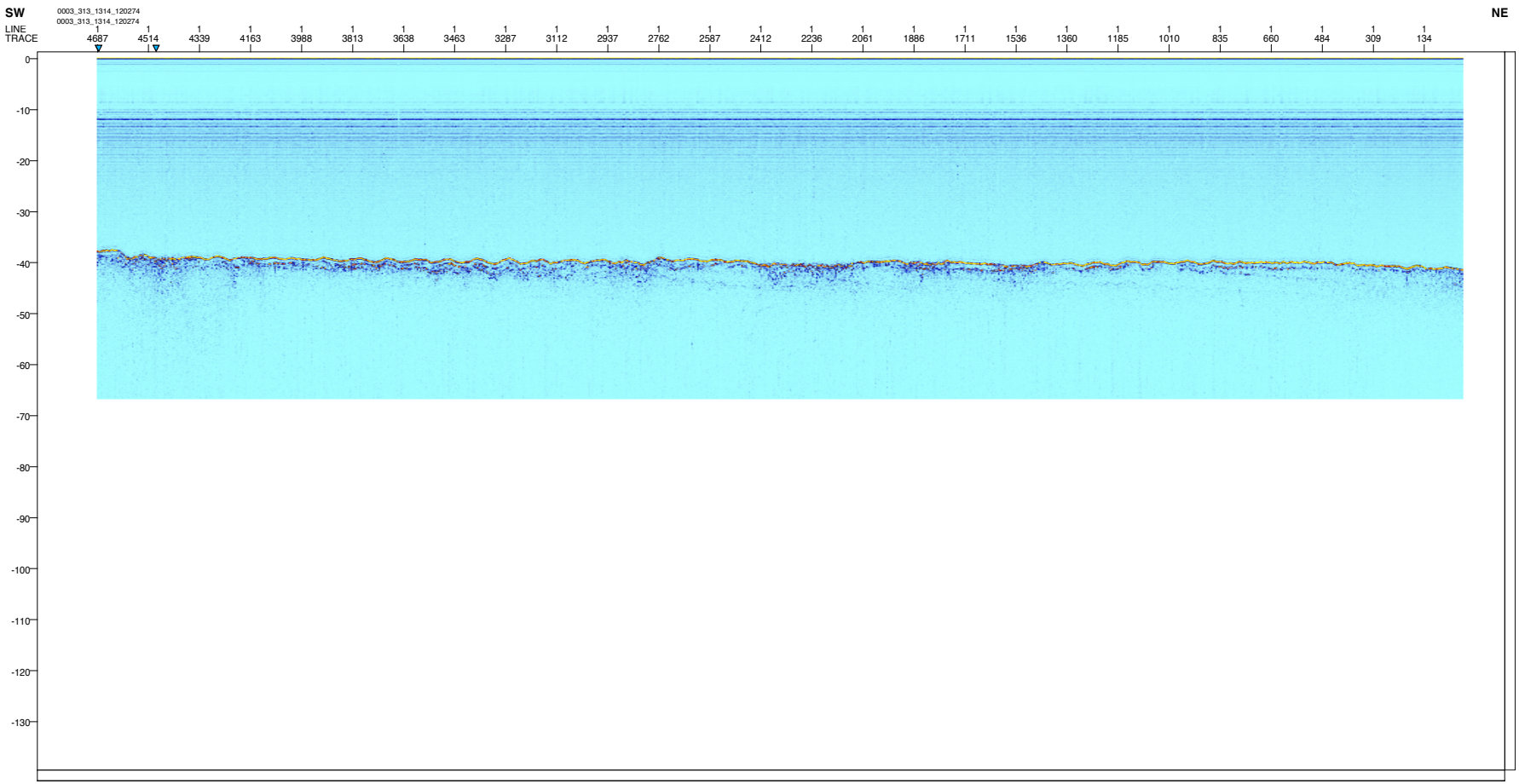
SW
NE
0003_313_1314_120274
0003_313_1314_120274
LINE
TRACE
1 4687
1 4514
1 4339
1 4163
1 3988
1 3813
1 3638
1 3463
1 3287
1 3112
1 2937
1 2762
1 2587
1 2412
1 2236
1 2061
1 1886
1 1711
1 1536
1 1360
1 1185
1 1010
1 835
1 660
1 484
1 309
1 134
0
-10
-20
-30
-40
-50
-60
-70
-80
-90
-100
-110
-120
-130

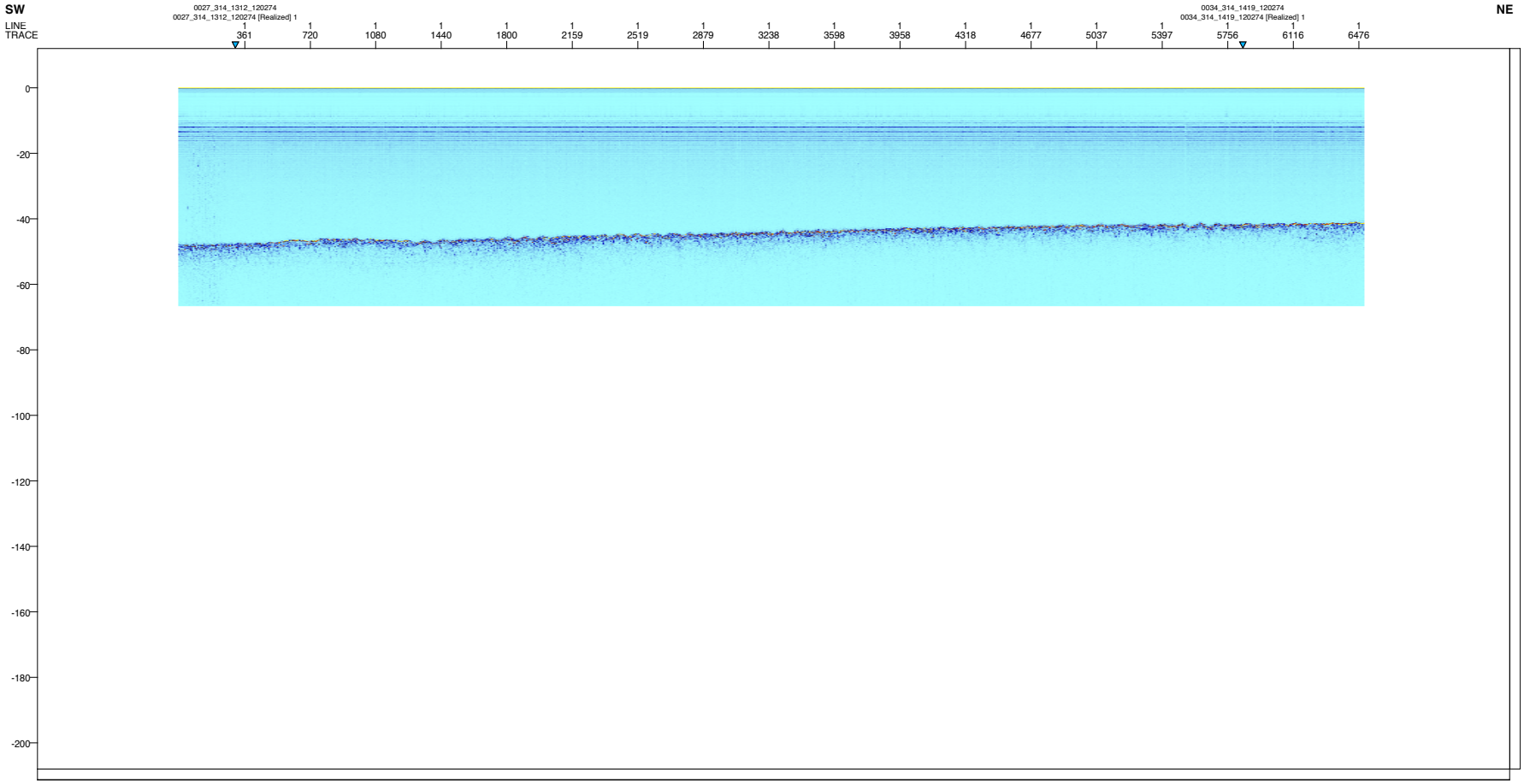
SW
NE
LINE
TRACE
0027_314_1312_120274
0027_314_1312_120274 [Realized] 1
0034_314_1419_120274
0034_314_1419_120274 [Realized] 1
1
361
720
1080
1440
1800
2159
2519
2879
3238
3598
3958
4318
4677
5037
5397
5756
6116
6476
0
-20
-40
-60
-80
-100
-120
-140
-160
-180
-200

Seismic line survey B, from shore-to-sea.

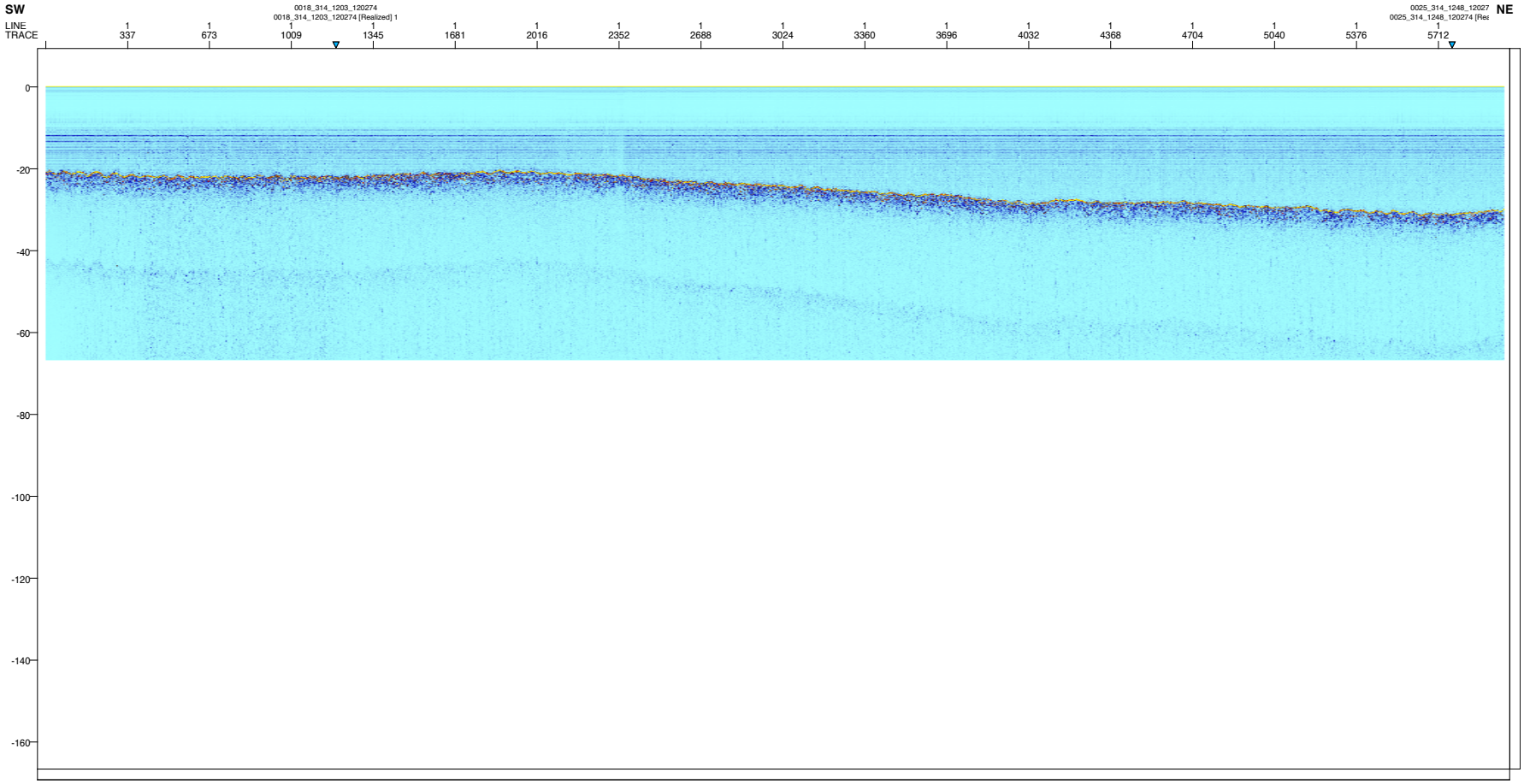

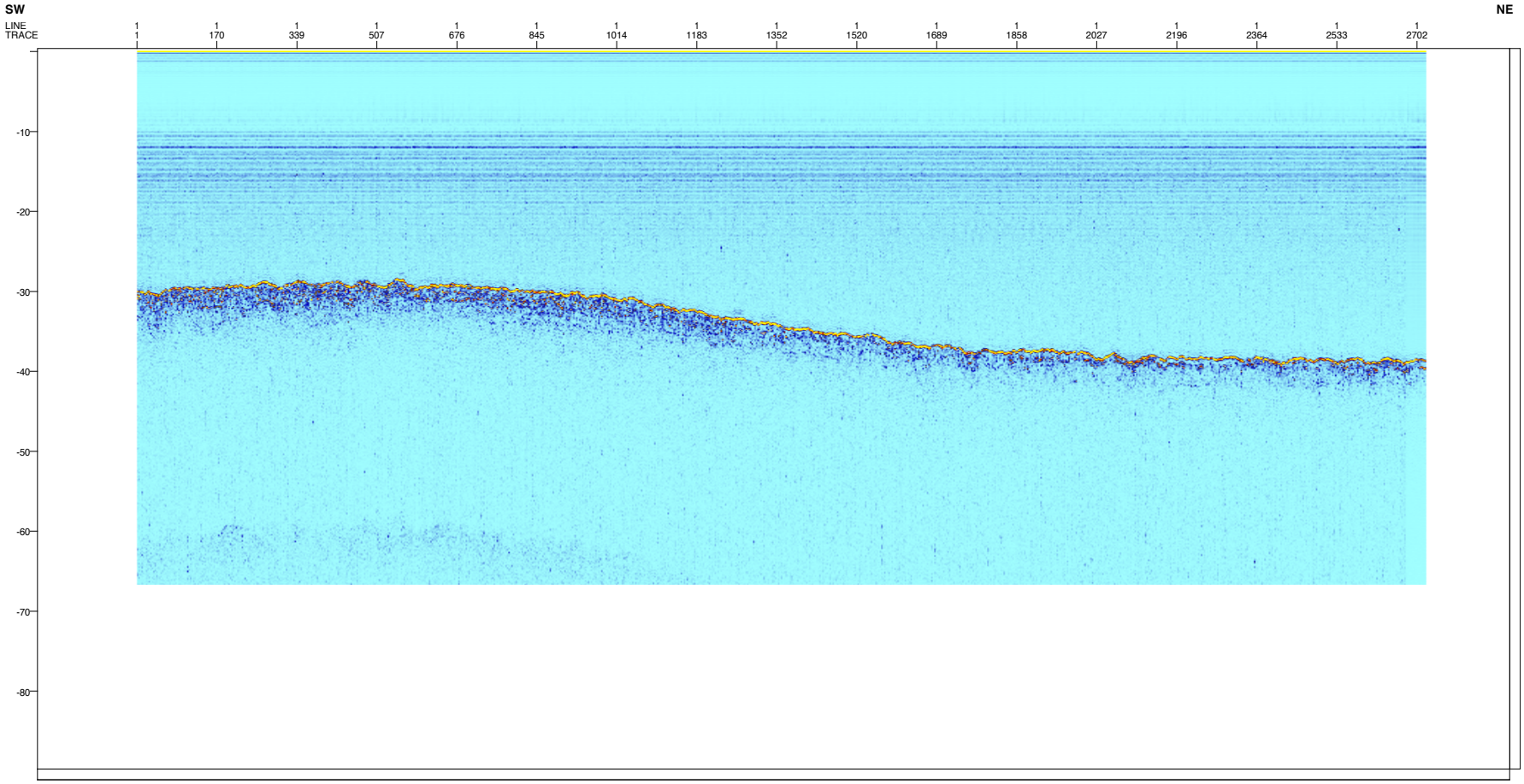
SW
NE
LINE
TRACE
1
1
1
170
1
339
1
507
1
676
1
845
1
1014
1
1183
1
1352
1
1520
1
1689
1
1858
1
2027
1
2196
1
2364
1
2533
1
2702
-10
-20
-30
-40
-50
-60
-70
-80

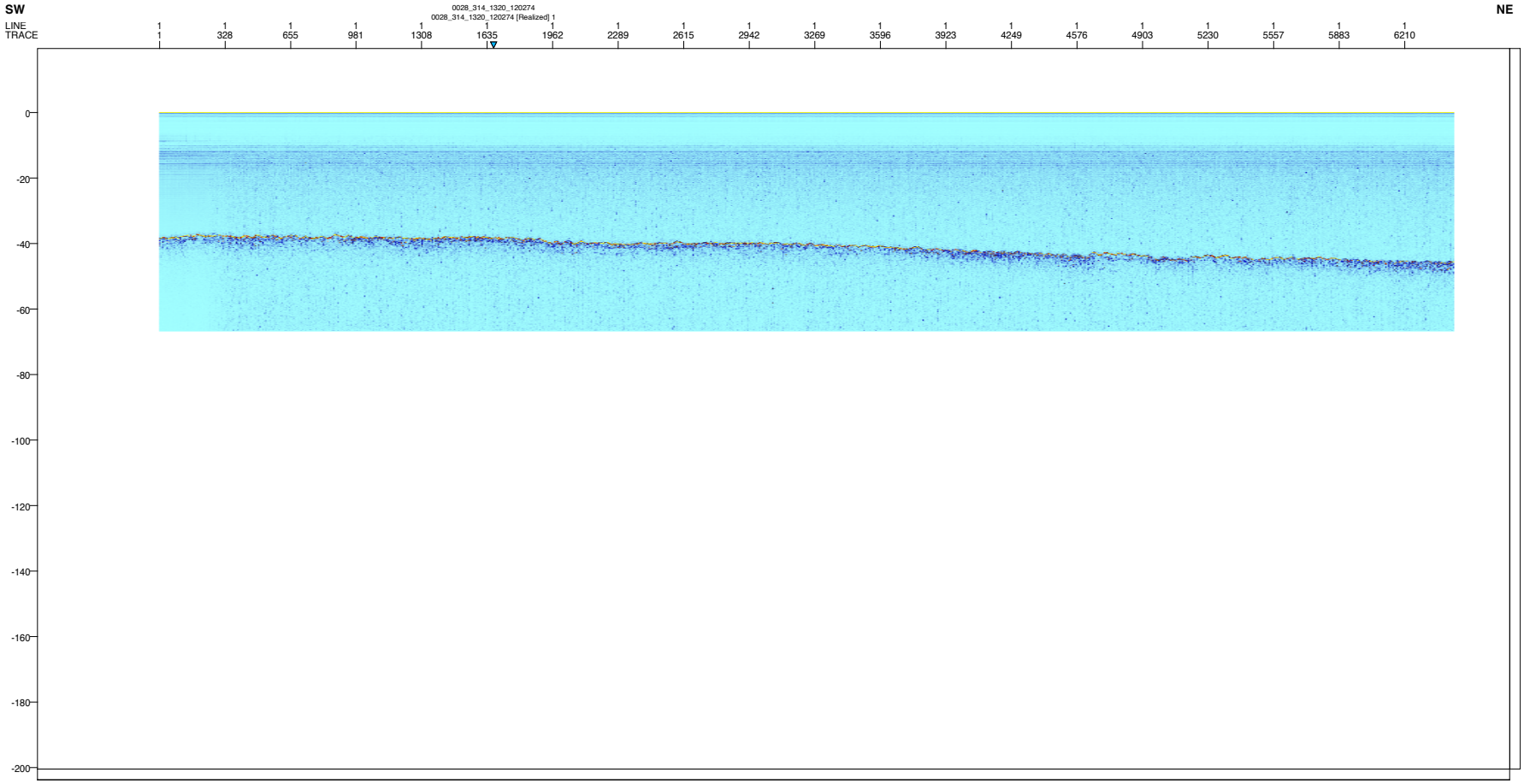
SW
NE
0028_314_1320_120274
0028_314_1320_120274 [Realized] 1
LINE
TRACE
1 1
1 328
1 655
1 981
1 1308
1 1635
1 1962
1 2289
1 2615
1 2942
1 3269
1 3596
1 3923
1 4249
1 4576
1 4903
1 5230
1 5557
1 5883
1 6210
0
-20
-40
-60
-80
-100
-120
-140
-160
-180
-200

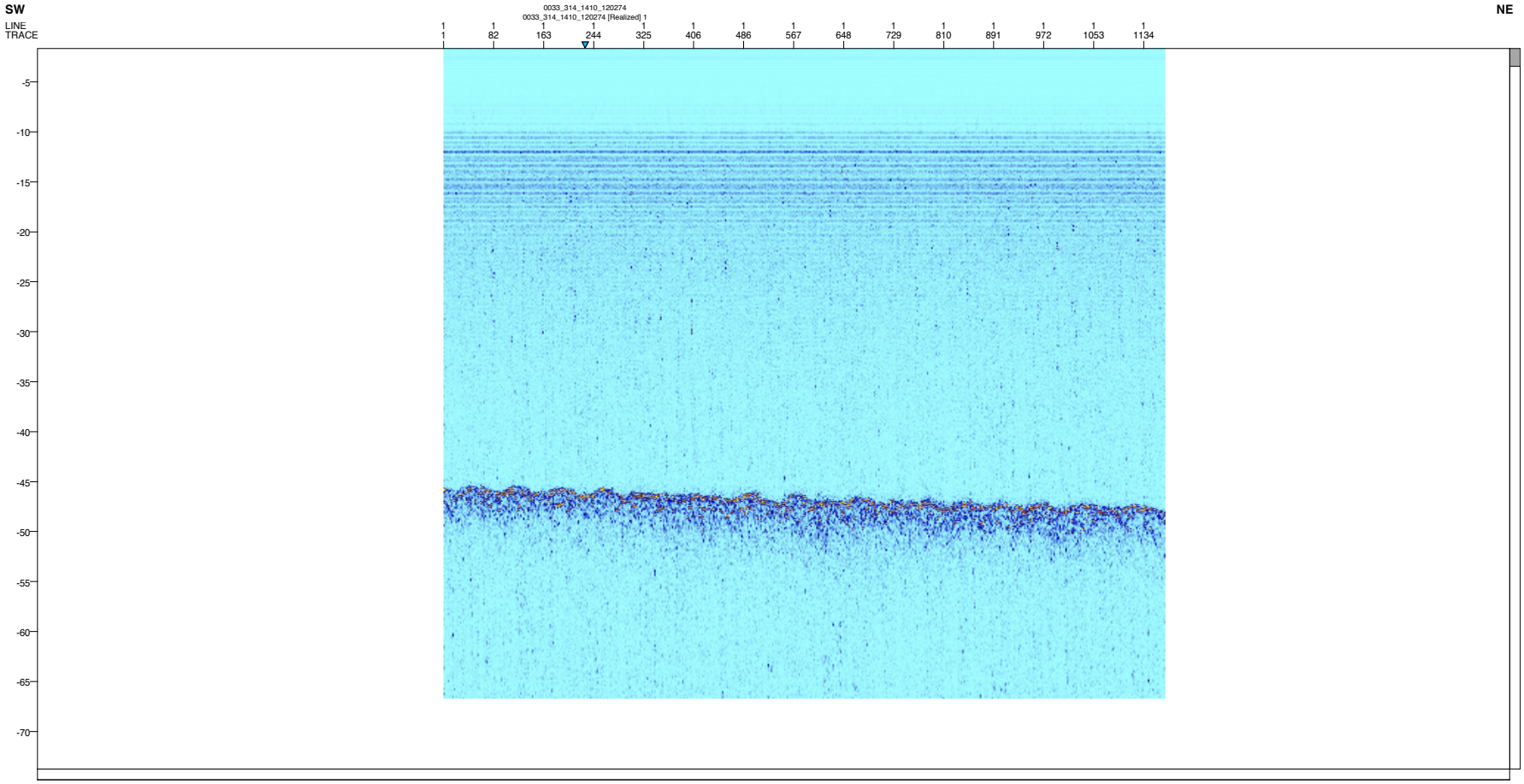
SW
NE
0033_314_1410_120274
0033_314_1410_120274 [Realized] 1
LINE
TRACE
1 1
1 82
1 163
1 244
1 325
1 406
1 486
1 567
1 648
1 729
1 810
1 891
1 972
1 1053
1 1134
-5
-10
-15
-20
-25
-30
-35
-40
-45
-50
-55
-60
-65
-70

Seismic line survey C, from shore-to-sea.

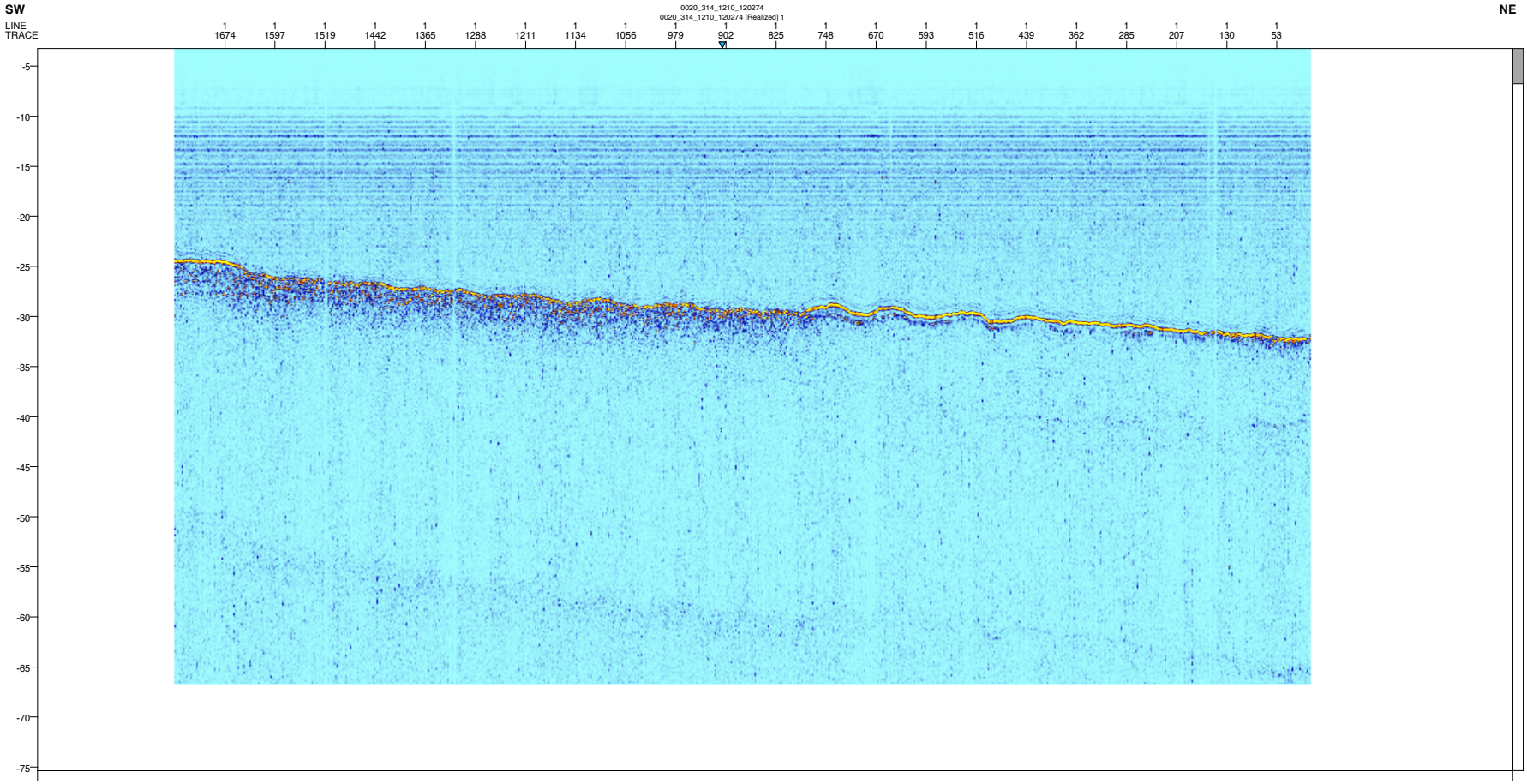

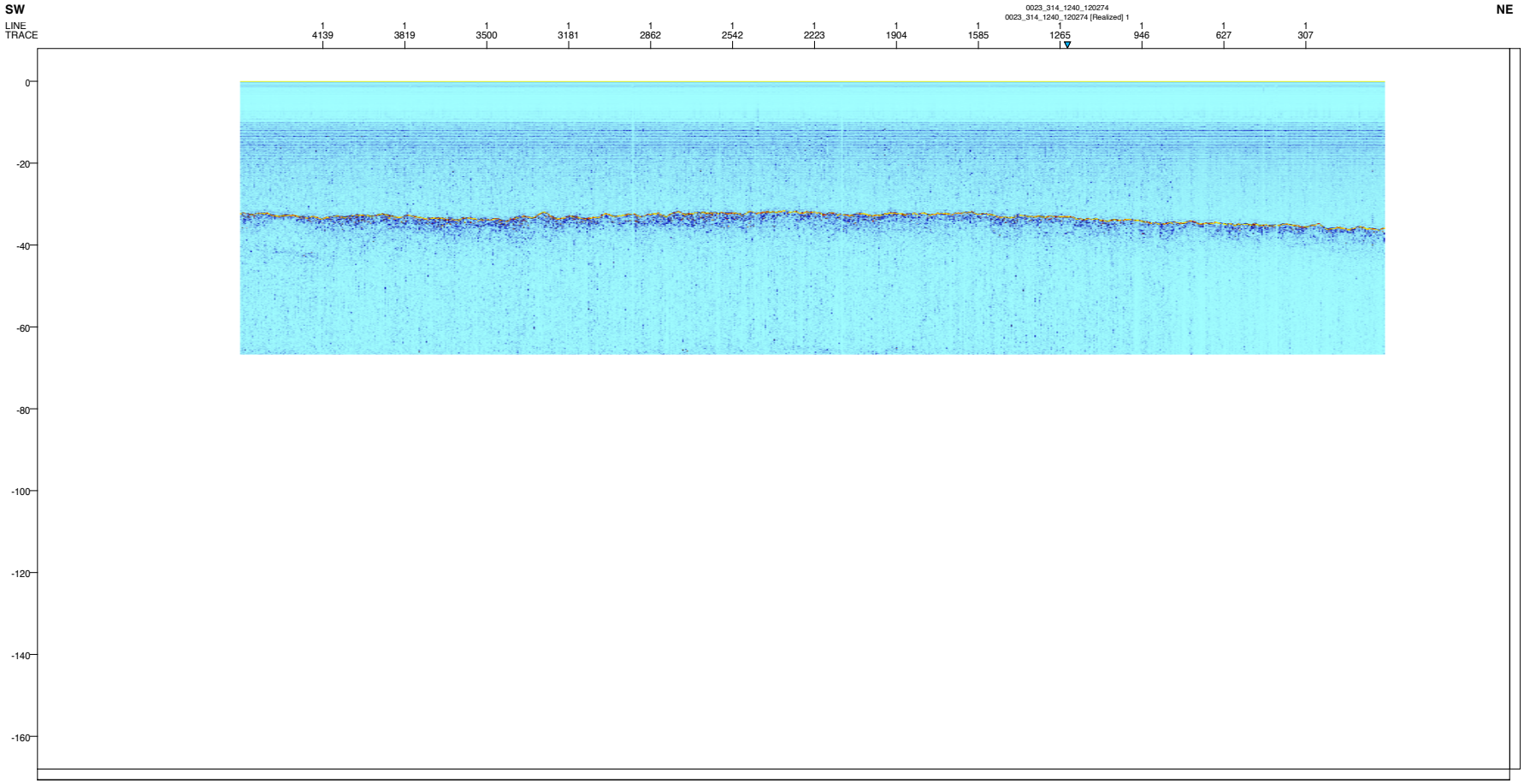
SW
NE
LINE
TRACE
0023_314_1240_120274
0023_314_1240_120274 [Realized] 1
1 4139
1 3819
1 3500
1 3181
1 2862
1 2542
1 2223
1 1904
1 1585
1 1265
1 946
1 627
1 307
0
-20
-40
-60
-80
-100
-120
-140
-160

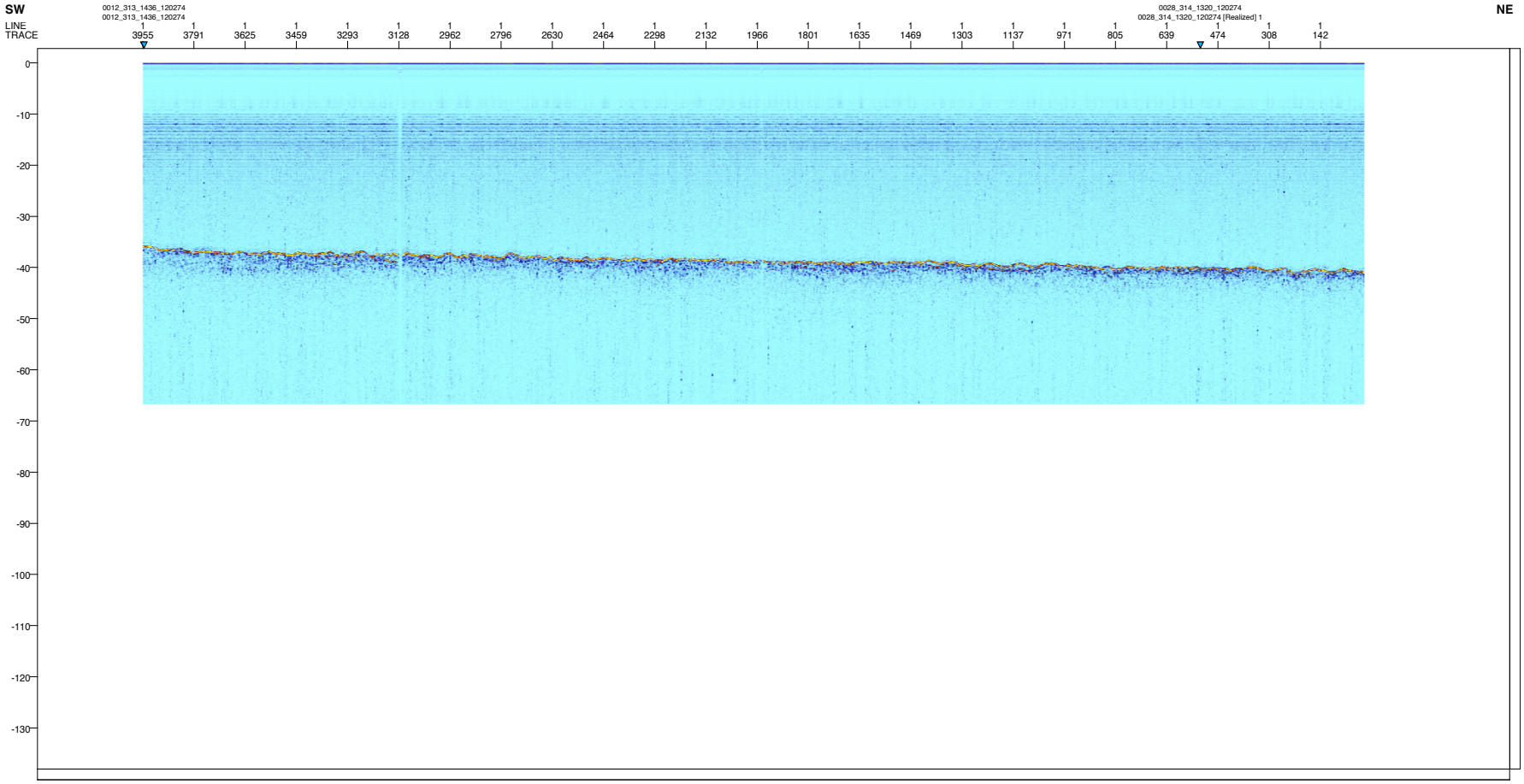
SW
NE
0012_313_1436_120274
0012_313_1436_120274
0028_314_1320_120274
0028_314_1320_120274 [Realized] 1
LINE
TRACE
3955
3791
3625
3459
3293
3128
2962
2796
2630
2464
2298
2132
1966
1801
1635
1469
1303
1137
971
805
639
474
308
142
0
-10
-20
-30
-40
-50
-60
-70
-80
-90
-100
-110
-120
-130

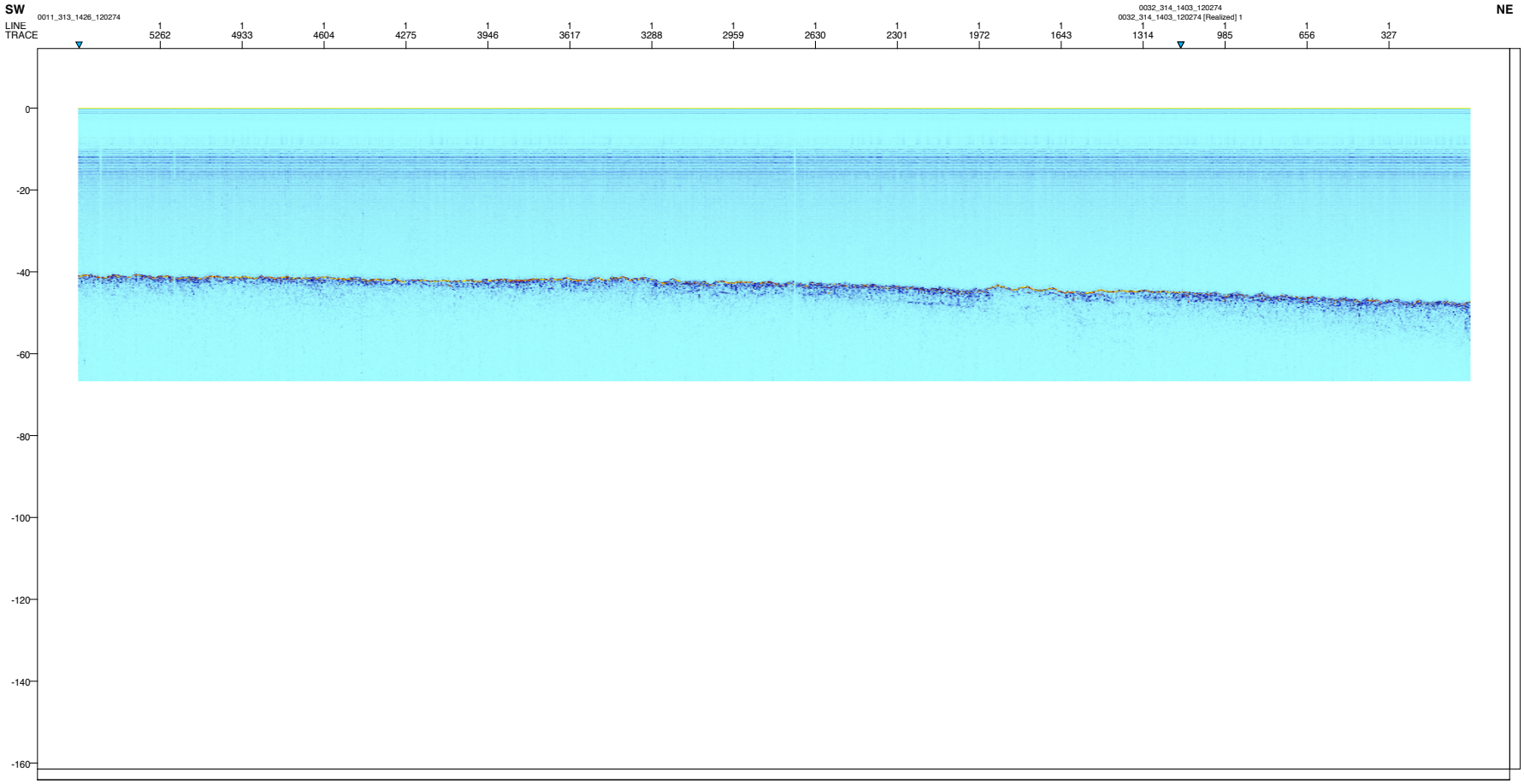
SW
NE
0011_313_1426_120274
0032_314_1403_120274
0032_314_1403_120274 [Realized] 1
LINE
TRACE
1 5262
1 4933
1 4604
1 4275
1 3946
1 3617
1 3288
1 2959
1 2630
1 2301
1 1972
1 1643
1 1314
1 985
1 656
1 327
0
-20
-40
-60
-80
-100
-120
-140
-160

Seismic line survey D, from shore-to-sea.

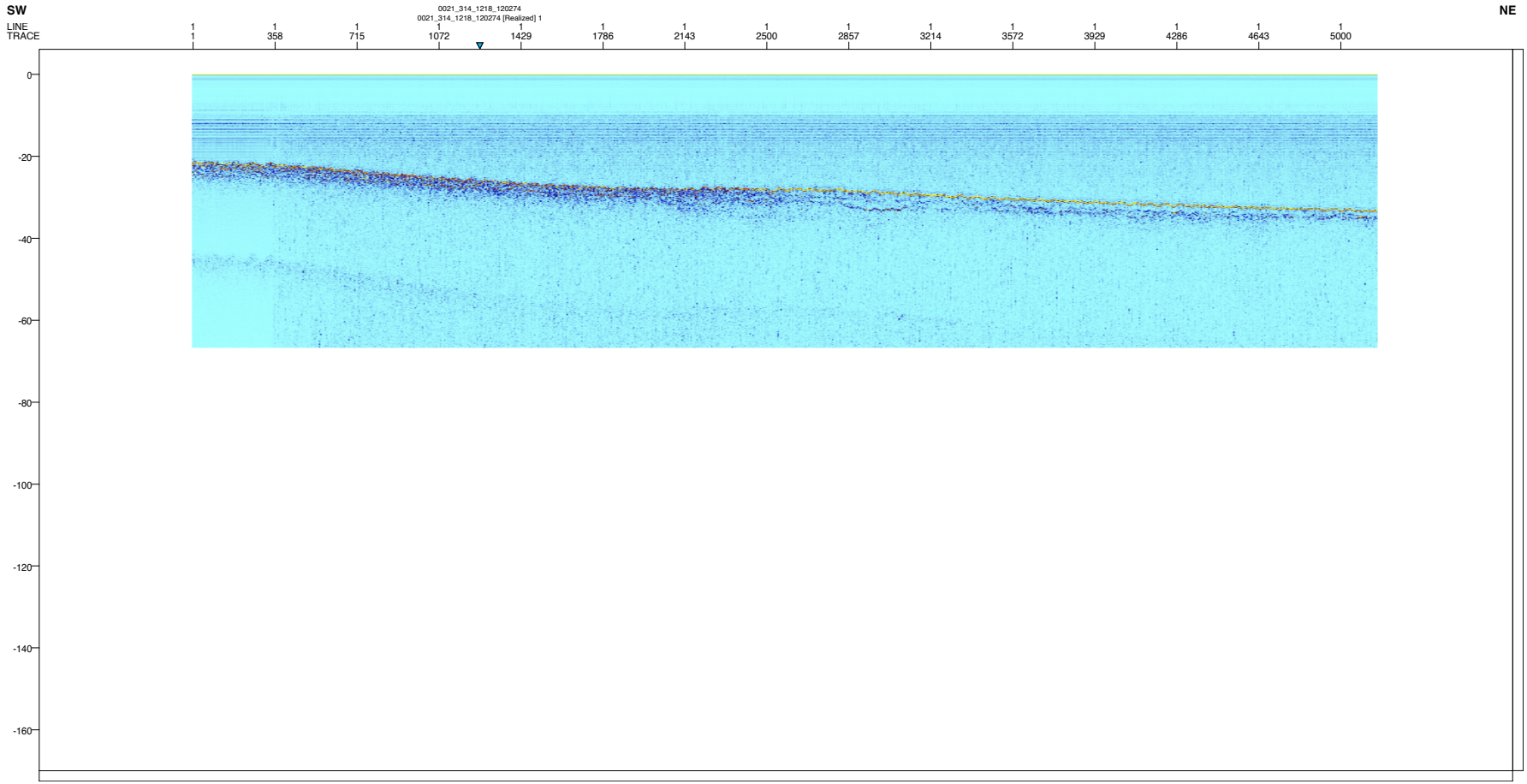

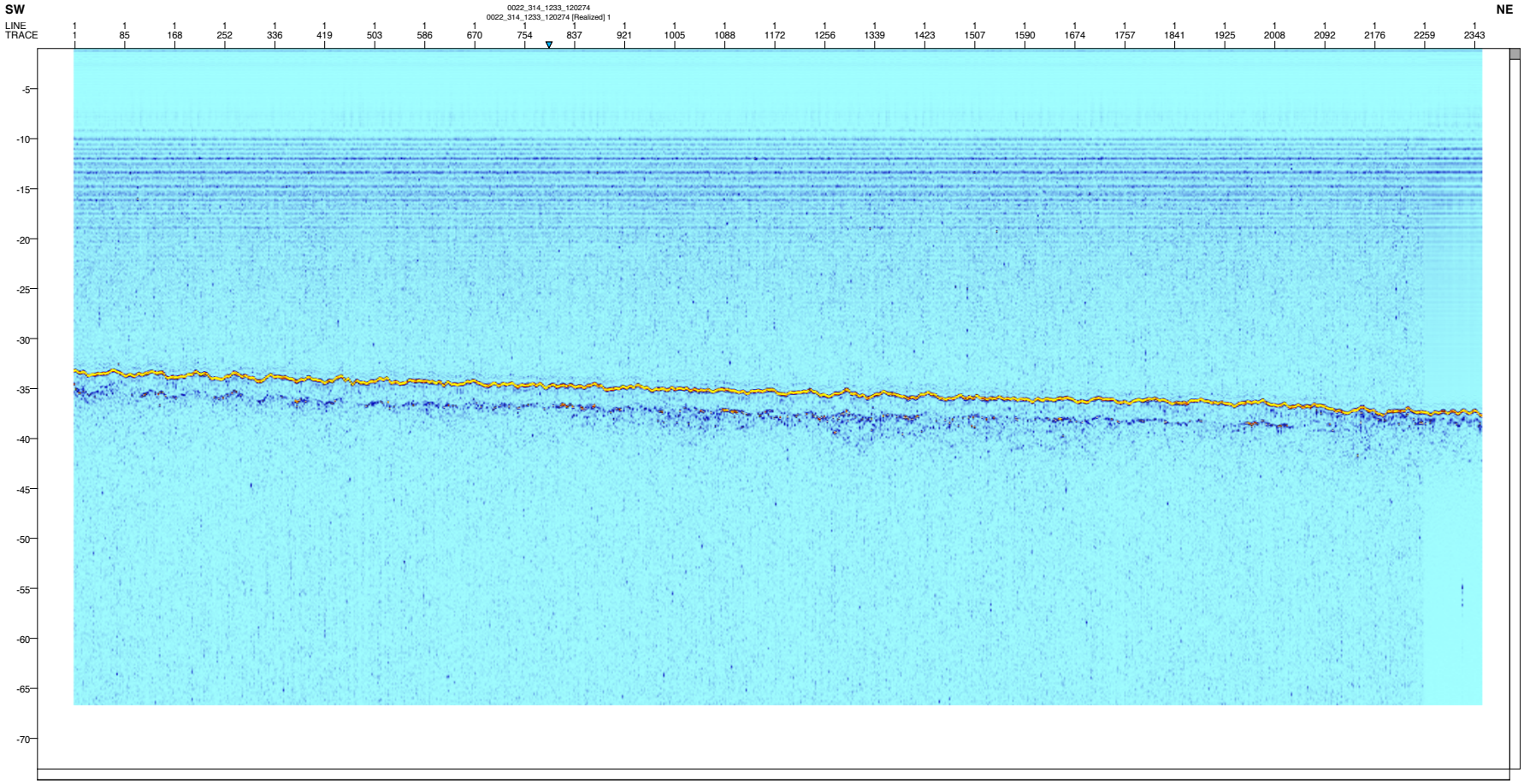
SW
NE
0022_314_1233_120274
0022_314_1233_120274 [Realized] 1
LINE
TRACE
1 1 85 168 252 336 419 503 586 670 754 837 921 1005 1088 1172 1256 1339 1423 1507 1590 1674 1757 1841 1925 2008 2092 2176 2259 2343
-5
-10
-15
-20
-25
-30
-35
-40
-45
-50
-55
-60
-65
-70

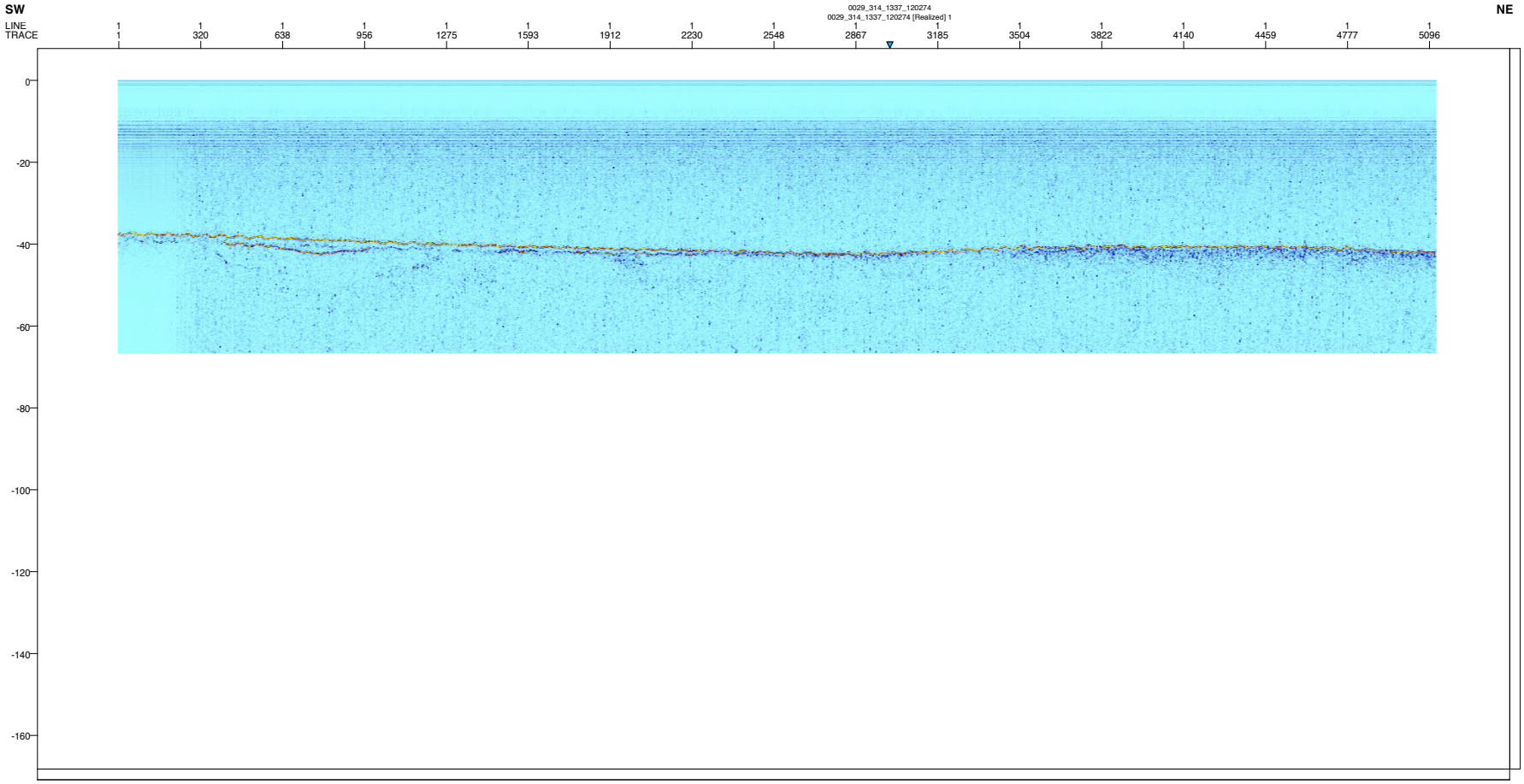
SW
NE
LINE
TRACE
0029_314_1337_120274
0029_314_1337_120274 [Realized] 1
1
1
320
638
956
1275
1593
1912
2230
2548
2867
3185
3504
3822
4140
4459
4777
5096
0
-20
-40
-60
-80
-100
-120
-140
-160

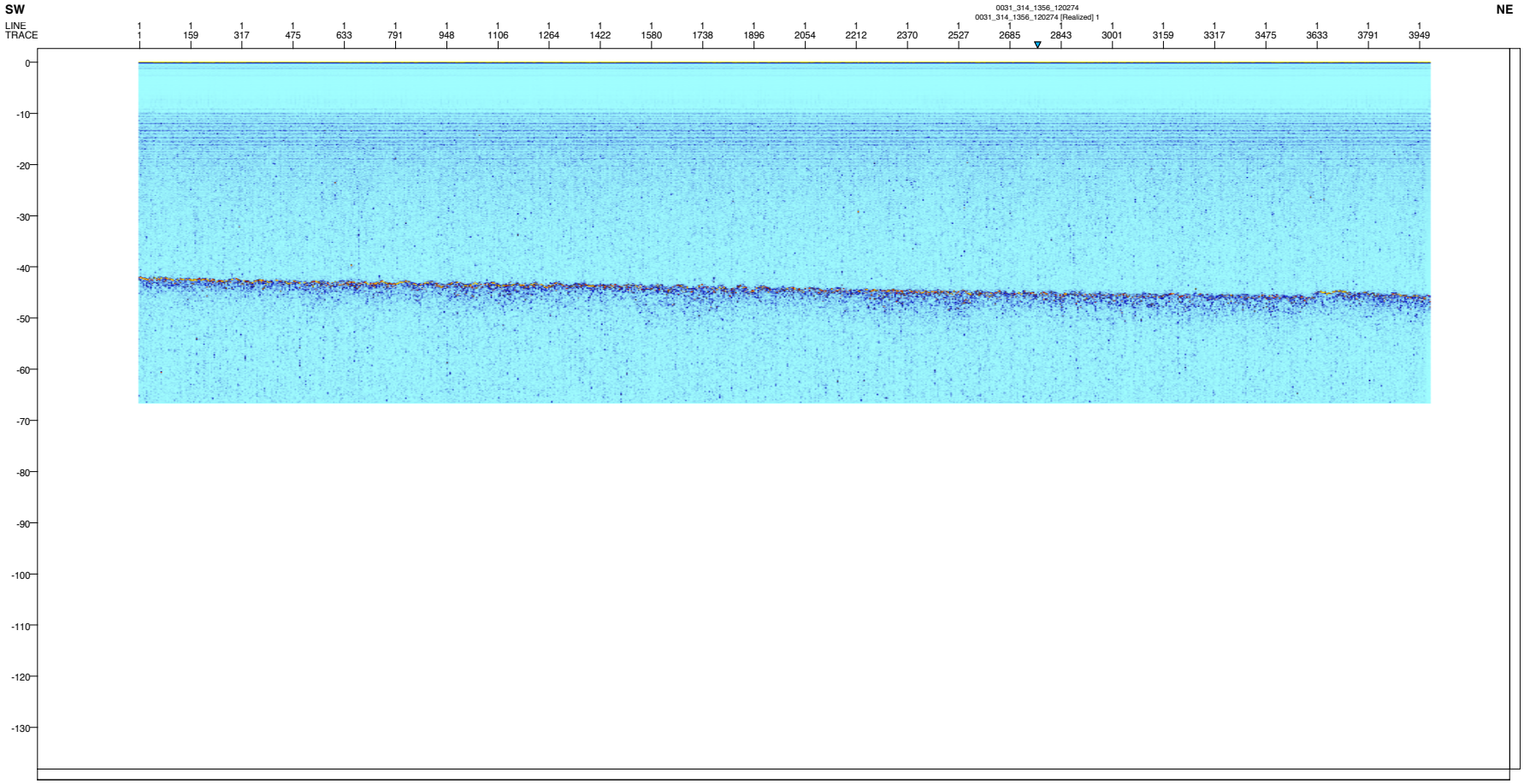
SW
NE
LINE
TRACE
0031_314_1356_120274
0031_314_1356_120274 [Realized] 1
1 1 159 317 475 633 791 948 1106 1264 1422 1580 1738 1896 2054 2212 2370 2527 2685 2843 3001 3159 3317 3475 3633 3791 3949
0
-10
-20
-30
-40
-50
-60
-70
-80
-90
-100
-110
-120
-130

Seismic line survey E, from northwest to southwest.

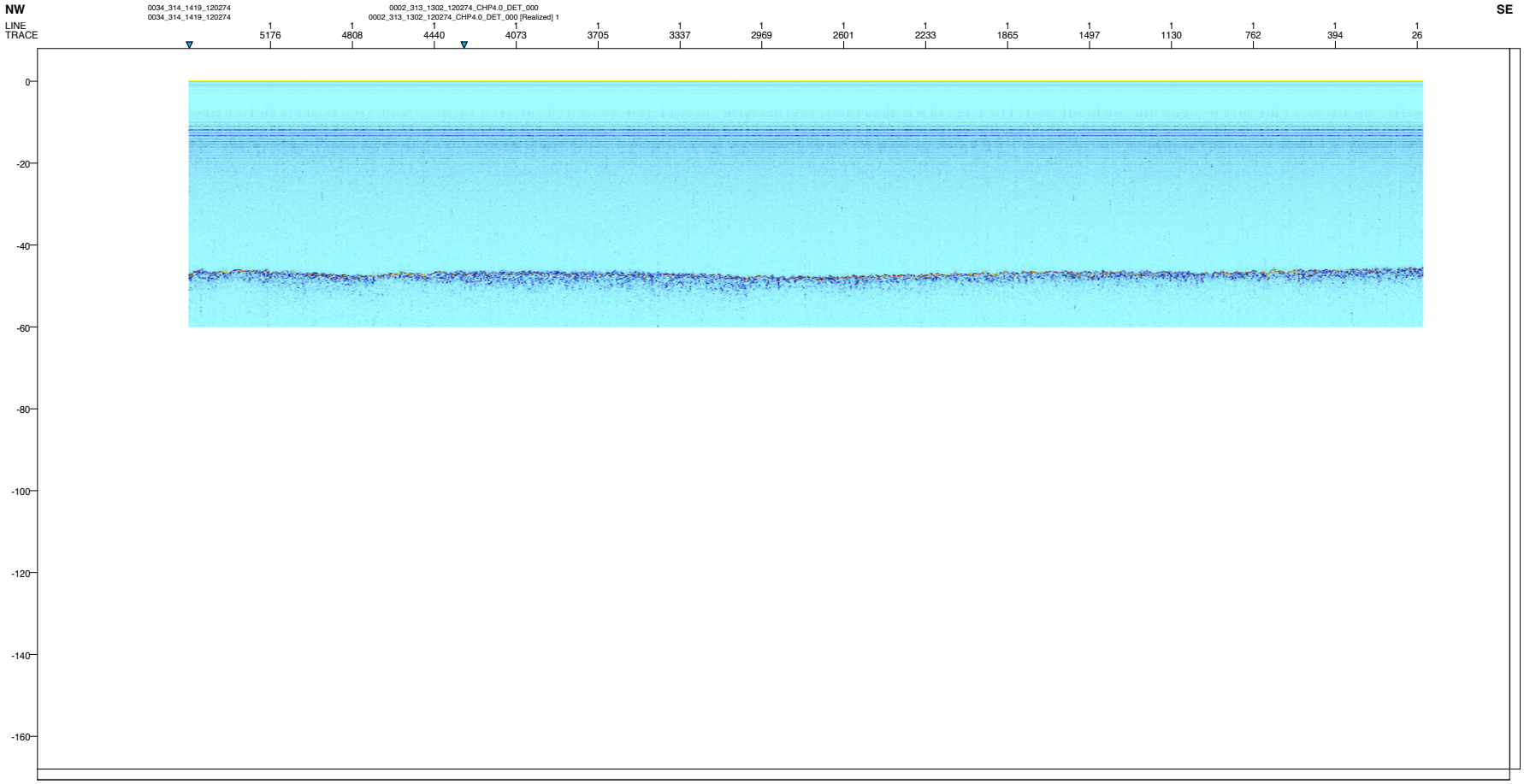

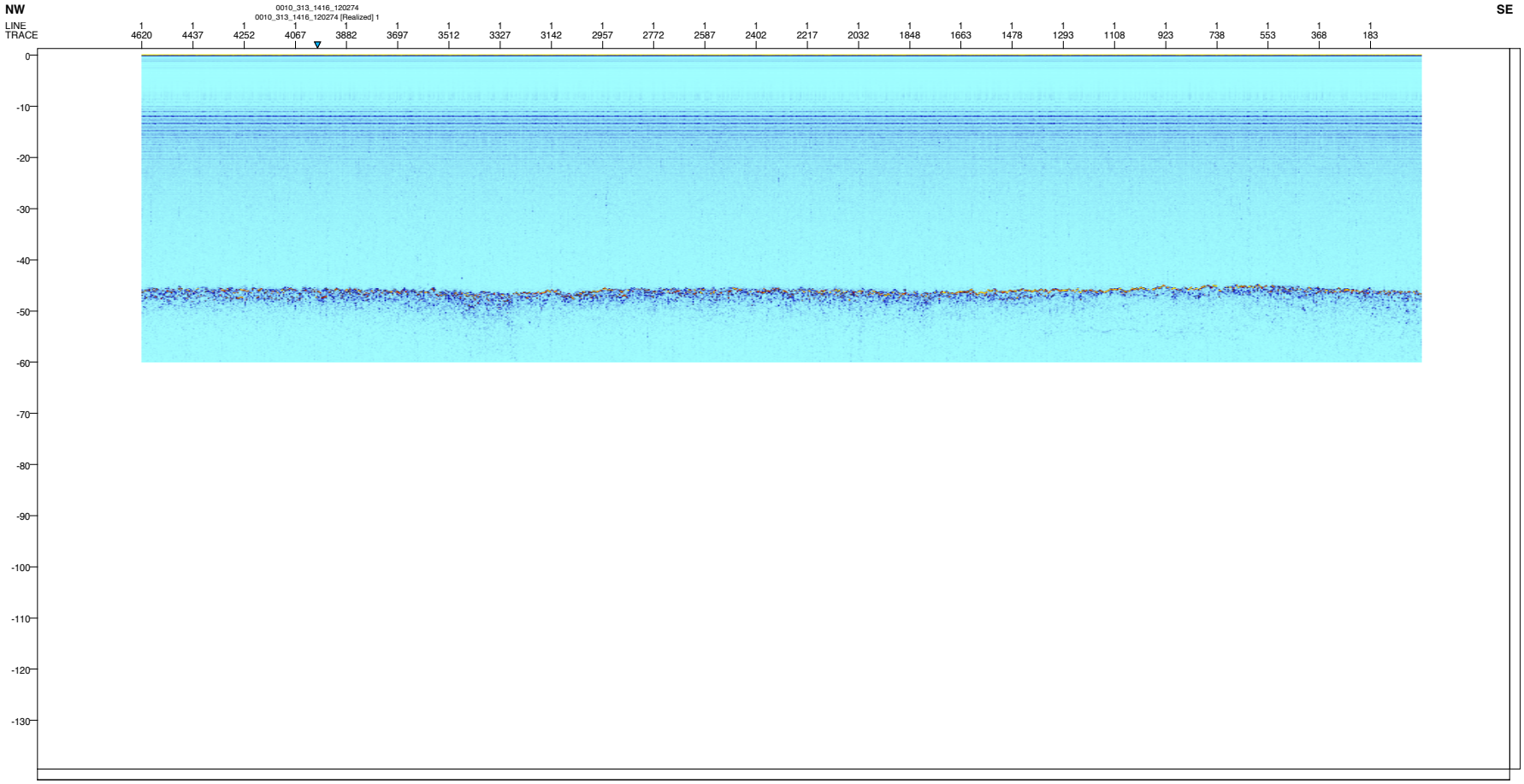
NW
SE
LINE
TRACE
0010_313_1416_120274
0010_313_1416_120274 [Realized] 1
4620
4437
4252
4067
3882
3697
3512
3327
3142
2957
2772
2587
2402
2217
2032
1848
1663
1478
1293
1108
923
738
553
368
183
0
-10
-20
-30
-40
-50
-60
-70
-80
-90
-100
-110
-120
-130

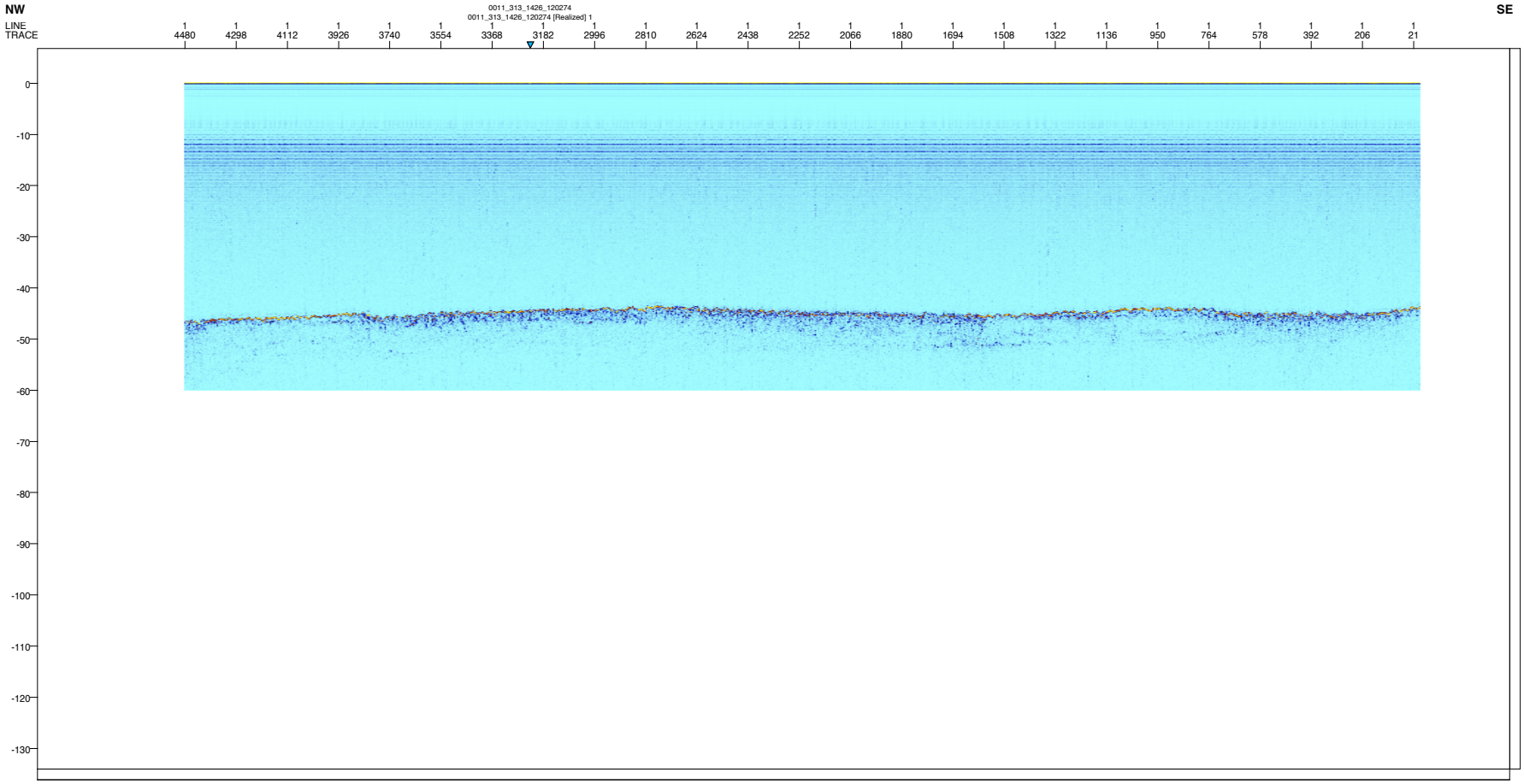
NW
SE
LINE
TRACE
0011_313_1426_120274
0011_313_1426_120274 [Realized] 1
4480
4298
4112
3926
3740
3554
3368
3182
2996
2810
2624
2438
2252
2066
1880
1694
1508
1322
1136
950
764
578
392
206
21
0
-10
-20
-30
-40
-50
-60
-70
-80
-90
-100
-110
-120
-130

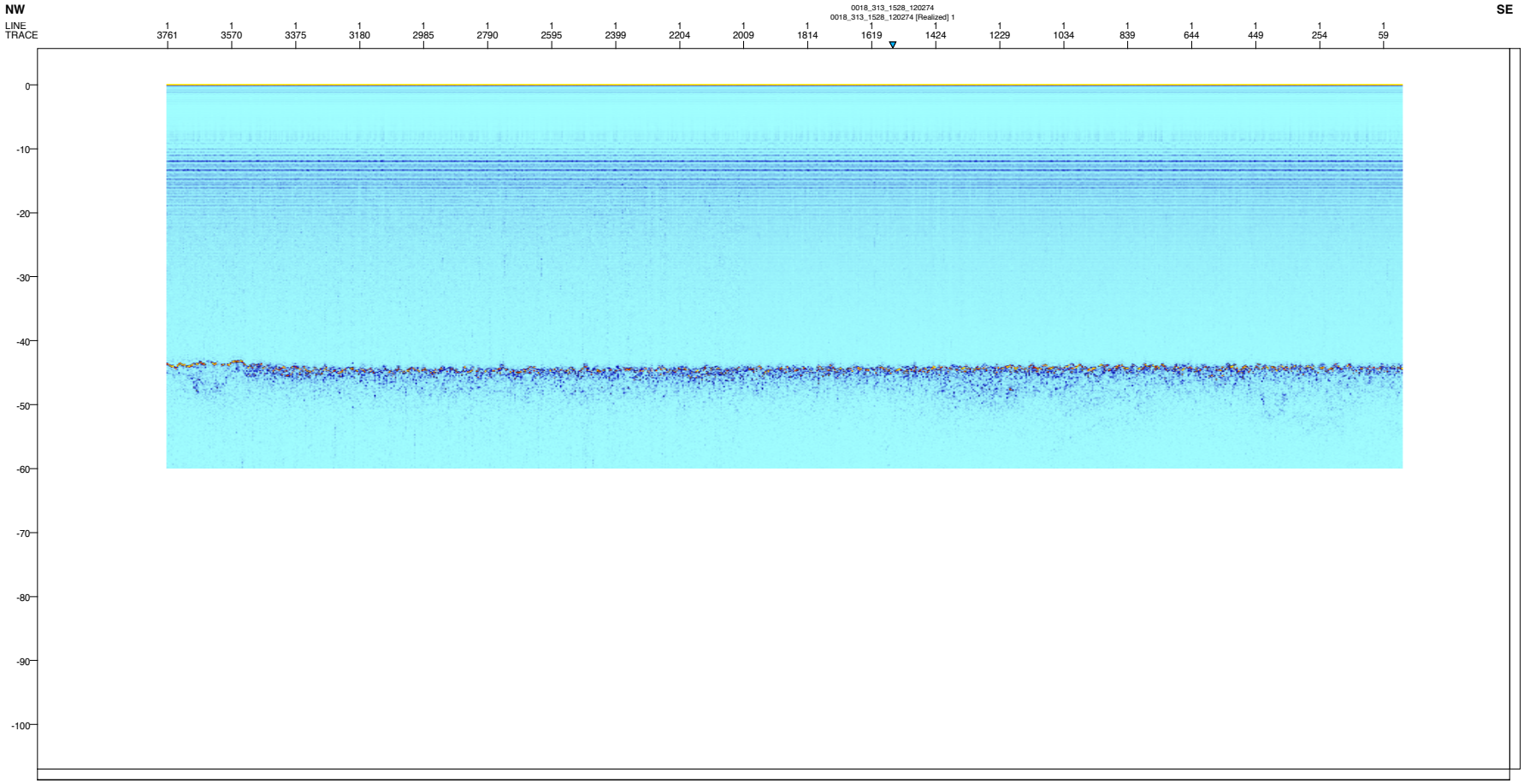
NW
SE
LINE
TRACE
0018_313_1528_120274
0018_313_1528_120274 [Realized] 1
1 3761
1 3570
1 3375
1 3180
1 2985
1 2790
1 2595
1 2399
1 2204
1 2009
1 1814
1 1619
1 1424
1 1229
1 1034
1 839
1 644
1 449
1 254
1 59
0
-10
-20
-30
-40
-50
-60
-70
-80
-90
-100

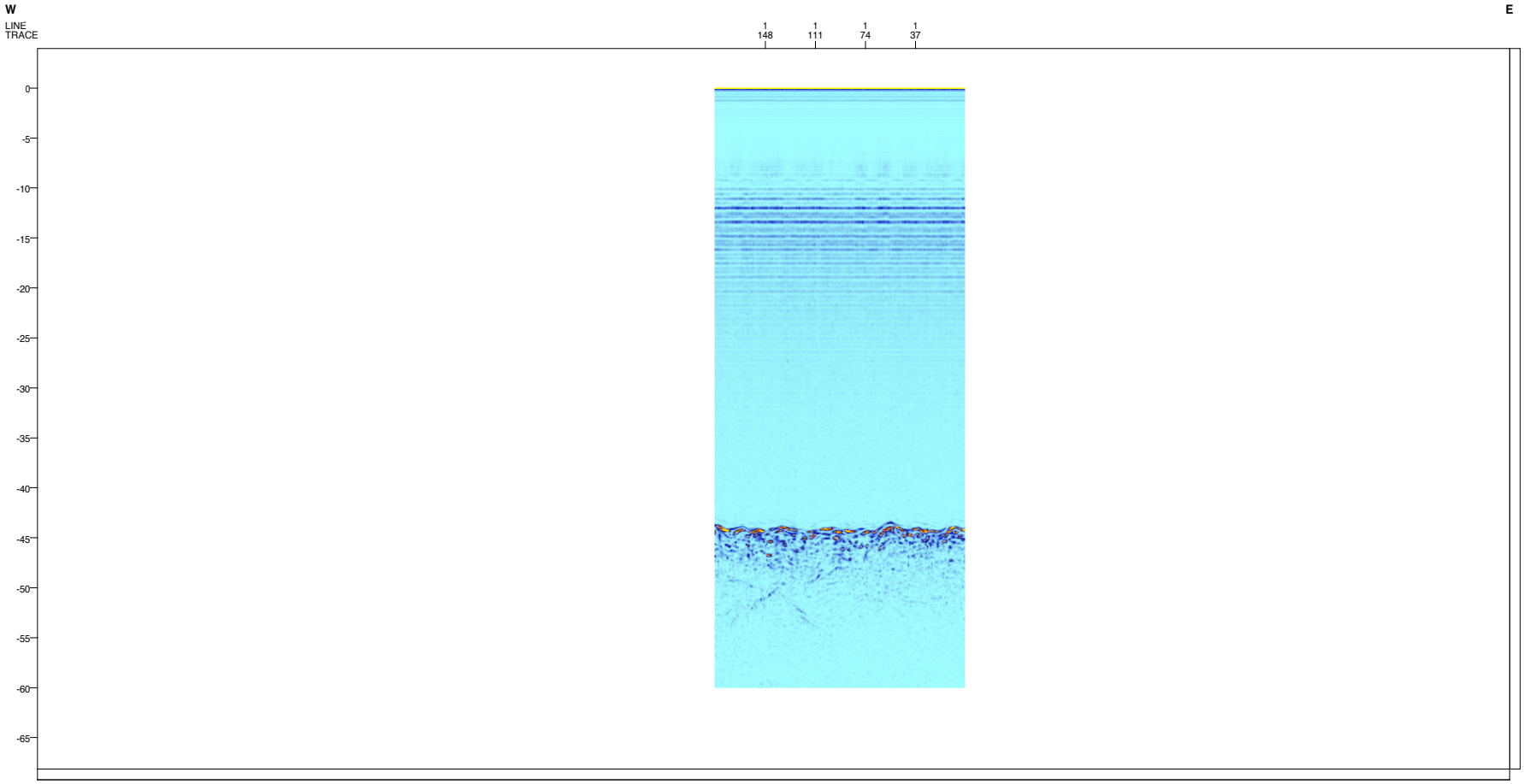
W
E
LINE
TRACE
1
148
1
111
1
74
1
37
0
-5
-10
-15
-20
-25
-30
-35
-40
-45
-50
-55
-60
-65

Seismic line survey F, from northwest to southwest.

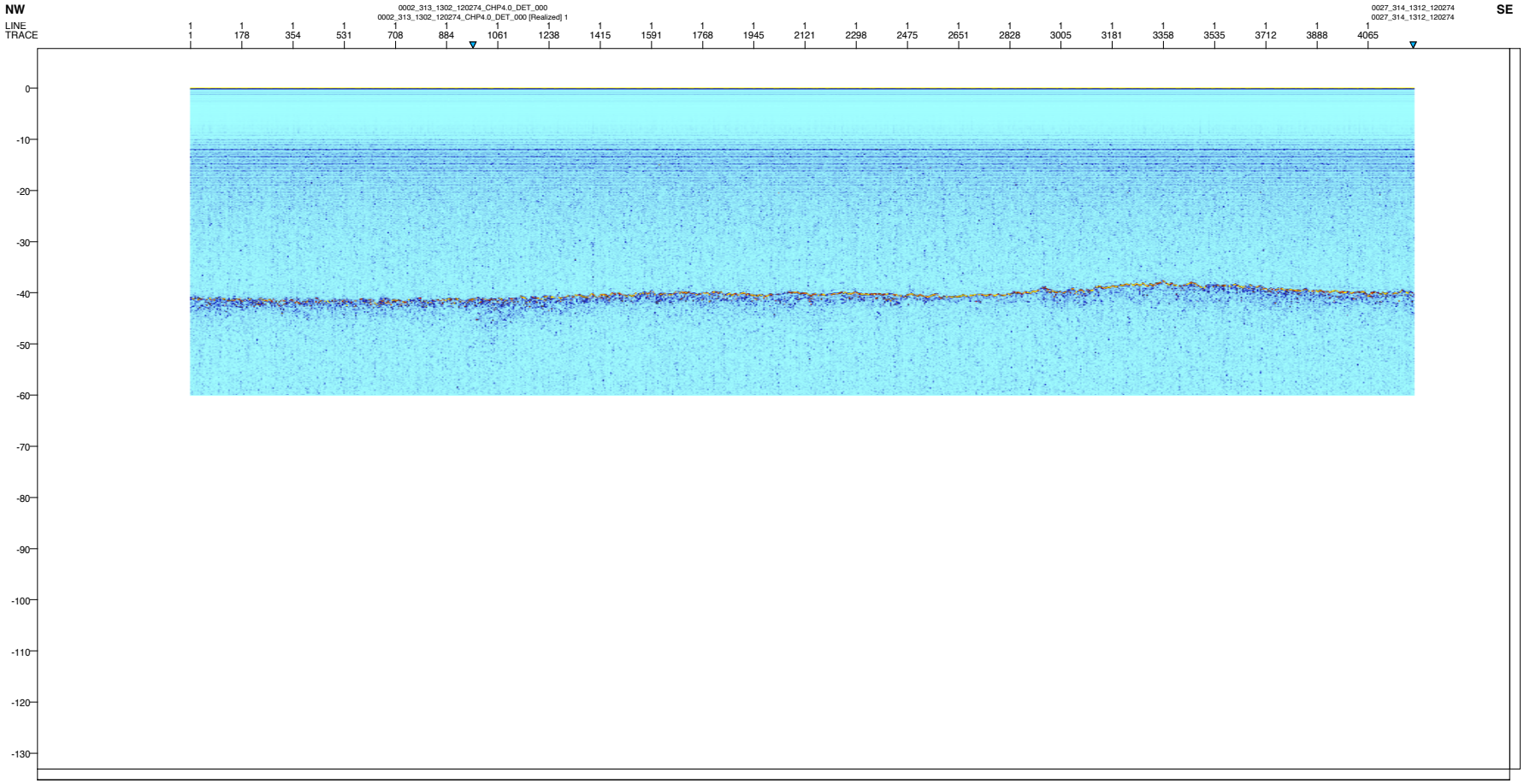

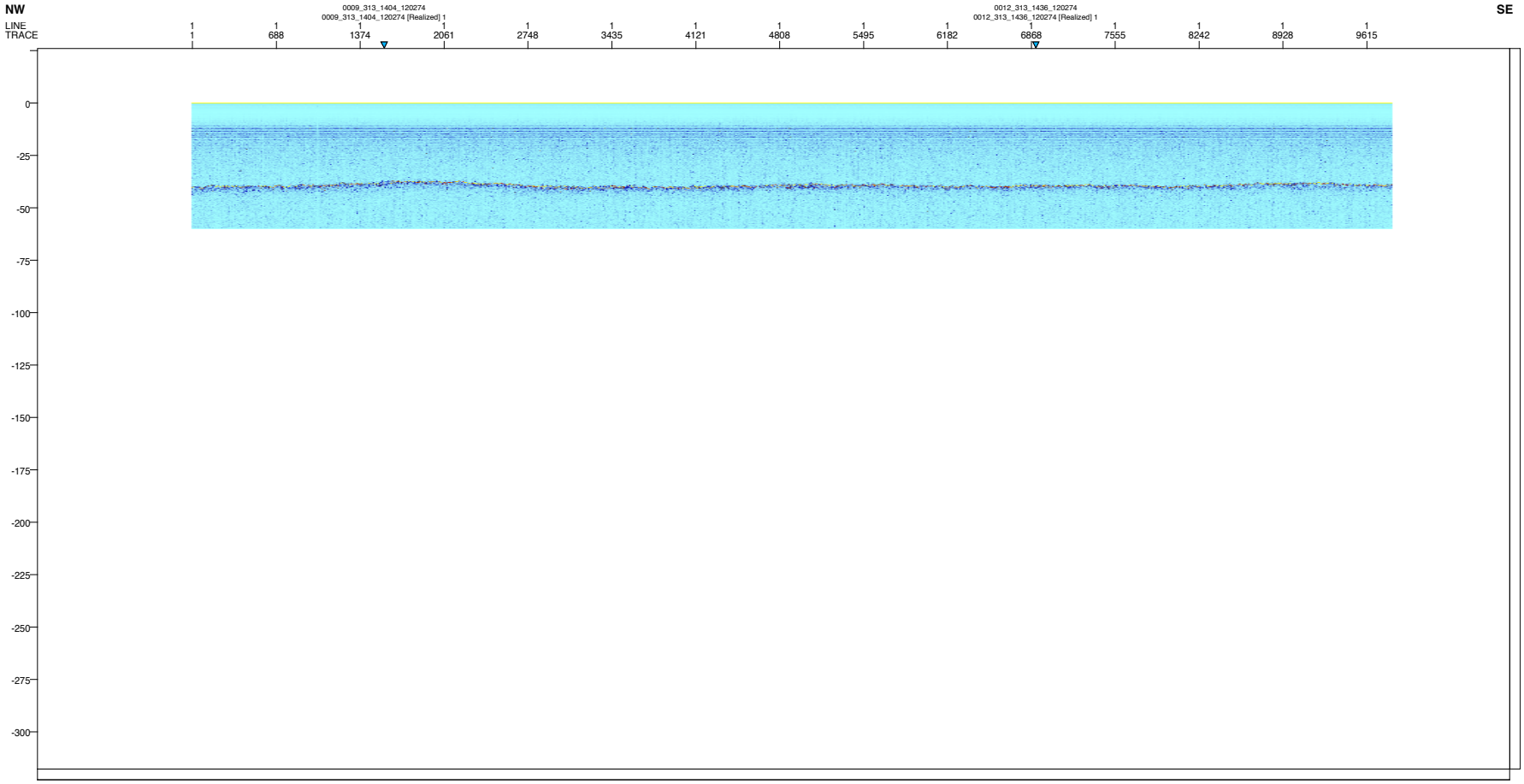
NW
SE
LINE
TRACE
0009_313_1404_120274
0009_313_1404_120274 [Realized] 1
0012_313_1436_120274
0012_313_1436_120274 [Realized] 1
1
1
688
1374
2061
2748
3435
4121
4808
5495
6182
6868
7555
8242
8928
9615
0
-25
-50
-75
-100
-125
-150
-175
-200
-225
-250
-275
-300

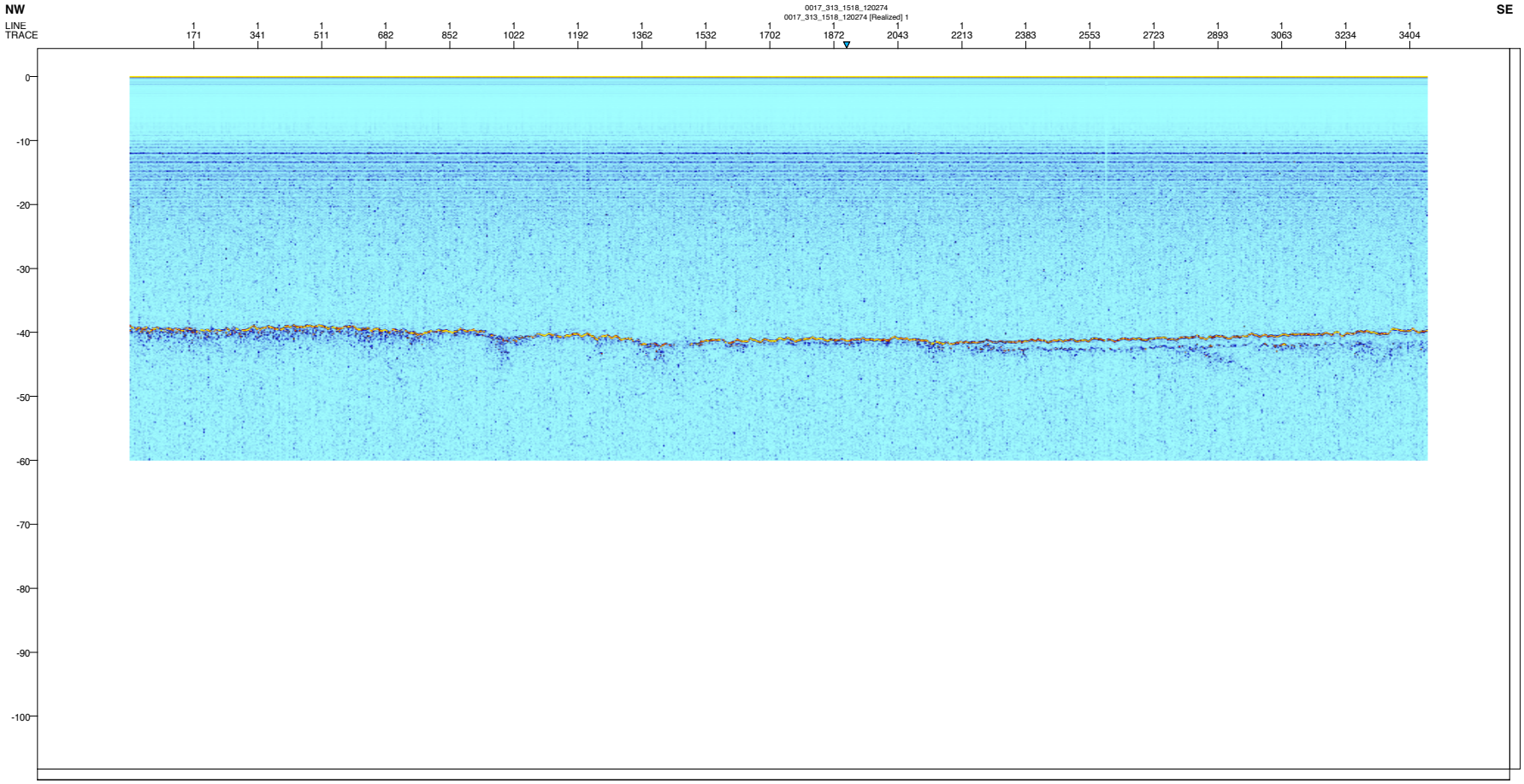
NW
SE
LINE
TRACE
0017_313_1518_120274
0017_313_1518_120274 [Realized] 1
1 171
1 341
1 511
1 682
1 852
1 1022
1 1192
1 1362
1 1532
1 1702
1 1872
1 2043
1 2213
1 2383
1 2553
1 2723
1 2893
1 3063
1 3234
1 3404
0
-10
-20
-30
-40
-50
-60
-70
-80
-90
-100

Seismic line survey G, from northwest to southwest.

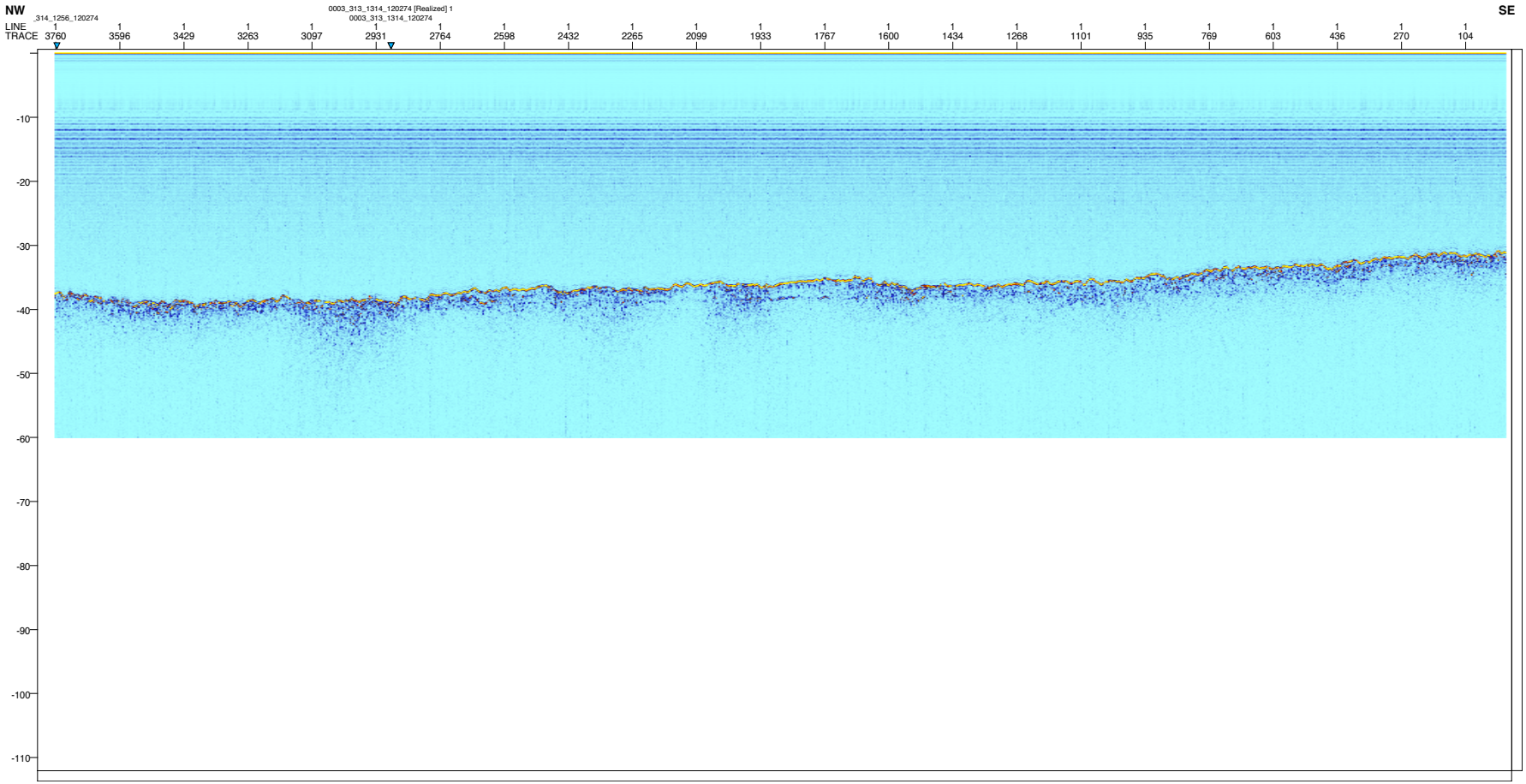

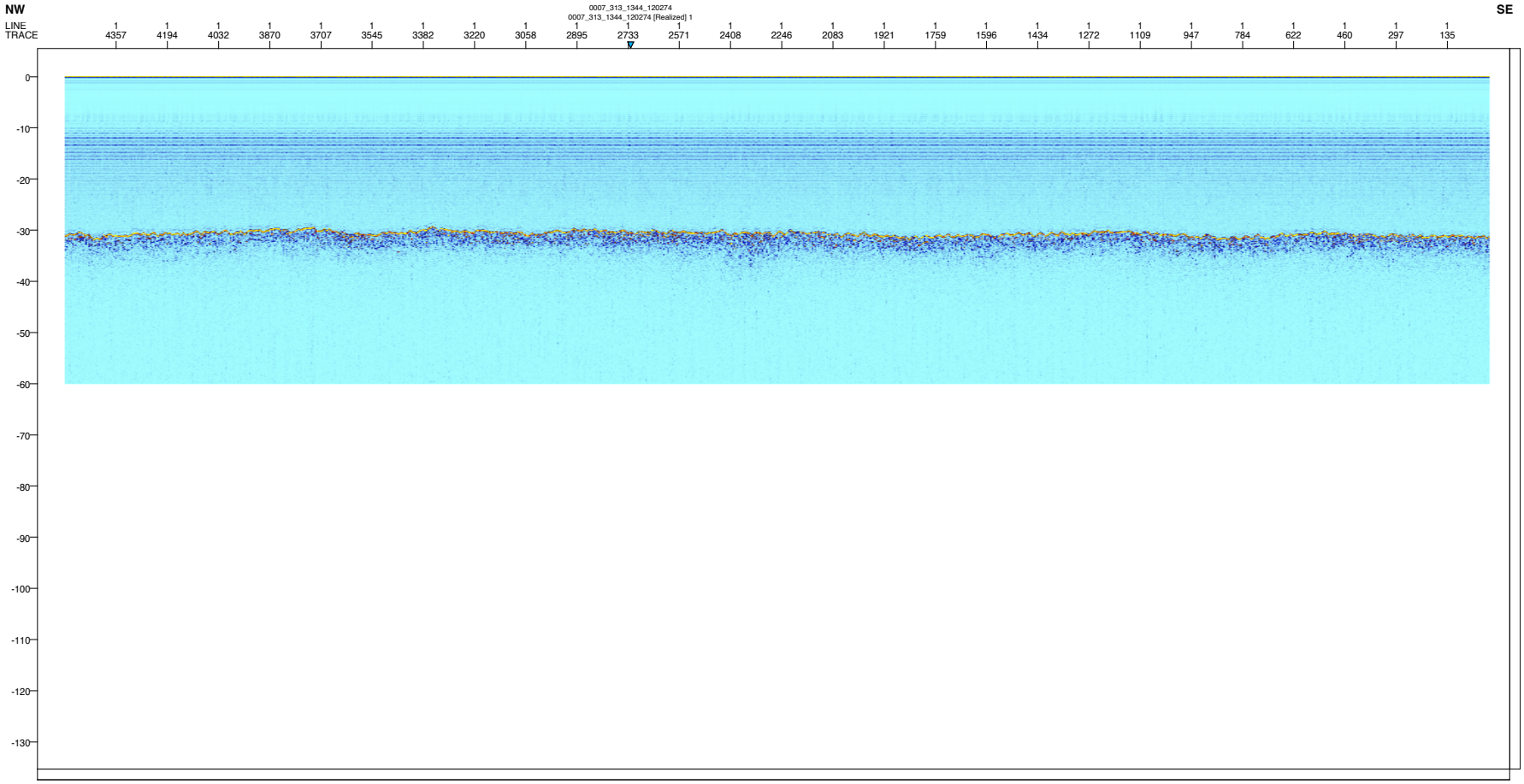
NW
SE
LINE
TRACE
0007_313_1344_120274
0007_313_1344_120274 [Realized] 1
4357
4194
4032
3870
3707
3545
3382
3220
3058
2895
2733
2571
2408
2246
2083
1921
1759
1596
1434
1272
1109
947
784
622
460
297
135
0
-10
-20
-30
-40
-50
-60
-70
-80
-90
-100
-110
-120
-130

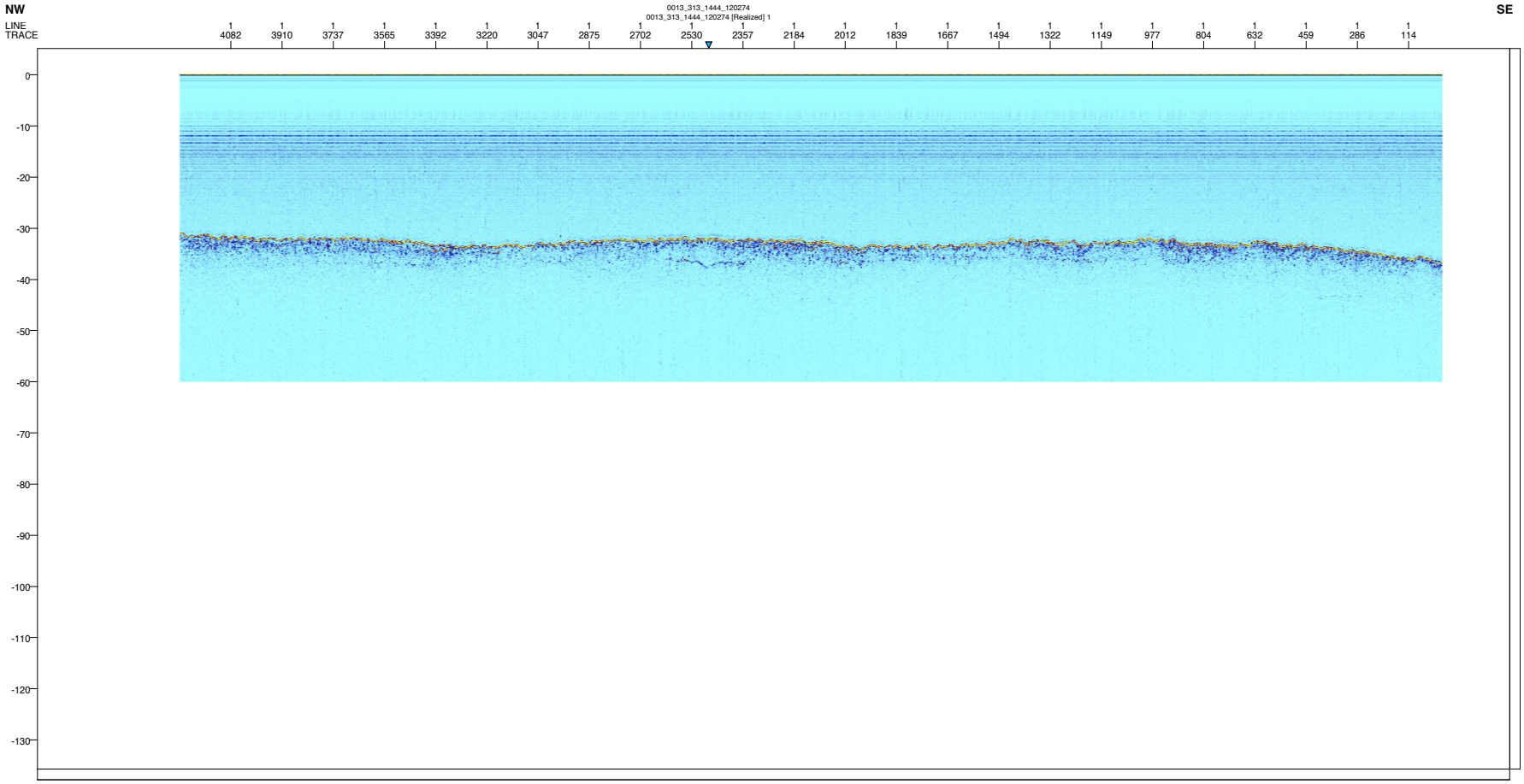
NW
SE
LINE
TRACE
0013_313_1444_120274
0013_313_1444_120274 [Realized] 1
1 4082
1 3910
1 3737
1 3565
1 3392
1 3220
1 3047
1 2875
1 2702
1 2530
1 2357
1 2184
1 2012
1 1839
1 1667
1 1494
1 1322
1 1149
1 977
1 804
1 632
1 459
1 286
1 114
0
-10
-20
-30
-40
-50
-60
-70
-80
-90
-100
-110
-120
-130

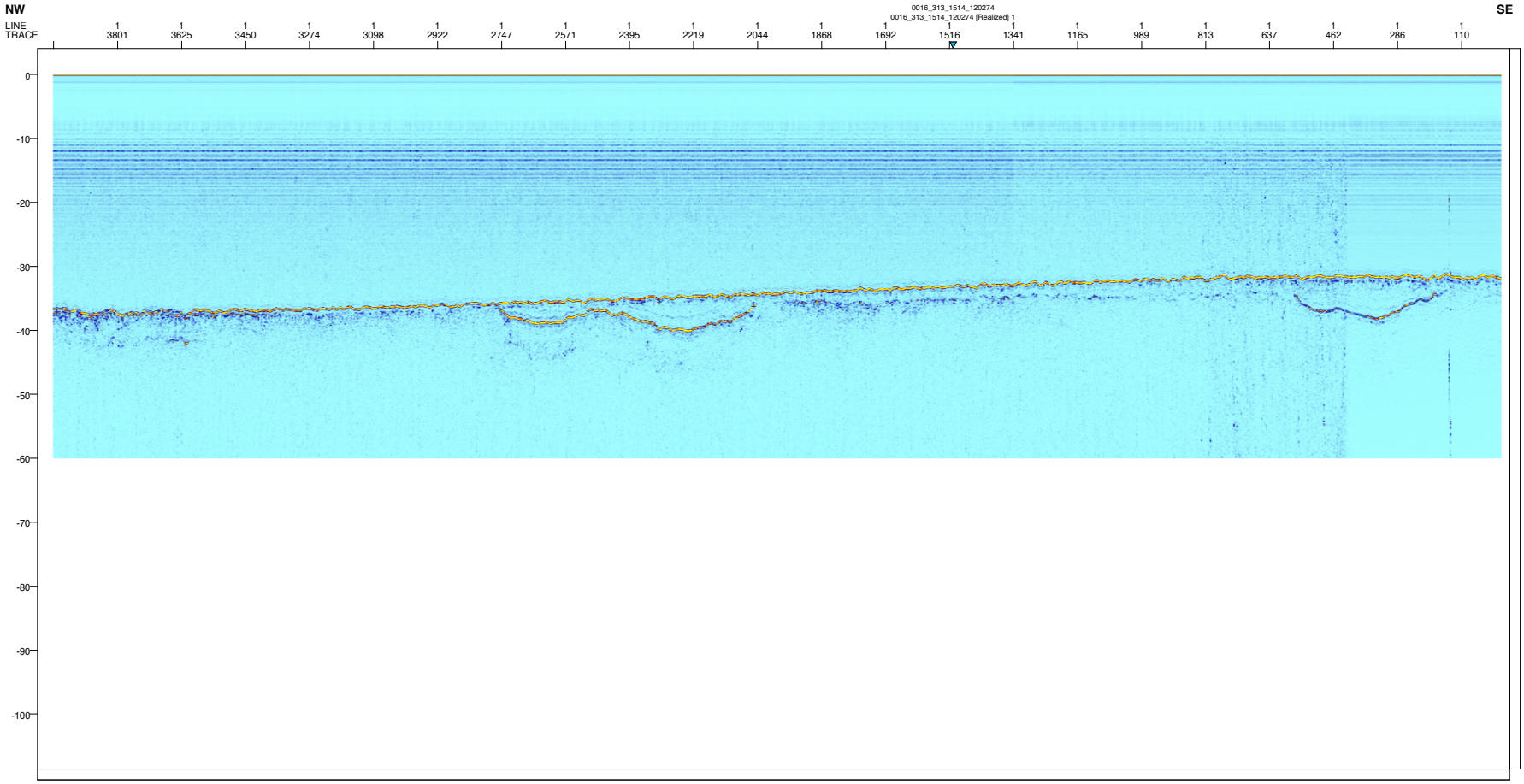
NW
SE
LINE
TRACE
0016_313_1514_120274
0016_313_1514_120274 [Realized] 1
1 3801
1 3625
1 3450
1 3274
1 3098
1 2922
1 2747
1 2571
1 2395
1 2219
1 2044
1 1868
1 1692
1 1516
1 1341
1 1165
1 989
1 813
1 637
1 462
1 286
1 110
0
-10
-20
-30
-40
-50
-60
-70
-80
-90
-100

Seismic line survey H, from northwest to southwest.

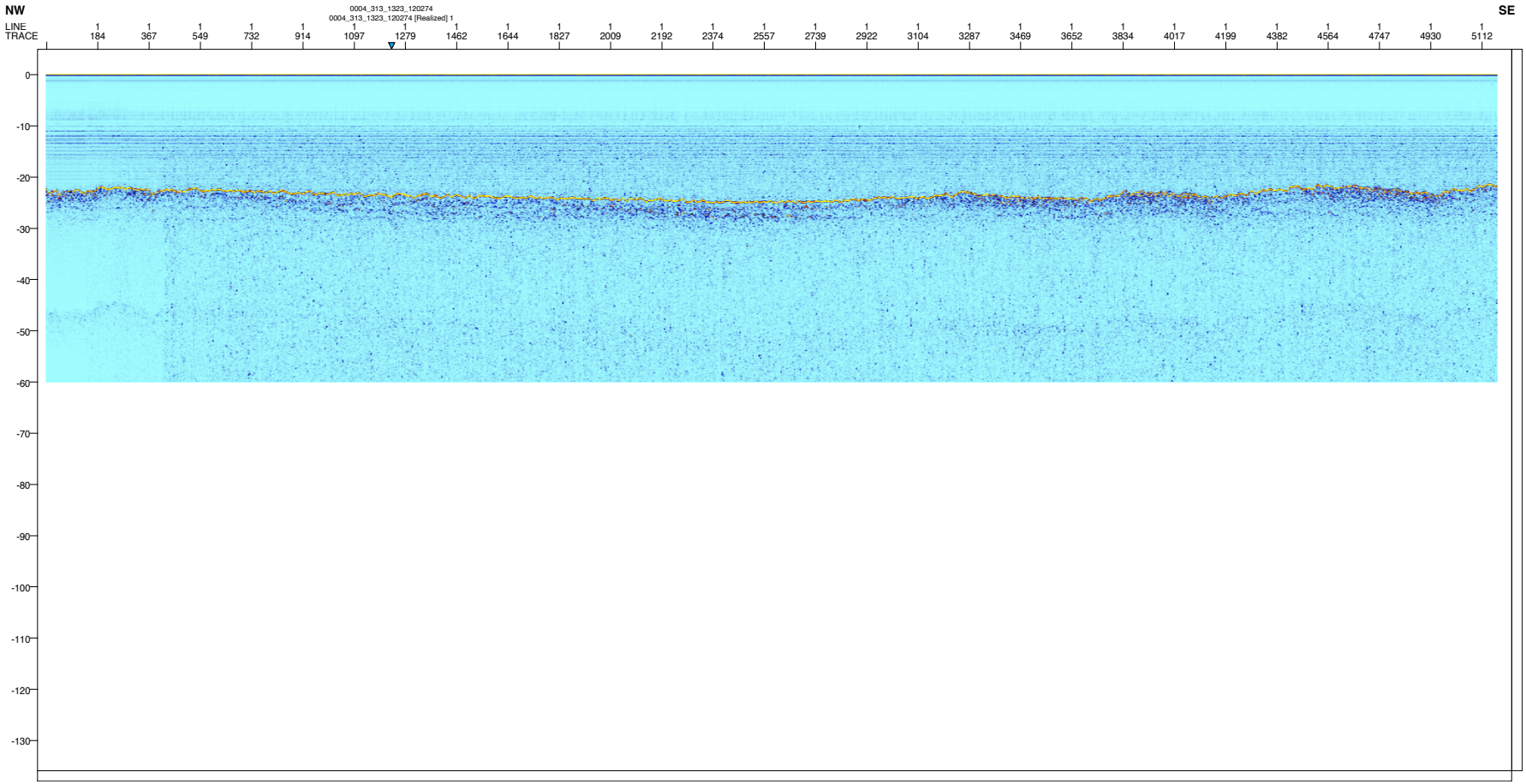

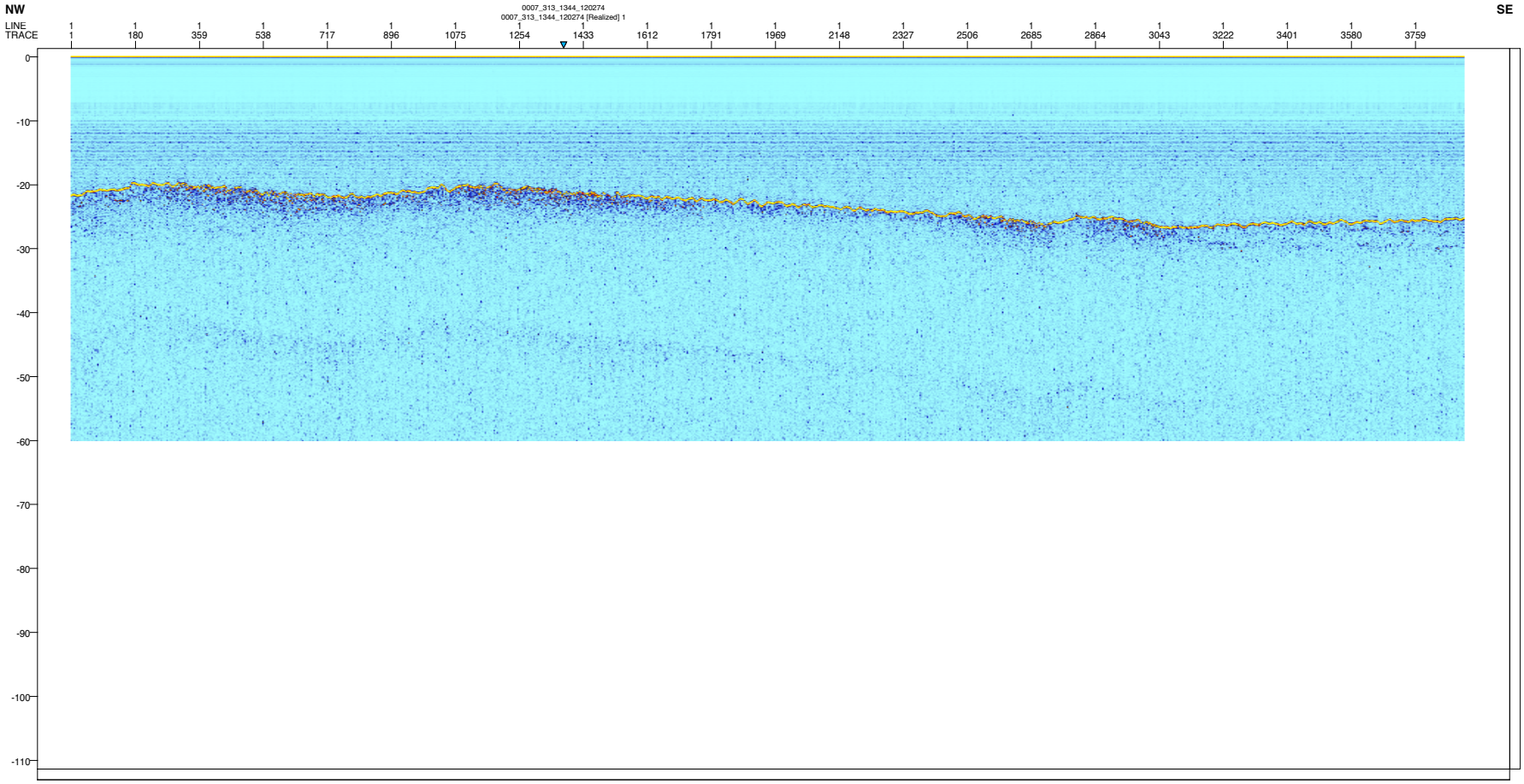
NW
SE
LINE
TRACE
0007_313_1344_120274
0007_313_1344_120274 [Realized] 1
1 1 180 359 538 717 896 1075 1254 1433 1612 1791 1969 2148 2327 2506 2685 2864 3043 3222 3401 3580 3759
0
-10
-20
-30
-40
-50
-60
-70
-80
-90
-100
-110

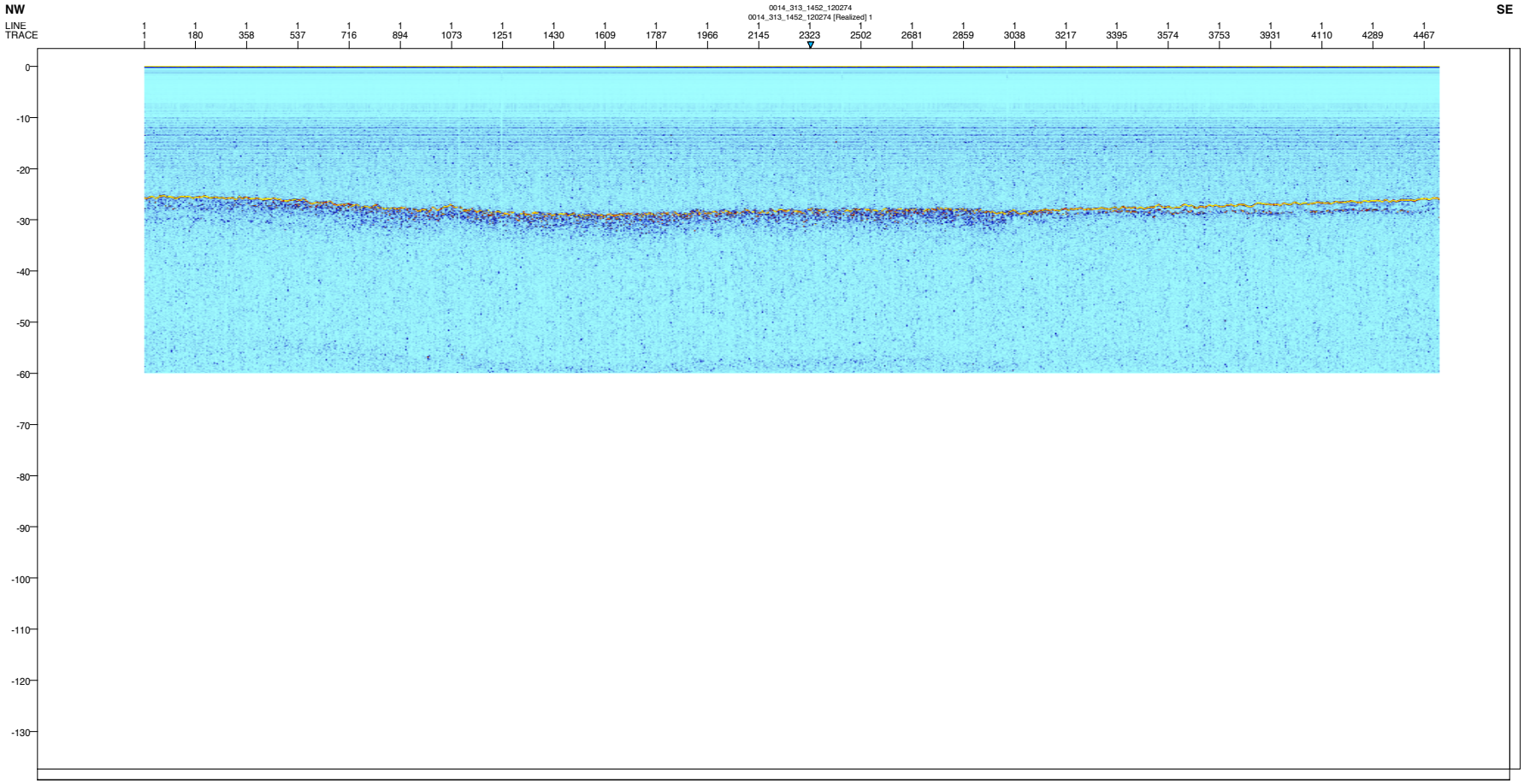
NW
SE
0014_313_1452_120274
0014_313_1452_120274 [Realized] 1
LINE
TRACE
1 1 180 358 537 716 894 1073 1251 1430 1609 1787 1966 2145 2323 2502 2681 2859 3038 3217 3395 3574 3753 3931 4110 4289 4467
0
-10
-20
-30
-40
-50
-60
-70
-80
-90
-100
-110
-120
-130

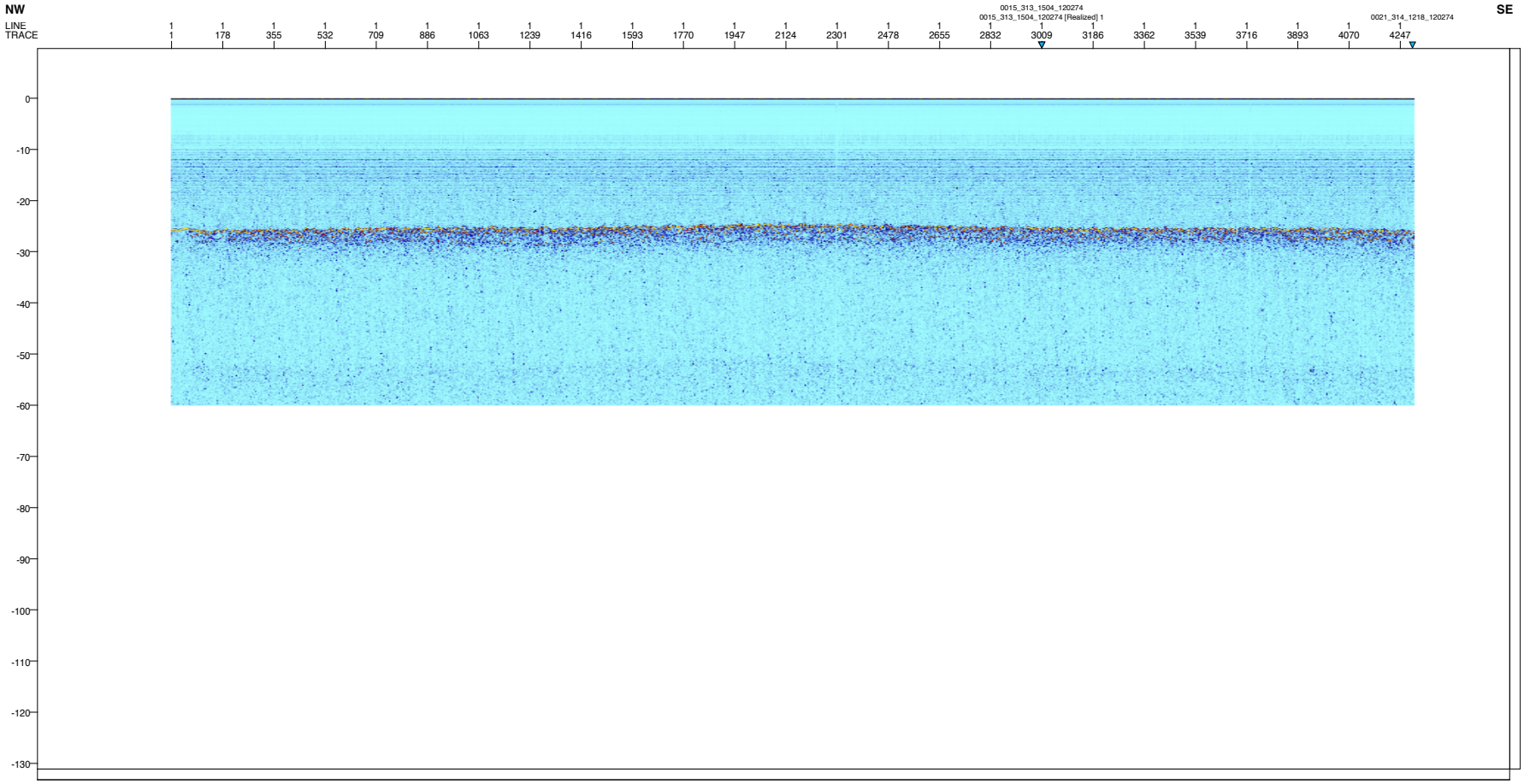
NW
SE
LINE
TRACE
0015_313_1504_120274
0015_313_1504_120274 [Realized] 1
0021_314_1218_120274
1 1 178 355 532 709 886 1063 1239 1416 1593 1770 1947 2124 2301 2478 2655 2832 3009 3186 3362 3539 3716 3893 4070 4247
0 -10 -20 -30 -40 -50 -60 -70 -80 -90 -100 -110 -120 -130

Appendix E. Core Logs of Vibracores

Digital core logs created using Applecore®

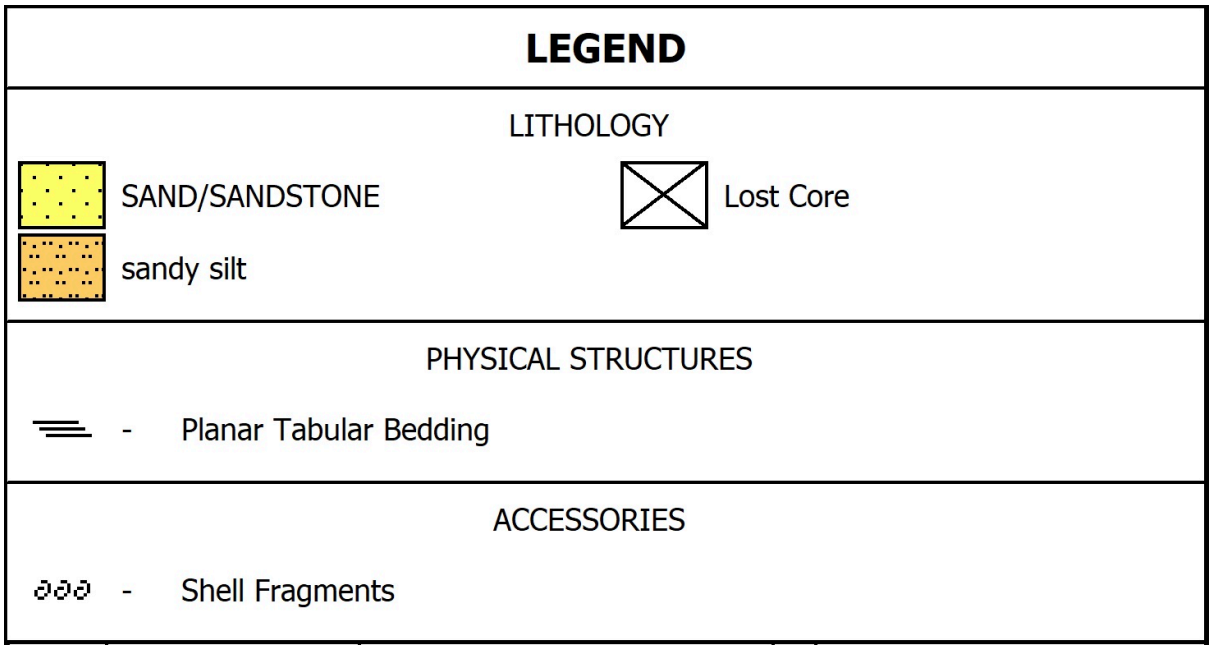

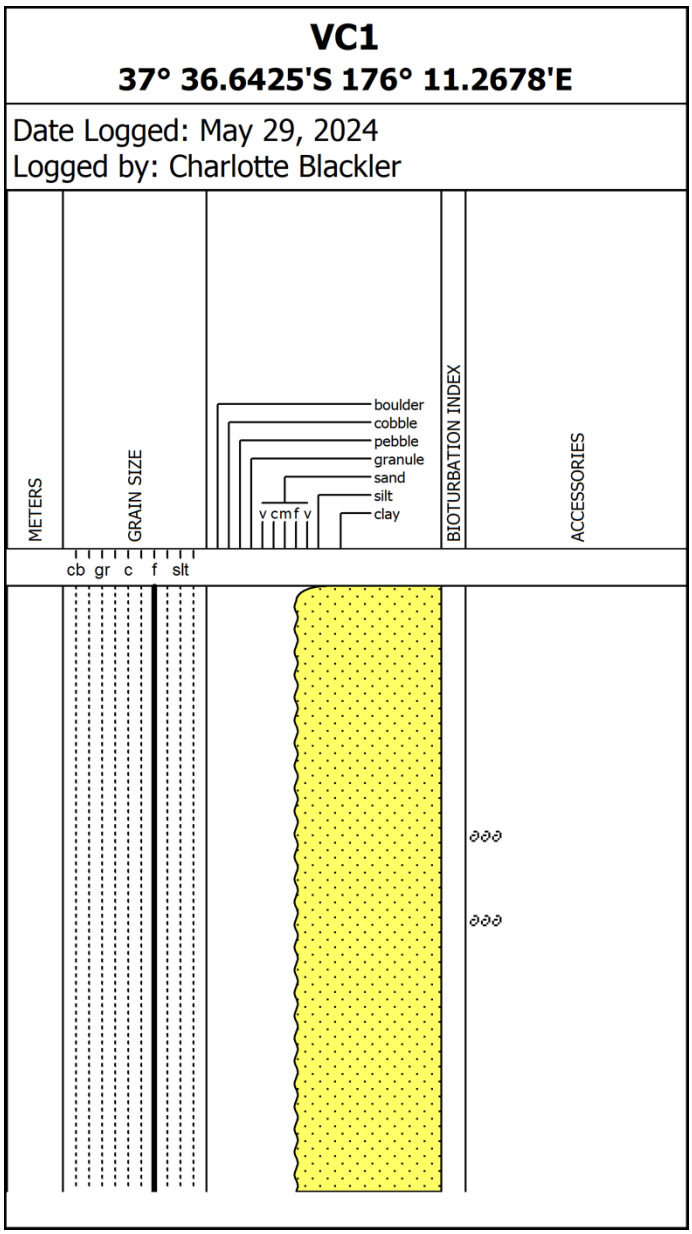
VC1
37° 36.6425'S 176° 11.2678'E
Date Logged: May 29, 2024
Logged by: Charlotte Blackler
METERS
GRAIN SIZE
cb gr c f slt
boulder
cobble
pebble
granule
sand
silt
clay
v c m f v
BIOTURBATION INDEX
ACCESSORIES

VC2

37° 36.683'S 176° 12.4454'E

Date Logged: May 29, 2024
Logged by: Charlotte Blackler
Remarks:

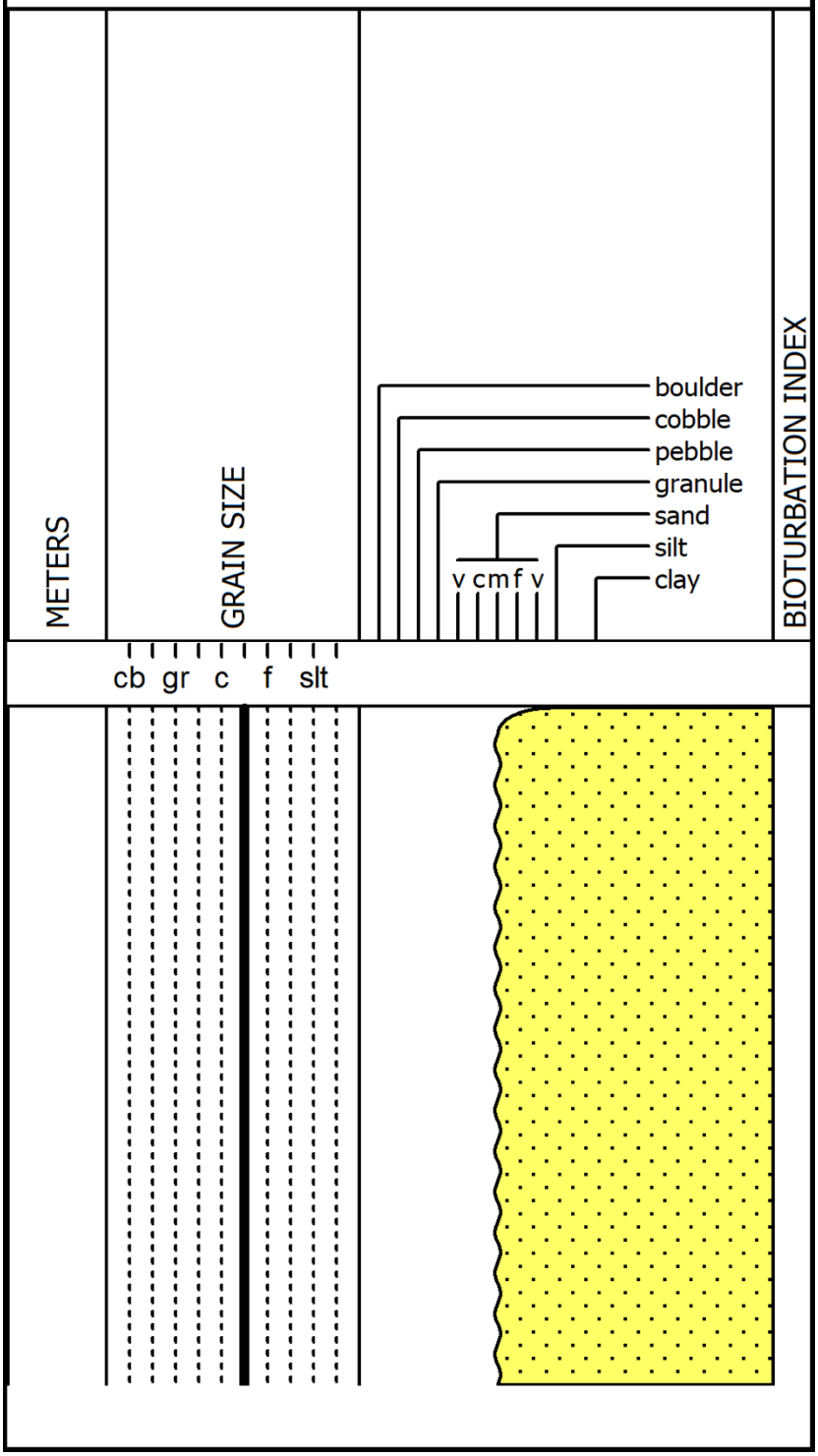

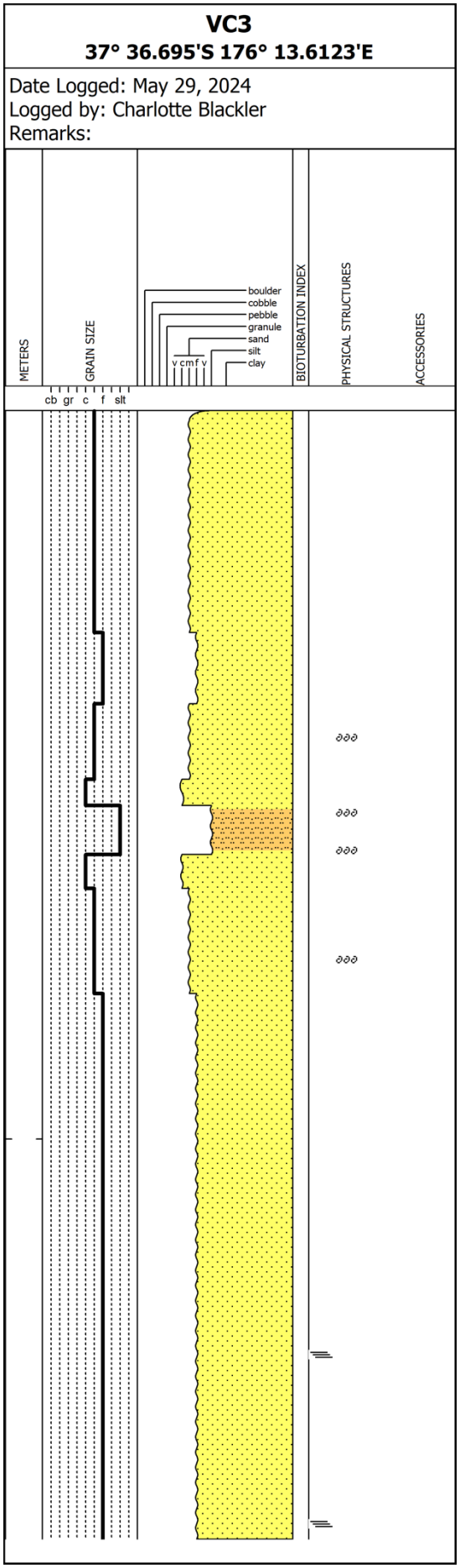
VC3
37° 36.695'S 176° 13.6123'E
Date Logged: May 29, 2024
Logged by: Charlotte Blackler
Remarks:
METERS
GRAIN SIZE
cb gr c f slt
boulder
cobble
pebble
granule
sand
silt
clay
v cm f v
BIOTURBATION INDEX
PHYSICAL STRUCTURES
ACCESSORIES

VC4

37° 36.6691'S 176° 14.8632'E

Date Logged: May 29, 2024
Logged by: Charlotte Blackler
Remarks: